INSA

CNRS CENTRE NATIONAL DE LA RECHERCHE SCIENTIFIQUE



# WORKSHOP :

# Applications of SQUID Magnetometrie

## INSA de Lyon
## 16 et 17 juin 1999
## Lyon - France



Professor Pierre-Louis VUILLERMOZ wishes to thank the following for their contribution to the success of this conference :

European Office of Aerospace Research and Development, Air Force office of Scientific Research , United States Air Force Research Laboratory.

# REPORT DOCUMENTATION PAGE

Form Approved OMB No. 0704-0188



1. AGENCY USE ONLY (Leave blank)

2. REPORT DATE

12 October 1999

3. REPORT TYPE AND DATES COVERED

Conference Proceedings

4. TITLE AND SUBTITLE

Applications of SQUID Magnetometry

5. FUNDING NUMBERS

F61775-99-WF058

6. AUTHOR(S)

Conference Committee

7. PERFORMING ORGANIZATION NAME(S) AND ADDRESS(ES)

Laboratoire de Physique de la Matiere, Batiment 502, INSA de Lyon
20, avenue Albert Einstein
Villeurbanne Cedex 69621
France

8. PERFORMING ORGANIZATION REPORT NUMBER

N/A

9. SPONSORING/MONITORING AGENCY NAME(S) AND ADDRESS(ES)

EOARD
PSC 802 BOX 14
FPO 09499-0200

10. SPONSORING/MONITORING AGENCY REPORT NUMBER

CSP 99-5058

11. SUPPLEMENTARY NOTES

12a. DISTRIBUTION/AVAILABILITY STATEMENT

Approved for public release; distribution is unlimited.

12b. DISTRIBUTION CODE

A

13. ABSTRACT (Maximum 200 words)

The Final Proceedings for Applications of SQUID Magnetometry, 16 June 1999 - 17 June 1999

This is an interdisciplinary conference. Topics include non-destructive evaluation, geophysics, biomolecular dynamics; and biomedical applications in neurology and cardiology.

14. SUBJECT TERMS

EOARD, Superconductivity, Aging Aircraft

15. NUMBER OF PAGES

220

16. PRICE CODE

N/A

| 17. SECURITY CLASSIFICATION OF REPORT | 18. SECURITY CLASSIFICATION OF THIS PAGE | 19, SECURITY CLASSIFICATION OF ABSTRACT | 20. LIMITATION OF ABSTRACT |
|---|---|---|---|
| UNCLASSIFIED | UNCLASSIFIED | UNCLASSIFIED | UL |

NSN 7540-01-280-5500

Standard Form 298 (Rev. 2-89)
Prescribed by ANSI Std. 239-18
298-102

# Introduction to SQUID Magnetometry and Its Applications (plus some examples of the author's research)

Harold Weinstock
US Air Force Office of Scientific Research
Arlington, VA 22203-1977 USA

Workshop on Applications of SQUID Magnetometry
INSA de Lyon
Lyon, FRANCE
June 16-17, 1999

# APPLICATIONS OF SQUID MAGNETOMETRY

## (TOPICS TO BE COVERED)

**Commercialization of SQUIDs**

**NDE of engineering structures and wires**

**RF amplifiers and dynamics of magnetic bacteria**

**Geophysical exploration**

**Magnetoencephalography (MEG)**

**Magnetocardiography (MCG)**

**Liver susceptometry and intestinal ischemia**

# SQUID

Superconducting QUantum Interference Device

$$\Phi_0 = 2.07 \times 10^{-15}\ \text{Wb} = \frac{h}{2e}$$

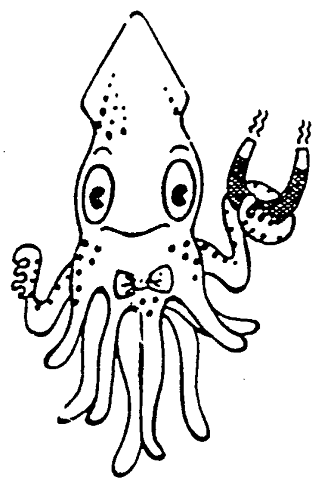

Squid, *Ommastrephes sagittatus*

Typical sensitivity $\approx 10^{-4}\,\Phi_0$

or $\approx 1 - 10\ \text{fT/Hz}^{1/2}$

(commercial instruments)

# ALTERNATIVE MAGNETOMETERS

- Variometer

  Rotation of a suspended magnet
  $10^{-10}$ THz$^{-1/2}$ at zero frequency
- Fluxgate $10^{-10}$ THz$^{-1/2}$ DC to kHz
- Induction Coil

  10 cm long, 10 cm diameter
  $10^{-13}$ THz$^{-1/2}$ at 10 Hz at room temperature
  $10^{-}13$ THz$^{-1/2}$ at 4 K
- Magnetic resonance magnetometers
- Hall effect
- Optical fiber
- SQUID $10^{-14}$ THz$^{-1/2}$ DC to 10's of kHz

"Magnetic quantities, units, materials and measurements," J.E. Zimmerman, in *Biomagnetism: an Interdisciplinary Approach,* S.J. Willia G.L. Romani, L. Kaufman, and I. Modena, Eds., (Plenum, New York, 1982) pp. 17-42.

**Never** Use a SQUID When

A Simpler,

Less Expensive Technology

is Adequate

# **Do** Use a SQUID When

- Extra Sensitivity is Required
- Nothing Else Will Meet Your Requirements

  (distant noise, high fields, spatial resolution, linearity)

# Magnetic Fields

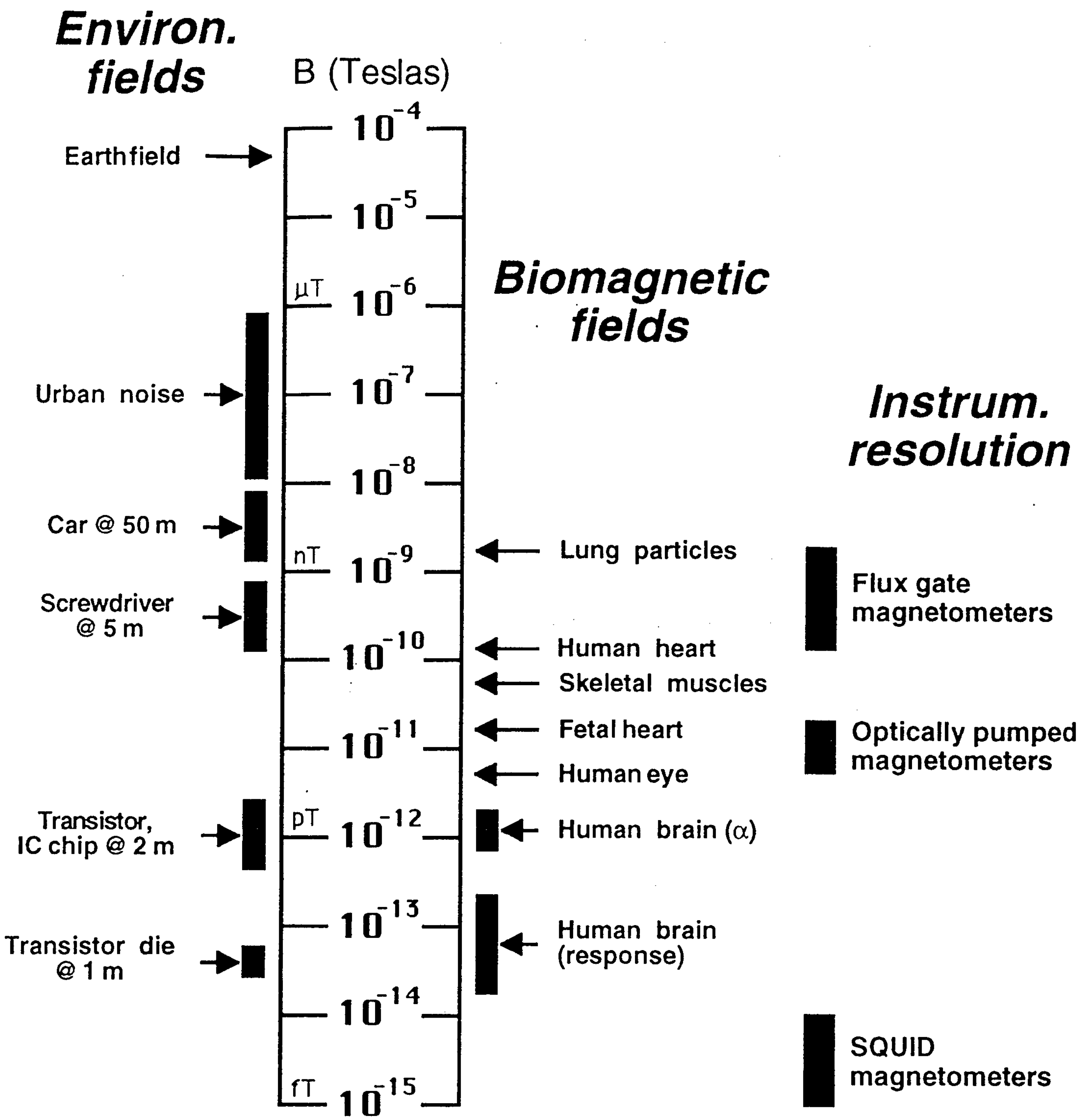


| | |
|---|---|
| Car = $10^{14}$ pT·cm$^3$ | Packaged IC chip or transistor = $10^7$ pT·cm$^3$ |
| Screwdriver = $10^{11}$ pT·cm$^3$ | IC chip or transistor die = $5 \times 10^4$ pT·cm$^3$ |

# SQUIDs

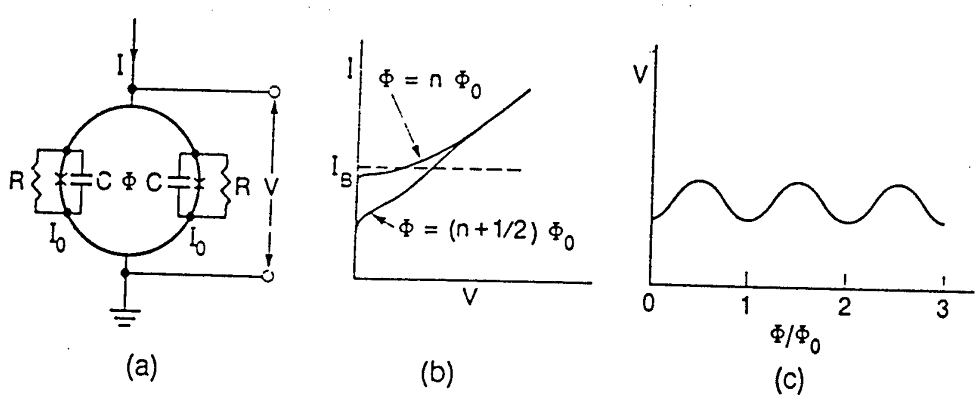


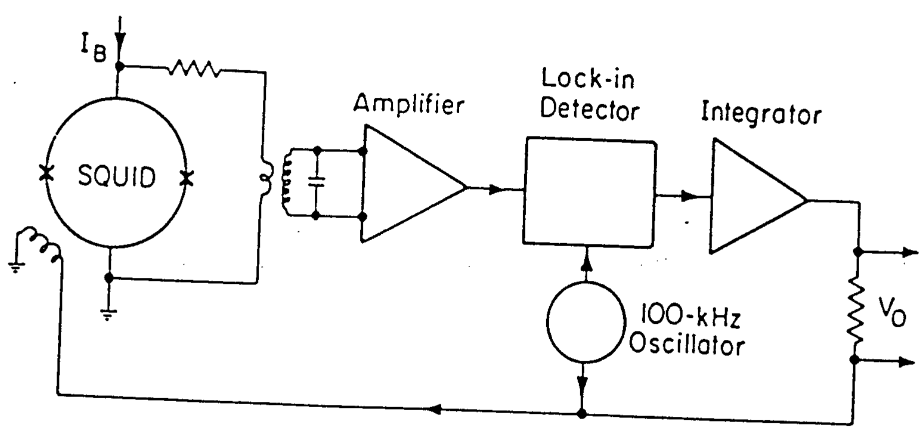


"Principles and applications of SQUIDS," J. Clarke, *Proc. IEEE* **77**: 1208-1223.

# MAGNETOMETERS

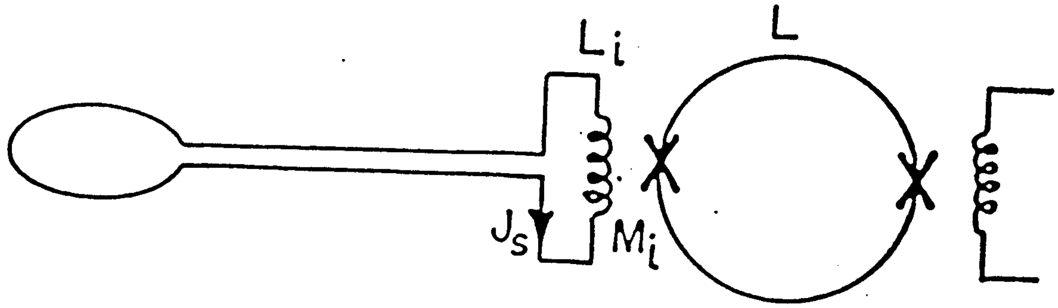


FLUX-LOCKED SQUID

- Single loop
- Multiple turns
- Field sensitivity proportional to coil area
- Sensitive to noise
- Sensitive to tilt in Earth's field

"Principles and applications of SQUIDS," J. Clarke, *Proc. IEEE* 77: 1208-1223.

# ENVIRONMENTAL NOISE

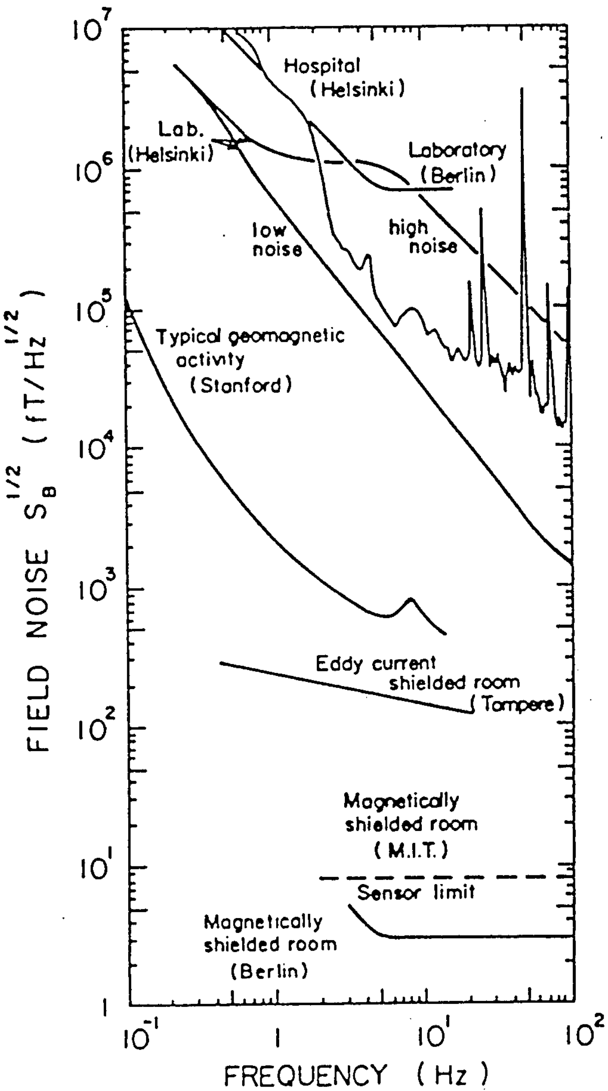


G.L. Romani, S.J. Williamson, and L. Kaufman, *Review of Sci. Instru.*, **53**: 1815 (1982)

# GRADIOMETERS

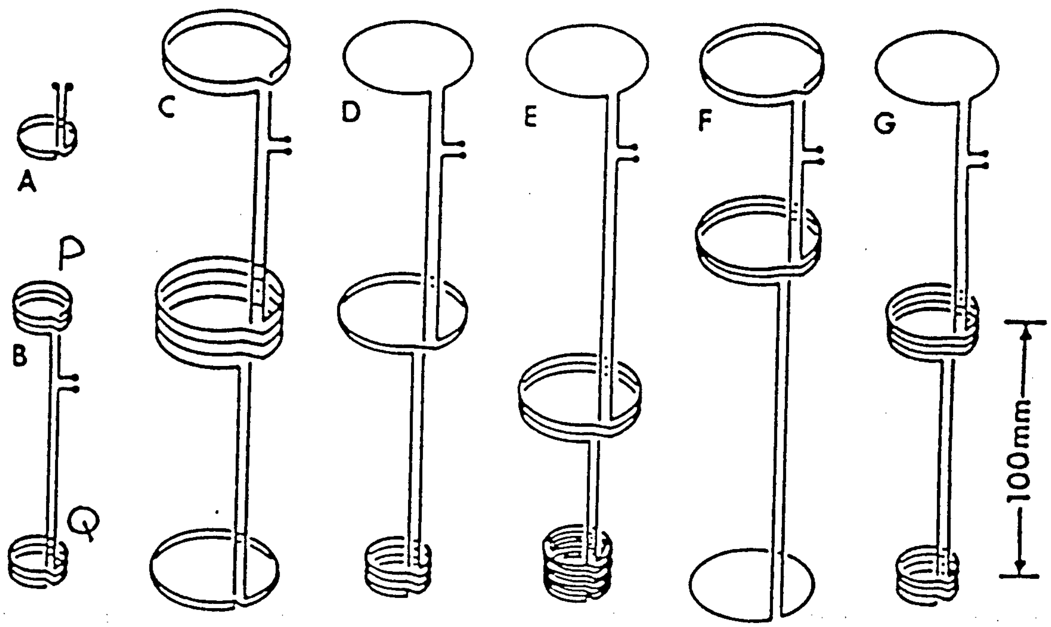


- Can be balanced to 1 part in $10^7$
- Insensitive to distant noise sources
- Insensitive to tilt in uniform fields
- Energy wasted in balance coils

"Optimization of SQUID Differential Magnetometers," J.P. Wikswo, Jr., *AIP Conf. Proc.*, 44: 145-149 (1978).

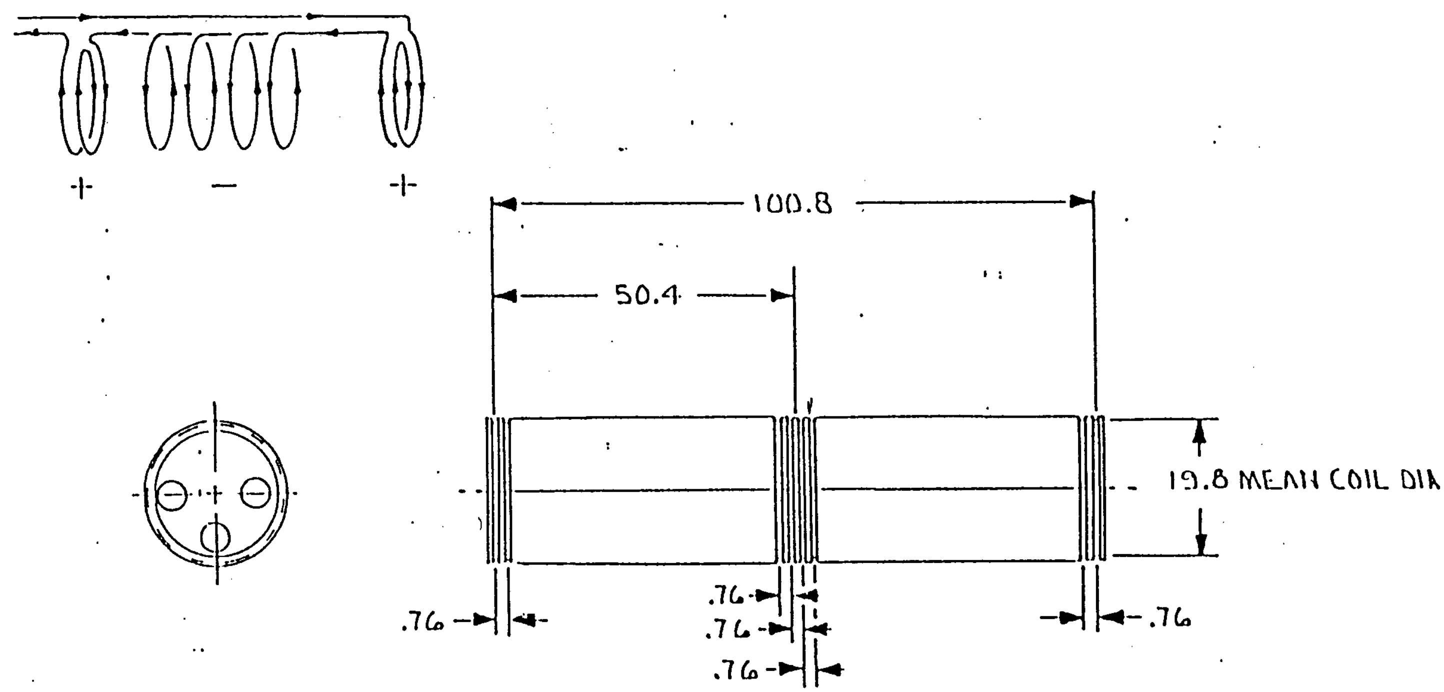


NOTES.
1. ALL DIMENSIONS ARE IN MM.

Figure 1-3. Model 601 Biomagnetometer Coil Form and Pick-Up Coil

A2001-327, Rev. C

# SQUID DEWAR DESIGN

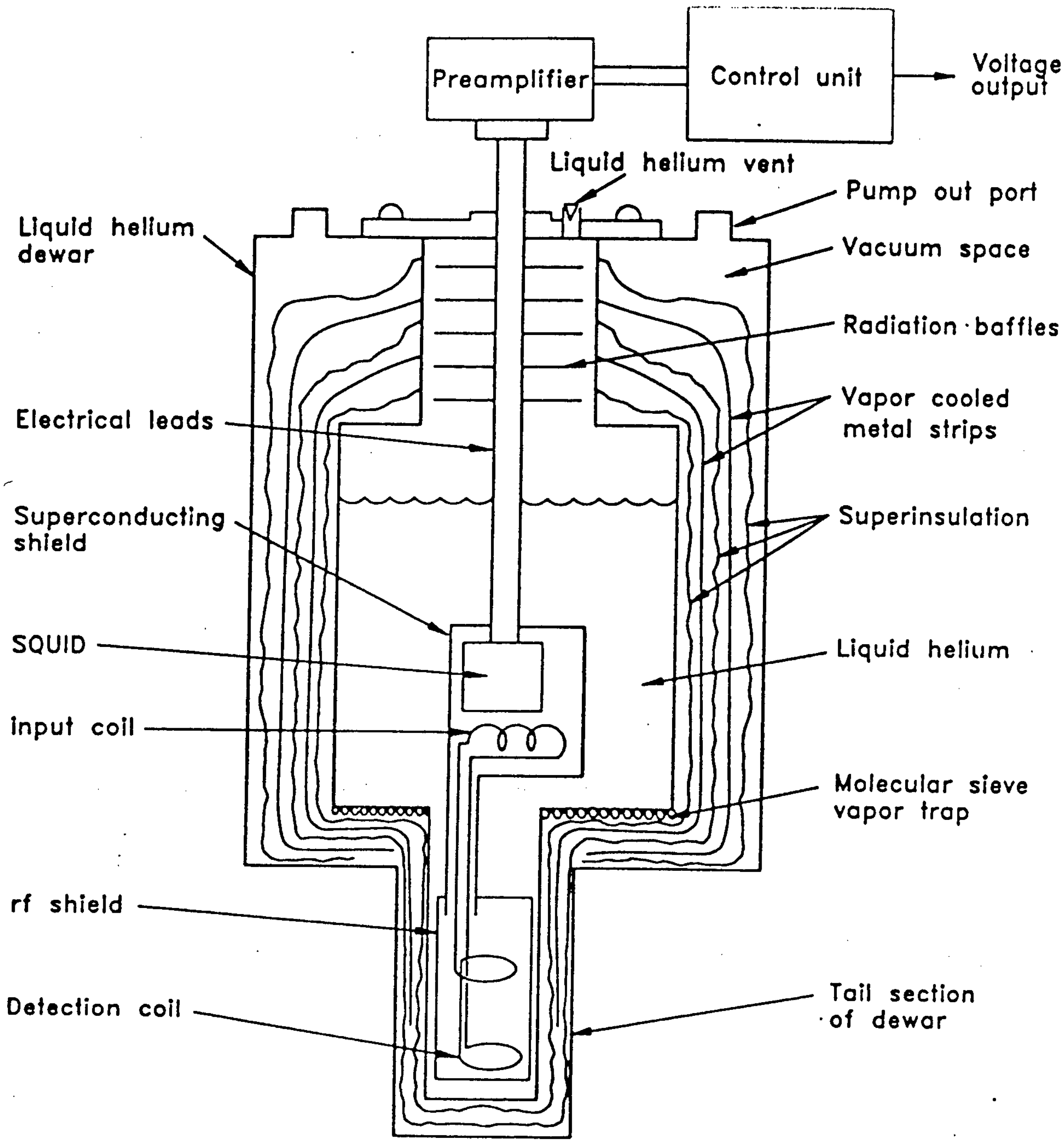


"Cryogenics," J.E. Zimmerman, in *Biomagnetism: an Interdisciplinary Approach*, S.J. Williamson, G.L. Romani, L. Kaufman, and I. Modena, Eds., (Plenum, New York, 1982) pp. 44-67.

# MCG Using HTS And LTS Magnetometer SQUIDs

Inside A Shielded Room (Courtesy PTB Berlin)

MCG With PTB LTS-SQUID

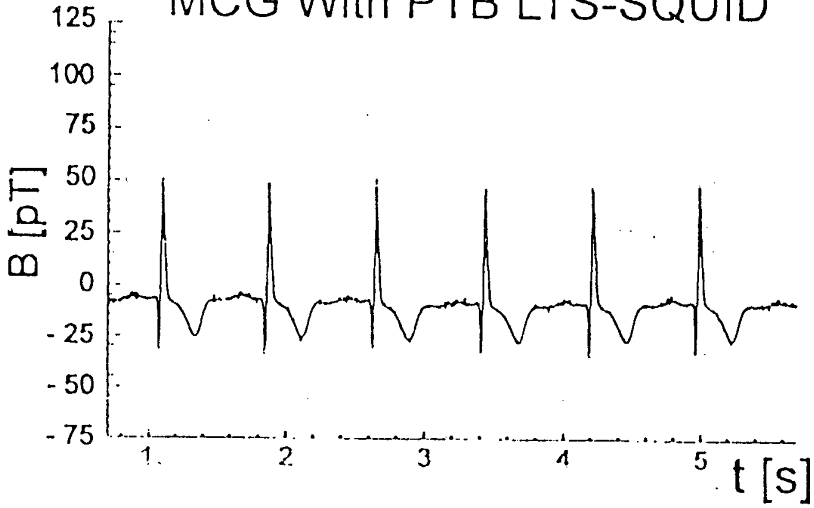


$B_N = 25\ fT/\sqrt{Hz}$

MCG With KFA HTS-SQUID

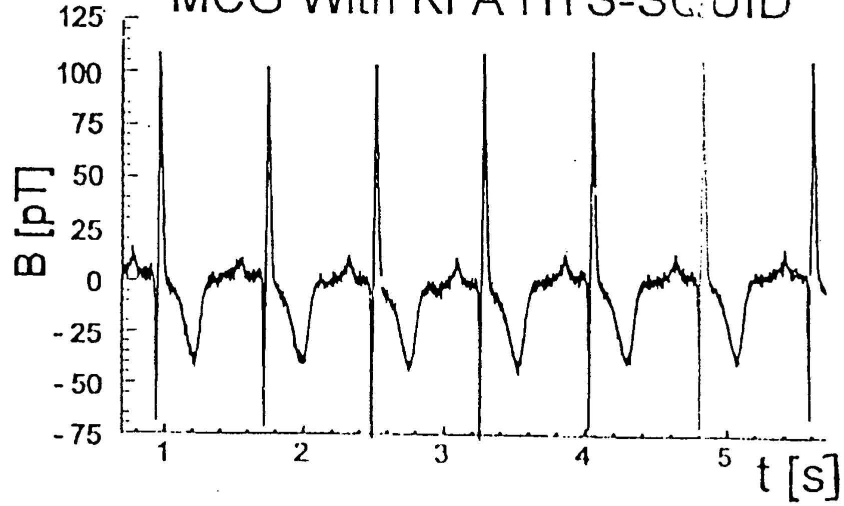


$B_N = 40\ fT/\sqrt{Hz}$

Video Bandwidth 250 Hz

$LN_2$ Makes A **Smaller Source-SQUID Distance** Possible!

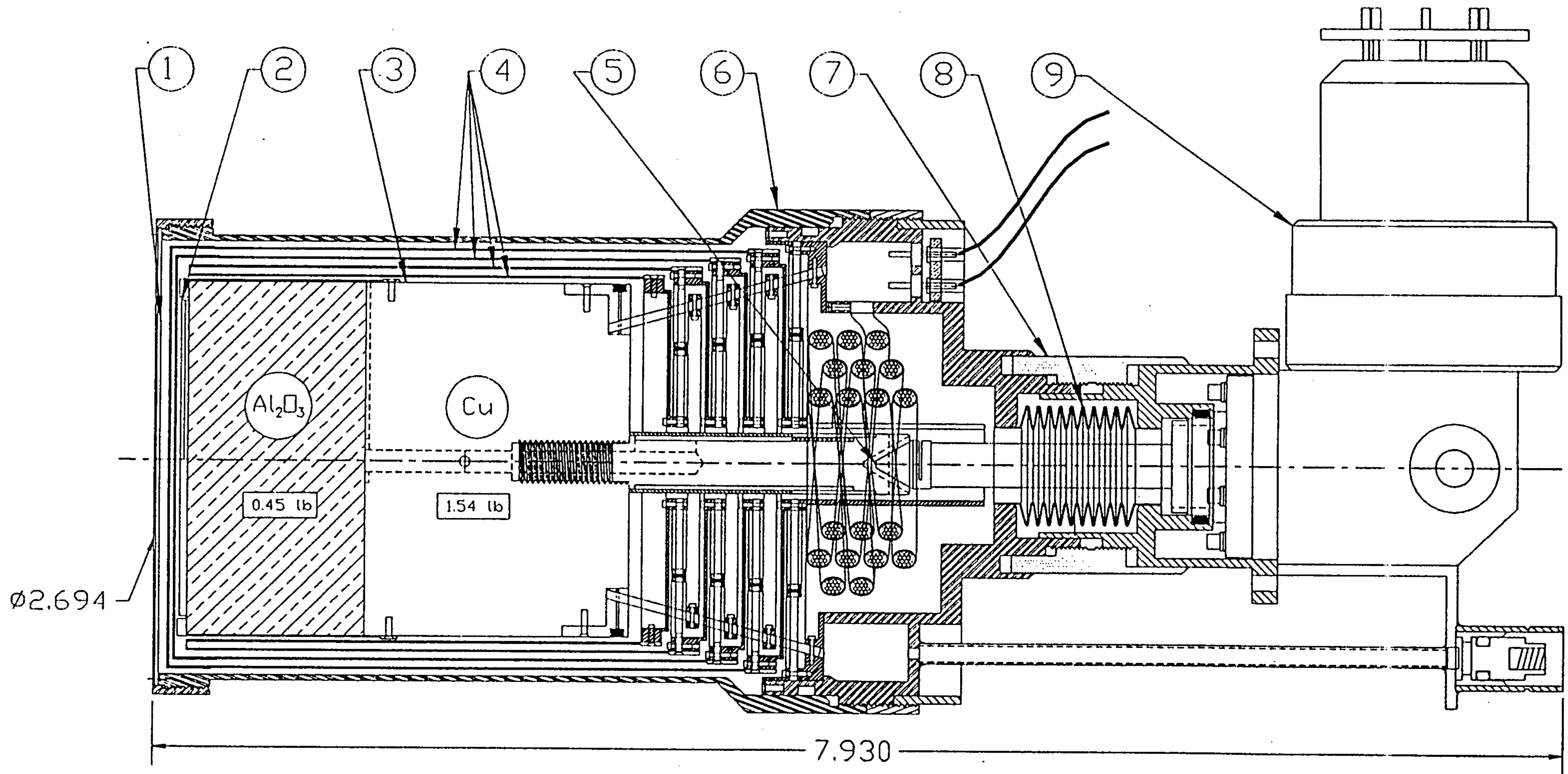


| | | |
|---|---|---|
| 1. sapphire window | 4. thermal shields | 7. coupling turnbuckle |
| 2. SQUID array | 5. refrigerator cold pad | 8. bellows |
| 3. cryobattery | 6. vacuum jacket | 9. microcooler |

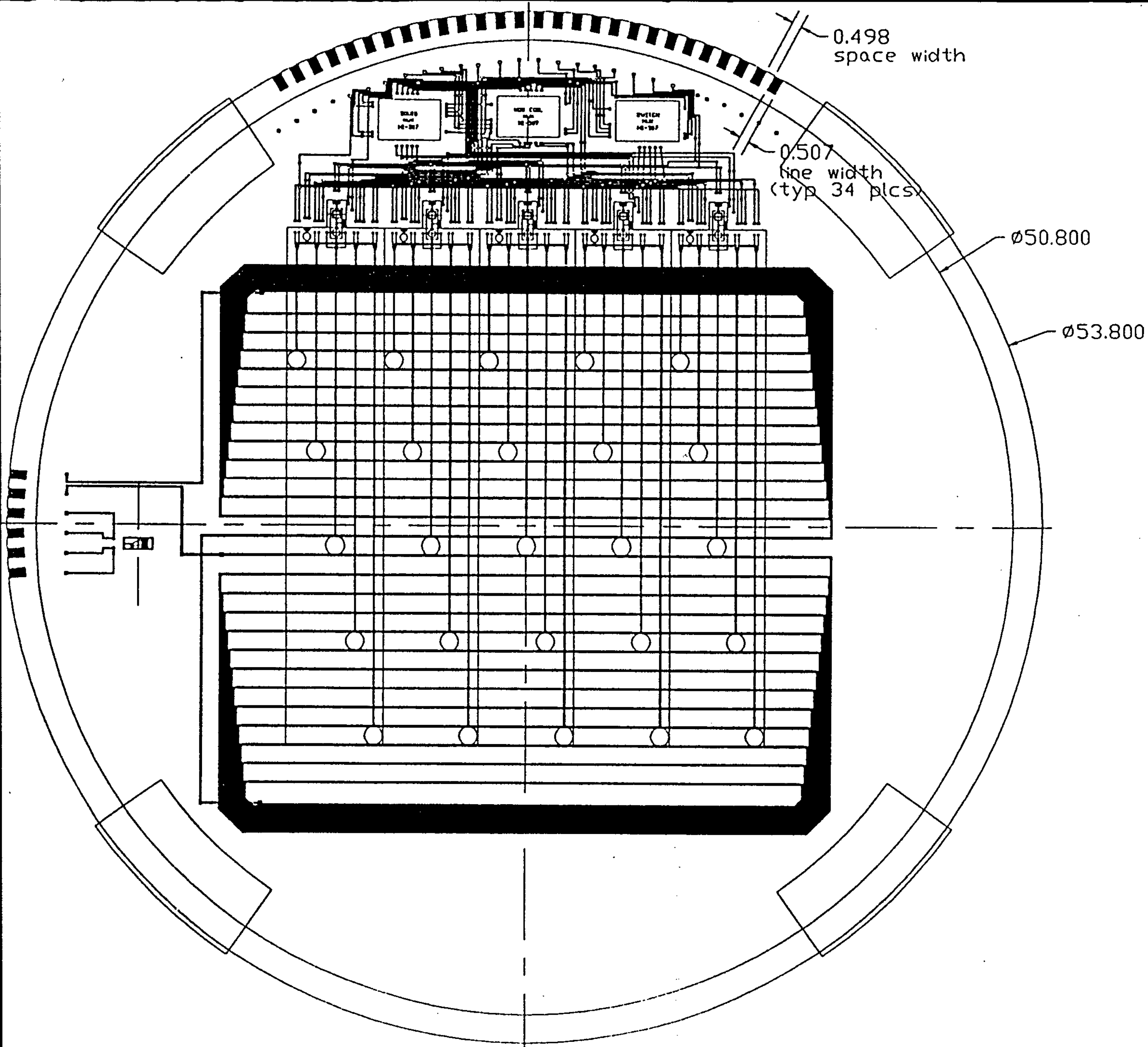


*** NOTE: ALL LINEAR DIMENSIONS IN MILLIMETERS

ALL TRACES AND JUMPERS 0.050 Ag EXCEPT
SOURCE COIL AND LEADS (0.100 YBCO)


1 mm

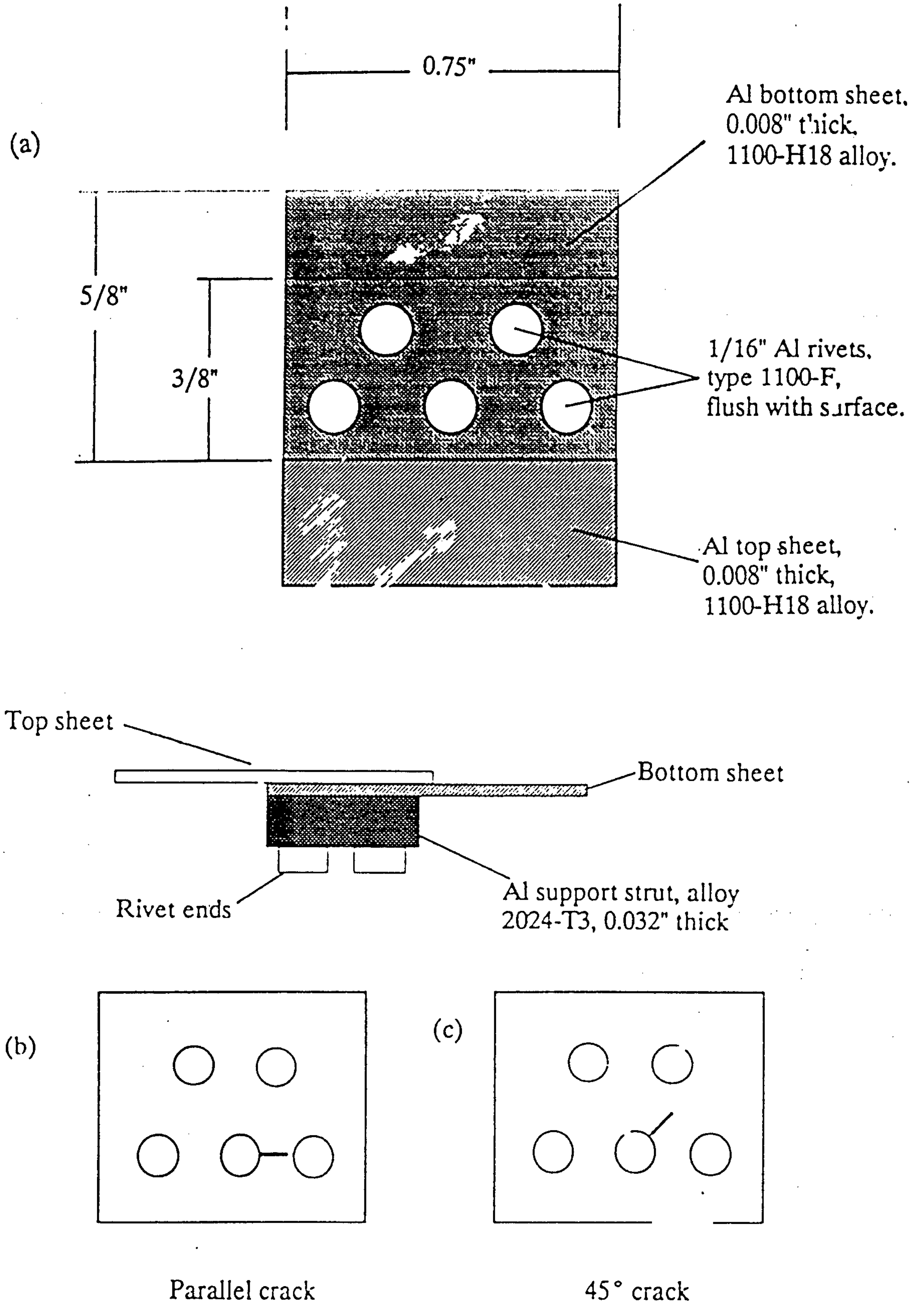


SAMPLE CONFIGURATION

Figure 3. (a) The top and side views of a model aluminum wing lap joint assembly. (b) A schematic of the lower aluminum sheet with a crack parallel to the lap joint and (c) the lower aluminum sheet with a crack at 45° to the lap joint.

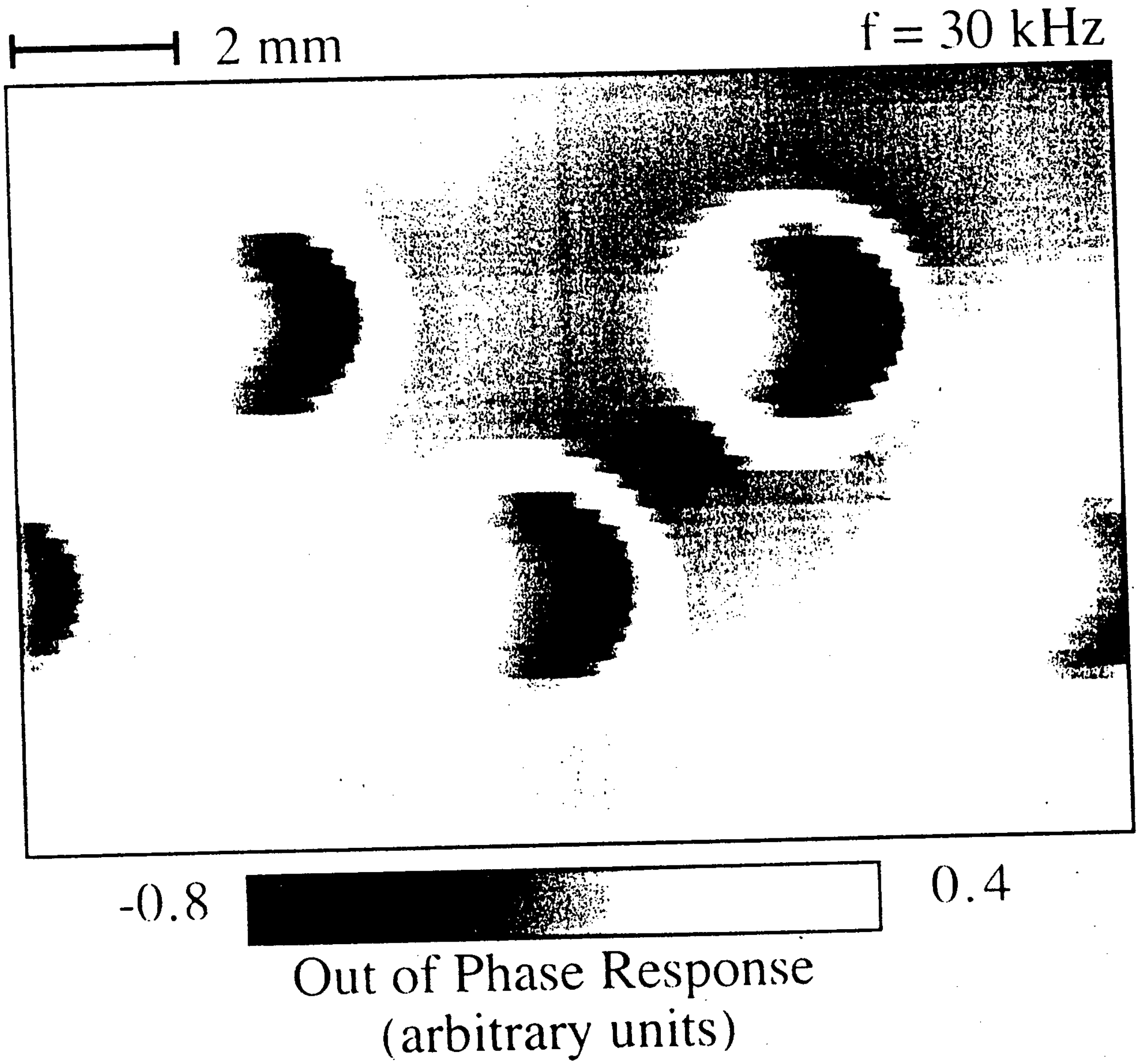


[illegible] current image of a lap joint sample containing a 45° crack.

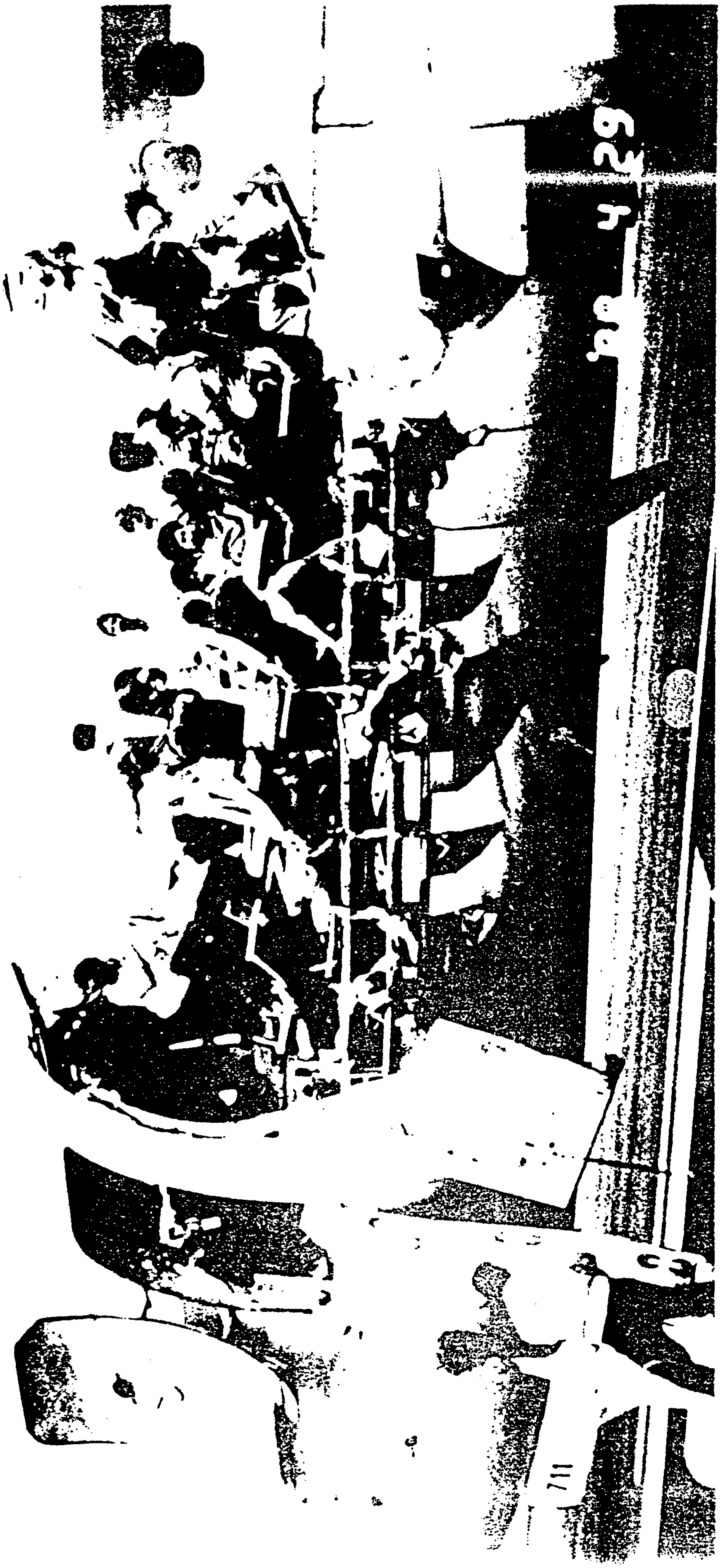

## TECHNICAL MISSION

**Perform basic research to contribute to the integrity and maintainability of aging aircraft and future aerospace systems**

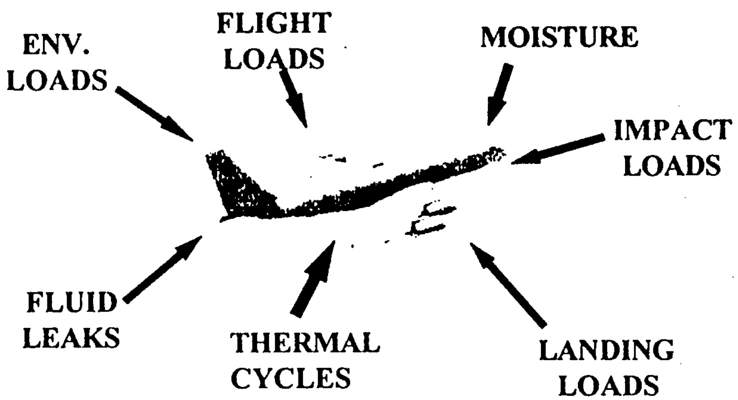


Causes of Damage

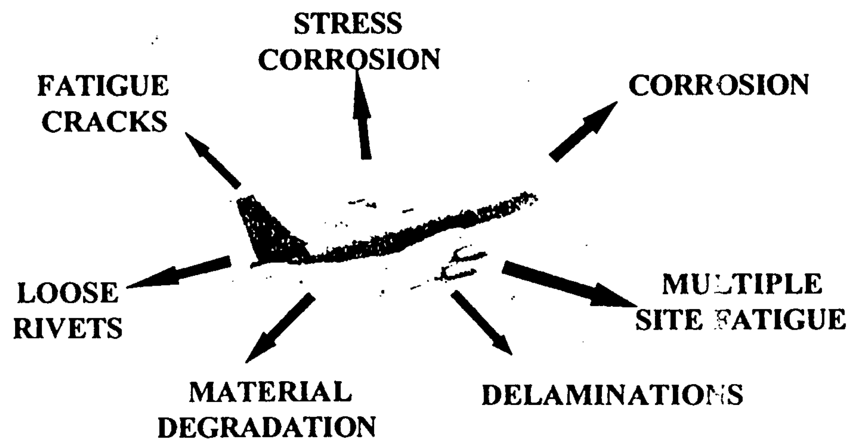


Forms of Damage

## EDUCATIONAL MISSION

**Produce qualified graduate and post-graduate students in fields relevant to AF needs**

FAST

# Air Force Aging Aircraft

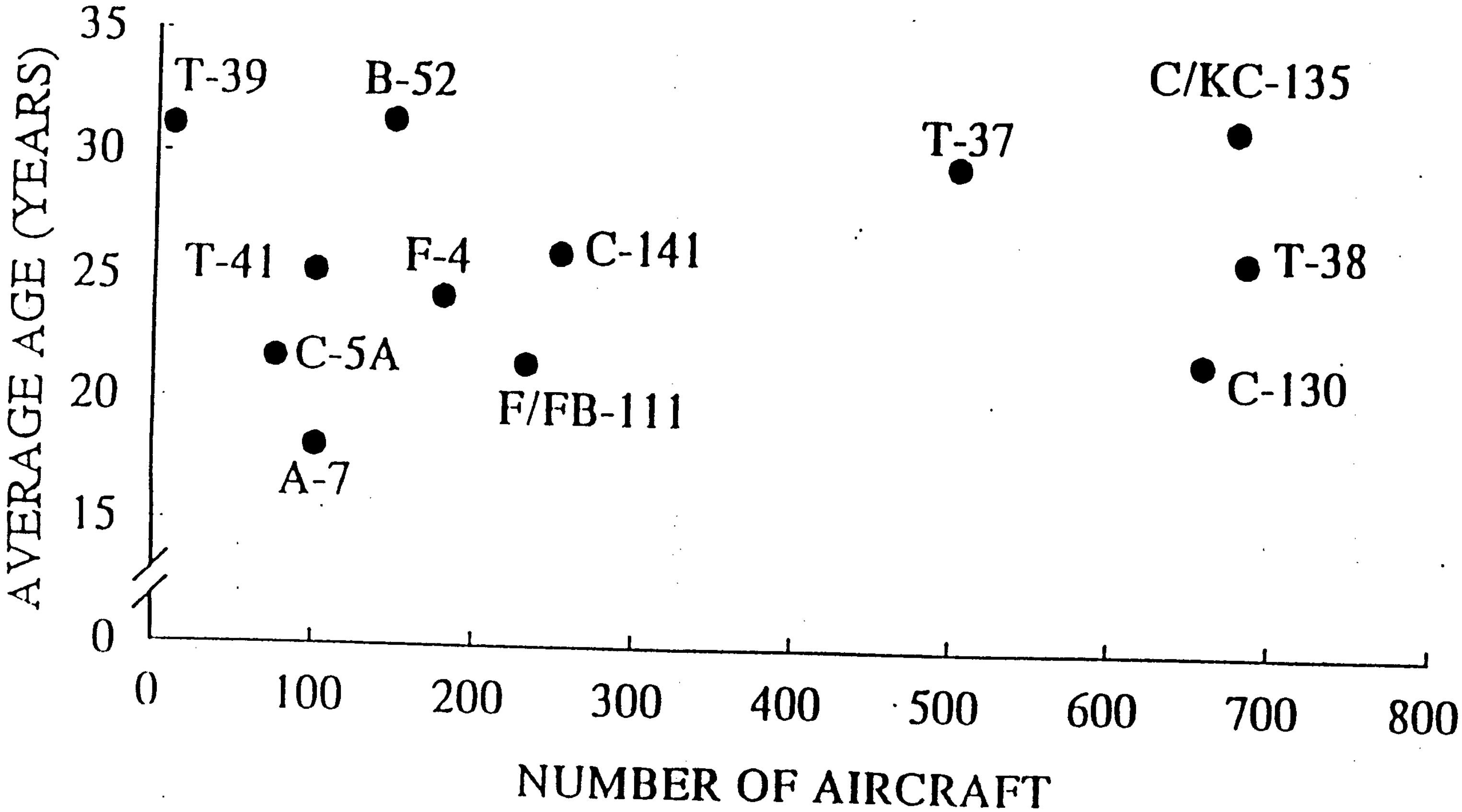


Rockwell - MIT Corrosion Panel 2/94

# Net magnetic flux per scan v.s. Time

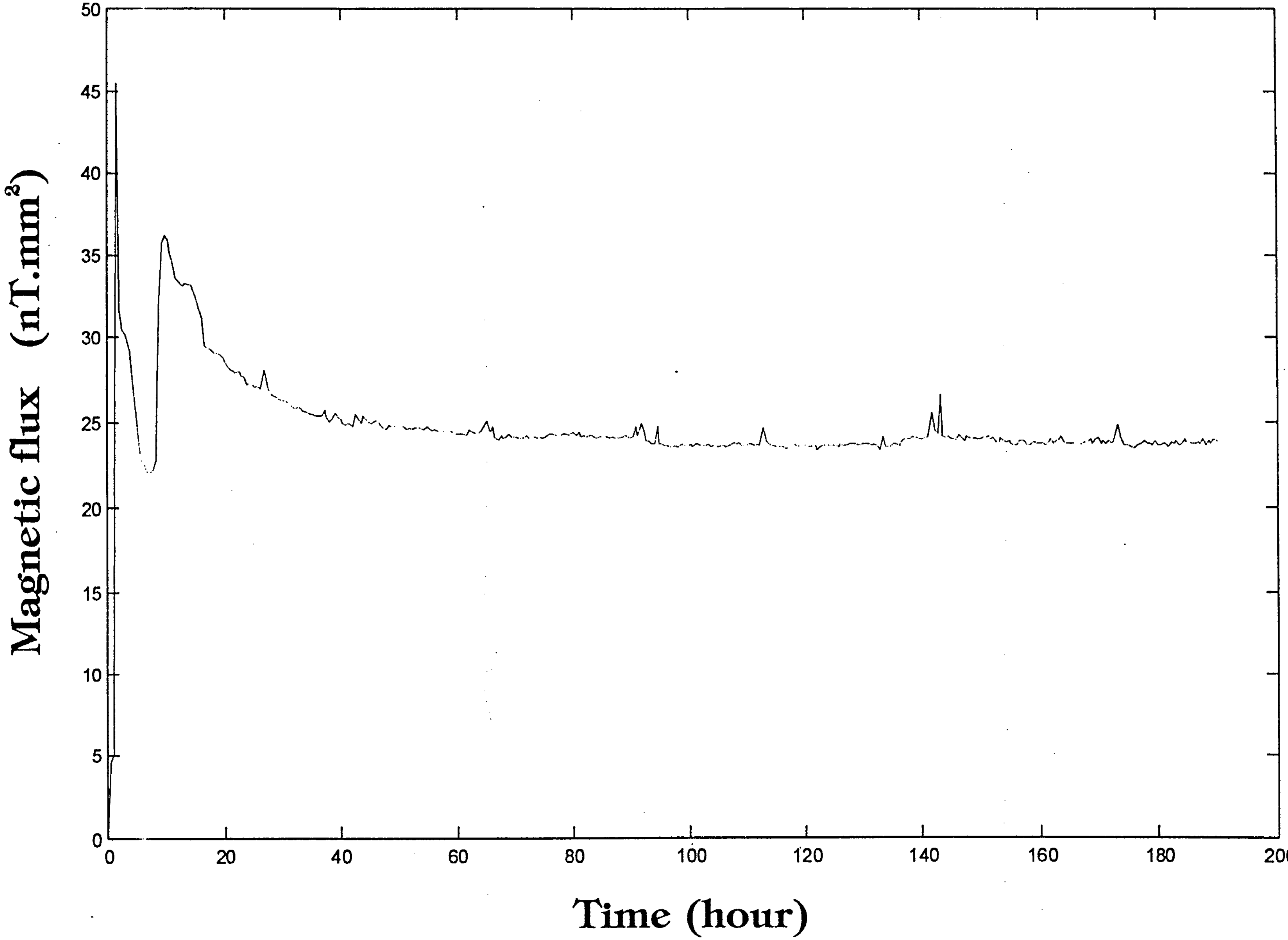

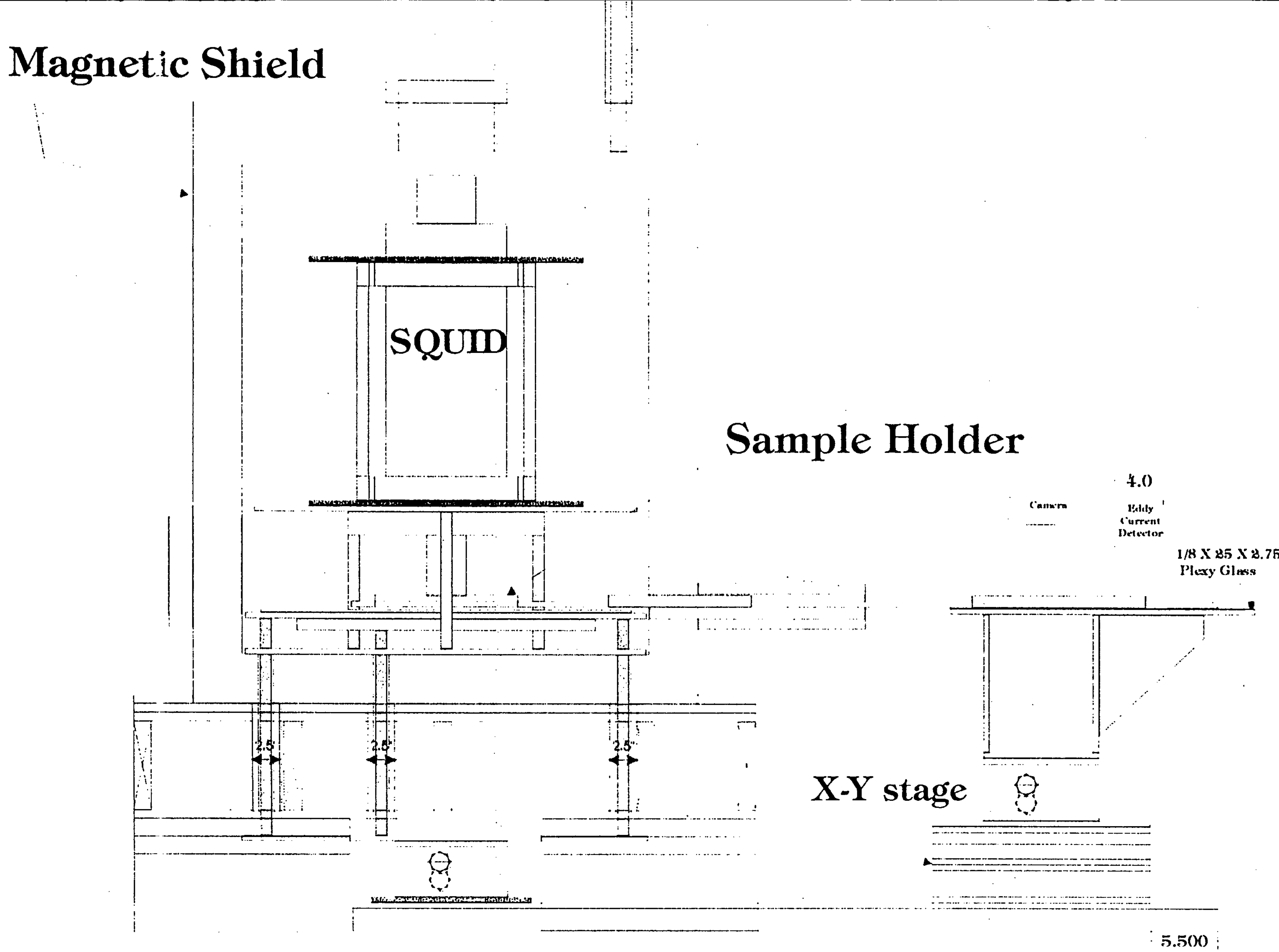

Magnetic Shield
SQUID
Sample Holder
4.0
Camera
Eddy
Current
Detector
1/8 X 25 X 2.75
Plexy Glass
2.5"
2.5"
2.5"
X-Y stage
5.500

# INSPECTION TECHNIQUES

VISUAL (80%)

PENETRANT

HIGH FREQUENCY EDDY CURRENT

LOW FREQUENCY EDDY CURRENT

SONIC

ULTRASONIC

X-RAY RADIOGRAPHY

NEUTRON RADIOGRAPHY

MAGNETIC PARTICLE METHODS

LASER-BASED OPTICAL METHODS

X-RAY DIFFRACTION

THERMAL WAVE IMAGING

ACOUSTIC EMISSION

POTENTIAL DROP METHODS

# Magnetopneumography

- Body is normally diamagnetic or paramagnetic
  - no naturally occurring ferro- or ferrimagnetic constituents
- Ferrimagnetic materials associated with particulate contaminates
  - dust in lungs of coal miners, welders, asbestos workers
  - magnetite dust tracer for lung clearance studies
- Allows lung clearance studies
  - $\mathbf{M} = \mathbf{m}_S\,(1 - e^{-3\,H/Q})$
    - 70 mT (5 sec) $\Rightarrow$ 90% saturation of ferrimagnetic particles
  - $\mathbf{M}_{H = \mathrm{constant}} = \mathbf{m}_S\,(1 - e^{-t/\tau_H})$
    - $\tau_{\mathrm{ferrimagnetism}}$ as short as minutes
- Example of Research, not Clinical Application

Tristan Technologies

# Magnetopneumography Measurement Techniques

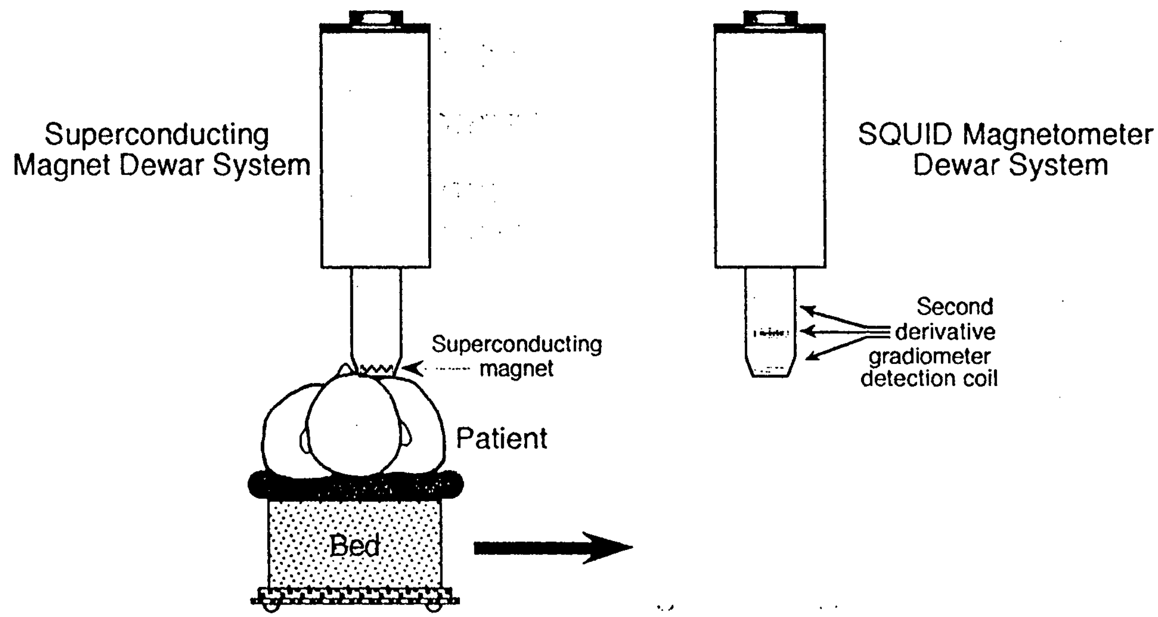


- Magnetize lung
  H ~ 100 mT 9 cm below magnet
- Move subject beneath magnetometer
- Scan magnetometer for remnant magnetism
  500 picogram/cc sensitivity ≈ 1 μgram total particulates
  $\Delta t \geq 10$ seconds

Tristan Technologies

# Mesenteric Ischemia

- Mesenteric arteries carry blood to the stomach, small and large intestine
- Blockage of the blood flow (ischemia) can lead to intestinal necrosis
- Symptoms are primarily abdominal pain, usually 30-90 minutes after eating
  - often ignored
- Diagnosis of mesenteric artery narrowing or blockage is by arteriogram
  - requires catheter and X-ray dye
  - limit on size of vessels that can be seen by X-ray
- Treatment requires surgical intervention
  - if intestinal tissue is necrotic, segment(s) must be removed or bypassed
  - if diagnosis delayed, mortality rate can exceed 50%

Tristan Technologies

# Basic Electric Rhythm

- Gastrointestinal (GI) tract exhibits two types of electrical activity
  - high frequency spiking associated with muscle contraction
  - **Low frequency oscillations known as electric activity or basic electric rhythm (BER)**

| | |
|---|---|
| Human gastric BER | $\approx 3.2 \pm 0.1$ Hz |
| Small intestine BER | $\approx 11.3 \pm 0.1$ Hz |
| duodenum BER | $\approx 12$ Hz |
| terminal ileum BER | $\approx 8$ Hz |

Tristan Technologies

# Ischemic Episodes Show Marked Reduction in BER

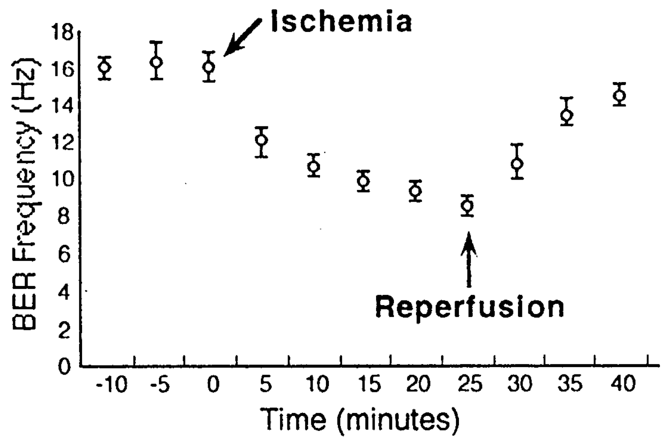


BER frequency before and after occlusion of mesenteric artery

Statistically significant frequency shift may permit diagnosis

Tristan Technologies

# Instrumentation for Ischemia

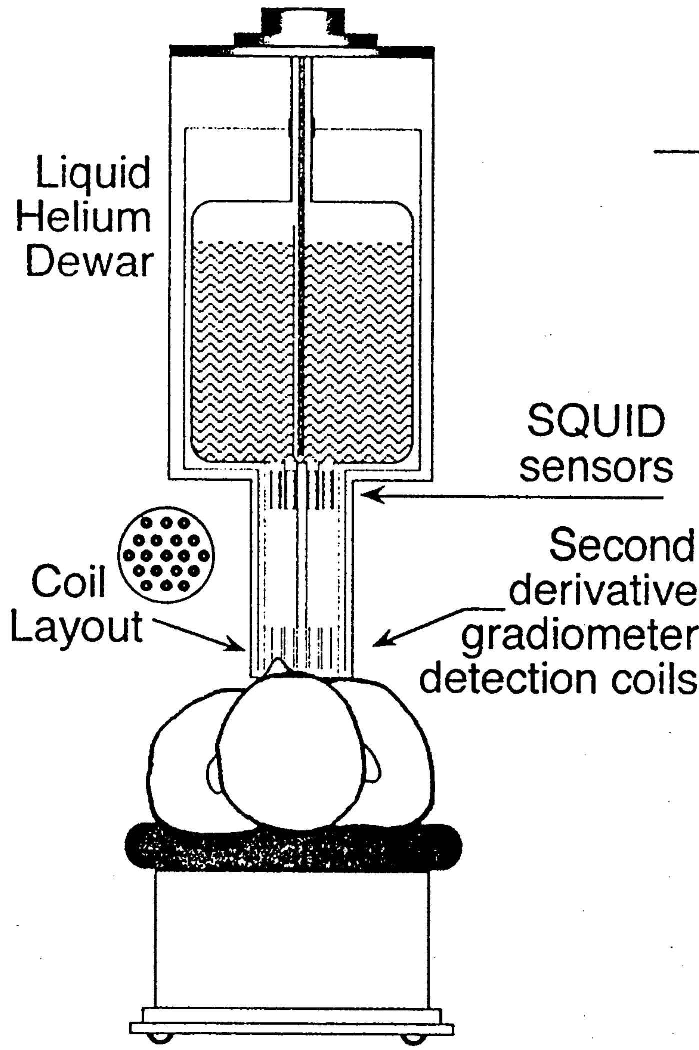


- Subcutaneous electrodes ~ mV
  - Highly invasive
  - *not a clinical procedure*
- SQUID Magnetometer ~ pT
  - Not invasive
- Status
  - First 3-channel system at Vanderbilt
  - Building 19 channel system for preclinical studies
    - has vector ($B_X$, $B_Y$, $B_Z$) channels
- Example of a Pre-Clinical Application

Tristan Technologies

# Biomagnetic Liver Susceptometry

- Medical Motivation
- Iron in the Human Body
- The Differential Measurement
- Calculation of Iron Concentration ($\chi$)
- Magnetic Detection First Shown in Animals
- The SQUID Magnetometer
- The Instrument
- Measurement Protocol
- Clinical Validation of Magnetic Measurement
- Conclusions

Tristan Technologies

# Medical Motivation

## Genetic diseases, which directly or indirectly cause iron overload

| Disease: | Hæmochromatosis | Thalassemia | Sickle-Cell Anemia |
|---|---|---|---|
| Symptoms: | none in early stages; diabetes, arthritis, myocardial infarction, cirrhosis, etc. in later stages, anemia, tiredness | anemia, tiredness | anemia, hypoxemia |
| Source of excess iron: | abnormal absorption from diet | transfusion, some excess absorption | whole blood transfusion |
| Therapy for Iron Removal: | phlebotomy | chelation | chelation |
| Other Therapy: | | spleenectomy, bone marrow transplantation | equal exchange transfusions |
| Incidence*: (U.S. figures) | 0.25% - 0.5 % affected ~10% have trait | 1.5% | 0.3% blacks affected, 7% have trait |
| Main Sub population affected | Northern European decent | Mediterranean decent | African or Hispanic decent |

**Consequences**: Long-term exposure to high levels of iron in the body cause diabetes, growth disturbances, arthritis, and irreversible damage to endocrine glands, heart and liver.

Tristan Technologies

# Iron in the Human Body

~ **4 Grams of Iron in Healthy Adult**

- ~ **3 grams involved in biochemistry, primarily oxygen transport**
- ~ **1 gram of iron is stored in specialized protein molecules** (*e.g.*, ferritin, hemosiderin).
  - The major storage location is the Liver
  - Secondary storage locations are the Spleen and, when overloaded, the Heart

**When greatly overloaded, as much as 50 gram of Iron stored in 1.5 kg liver**

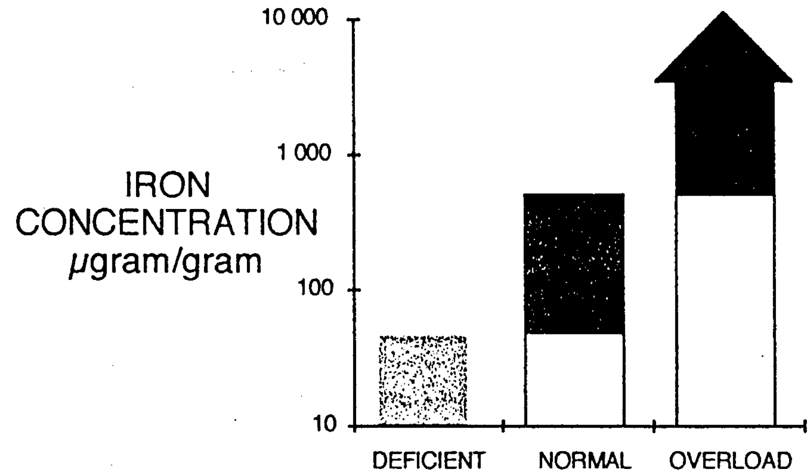


**The iron stored in the ferritin molecule is paramagnetic**

The concentration of iron can be determined by a magnetic susceptibility measurement $\chi = B/H$

Tristan Technologies

# The Differential Measurement

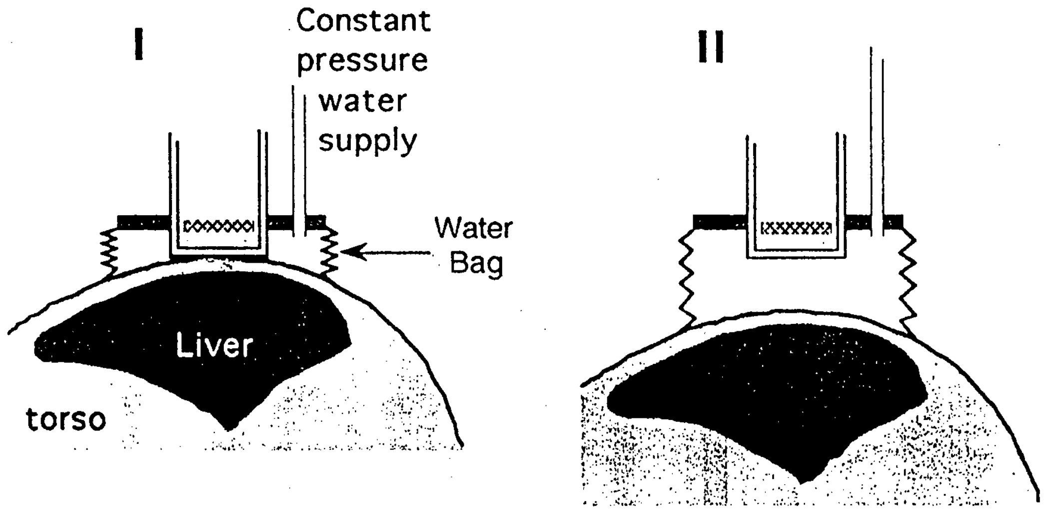


- Susceptibility of Liver sum of iron ($\propto$ [Fe]) and liver tissue
- The Liver is surrounded by tissue
  - $\chi_{tissue}$ is non-zero
  - $\chi_{tissue} \approx \chi_{water}$
- Use of Water Bag simulates uniform medium
  - Measurement is made by lowering the subject (**I**)
  - Water effectively replaces the torso by water (**II**)

Tristan Technologies

# Calculation of Iron Concentration ($\chi$)

## First Order

$\chi_{\text{liver}} << \chi_{\text{tissue}}$ *(skin, fat, muscle, ribs,...)*

$$V(z) = C\,\Delta\chi_{liver}\,\Phi + \Delta V_{system}(z) + V_O(z)$$

$$\Phi(z) = \int H_{magnet} \cdot B_{coils}\, dr^3$$

## Second Order

$\chi_{\text{liver}} \leq \chi_{\text{tissue}}/10$

$$V(z) = C\,\{\Delta\chi_{tissue}\,\Phi_{tissue} + \Delta\chi_{liver}\,\Phi_{liver}(z + z_{liver})\} + \Delta V_{system}(z) + V_O(z) + O_3$$

By fitting output voltage as a function of depth, $\chi$ can be determined

Tristan Technologies

# Magnetic Detection First Shown in Animals

"Estimation of Hepatic Iron Stores by In-Vivo Measurement of Magnetic Susceptibility"
John H. Bauman and John W. Harris, *The Journal of Laboratory and Clinical Medicine*, **70**, 246 - 257 (1967)

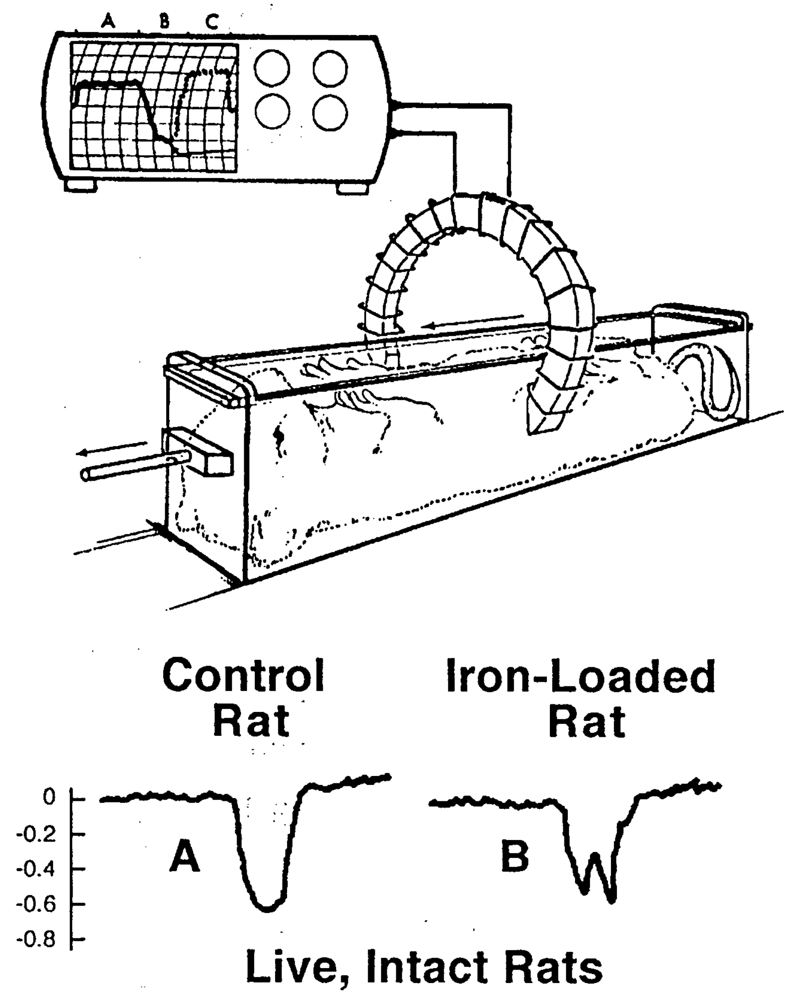


Tristan Technologies

# The SQUID Magnetometer

- Amplifier is Superconducting QUantum Interference Device (SQUID)
  - Operates at cryogenic temperatures
- Measures Magnetic Fields better than anything else
  - Sensitivity as low as femtoTesla
- Highly Stable and Repeatable in large magnetic fields
  - better than parts per million/hour in Tesla fields
- Very Reliable
  - Fundamental technology commercially available since 1970
  - 12 year operational history as measurement of iron stores
- Sites in Hamburg, Germany and New York
  - Systems under construction for Torino, Italy and California

Tristan Technologies

# Clinical Biomagnetism

- Advantages of Biomagnetism
- Magnetopneumography
- Biomagnetic Liver Susceptometry
- Intestinal Ischemia
- Issues in Clinical Applications

Robert L Fagaly
Tristan Technologies,
San Diego, USA

Tristan Technologies

# Introduction

- Useful in identifying electrophysiological activity
- Biomagnetism has significant advantages over electrical recordings
  - Non-Invasive
    - *e.g.*, Intestinal Ischemia
  - Measures a vector quantity—magnetic field, rather than a scalar quantity—voltage
- Many magnetic analogs to electrical activity
  - MCG (Baule & McFee)
  - MEG (Cohen)
- There are also biomagnetic signals that have no electrical analogs.
  - Biomagnetic Liver Susceptometry
  - Magnetopneumography

Tristan Technologies

# The Instrument

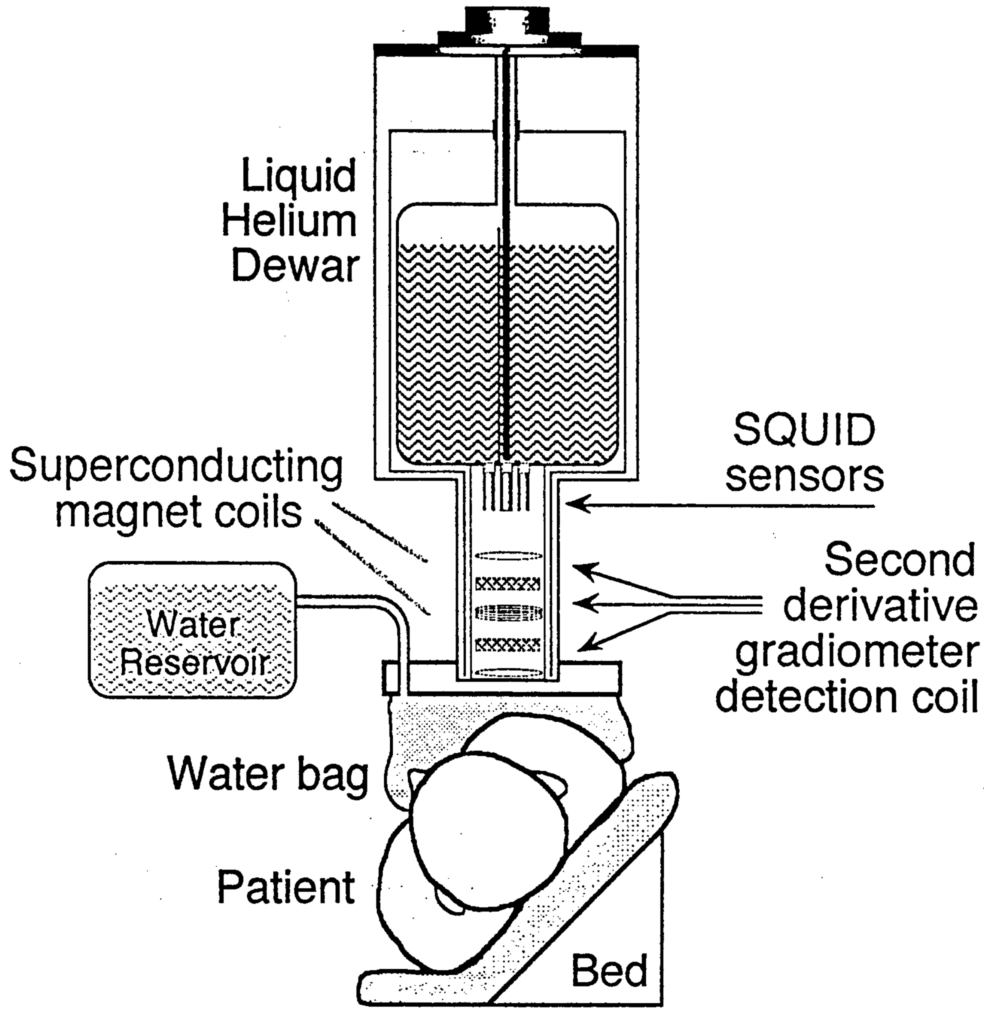


Tristan
Technologies

# Measurement Protocol

- Ultrasound Measurements
- Patient Positioned Beneath Detection Coils
- Patient Raised to Bottom of Dewar Tail - Water Bag Filled
- Patient Lowered - Water Bag Filling
- SQUID Electronics Yield Voltage Change
- Calculation of Hepatic Iron Concentration ($\chi$)
- Patient Report

Tristan Technologies

# Clinical Validation of Magnetic Measurement

G. M. Brittenham *et al*, "Magnetic-Susceptibility of Human Iron Stores", *New England Journal of Medicine* **307** 1671 (1982)

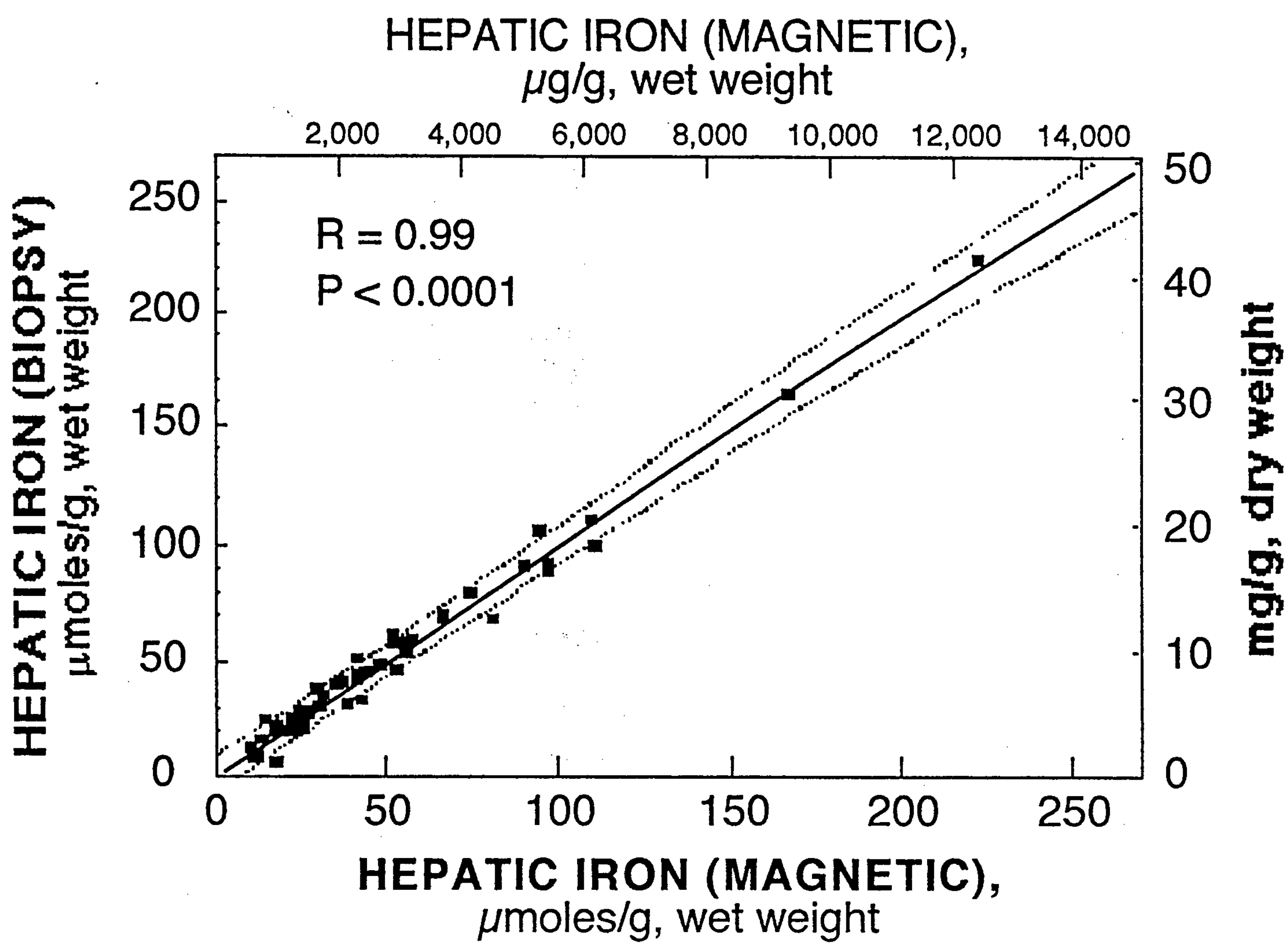


Comparison of hepatic iron concentration as determined by magnetic susceptometry and by chemical analysis of liver tissue obtained by clinically indicated biopsy. Magnetic and biochemical measurements were made within 1 month; patients with cirrhosis or with biopsy specimens less than 5 mg, wet weight, were excluded..

Tristan Technologies

# Conclusions

- The magnetic biopsy gives accurate assessment of iron stores
  - Direct measurement of iron
  - Repeatability better than 5%
- Non-invasive!
  - Allows serial measurements
  - Allows pediatric measurements
- Rapid Results
  - Measurement time (including ultrasound) < 30 minutes
- Proven Technique
  - >2,100 Patients measured
- Commercially available

Tristan Technologies

# Issues That Must Be Solved For Any Biomagnetic Measurement System to Gain Market Acceptance

- Must be a *Clinically* Accepted Method (efficacy)
- Must offer *significant* improvement over conventional methods or,
- Must offer new information not achievable by conventional methods
- Must be cost effective
  - either address a large patient population
    - Cost not the sole decision driver
  - or, if addressing an orphan disease
    - Cost becomes significant
- Must be “easy” to use
  - staffing requirements can significantly effect acceptability
  - need to minimize visibility of cryogens
- Third Party Reimbursement important
  - see above

Tristan Technologies

# Commercialization of SQUIDs

- The Basic Instrument
- Applications
- Product Costs
- Market Sizes
- History
- Commercial Companies
- Obstacles
- Conclusions

Robert L Fagaly
Tristan Technologies,
San Diego, USA

Tristan Technologies

# Why SQUIDs?

- It is the **most** sensitive amplifier known
- True dc response
- GHz bandwidth
- Zero phase distortion
- Noise levels below $10^{-31}$ J/Hz
- High dynamic range: >180 dB
- Excellent linearity:1:$10^{7}$
- Physically compact

Tristan Technologies

# The Basic Instrument

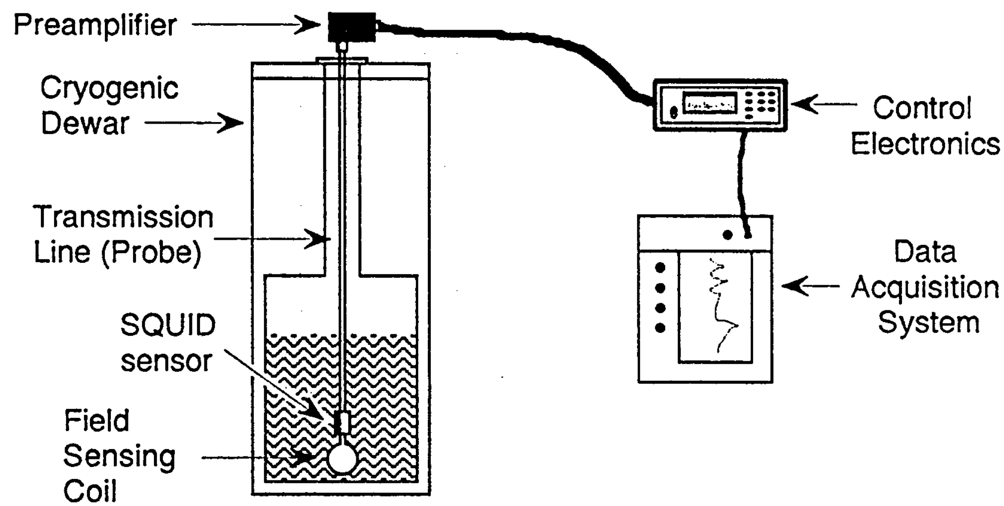


Tristan Technologies

# What Can I Do With It?

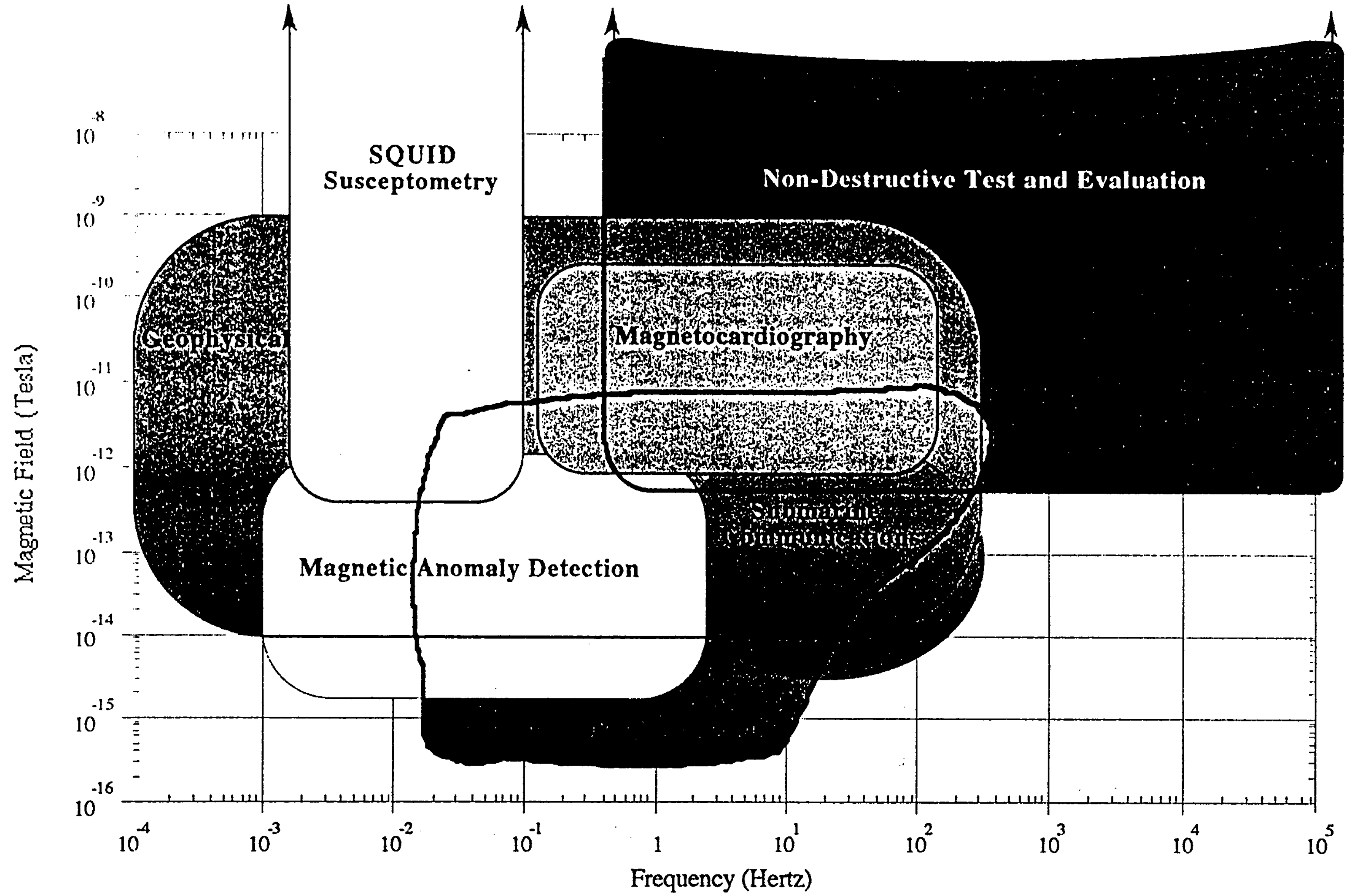


Tristan Technologies

# HTS DC-SQUID flip-chip magnetometers

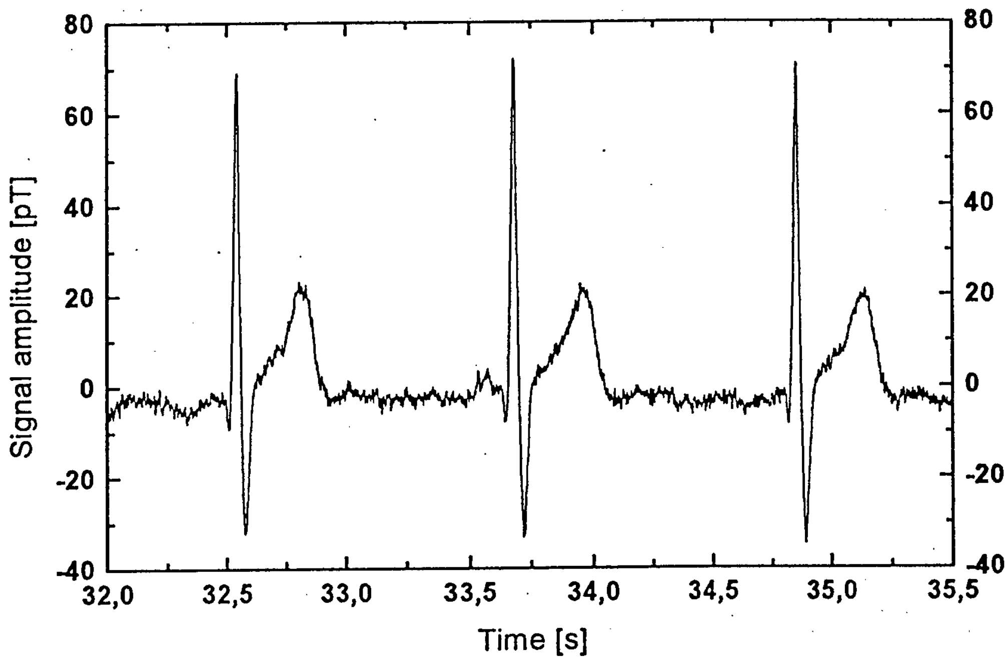


An example of a real-time MCG-measurement with the flip-chip magnetometer.

Forschungszentrum Jülich

Dr.M.I.Faley
IMF-IFF

# Sensor head for a DC-SQUID microscope

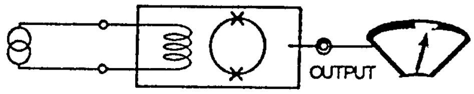


ac and dc Current

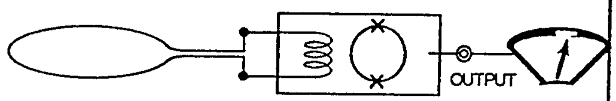


Magnetic Field

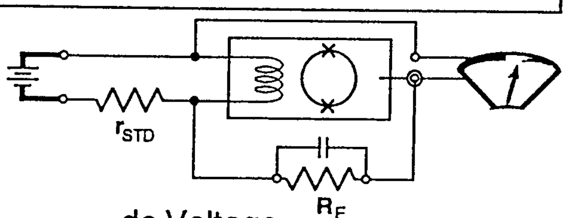


dc Voltage

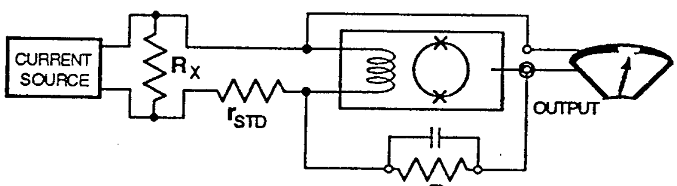


dc Resistance

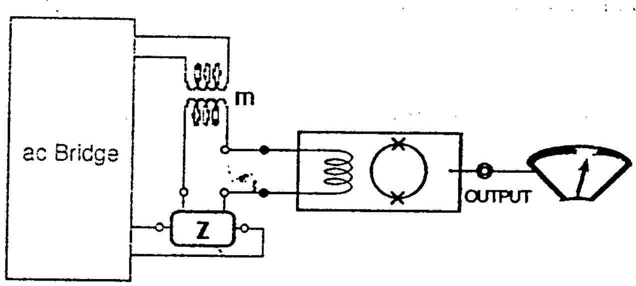


ac Resistance/Inductance Bridge

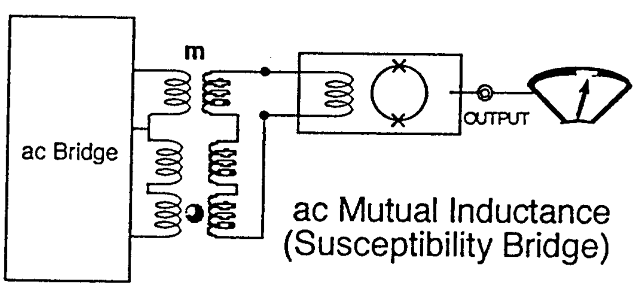


ac Mutual Inductance
(Susceptibility Bridge)

# Applications

## • Laboratory

| | |
|---|---|
| Ammeter: | $10^{-12}$ ampere/√Hz |
| Voltmeter: | $10^{-14}$ volt |
| Ohmmeter: | $10^{-12}$ Ω |
| Mutual/Self Inductance: | $10^{-12}$ henry |
| **Magnetic Susceptibility**: | $10^{-10}$ emu & single electron spins |
| Magnetic Fields: | $10^{-15}$ tesla/√Hz |

Nuclear Magnetic Resonance

## • Geophysical

Oil Exploration
Airborne Exploration Systems
Oceanographic Measurements

## • Biomedical

Studies of the Brain—**Neuromagnetism**
Studies of the Heart—MagnetoCardiography
Liver, Lung, Intestines, other biological activity

## • NDE

Defect Detection in Ferrous and Non-Ferrous Metals
Insulating Material Analysis
Infrastructure (Bridges, Runways, Buildings)
Aerospace
**Magnetic Microscopy**

## • Military

Mine Detection and Unexploded Ordinance (UXO)
Submarine Communication and Detection

## • non-SQUID Electronics *(but interesting)*

Digital switching
Cellular filters
NMR and MRI receiver coils

*Tristan Technologies*

# Environmental Noise

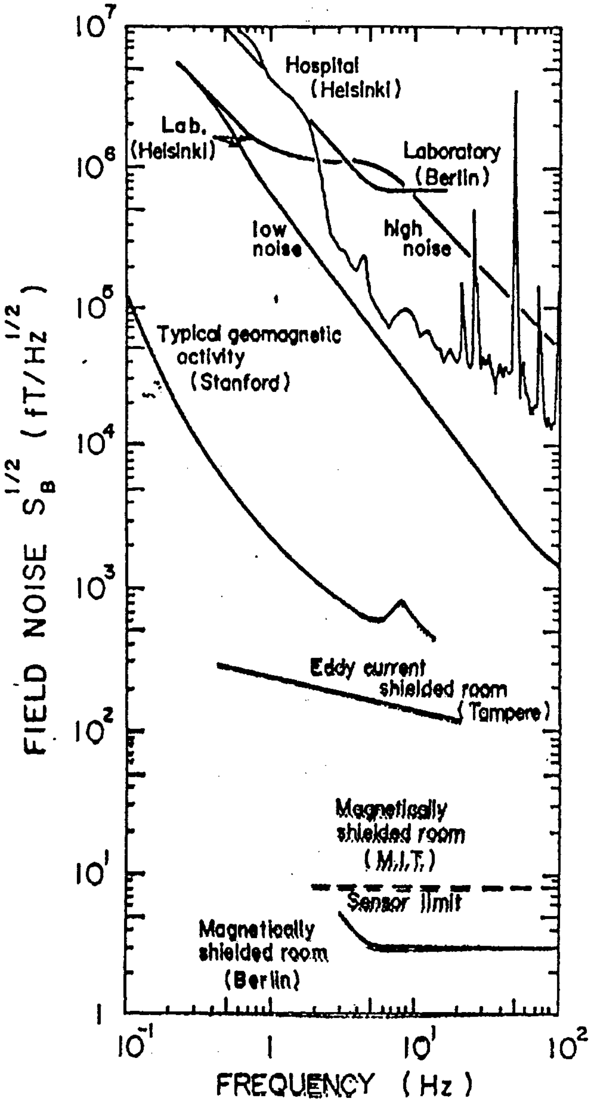


Tristan Technologies

# Impact of High Temperature Superconductivity

- 1986: Discovery of High Temperature Superconductivity
- Higher Operating Temperatures and Reduced Cooling Requirements
- Primarily Thin-Film Fabrication (not really HTS, but parallel development)
- **Positives**
  - Simplified cryogenics
    ratio of latent heats/unit volume
    ($LN_2$/LHe) $\approx 50$
    single-stage closed cycle cooling possible
  - Reduced size and operating costs
- **Negatives**
  - Noise power power proportional to temperature
    but at acceptable levels: $10^{-30}$ J/$\sqrt{\text{Hz}}$
  - Planar devices suitable only for:
    Magnetometers: $B_x$
    planar gradiometers: $\frac{\partial B_z}{\partial x}$
  - Need $< 10^{-12}\ \Omega$ joint resistances for dc response
    Problem of interconnects for 3D structures $\frac{\partial B_z}{\partial z}$

Tristan Technologies

Forschungszentrum Jülich

Dr.M.I.Faley
IMF-IFF

# HTS DC-SQUID flip-chip magnetometers

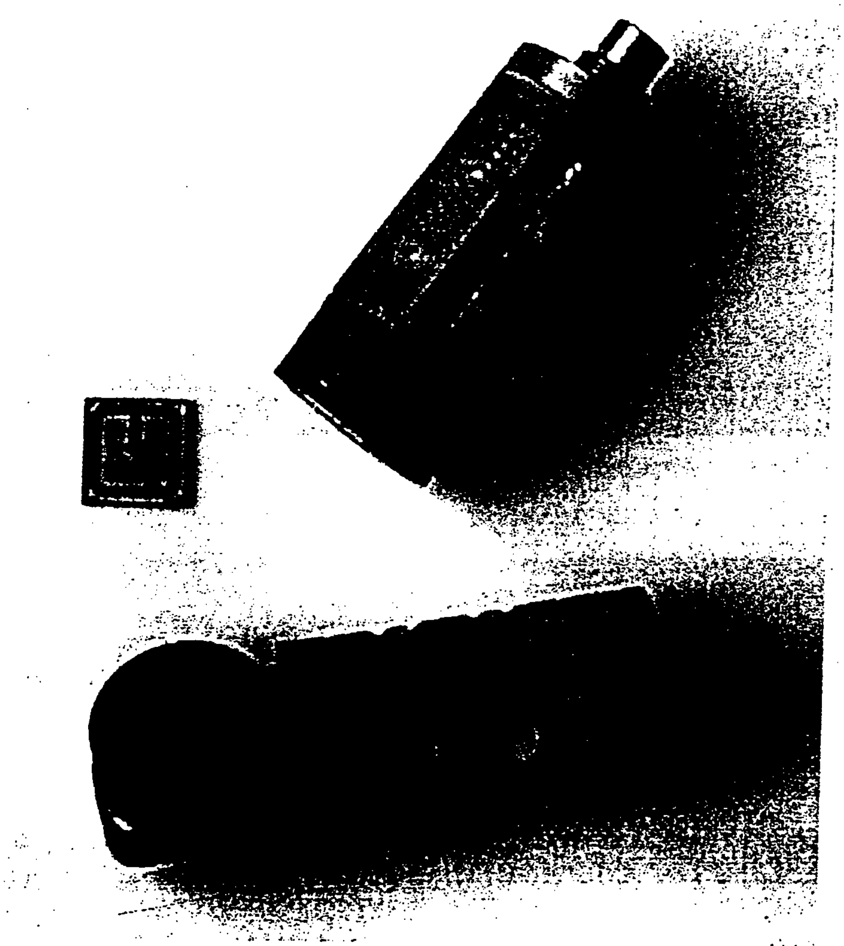

Multilayer flux transformer on 10 mm x 10 mm $SrTiO_3$ substrate and encapsulated dc-SQUID magnetometers. The magnetometers are fixed on standard dc-SQUID packages (axial and 90°) designed for operation together with iMAG electronics.

Dr.M.I.Faley
IMF-IFF

# HTS DC-SQUID flip-chip magnetometers

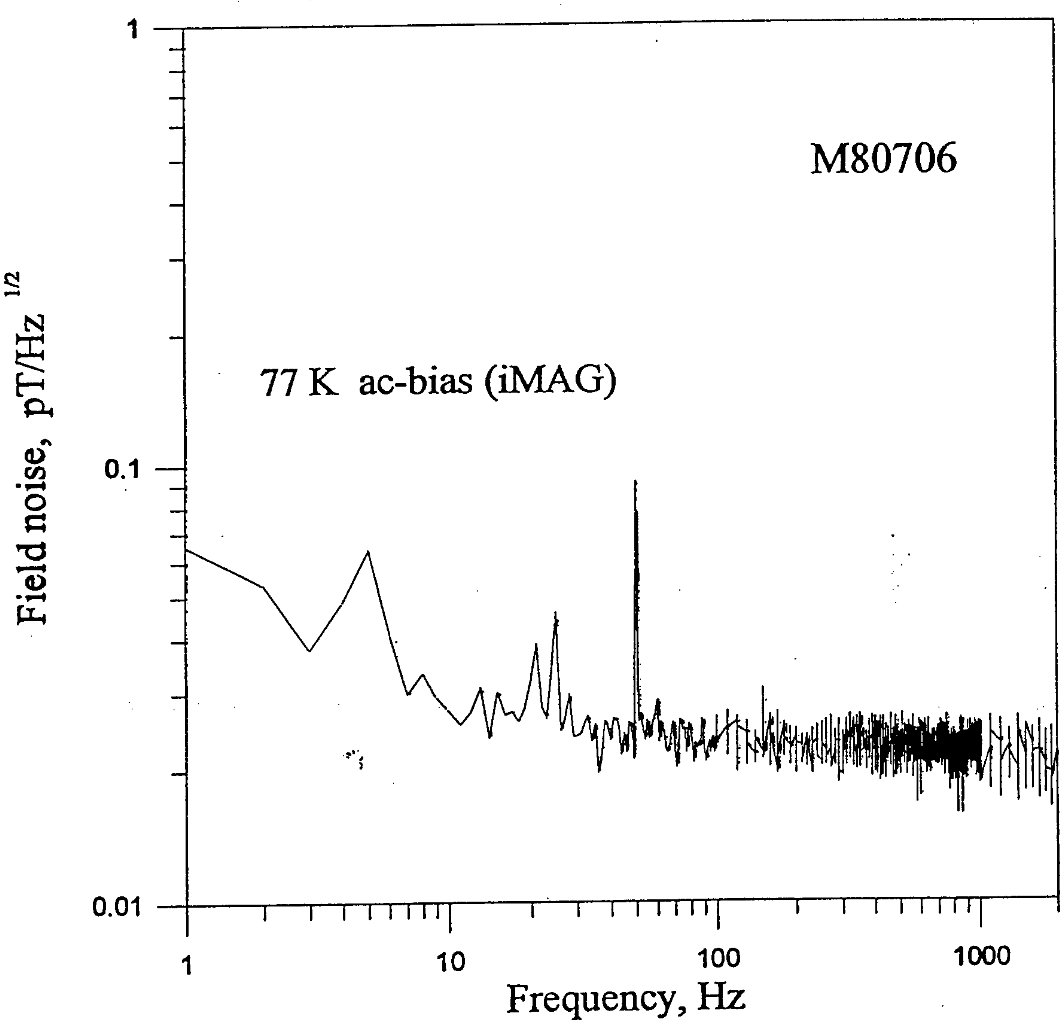


An example of a noise measurement with the flip-chip magnetometer, having a 8 mm x 8 mm pick-up loop of the flux transformer, measured inside a four layers μ-metal shield.

# Product Costs

- Laboratory
  - Basic measurement system $10,000
  - SQUID susceptometer $150,000
- Geophysical
  - 3-axis HTS magnetometer $40,000
  - Rock magnetometer $150,000
- Biomedical
  - 150 channel neuromagnetometer $2,000,000
  - Single channel biomagnetometer $50,000
  - Liver-Iron biosusceptometer $750,000
  - Custom biomagnetometer $100,000 - 300,000
- NDE
  - Basic measurement system $20,000
  - Magnetic microscope $380,000
  - Custom NDE system $50,000 - 500,000

Tristan Technologies

# Market Sizes

1989

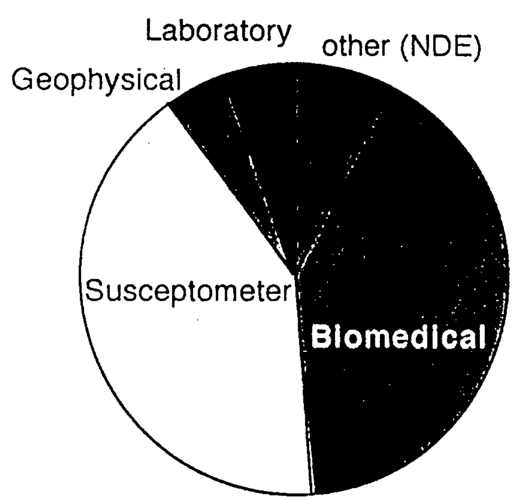


**25 M$**

1998

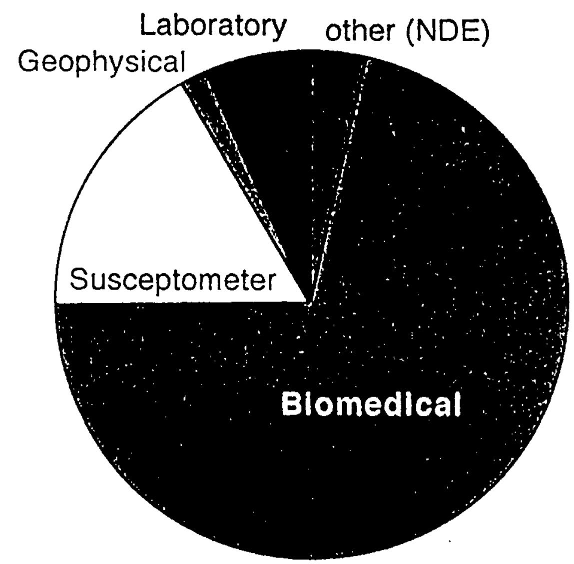


**30 M$**

- SQUID susceptometer market saturated
- 1999 Biomagnetism market increasing
  60+ whole head systems installed
  as many as 10 more in 1999
- SQUID NDE (primarily Microscopy)
  could be 10 M$ in 2000

Tristan Technologies

# TimeLine

| | |
|---|---|
| 1962 | Josephson Junction |
| 1964 | 1st SQUID |
| 1970 | 1st Commercial rf SQUID |
| 1974 | Toroidal rf SQUID (ruggedized) |
| 1980 | Hybrid (thin film) rf SQUID |
| 1982 | 1st Commercial dc SQUID |
| 1984 | Biomagnetism emerges |
| 1986 | High Temperature Superconductivity |
| 1993 | Mr. SQUID (1st Commercial HTS device) |
| 1994 | 1st Commercial HTS SQUID |

Tristan Technologies

# Commercial SQUID Companies

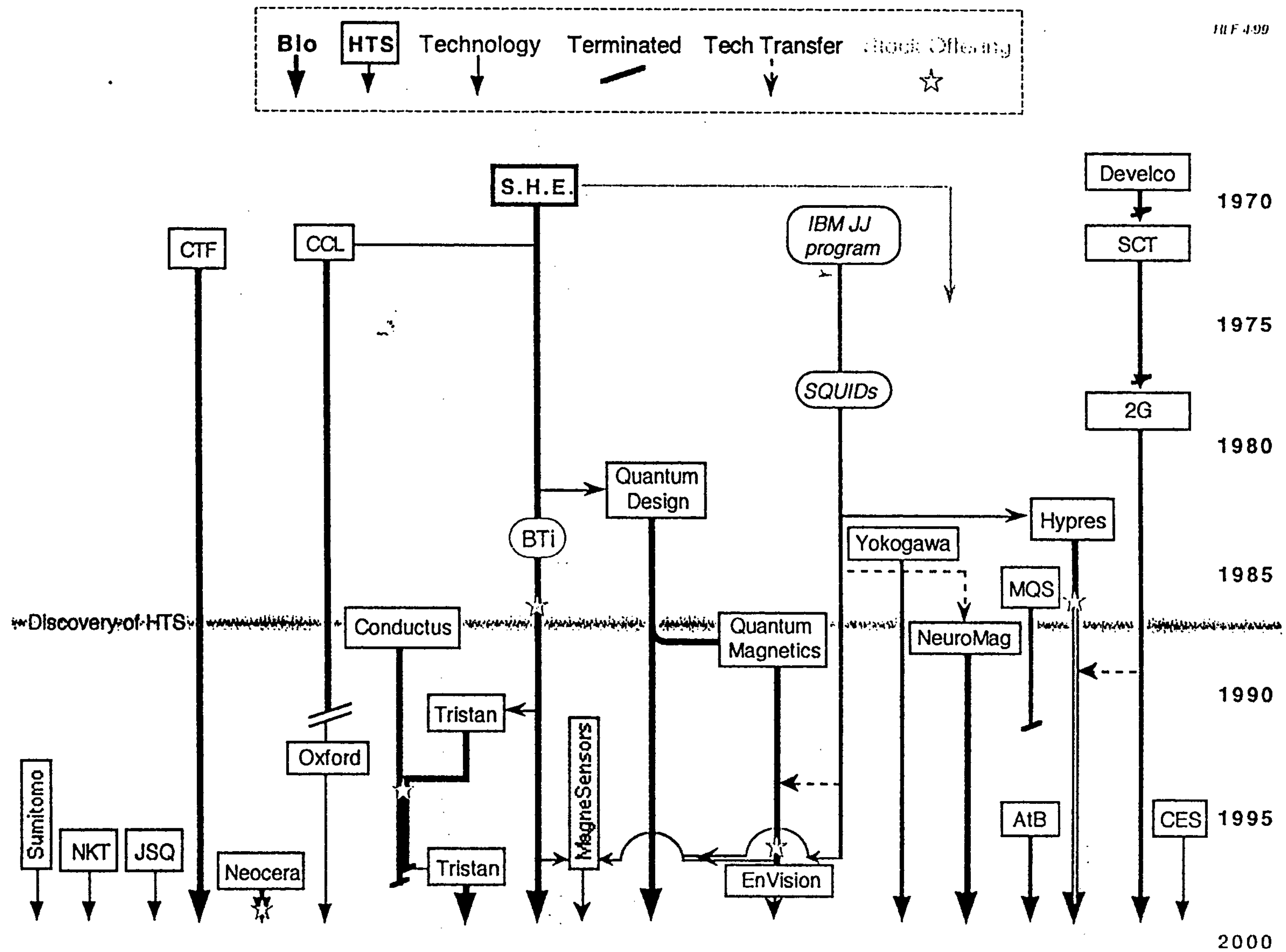


Tristan Technologies

# Corporate Types

- Type I
  - Large
    - > $100,000,000
    - > 500 employees
  - Diversified Technologies
    - multiple manufacturing sites
  - Profitable
  - *IGC, Oxford*
- Type II
  - Moderate size
    - ~ $10,000,000
    - < 100 employees
  - Single underlying technology products
    - single manufacturing site
  - Profitable
  - Quantum Design, Neuromag
- Type III
  - Products centered around single technology
  - Venture Capital/IPO Funded
    - Funding based upon market prospects > $100,000,000
    - Rapid growth after funding
    - > 100 employees
    - $5,000,000 - 10,000,000 annual expenditures
  - Retrenchment Phase
    - Market **Non-Acceptance** of Product
    - < 50 employees
    - more realistic market approach *(hopefully)*
    - BTi, Conductus, Hypres

Tristan Technologies

# Obstacles

- **Perceived**
  - Need for cryogens
  - Environmental noise
    - Need for shielding or sophisticated noise rejection
  - Motion induced noise
    - SQUIDs are vector devices
  - Cost
- **Applications**
  - Science establishes capability
  - Users establish need
- **Market Resistance**
  - Too often Technology Push, rather than Market Pull
- **Must Establish Need!**
  - Biomagnetism: Compelling Clinical Requirement
  - Industrial: Capability that saves user many M$

Tristan Technologies

# Conclusions

need to state influence of outside capital
what does it take to become a type I?
Product saturation vs. expanding markets

- SQUIDS offer *Significant* Technical Advantages
- There are Product Applications
- Only a "killer" Application gets you to Type I
- If the Market is Small, a Type II Company is appropriate

Tristan Technologies

# SQUIDs for Geomagnetic Exploration

**A.I. Braginski**

*Institut für Schicht- und Ionentechnik (ISI)*
*Forschungszentrum Jülich GmbH (FZJ), D-52425 Jülich*
**(Retired)**

**Partial support: BMBF Project No. 13 N 6527**

# Acknowledgements

*Leading Project Collaborators:*
M. Bick, K.-D. Husemann, R. Otto, G. Panaitov, N. Wolters, Y. Zhang and E. Zimmermann

*Project Partners:*
GERMANY: IPHT-Jena, Metronix GmbH, Tech. Univ. Berlin; CHINA: IGGE, Univ. of Peking

*Unpublished Data:*
Courtesy of C. Foley et al. CSIRO, Australia

# Outline

- Introduction
- Electromagnetic Methods of Geophysical Exploration
- Areas of Possible SQUID Applications in Geomagnetism
- Performance Requirements for SQUID Magnetometers
- History of LTS SQUID Uses in Geophysics
- Status of HTS SQUID Developments, rf and dc Magnetometers
- HTS SQUID Field Data
- Conclusions & Outlook

Forschungszentrum Jülich

# Principle of EM Methods in Geophysics

## target parameter: electrical ground conductivity

distinguish geological structures
by differences in conductivity

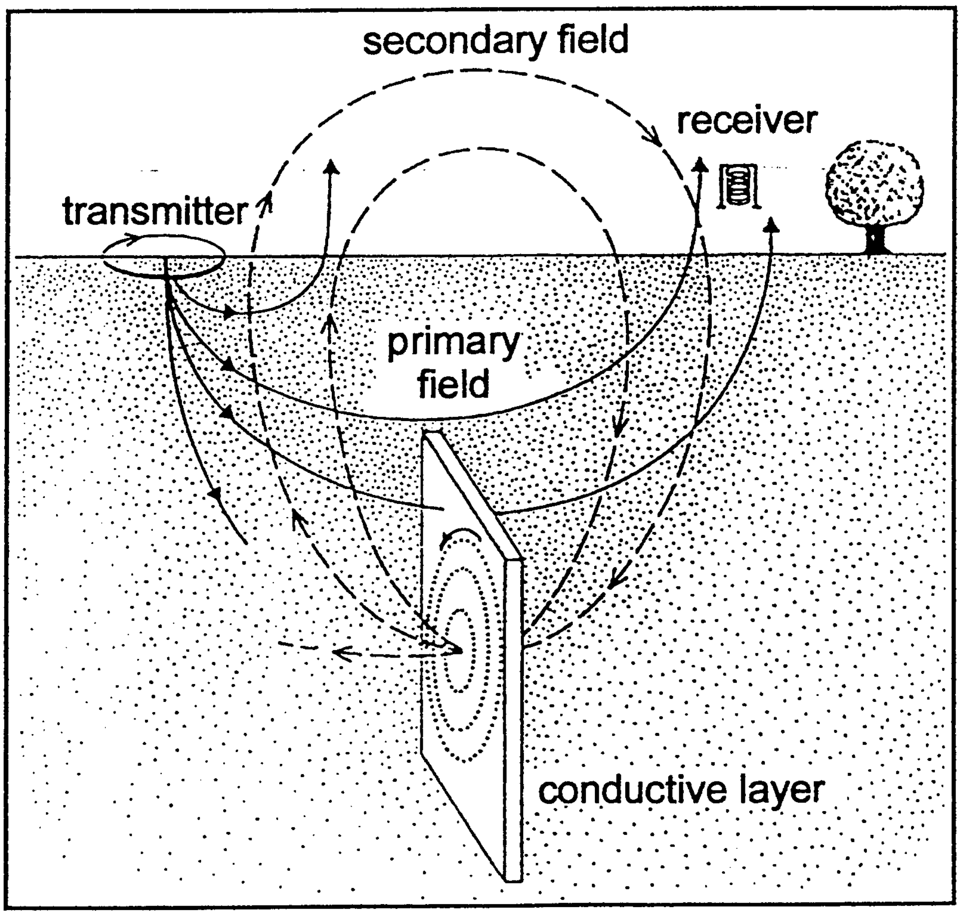


$$\text{skin depth} \quad z \sim \sqrt{\frac{1}{\sigma \cdot f}}$$

$\sigma$ = conductivity; f = frequency

GEOprincasc.cdr

# Electromagnetic Methods in Geophysics

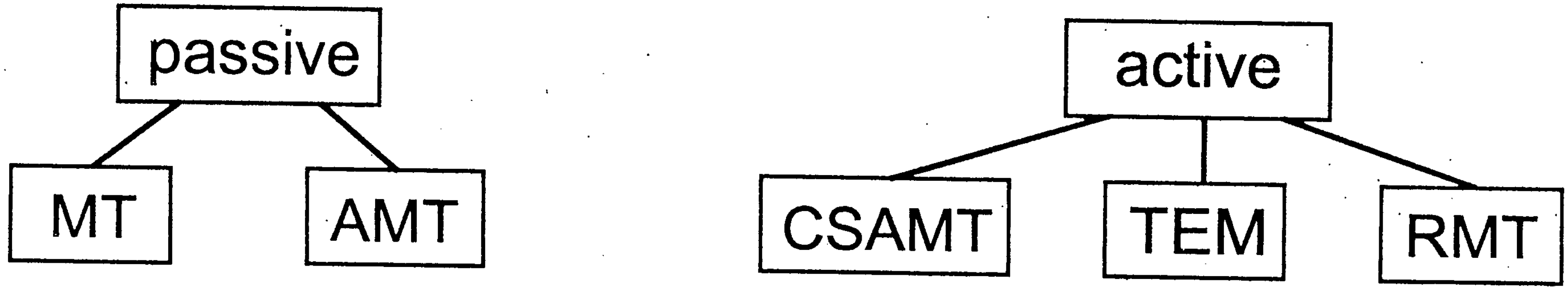


**claim:** - **one** sensor for **all** methods
- improved resolution for **great** depths

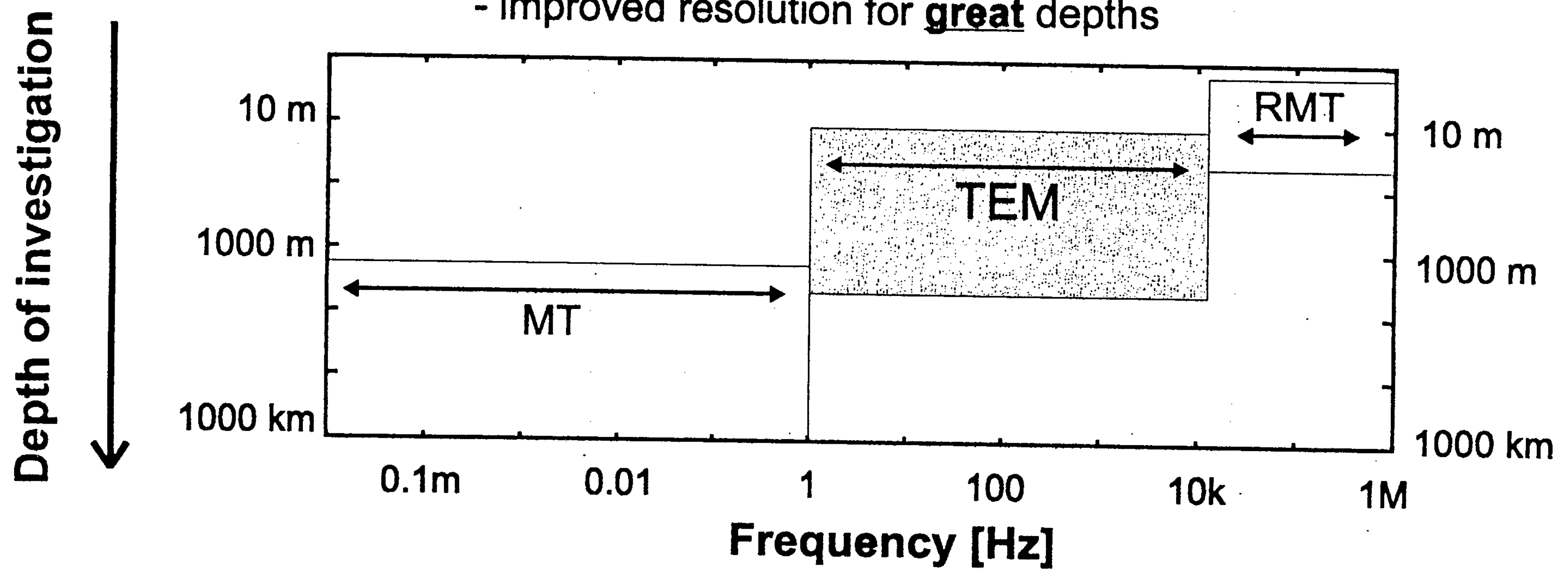

Forschungszentrum Jülich

# Application of Electromagnetic Methods for Geological Investigations

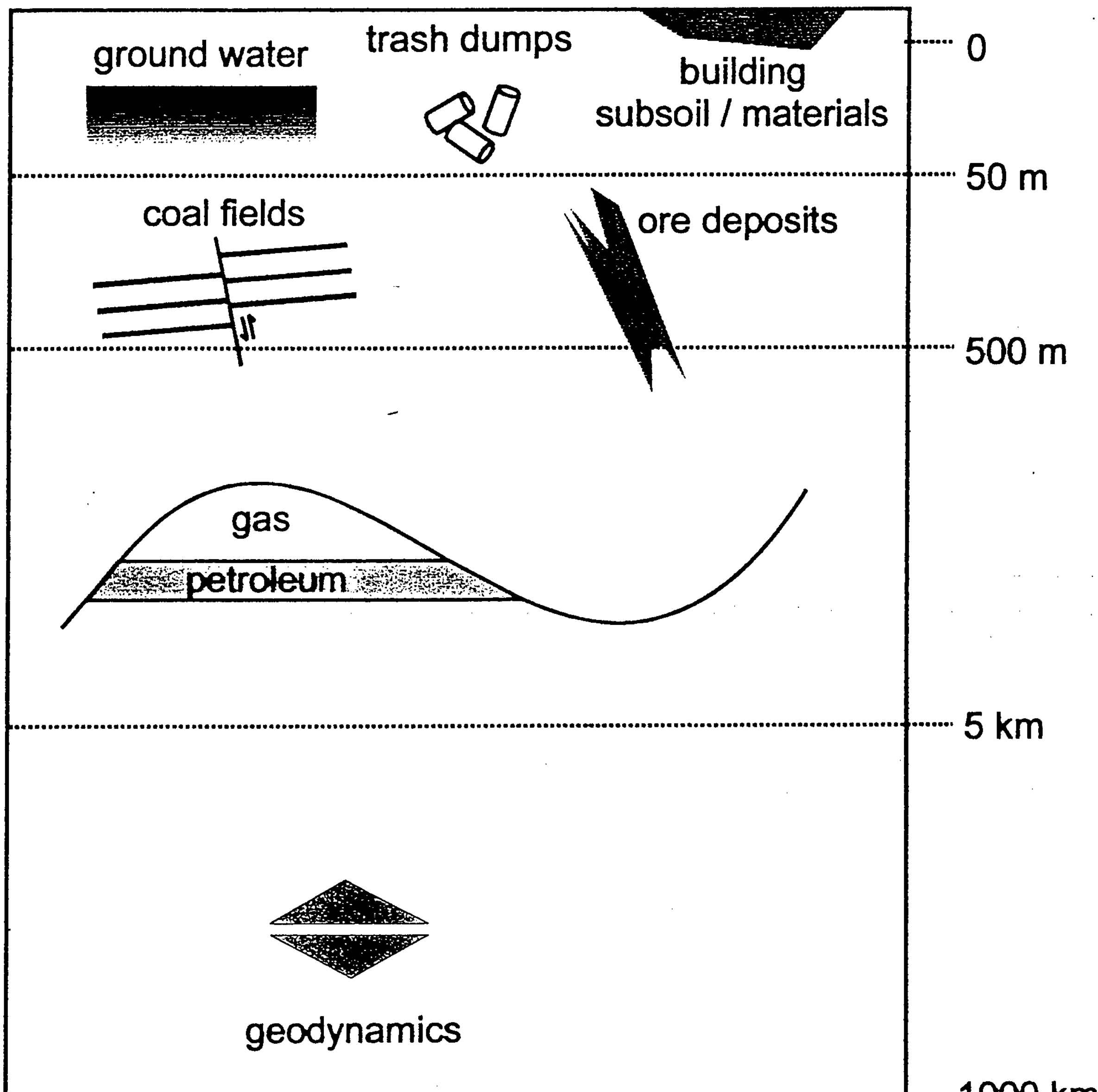


T. Radic, TU Berlin

GEOanwasc.cdr

# Electromagnetic Methods of Geophysical Sounding

*Time Domain:*

* Transient Electromagnetic Method (TEM)

* Long-Offset TEM (LOTEM)

*Frequency Domain:*

* Magnetotelluric (MT, AMT)

* Controlled-Source MT, AMT (CSMT, CSAMT)

* Very Low Radio Frequency Resistivity (VLF-R)

* Radiomagnetic Sounding (RMS)

# Magnetotellurics

- Natural or controlled source EM excitation, from $10^{-3}$ to > $10^{3}$ Hz
- Determine at earth surface:

$$Z_{xy}(\omega) = \mu_o \mu E_x(\omega)/B_y(\omega)$$

$$(\mu \approx 1)$$

- For a homogeneous earth:

$$\rho_{xy} = 1/\mu_o \mu \omega \,|\, Zxy(\omega) \,|^2$$

- For inhomogeneous subsoil one can use the apparent resistivity $\rho_a(\omega)$:

$$\rho_a \approx 0.2t\ [E_x/H_y]^2$$

where: $\rho_a$ [$\Omega$], t [sec], $E_x$ [mV/km], $H_y$[nT]

- Depth of penetration:

$$p \approx 1/2\pi(10\rho_a t)^{1/2}$$

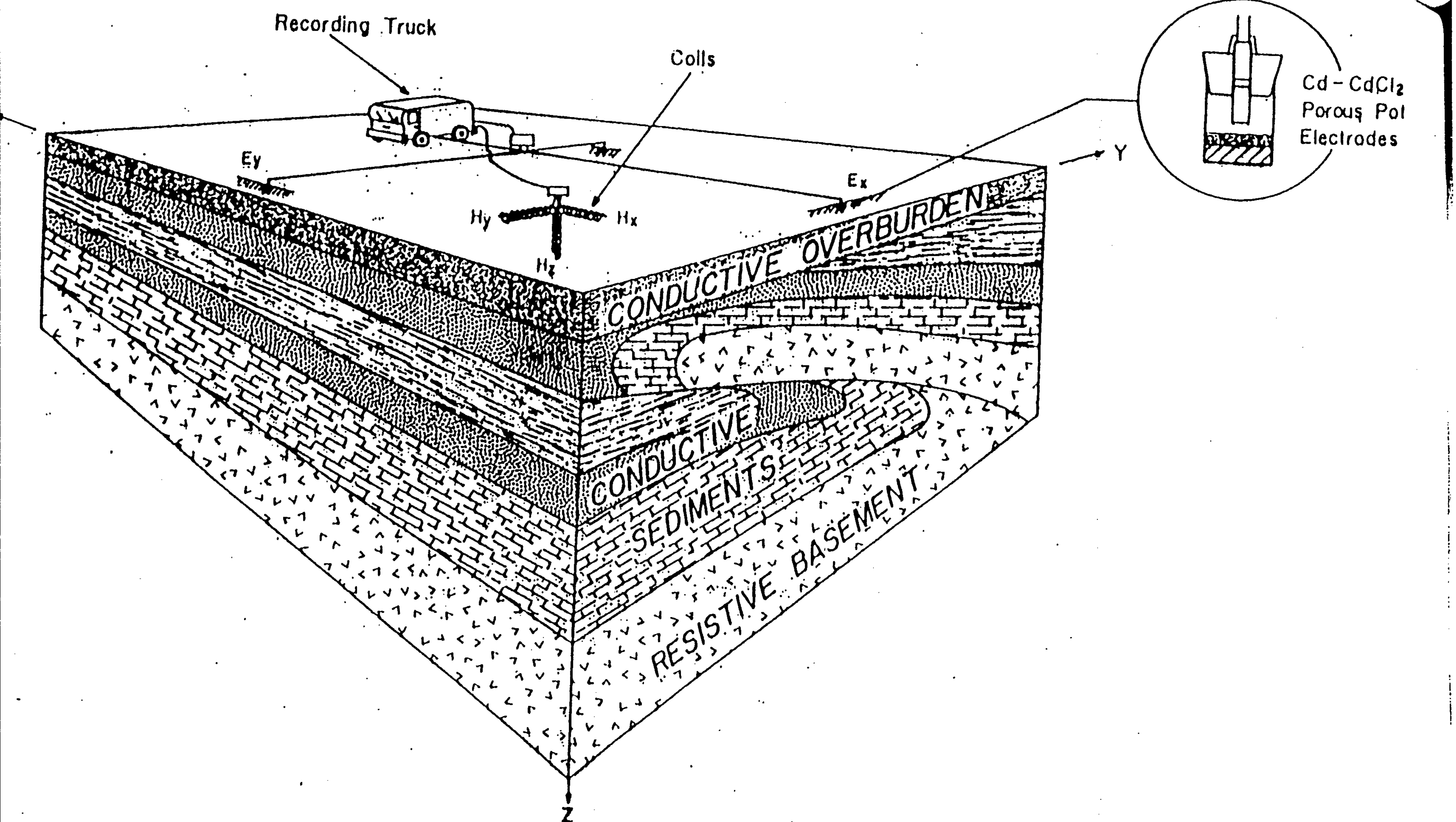

Recording Truck
Coils
Cd - CdCl2
Porous Pot
Electrodes
Ey
Ex
Hy
Hx
Hz
Y
Z
CONDUCTIVE OVERBURDEN
CONDUCTIVE
SEDIMENTS
RESISTIVE BASEMENT

# Principle of Transient Electromagnetics (TEM)

- transmitter generates magnetic field in the ground
- decay of secondary signal measured by SQUID
- improvement of SN-ratio by using bipolar transmitter signal

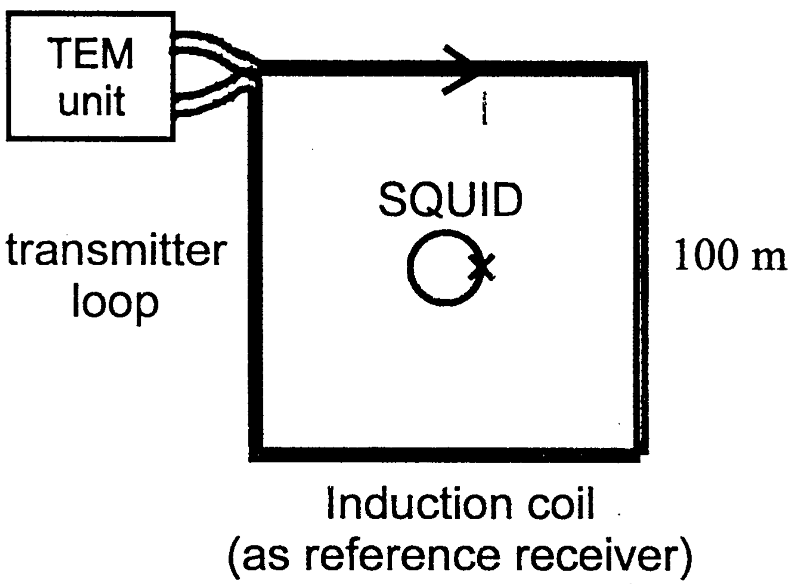


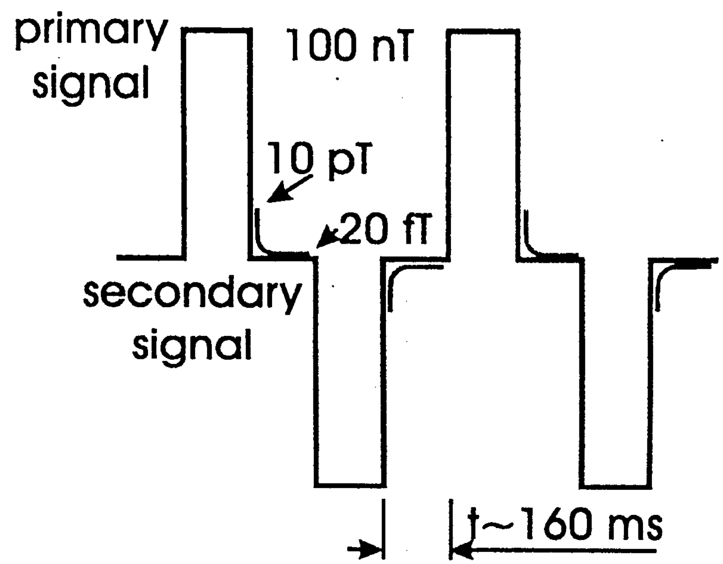


GEOtemprincasc.cdr

# Principle of Transient Electromagnetics (TEM) Measurements in Geophysics

decay of secondary field measured by rf SQUID

for homogeneous halfspace expected:

$$B \sim t^{-1.5}$$

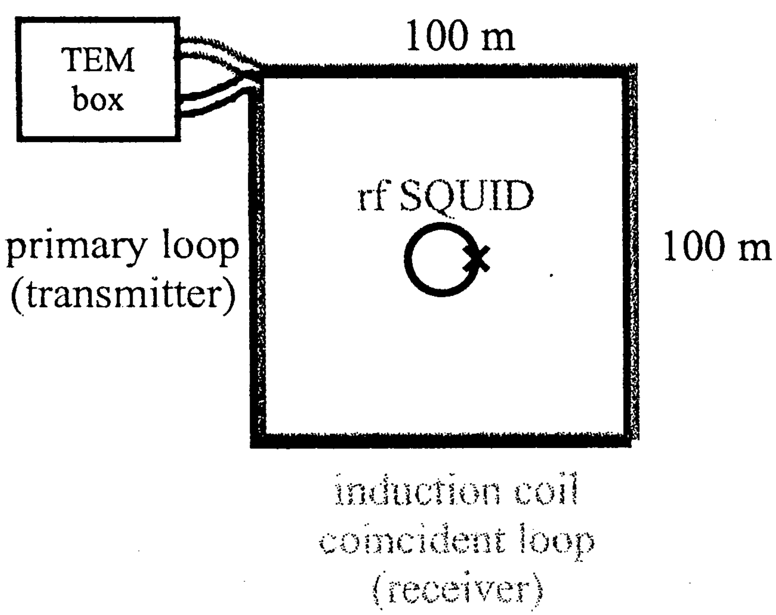


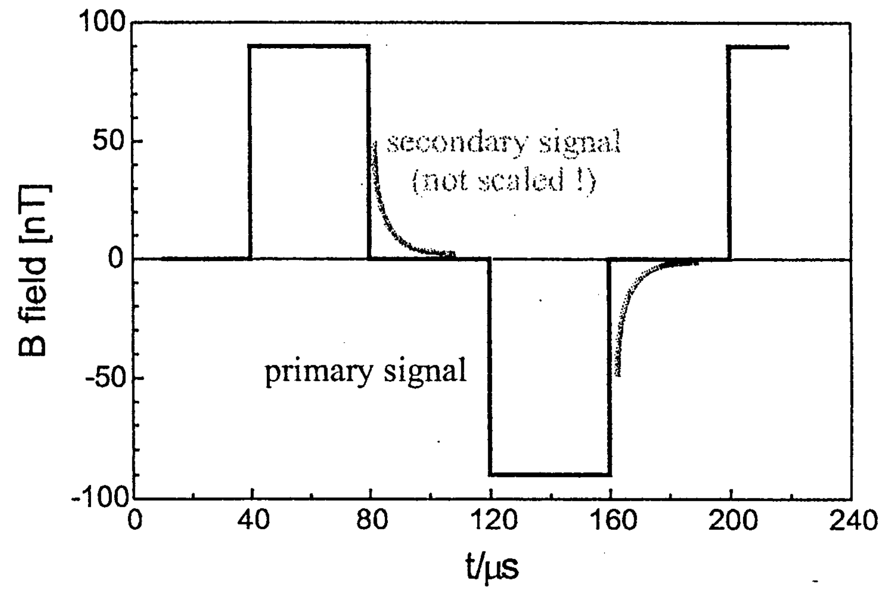

# Setup of TEM Field Trial

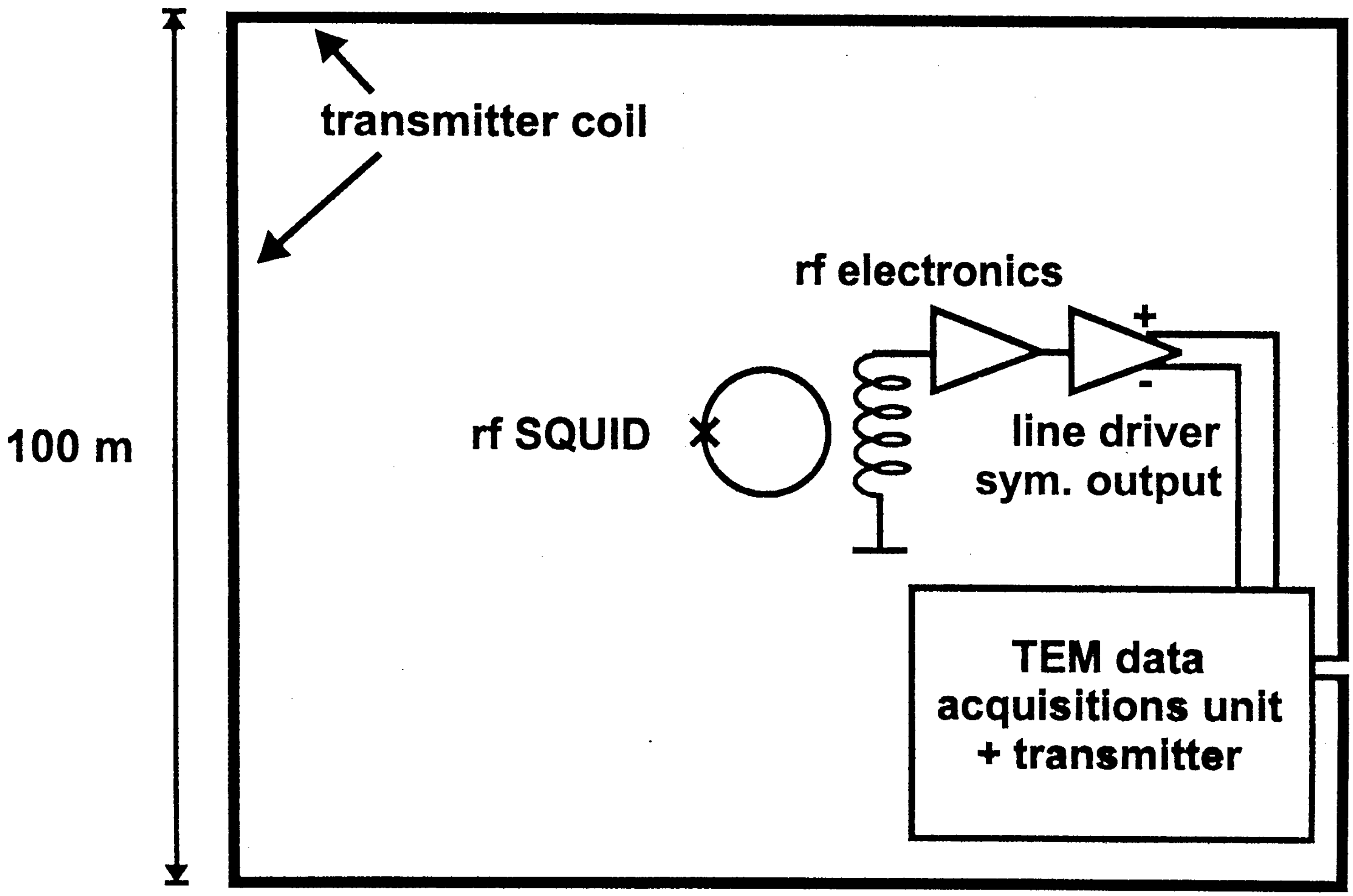

# Principle and Setup of LOTEM

- Investigation depths: several km
- Targets: oil and ore deposits

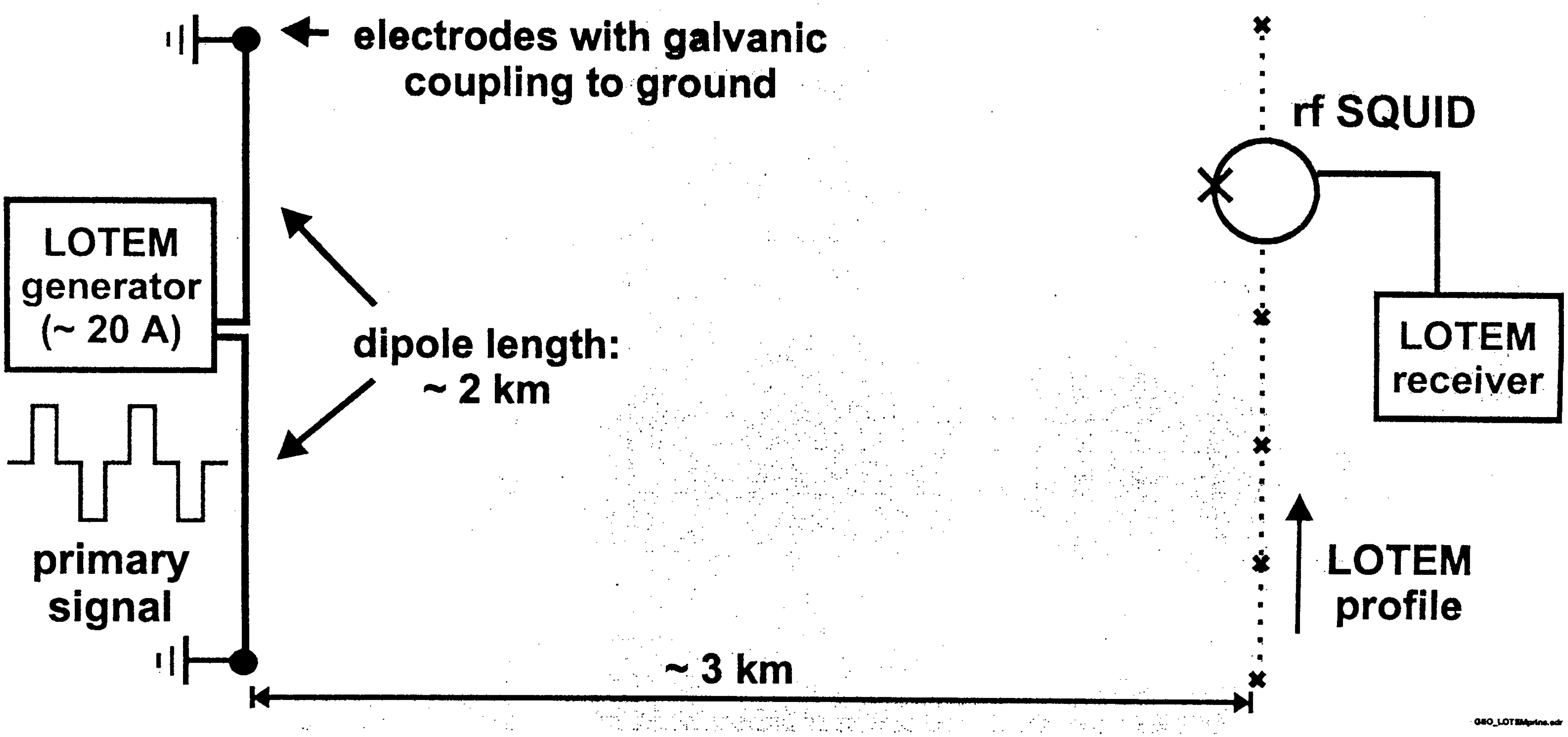

*The Bible:*

**Electromagnetic methods in Applied Geophysics – Applications, Parts A, B**

*Editor:*

**M.N. Nabighian**

*First Published in 1991 (last edition 1996) by:*

**Society of Exploration Physicists**
**P.O.Box 702740, Tulsa Oklahoma 74170-2740**

# Possible Applications of SQUID in Geomagnetism

- Paleomagnetism (Rock Sample Magnetometry)
- Prospecting/Surveying for Ore, Coal, etc. Deposits
- Prospecting for Oil Deposits
- Exploration for Geothermal Energy
- Small-Area Prospecting for Water, Buried Waste, Archeological Objects
- Volcanic Eruption and Earthquake Prediction
- Fluid Interface Detection

*Source:*

**SQUID Applications to Geophysics**

*Editors:*

**H. Weinstock & A.C. Overton**

*Published in 1981 by:*

**Society of Exploration Physicists**
**P.O.Box 702740, Tulsa Oklahoma 74170-2740**

# Advantages of HTS SQUIDs

## Size:

triple of induction coils
(e.g. product of Metronix)

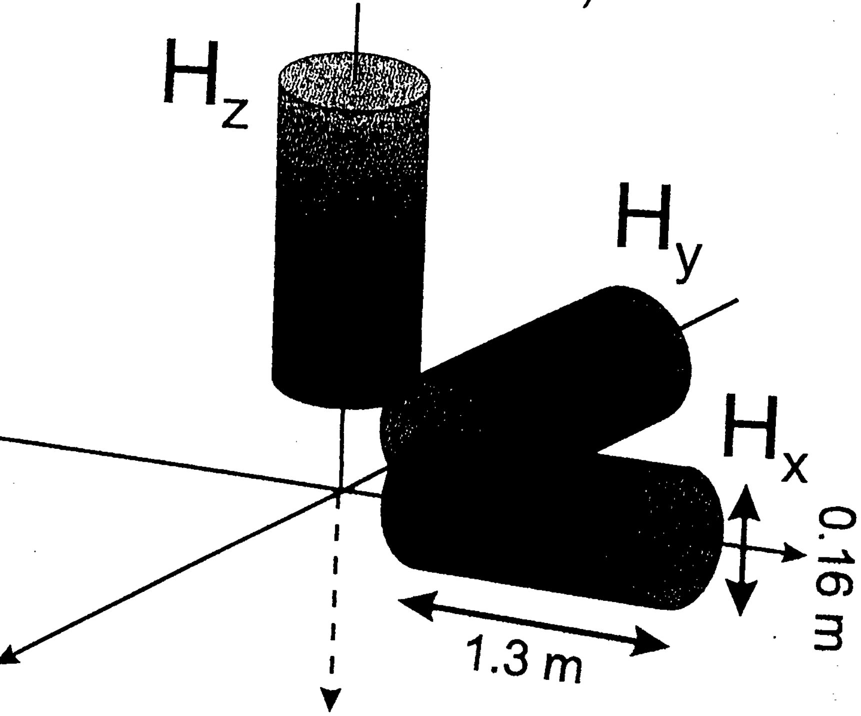


triple of
HTS SQUIDs

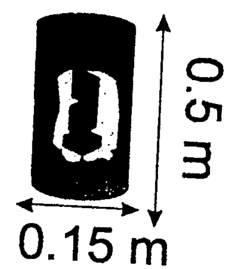


- compact, low weight:
  - easy handling
  - borehole potential
- broadband sensor (dc - 20 kHz / 10MHz)
- high sensitivity at low frequencies
- B-field sensor

## Requirements:

- field proven
- dyn. range > 120db
- slew rate > 1mT/sec

GEOsquvortasc.cdr

# TEM Method: Principle Advantage of SQUID

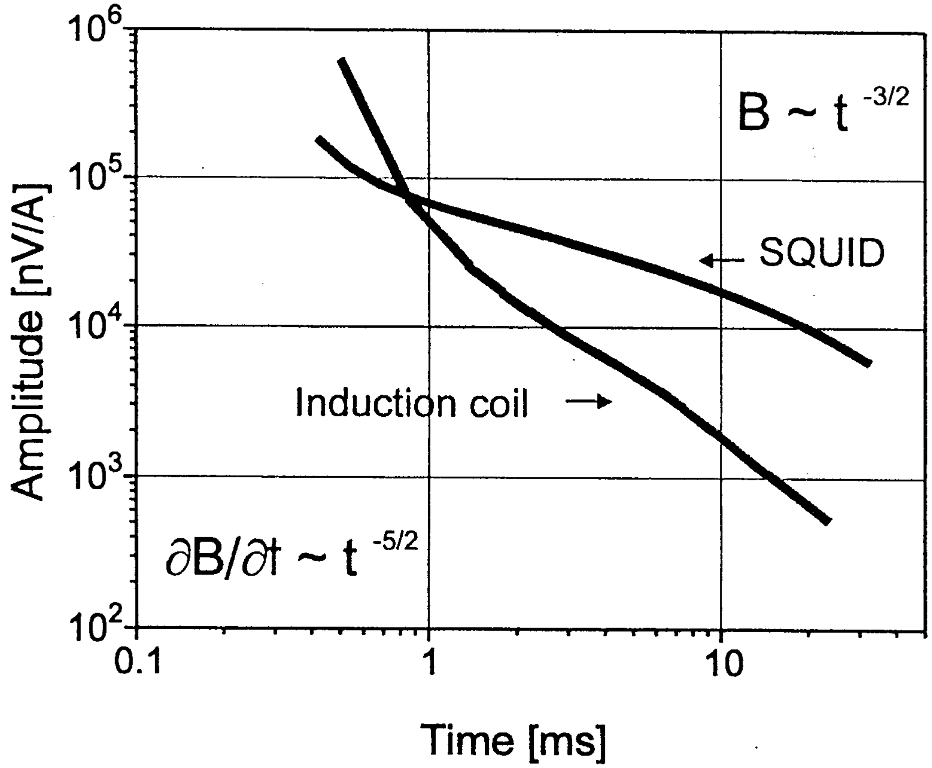


- **Disadvantage of coil:** $\partial B/\partial t$ receiver

  depth of investigation $z \propto \left(\frac{I \cdot A}{\sigma \cdot \eta_v}\right)^{1/5}$

- **Advantage of SQUID:** B-field sensor

  depth of investigation $z \propto \left(\frac{I \cdot A}{\eta_B}\right)^{1/3}$

[Spies, 1989]

GEOlemvortellasc.cdr

# Magnetic field noise for HTS rf SQUID and induction coil

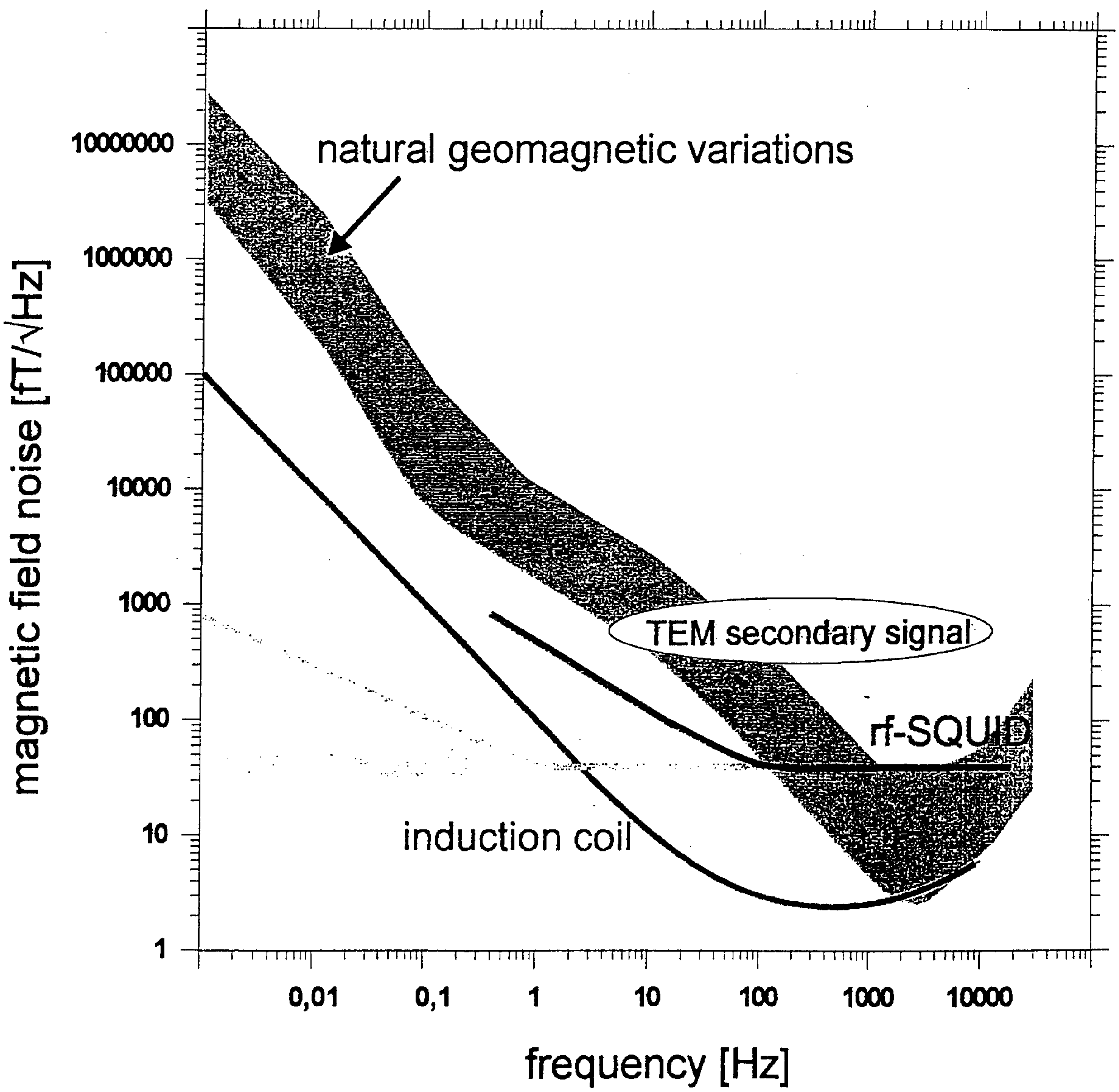

# Geomagnetic Exploration

## Objective:

**Improve portability, versatility, also attain mobility, beyond limitations of conventional induction coil equipment, but without sacrificing and possibly improving sensitivity of detection**

## EM Methods Investigated:

- **Transient EM (time domain)**
- **Controlled-source audio magnetotellurics (frequency domain)**
- **Radiometric detection of water & environmental waste**

# System Geometry

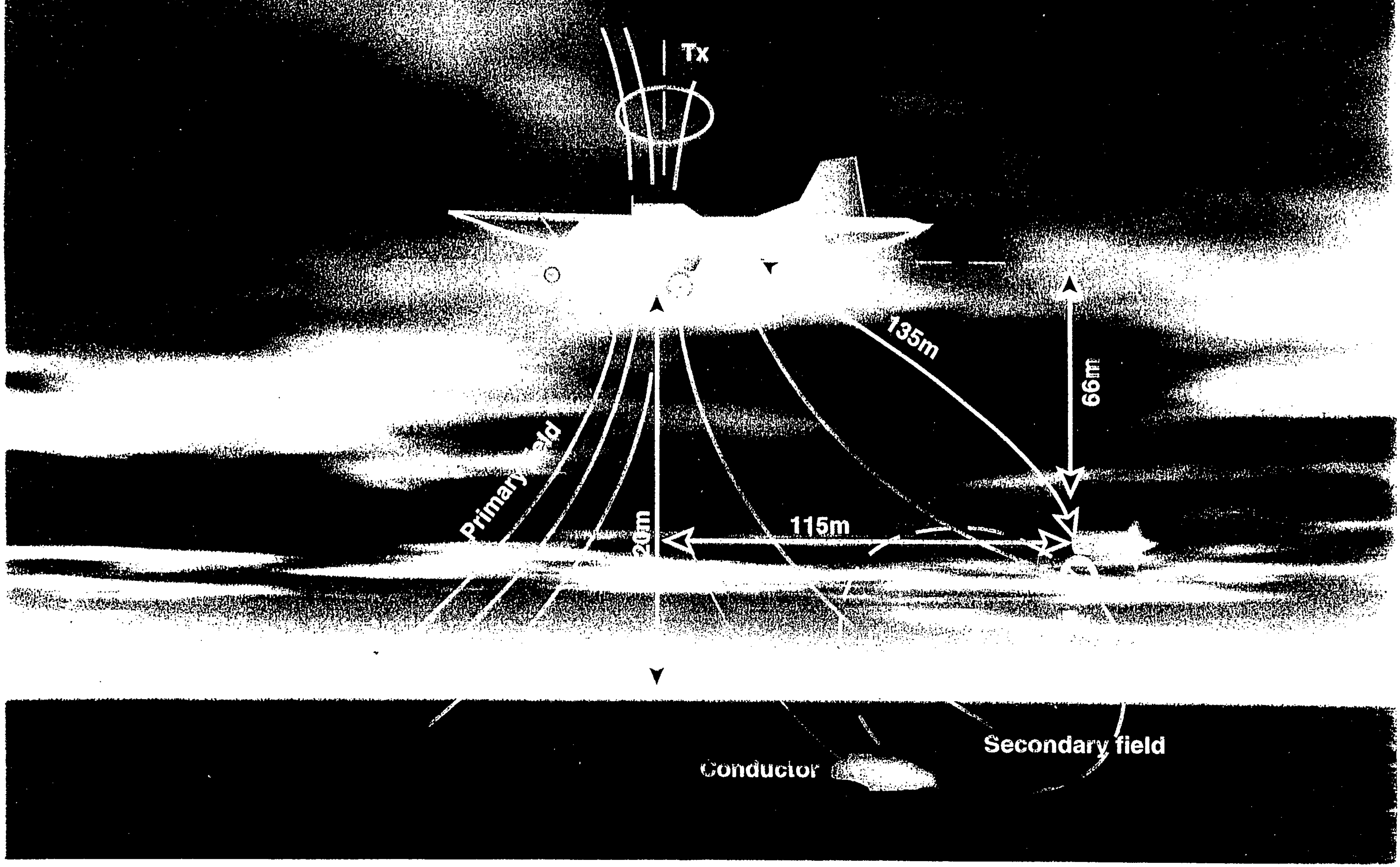

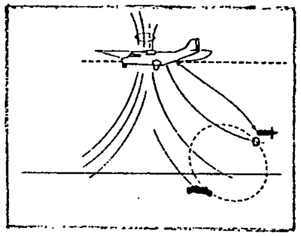

## AIR BORNE RESULTS
(Conductivity)

CSIRO

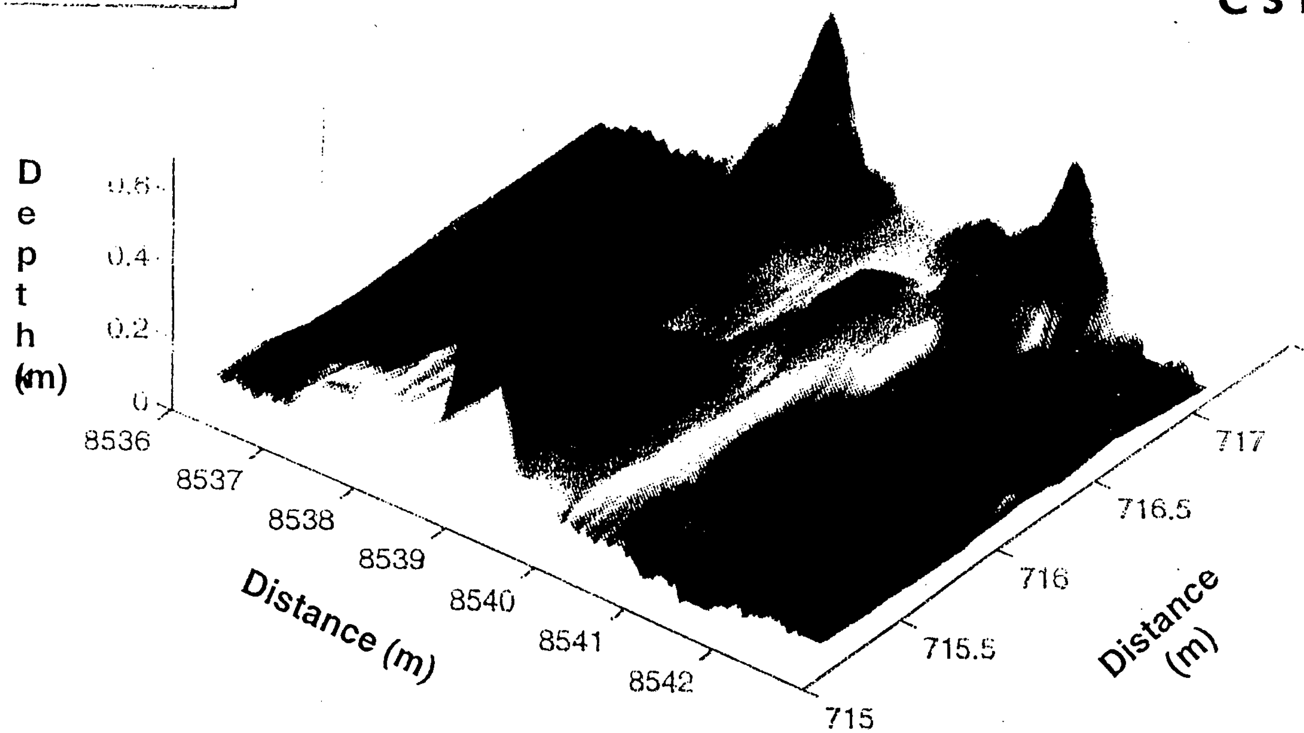

Project Supported by German Government (BMBF)

metronix

Technische Universität Berlin

IGGE

## SQUID Magnetometers for Geophysical Applications

IPHT JENA

Forschungszentrum Jülich

# Objectives:

Development of a compact, broadband vector magnetometer

Demonstration of geophysical exploration

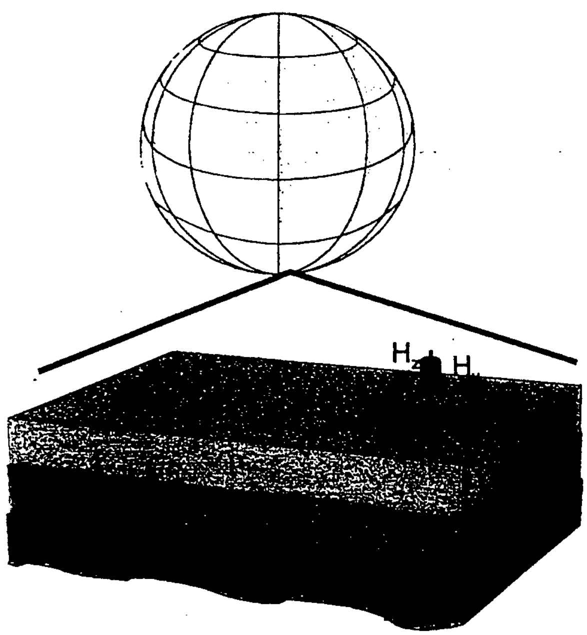

# Sensor Set-up of HTS rf SQUID Vector Magnetometer

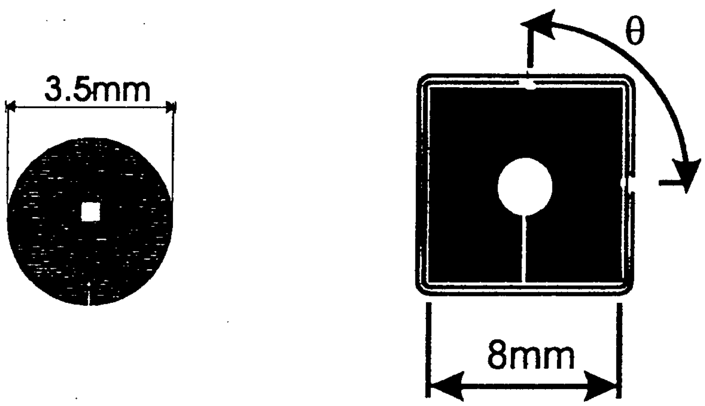


- **sensor:** rf washer SQUID and coplanar resonator in flip-chip configuration

**SQUID:**

| | |
|---|---|
| - YBCO washer: | ∅ = 3,5mm |
| - loop: | $100 \times 100\ \mu m^2$, $10 \times 500\ \mu m^2$ |
| - junction type: | step edge junction |
| - junction width: | $4\ \mu m$ |

**resonator:**

| | |
|---|---|
| - coplanar: | ∅ = 8mm on $1 cm^2$ substrate |
| - frequency: | 650 MHz – 1 GHz |
| - $\partial B/\partial\Phi$ = | $3{,}9\ nT/\Phi_0$ , $2{,}7\ nT/\Phi_0$ |

GEO3chnengeufbeec.cdr

# Sensor Module of HTS rf SQUID Vector Magnetometer [YBCO]

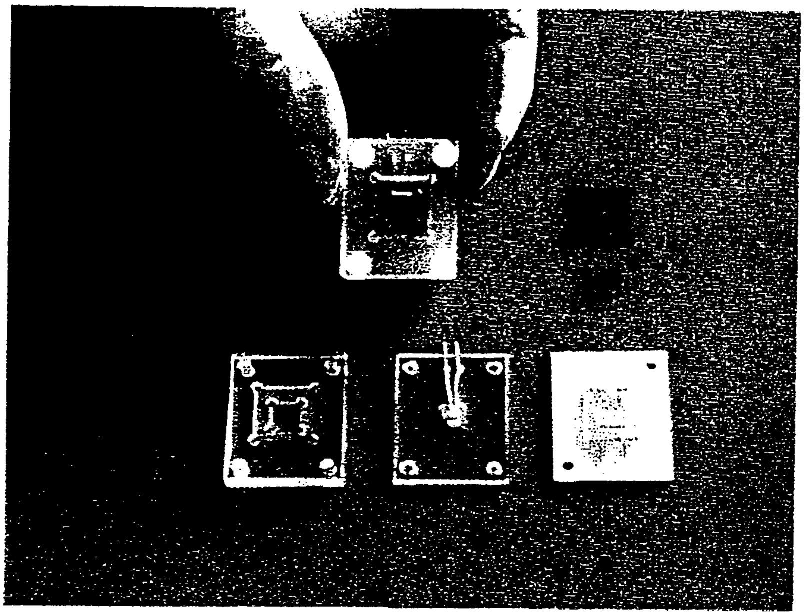

rf SQUID, coplanar resonator and planar coupling coil
integration of heater to eliminate trapped magnetic flux

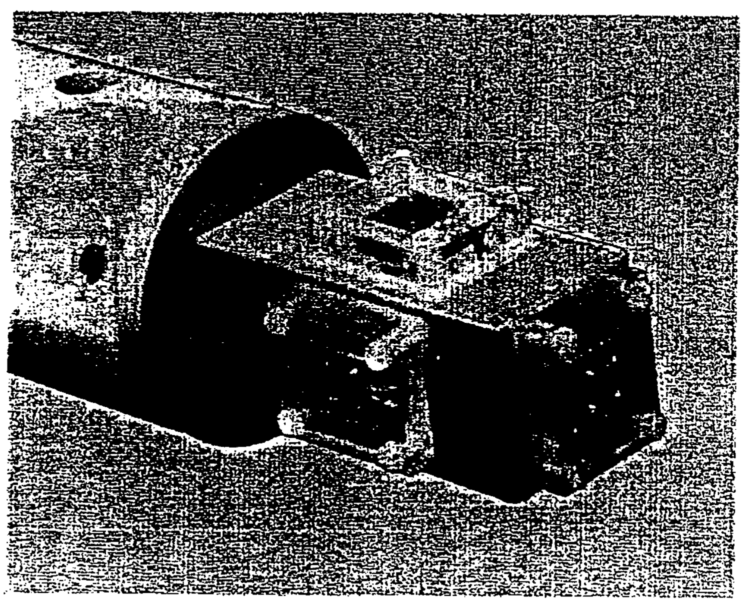

triaxial sensor head

# 3-axis HTS rf SQUID Vector Magnetometer

## Field Trial at Erbendorf, Oberpfalz

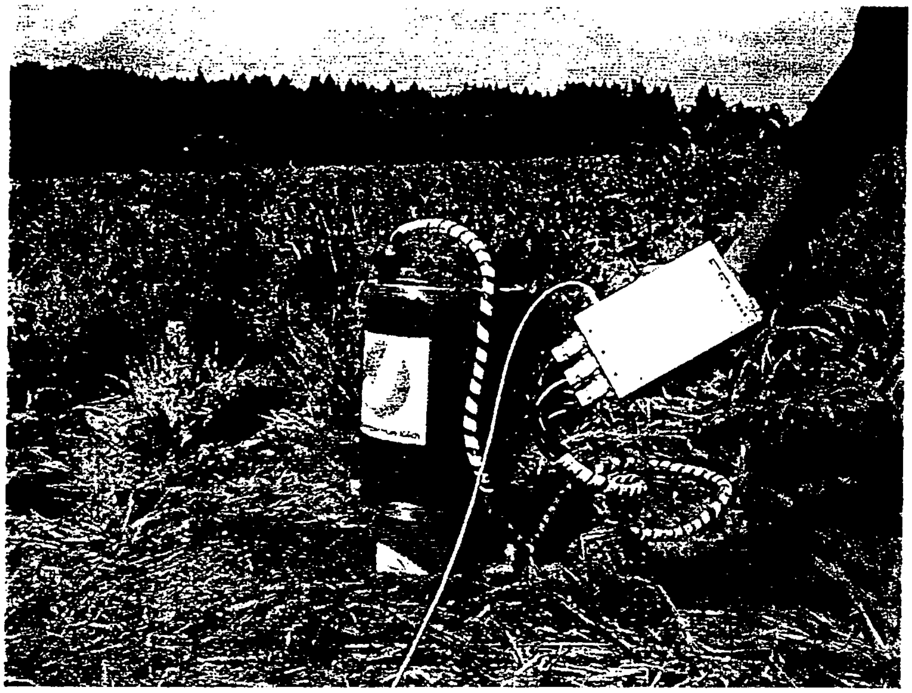

System includes heater and automatic adjustment of SQUID parameters; well shielded against rf noise

# TEM Survey with SQUID System

Cloncurry, Australia, October 1998

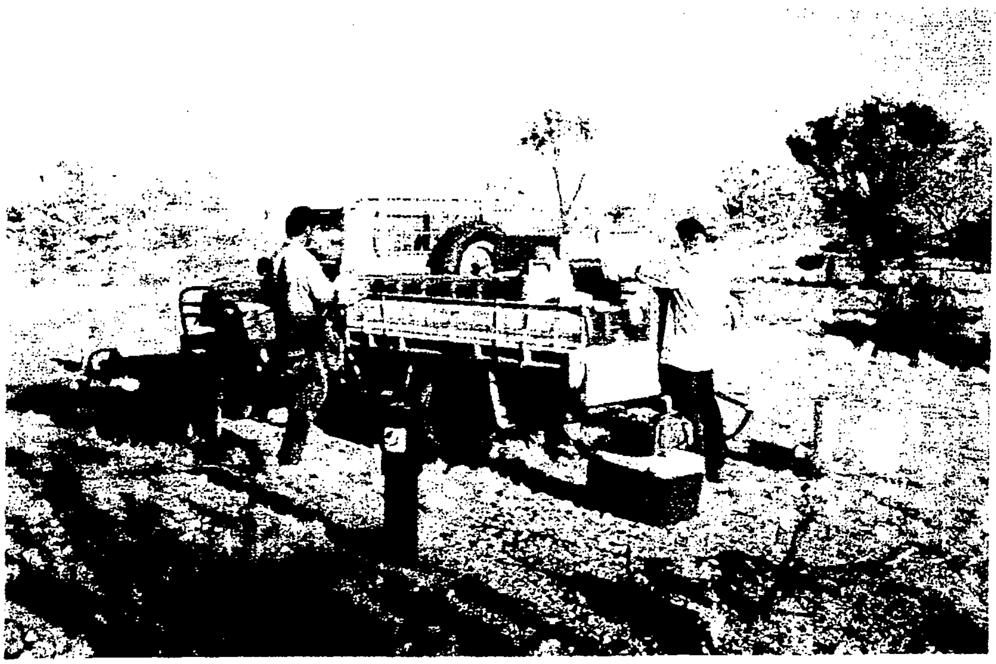

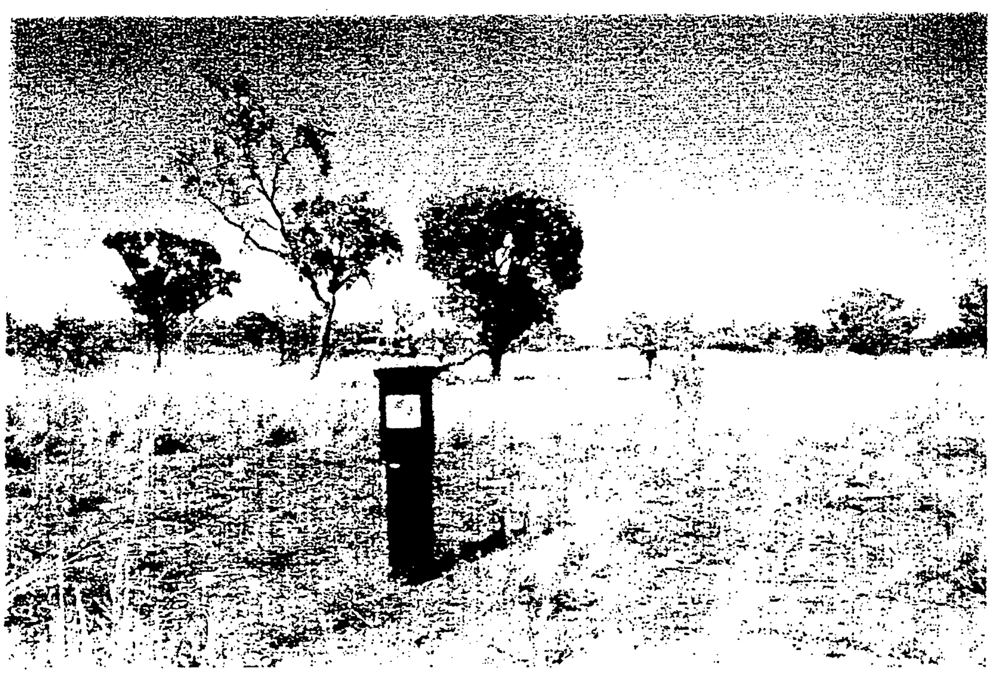

GEO_fieldsurvey.cdr

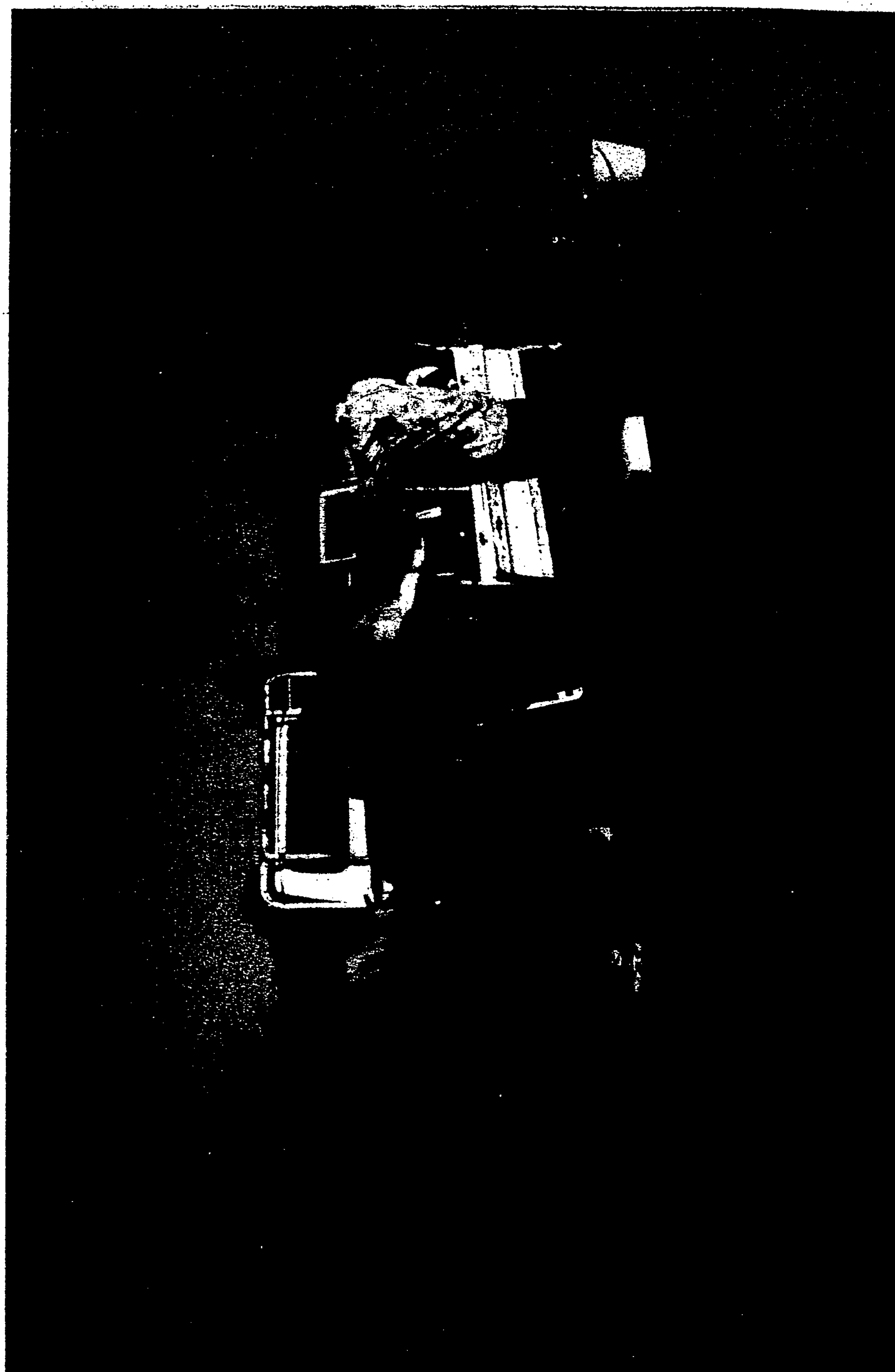

# Improved HTS SQUID Vector Magnetometer
# Presented at the Industrial Geophysical Exhibition SEG '98

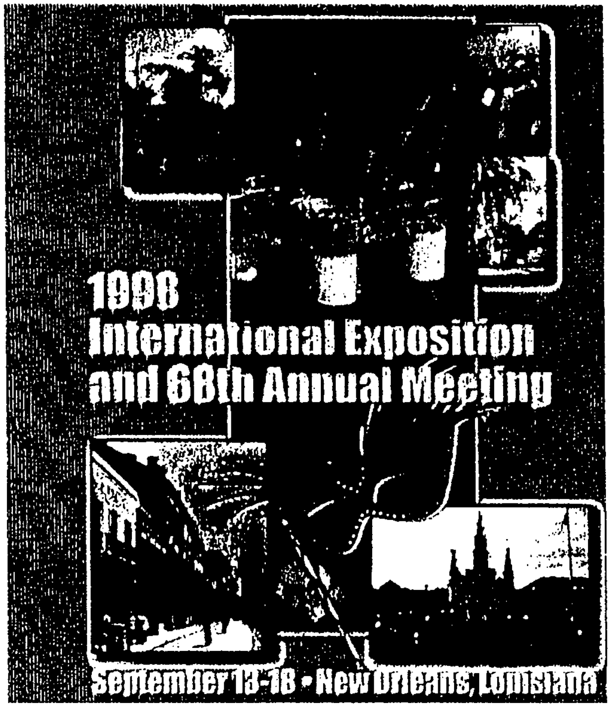


Booth # 2660 of Metronix GmbH

# Characteristics of HTS rf SQUID Vector Magnetometer

- **sensor set up:** orthogonal, capsulated
- **bandwidth:** dc – 20 kHz
- **dynamic range:** > 130 dB
- **slew rate:** ~ 2mT/s [~ $5x10^5$ $\Phi_0$/s]
- **cross talk:** < 0.5 %
- **hold time of dewar:** > 30 h
- **implemented heater**

- **field resolution:**

| | | |
|---|---|---|
| white noise | 40 fT/√Hz | [typical] |
| 1/f – onset | @ 100 Hz | [best channel] |

⇒ **Requirements for TEM fulfilled**

⇒ **Stable operation of all 3 channels in urban environment proved**

# Noise Spectra of Vector Magnetometer (Z-channel) in and Outside Magnetic Shielding

1/f-onset @ ~ 7 Hz in shielding
@ ~ 100 Hz outside shielding

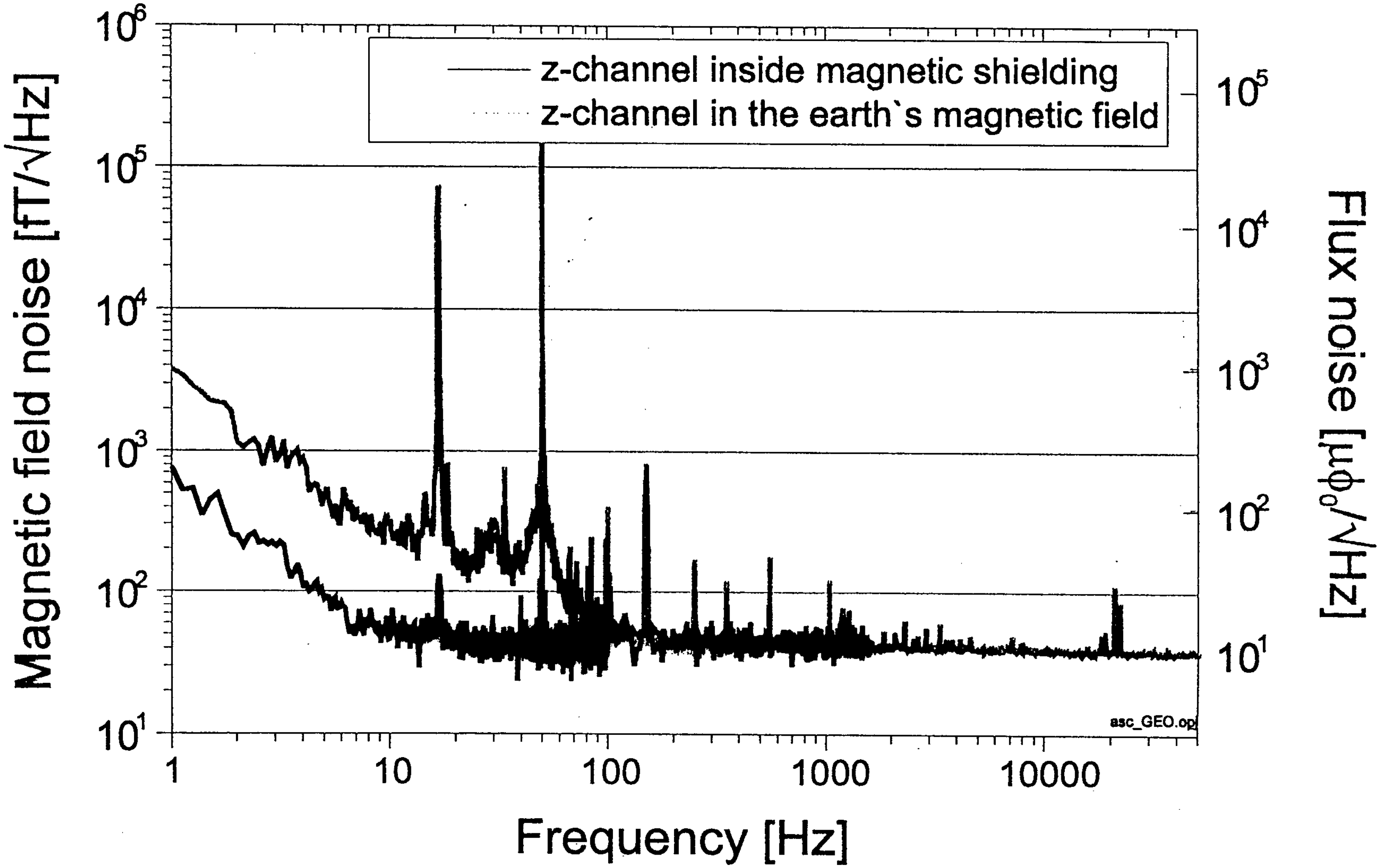

# Noise Spectra of Vector Magnetometer Inside 3-layer μ-metal Shielding

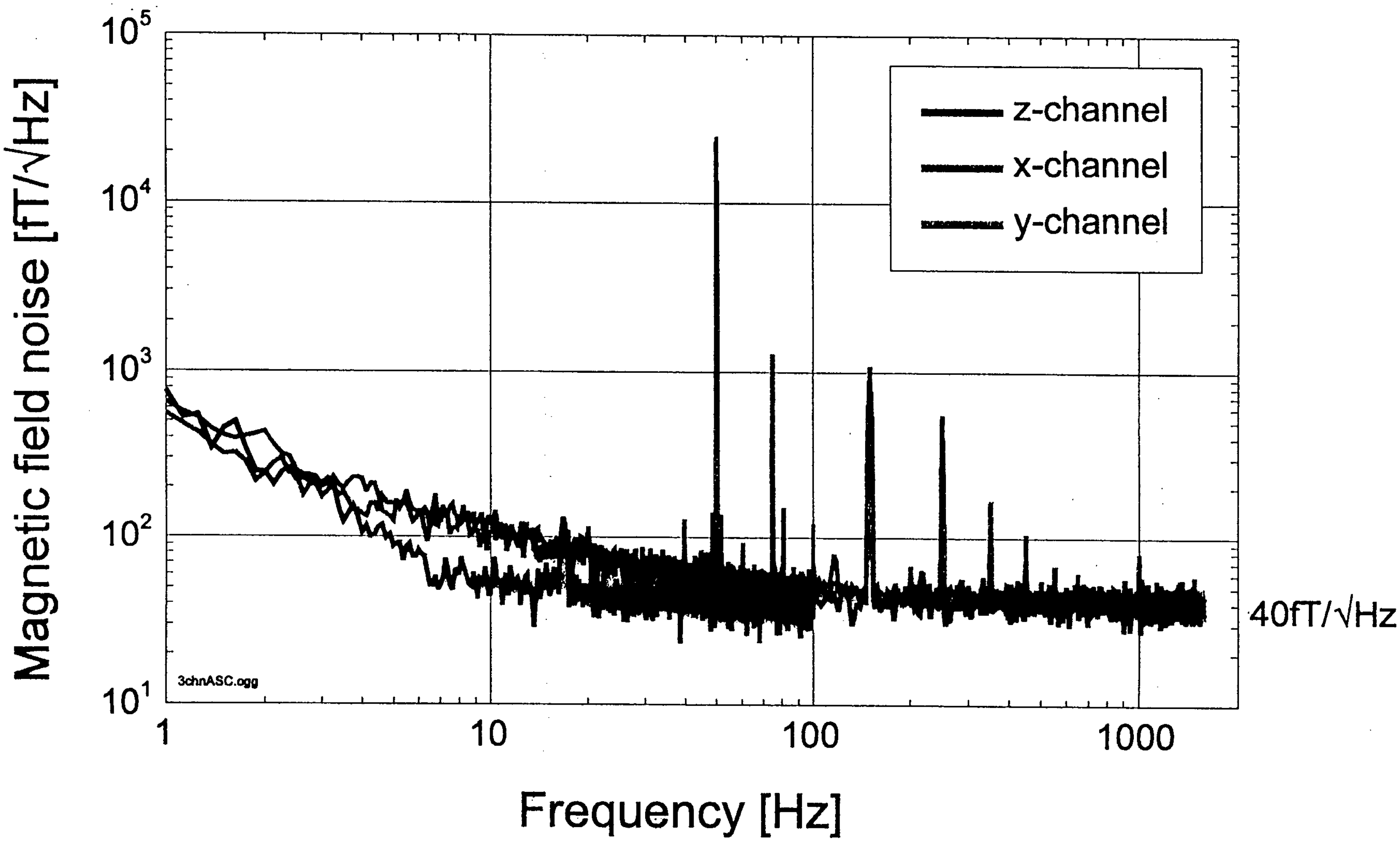

# Performance of Heater:
# Noise Spectra Before and After Heating (X-channel) During Field Trial

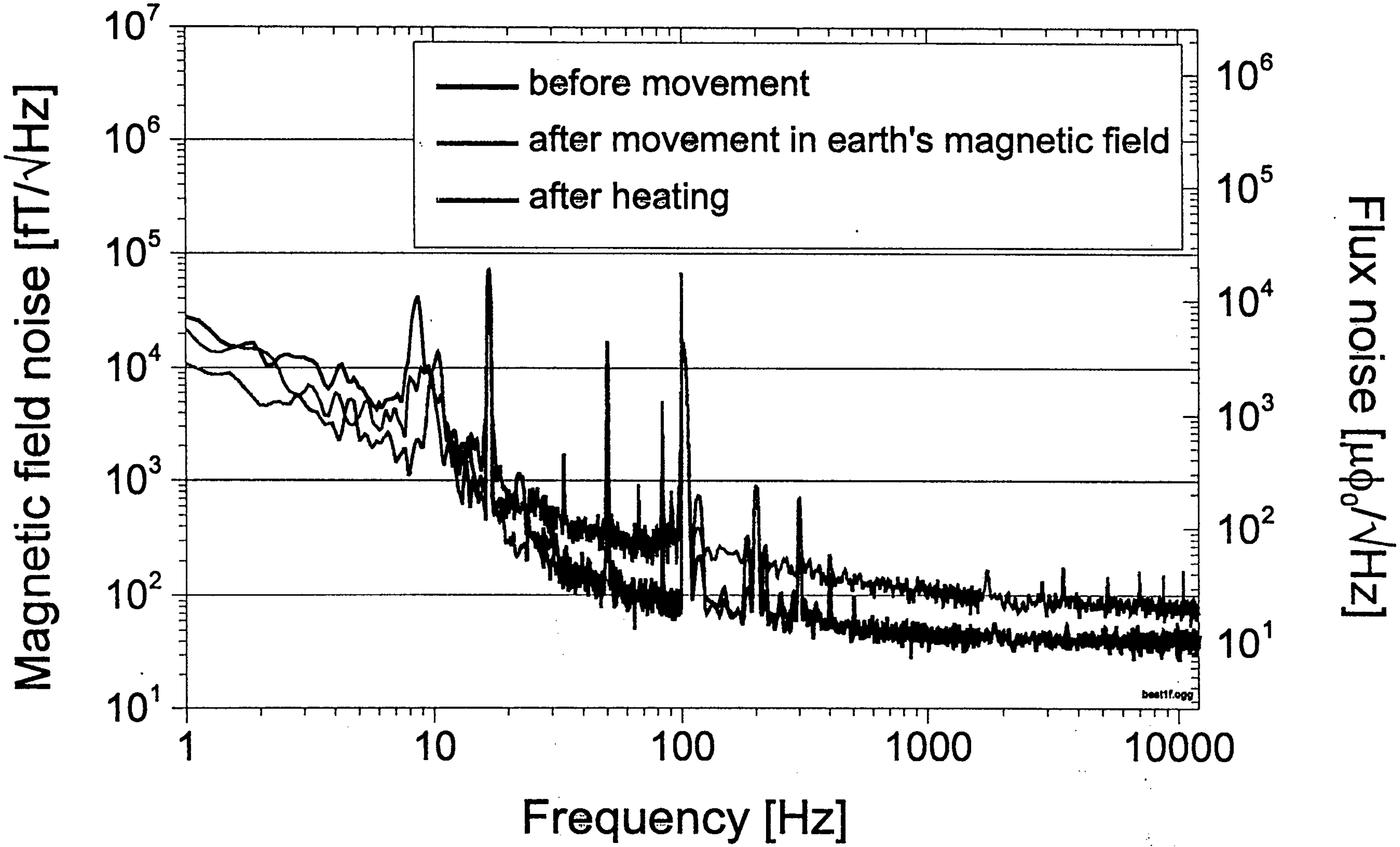

# Geophysical Transient Electromagnetics (TEM) Measurements:
## Advantage HTS rf SQUID over Coil for Late Times

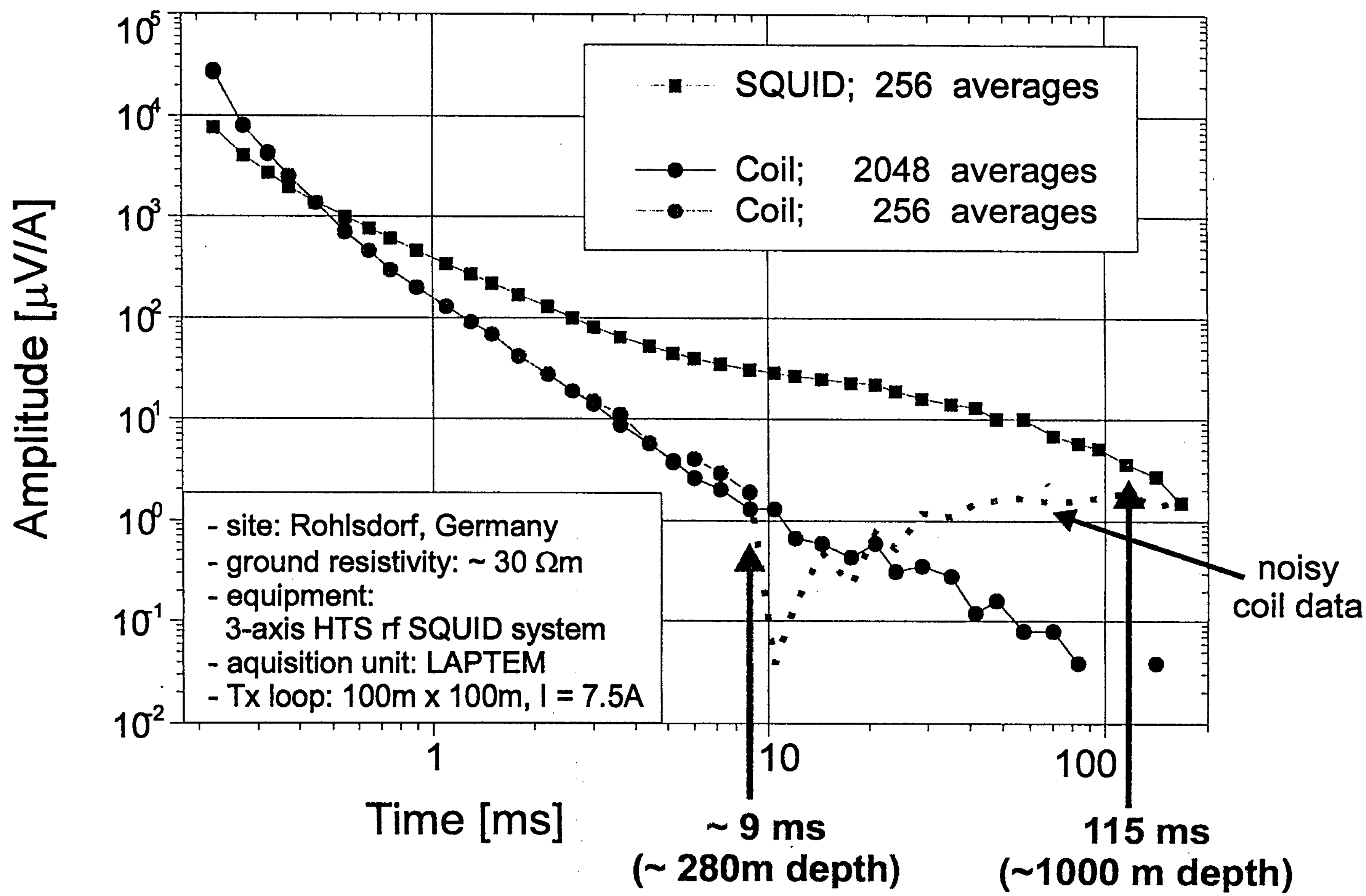

# TEM Measurements:
# Advantage HTS rf SQUID Over Coil for Late Times

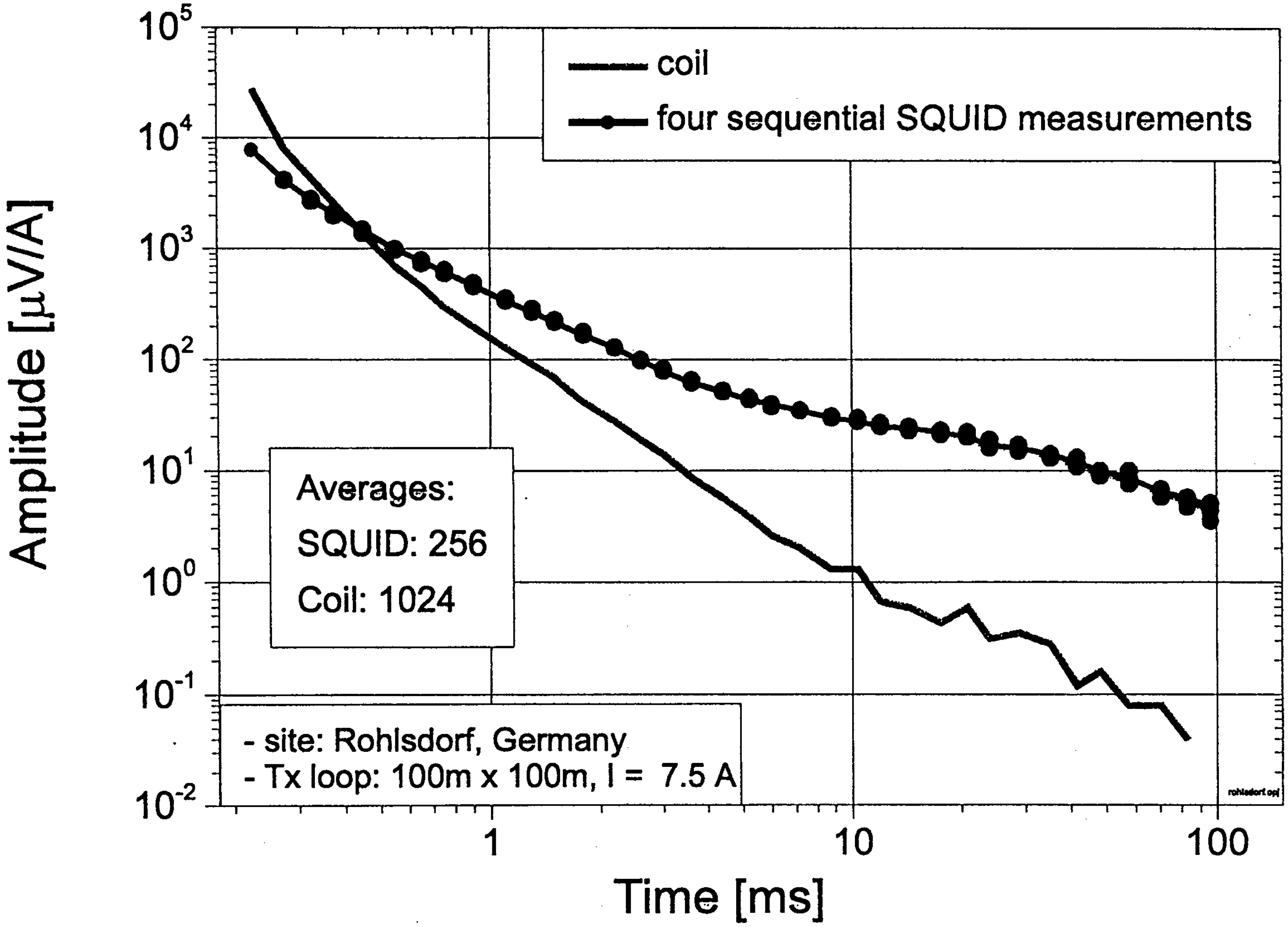

Geophysical Transient Electromagnetics, Measured at Martinsbüttel, Germany

## HTS SQUID Provides Better SNR Than Conventional Coil

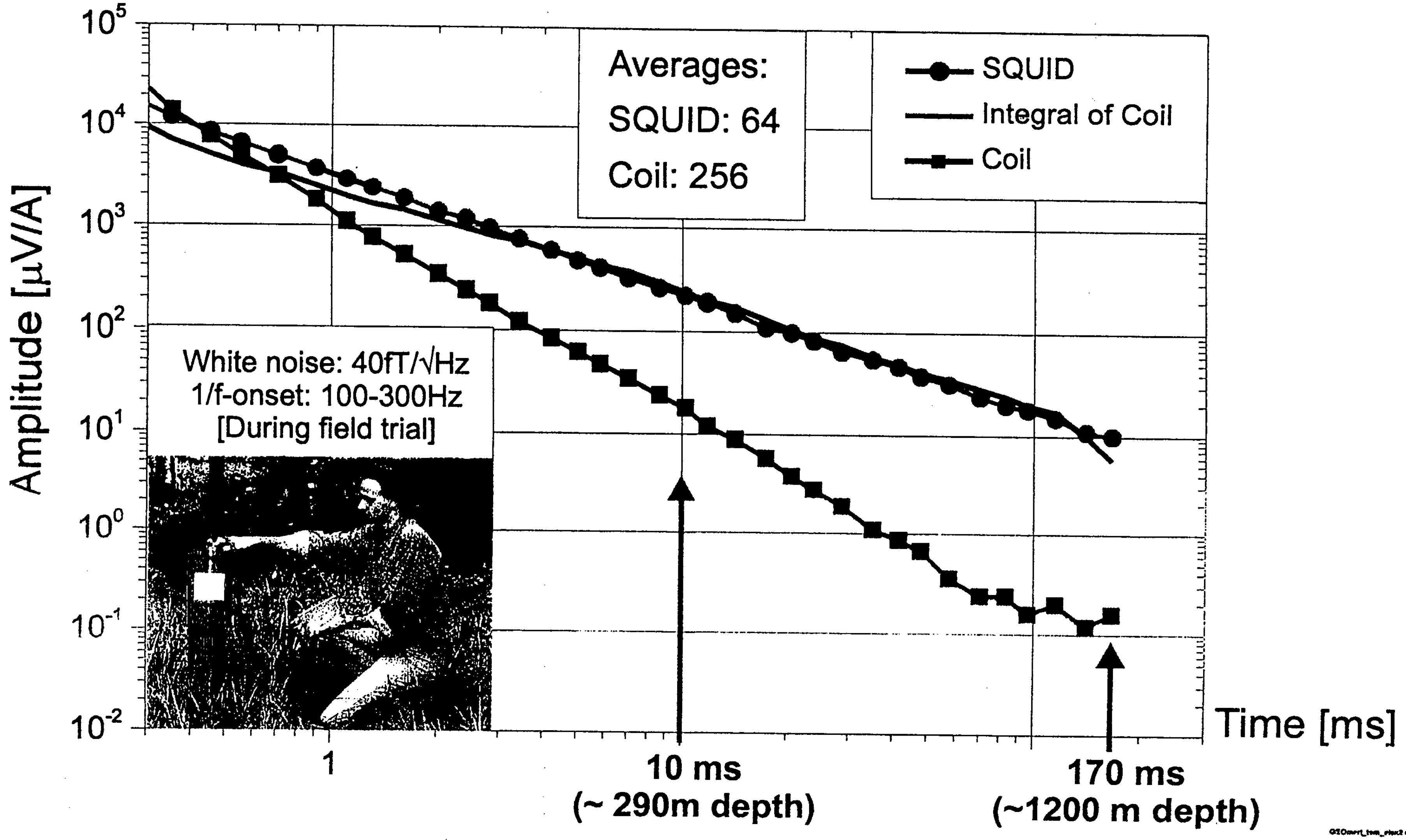

# Correlation SQUID - Coil for Late Times
# SQUID Provides Better SNR Than Coil

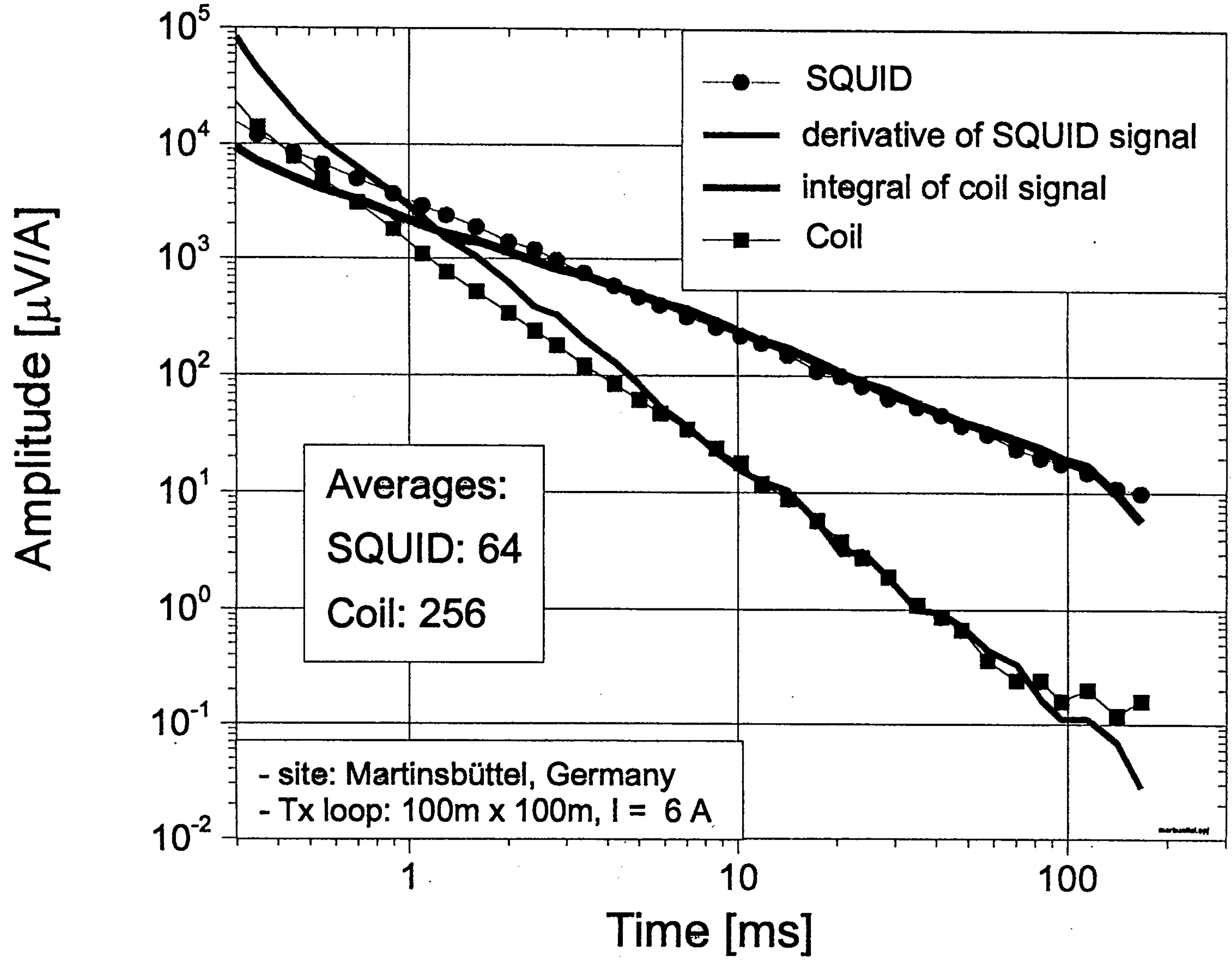


GEOmart_tem.cdr

# Reproducibility of Geophysical SQUID TEM Measurements

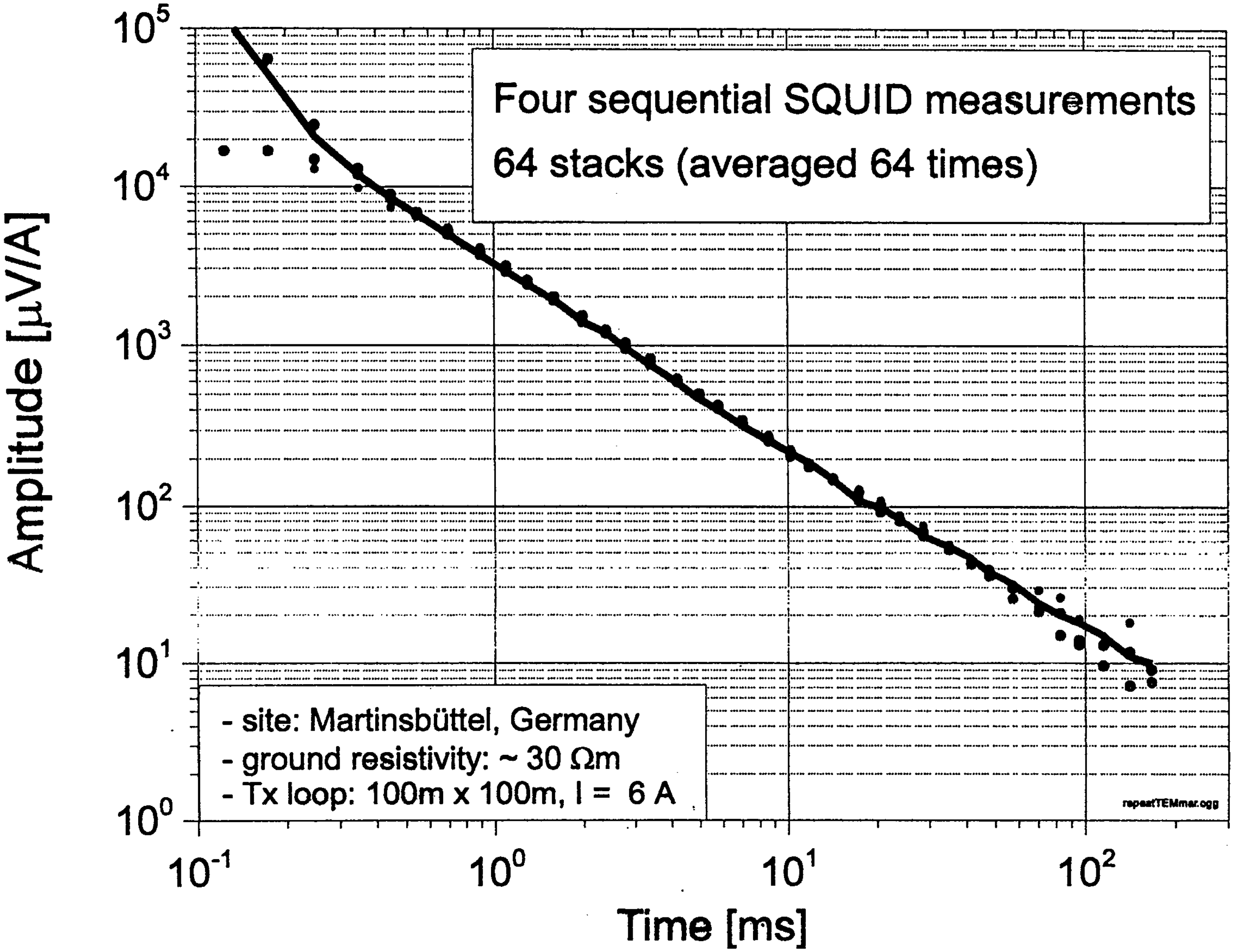


GEOrepeat_asc.cdr

VERTICAL COMPONENT B'(Z)

FZJ - SQUID

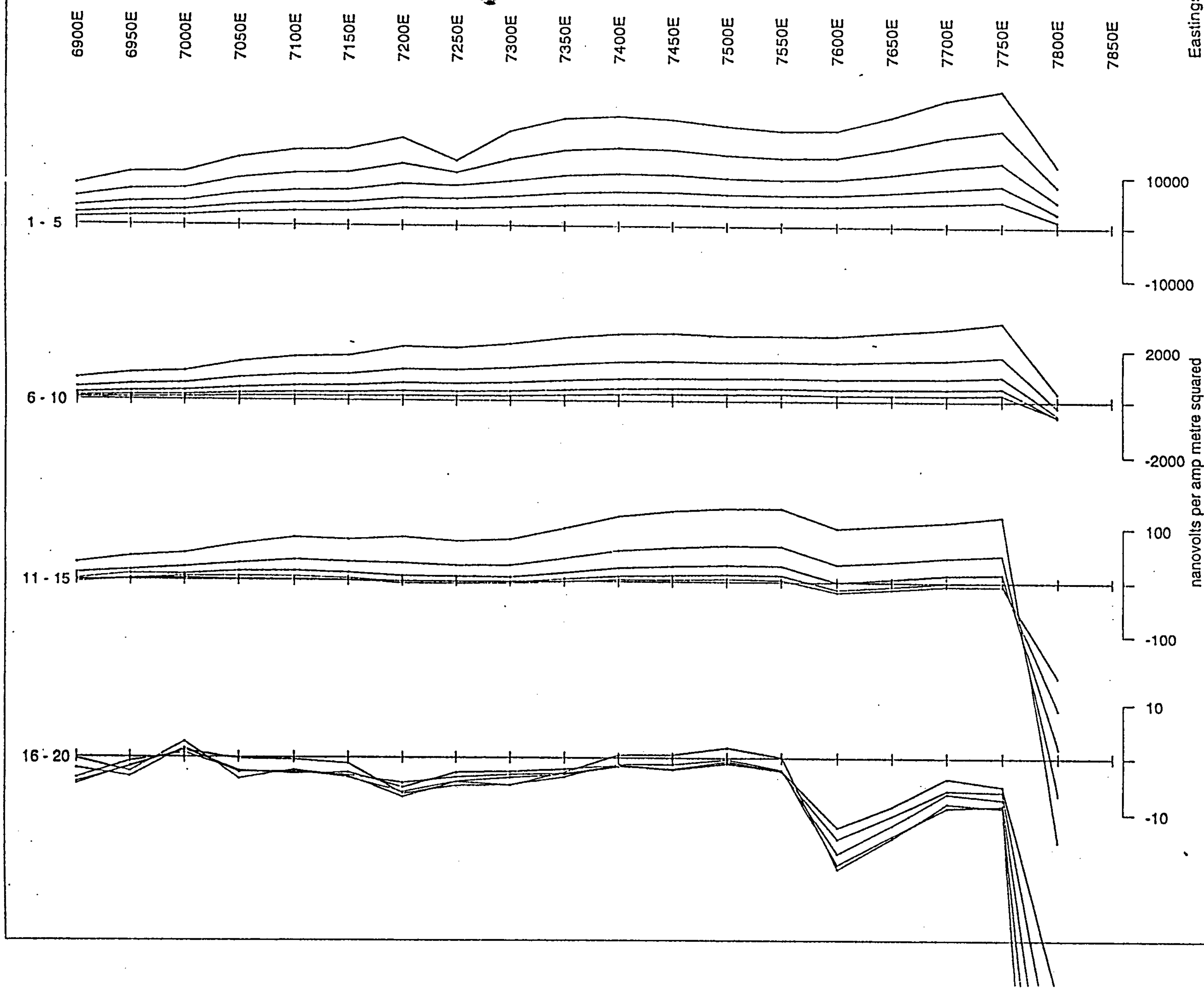


F

TR/

ELECTROMOT
SEC(

TIME DERIVA

Eloise,
Queensland

TX LOOP SIZE
TX TURN OFF TIME
FIRST GATE TIME
CURRENT
FREQUENCY
INTEGRATION TIME
SYNC MODE
HORIZONTAL SCAL
SURVEYED BY
DATE

geoterre

CLIENT : G
PROJECT : T
AREA : T
LINE : 8

TEM-PROFILE

VERTICAL COMPONENT B'(Z) October 24, 1998

IPHT - SQUID

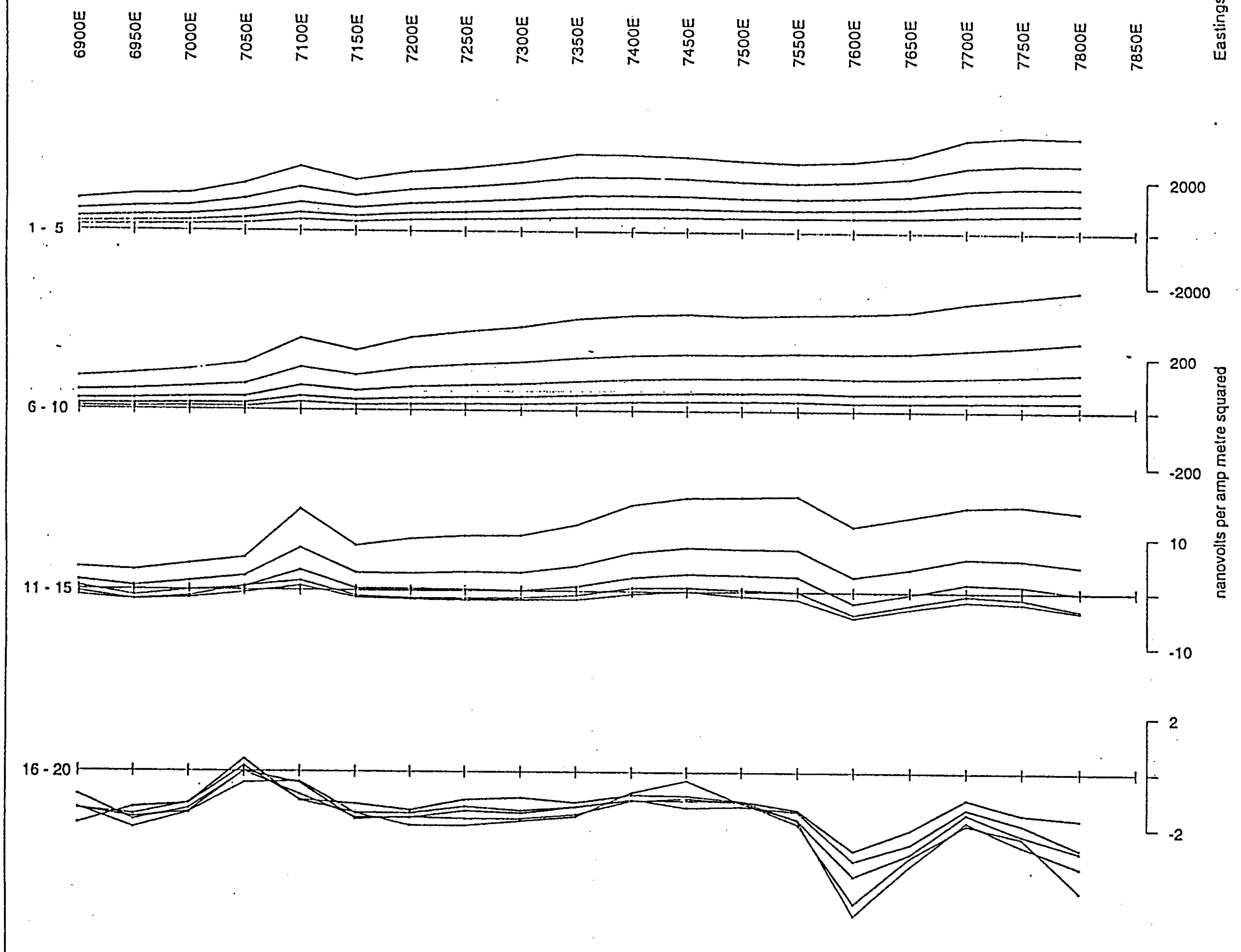


F

TR

ELECTROMOT
SEC

TIME DERIVA

Eloise, Queensland

TX LOOP SIZE
TX TURN OFF TIME
FIRST GATE TIME
CURRENT
FREQUENCY
INTEGRATION TIME
SYNC MODE
HORIZONTAL SCAL
SURVEYED BY
DATE

geoterre

CLIENT : G
PROJECT : T
AREA : T
LINE : 8

TEM-PROFILE

October 24, 1998

VERTICAL COMPONENT B'(Z)

GEOTERREX - COIL

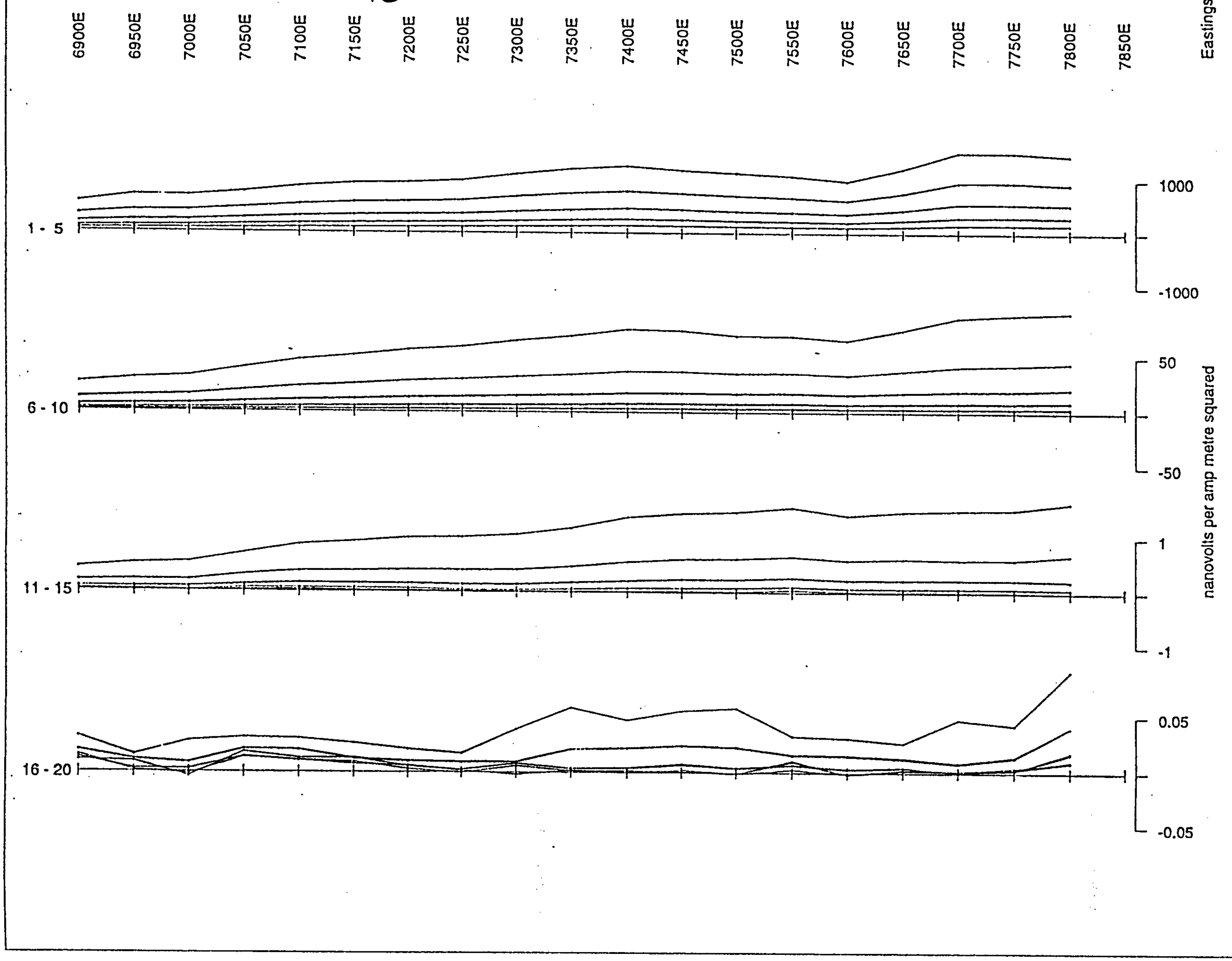


F

TR

ELECTROMOT
SEC

TIME DERIV

Eloise, Queensland

TX LOOP SIZE
TX TURN OFF TIMI
FIRST GATE TIME
CURRENT
FREQUENCY
INTEGRATION TIM
SYNC MODE
HORIZONTAL SCAI
SURVEYED BY
DATE

geoterre

CLIENT :
PROJECT :
AREA :
LINE :

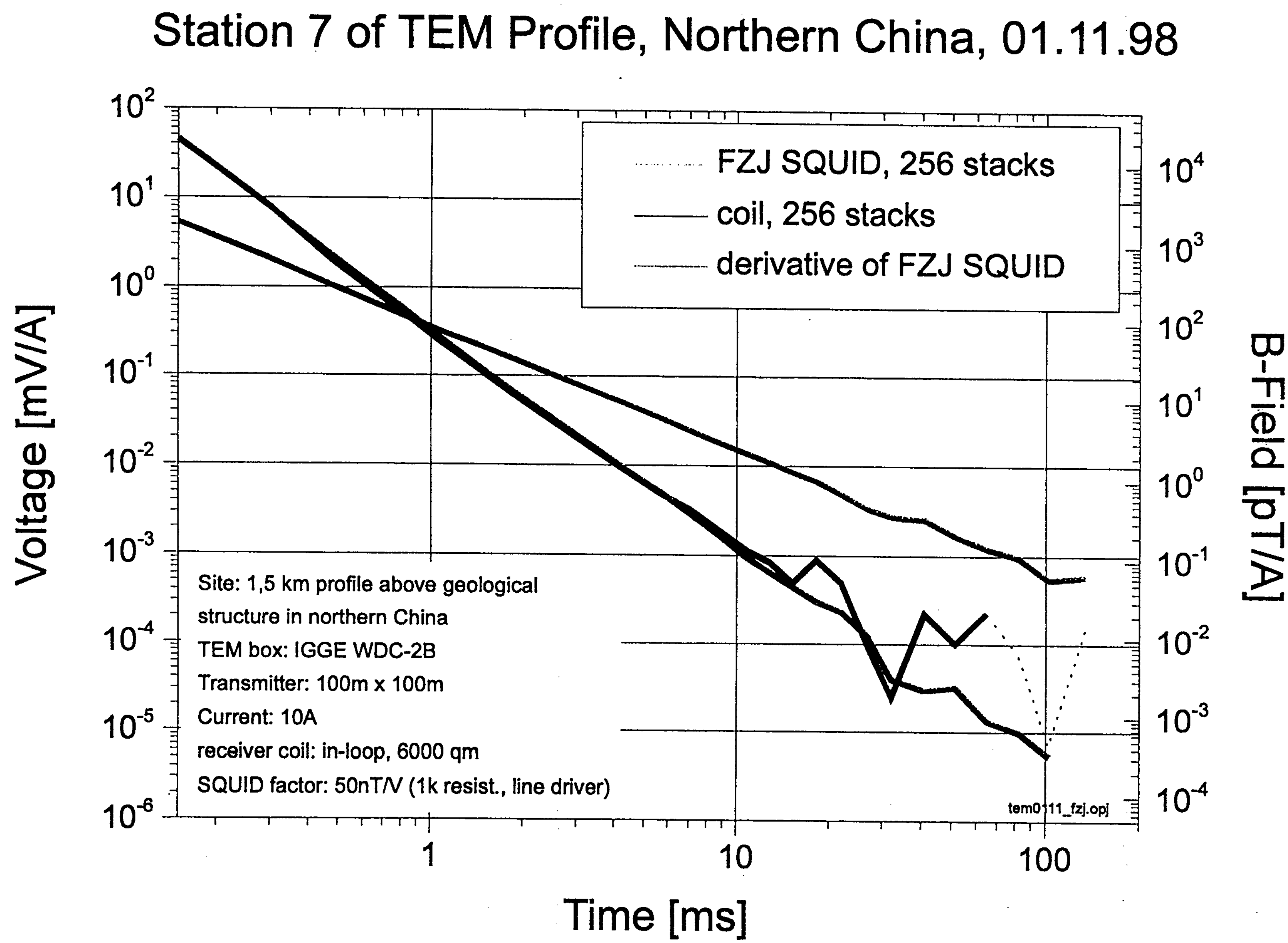
Station 7 of TEM Profile, Northern China, 01.11.98
FZJ SQUID, 256 stacks
coil, 256 stacks
derivative of FZJ SQUID
Site: 1,5 km profile above geological
structure in northern China
TEM box: IGGE WDC-2B
Transmitter: 100m x 100m
Current: 10A
receiver coil: in-loop, 6000 qm
SQUID factor: 50nT/V (1k resist., line driver)
tem0111_fzj.opj
Voltage [mV/A]
B-Field [pT/A]
Time [ms]
1
10
100

# SQUID-LOTEM Profile above
## Geological Structure in Northern China

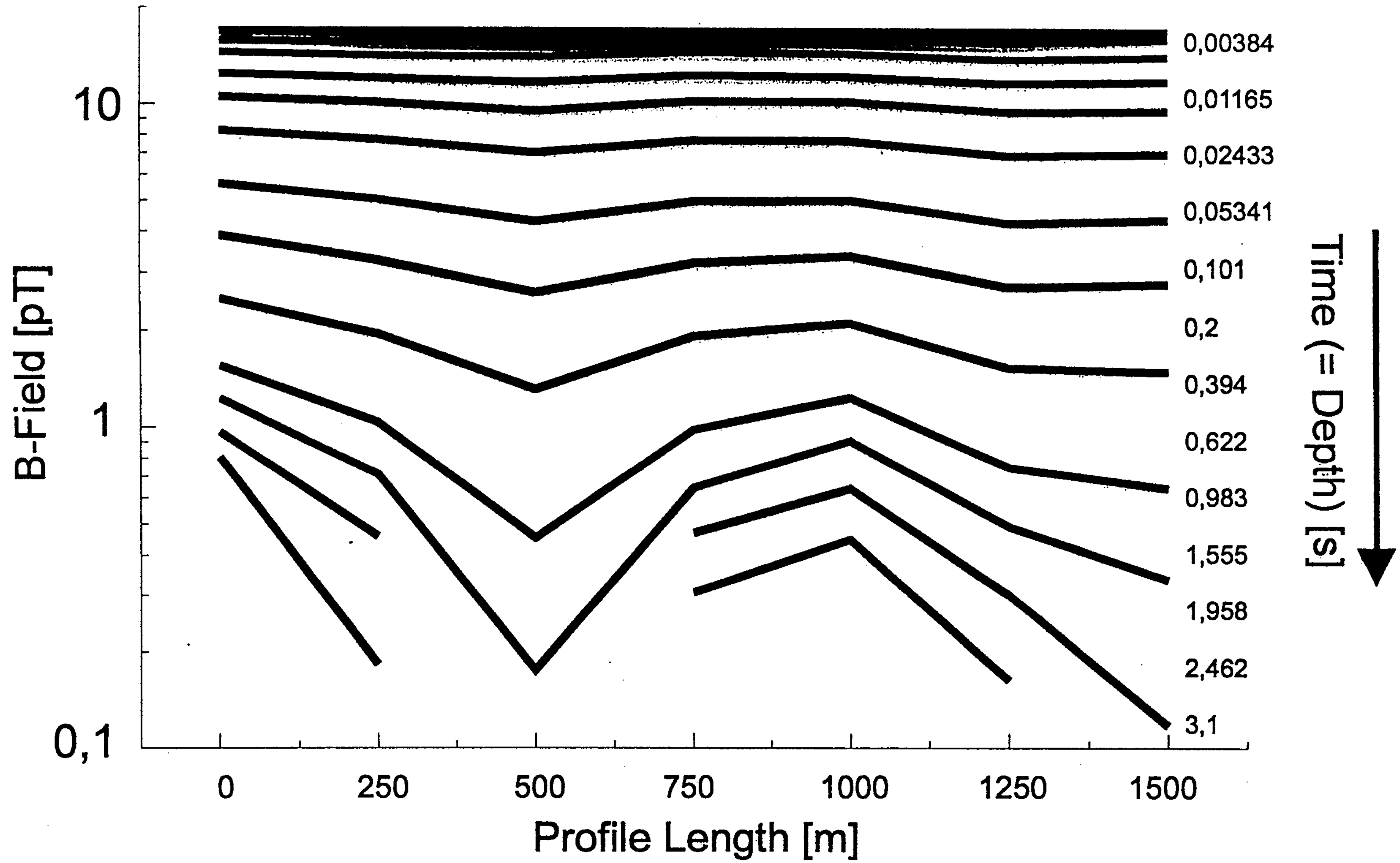


GEO_LOTEMmessung.cdr

LOTEM, Station 2, Northern China, 03.11.98

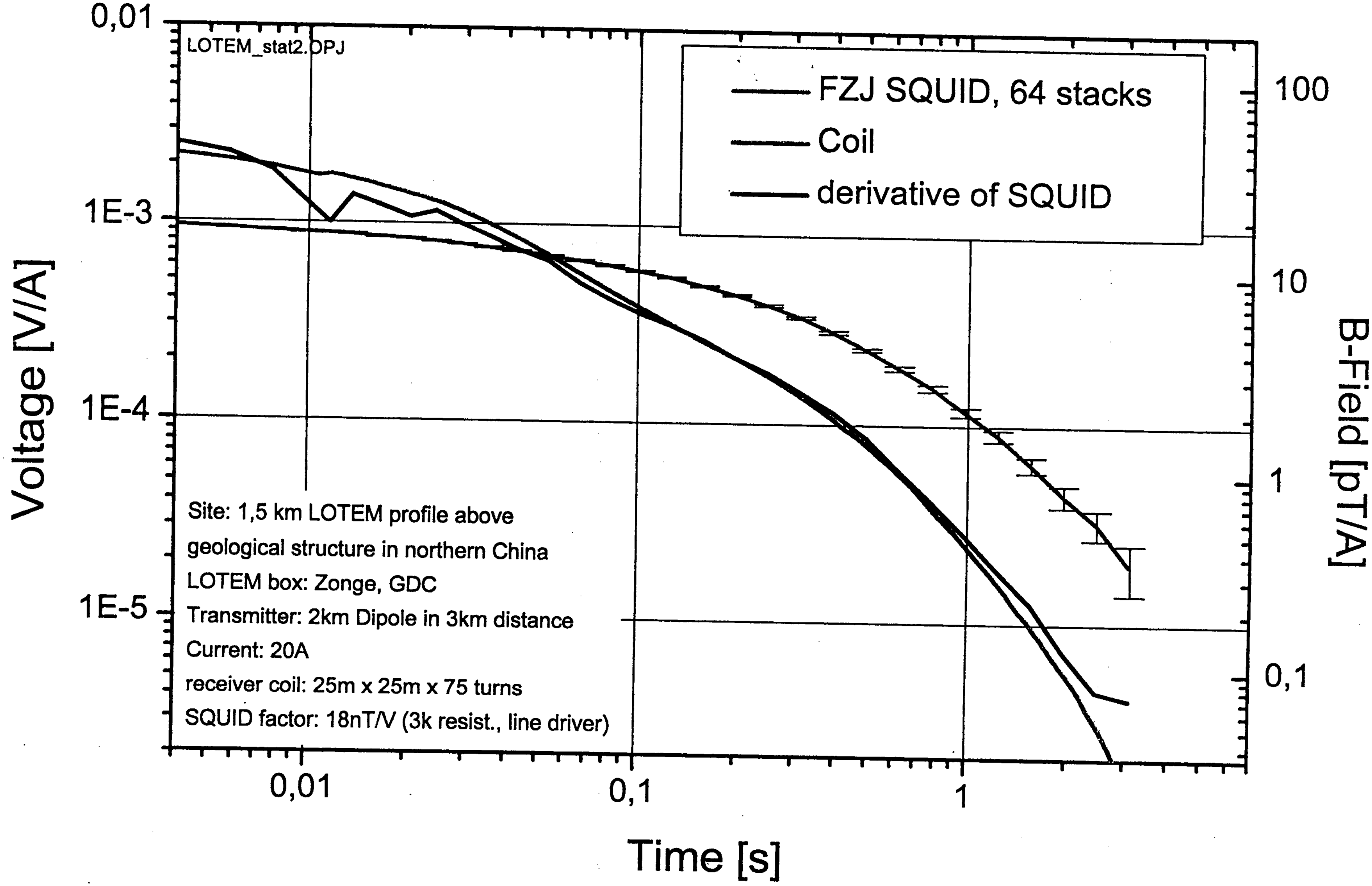

# Radiomagnetic Sounding

- Above 100 kHz, $E_x$ difficult to measure (sensor dimensions comp. to $\delta$)

- Measure B gradient instead:

$$\text{Curl } B(\omega) = \mu_0\mu(1/\rho_a - j\omega\varepsilon)E(\omega)$$

- When $\rho < 100\ \Omega\text{cm}$, $f < 1 - 2$ MHz, $j\omega\varepsilon$ is negligible, and we have:

$$Z_{xy}(\omega) \cong -\rho^*/\Delta z\big(\Delta B_y(\omega)/B_y(\omega)\big)$$

(with $\Delta B_y$, $\rho^*$ just below surface, $\Delta z \ll \delta$)

- For homogeneous earth ($\rho = \rho^*$):

$$\left|\Delta B_y(\omega)/B_y(\omega)\right| \cong 2^{1/2}\Delta z/\delta$$

$\Rightarrow \quad |\Delta B_y| = 8 - 800$ fT

for

$|B_y| = 1 - 100$ pT

# Schematic of LTS RMS (RMT) System

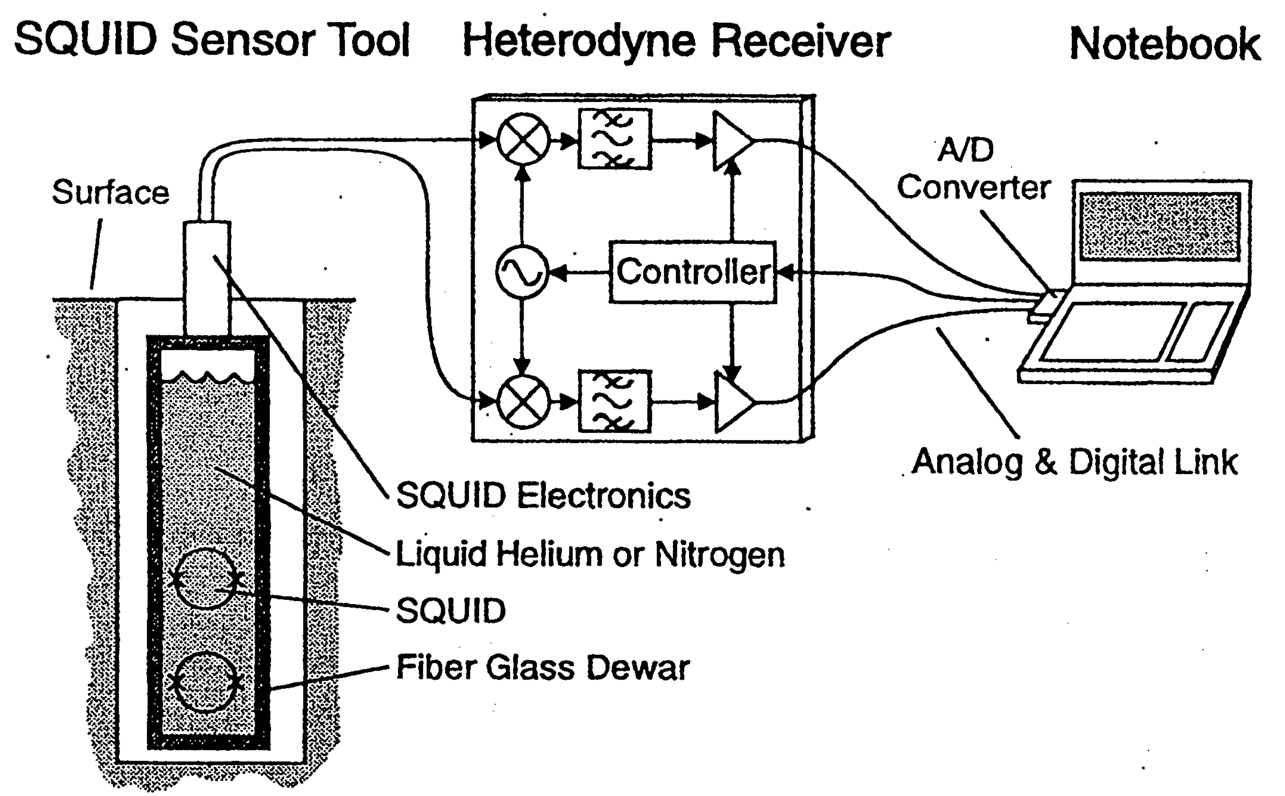


Drung, Radic et al., IEEE Trans. Appl. Supercond. 7, 3283 (1997)

# Main Noise Sources in TEM Determining SNR

## 1. Intrinsic noise of sensor

## 2. External disturbances:

- **high frequency [>20kHz - GHz]**

  radio / TV transmitter, mobile phones

⇒ directly affect SQUID's operation

- **low frequency [dc - 20kHz]**

  - wind noise (vibrations)
  - LF drifts of earth's magnetic field (~0,3nT/min)
  - cultural noise ($16^2/_3$Hz, 50Hz)
  - sferics

# 2. Intrinsic noise of sensor determining SNR

**Increased LF excess noise outside magnetic shielding.**

**Reasons:**

- **Penetration of flux into junction: suppression and fluctuation of critical current**

  possible solution: narrow junction

- **Thermally activated hopping of flux vortices in YBCO film**

  possible solutions:

  - high quality YBCO film
  - narrow line width of SQUID's structure ($w<\pi\Phi_0/4B_{earth}$)
  - pinning centres (antidots)

# Conclusions

- The usefulness of SQUID in geophysics was convincingly demonstrated with LTS SQUID, but LHe cooling was prohibitive; $LN_2$ is not
- Recent field tests using HTS SQUID demonstrators have been confirming their potential in TEM and RMS
- Further reduction of HTS SQUID low-frequency noise is required, especially for use in magnetotellurics
- Also required is ruggerizing & automating of SQUID systems, long cryogen hold time, cryocoolers, borehole-compatible systems
- There is potential in HTS SQUID use for prediction of earthquakes and volcano eruptions (and other)

# Outlook

- Existing interest of industry and users should lead to commercial availability of HTS SQUID systems for TEM in a few years (2000–2005)

- New developments in SQUID sensors (Berkeley), may also permit CSAMT systems at a comparable time scale

- The RMS using HTS SQUID might find the relatively largest market, after additional development efforts

- Novel (electrokinetic) methods, possible only with SQUID, might have a large economic potential in a more distant future

# Typical Magnetic Field Noise of Vector Magnetometer During Field Trial Outside Magnetic Shielding

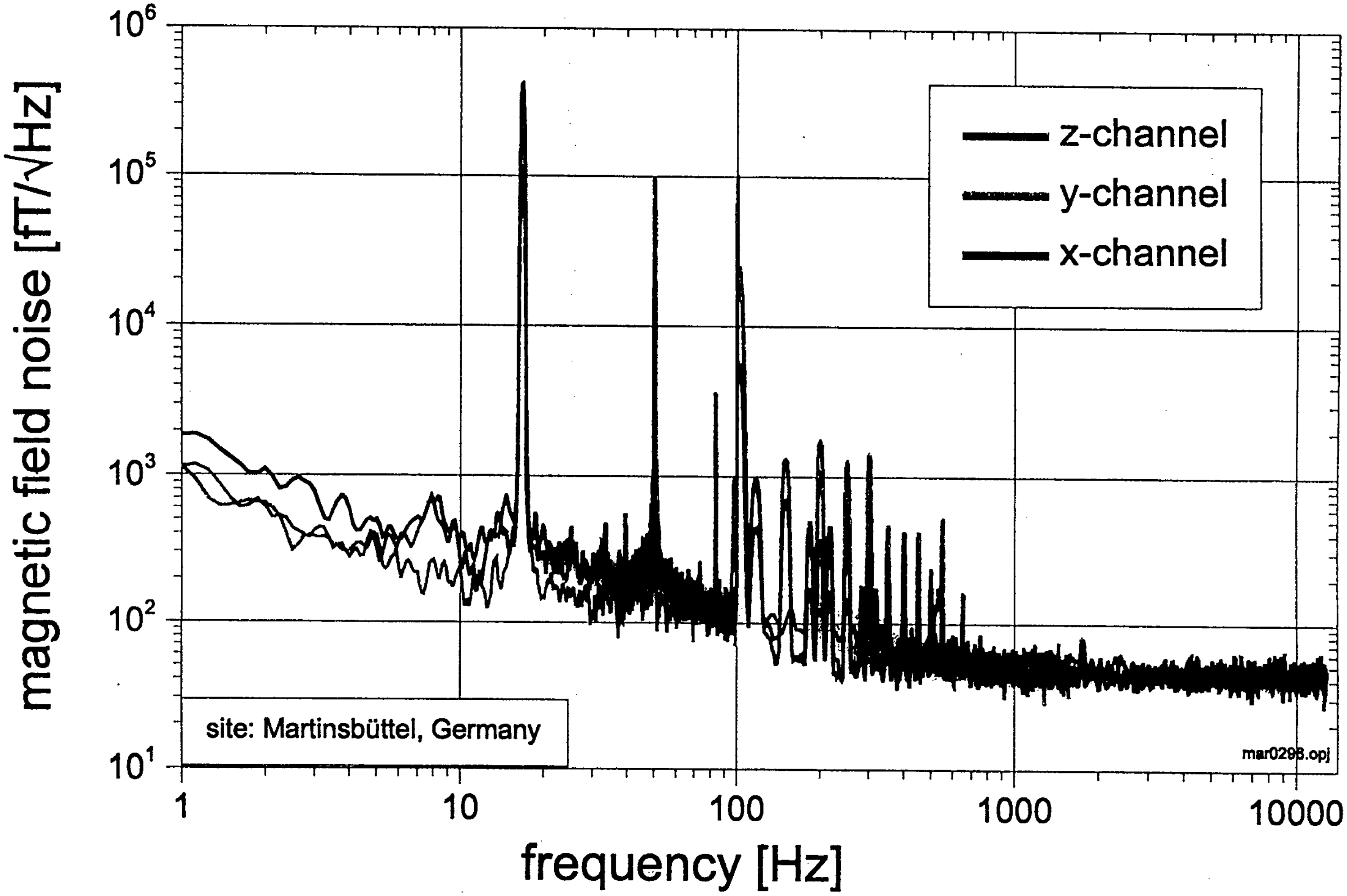

## SQUIDs, Axions, Bugs and Hearts

- SQUIDs – a short review
- The axion detector: a new mode for SQUIDs
- The SQUID microscope: magnetotactic bacteria
- Unshielded magnetocardiography with a high-$T_c$ second-derivative gradiometer

Lyon
16 June 1999

# Low-Noise rf Amplifiers Based on dc SQUIDs

(LOW-Tc)

Michael Mück and Marc-Olivier André
*Department of Physics*
*University of California, Berkeley*

In collaboration with:

Jost Gail and Christoph Heiden
*Institut für Angewandte Physik*
*Justus-Liebig Universität Gießen, Germany*

XIAOFENG MENG
(VAN DUZER/MICROLAB)

# LC - Resonator Input

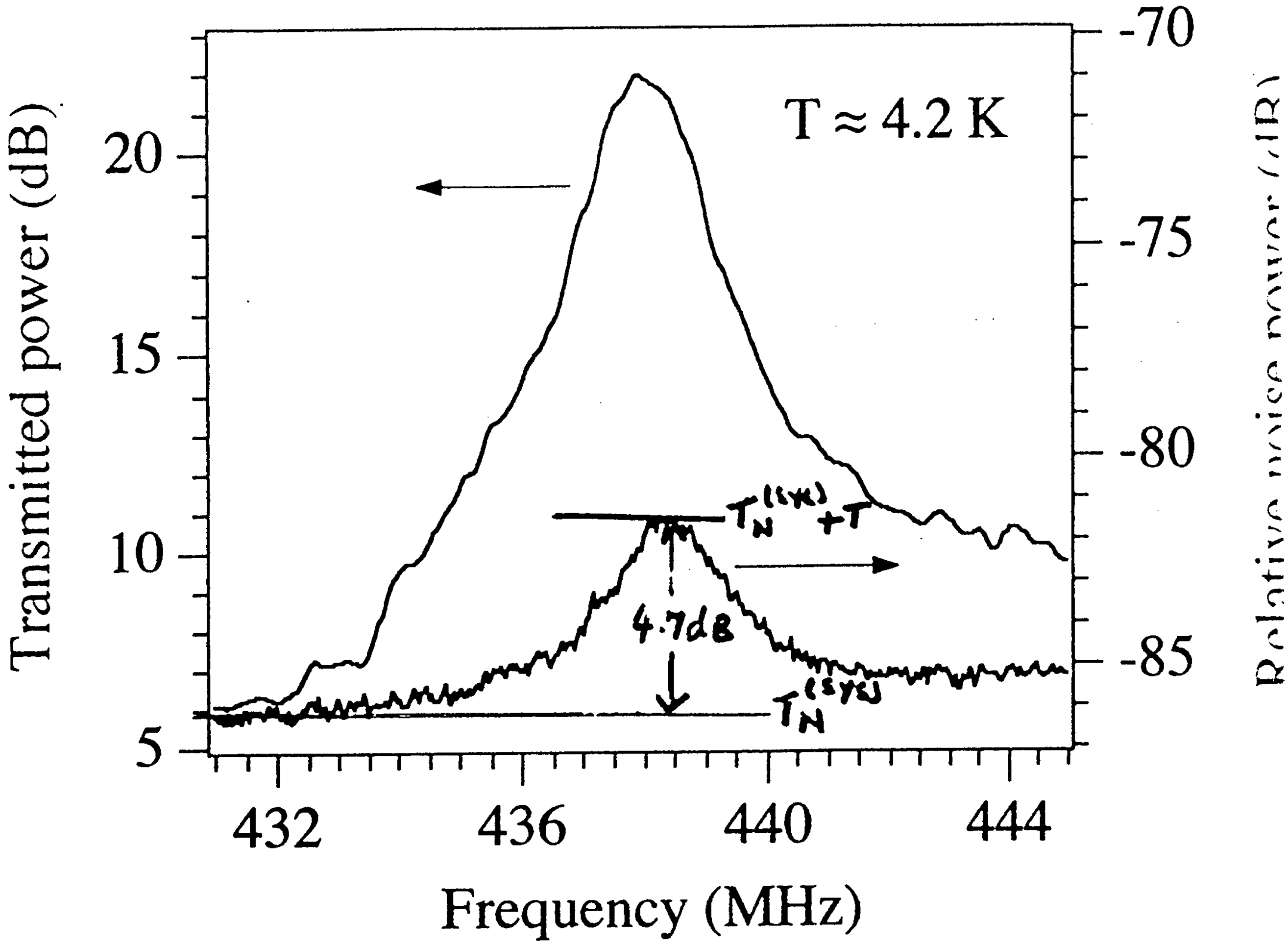


WITH 2dB COUPLING LOSS, PEAK HEIGHT ≈ 6.7dB

HENCE $10 \log_{10} [T_N^{(SYS)} + T] / T_N^{(SYS)} \approx 6.7$

$T_N^{(SYS)} \approx \underline{1.1K}$

[MEASURED : $T_N^{(SYS)} = 1.4 \pm 0.18K$]

# LC - Resonator Input

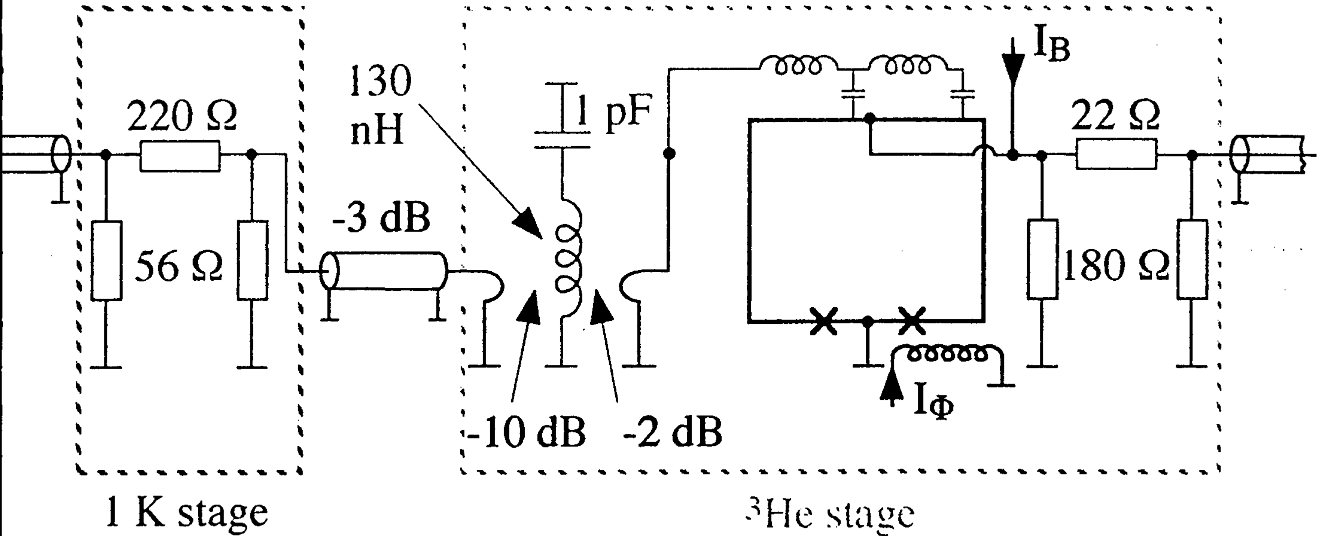

# NOISE TEMPERATURE

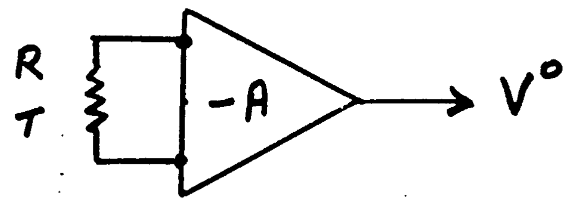


$$S_V^{\circ}(f) = A^2 \, 4k_B \, (T+T_N) R$$

WHERE $T_N = T_N(R)$

# Axions

- The axion is a candidate particle for dark matter
- Energy constrained to $10^{-6} - 10^{-3}$ eV (0.24 - 240 GHz)
- In a magnetic field $B_0$ an axion can convert into a photon
- In a resonant cavity of volume V and quality factor Q, conversion rate $\propto B_0^2 VQ$

## LLNL/MIT Axion Detector

- Cavity 1 m long, 0.5 m diameter : $T_c \approx 1.3$ K
- Frequency range 0.7 - 0.8 GHz
- Output from cavity detected by HEMT amplifier : $T_A \approx 1.7$ K
- System noise temperature $T_S = T_c + T_A \approx 3$ K
- Since integration time $\propto T_S$, there is great incentive to run the detector at a lower temperature (say, 0.3 K) provided one has a much quieter amplifier

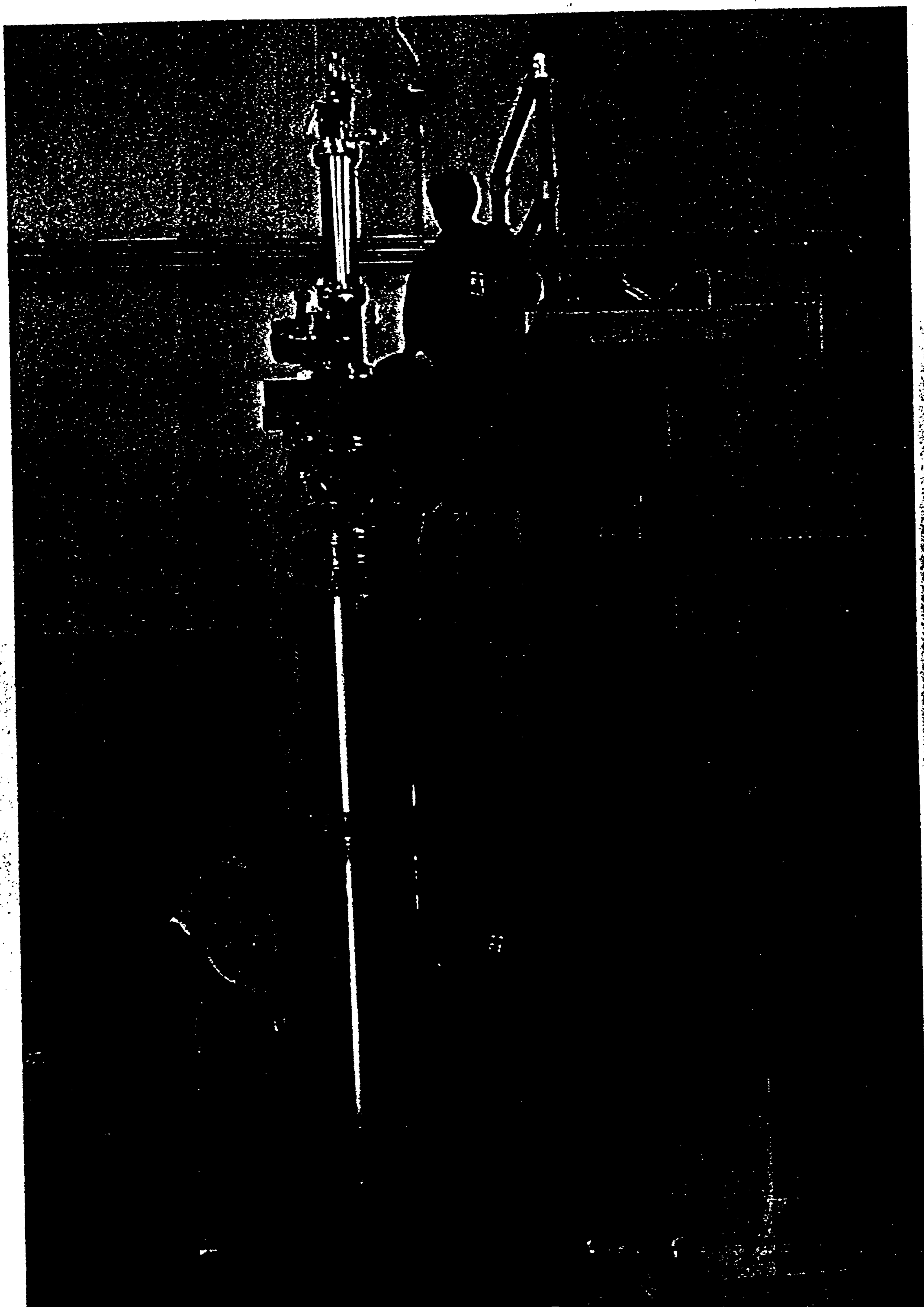

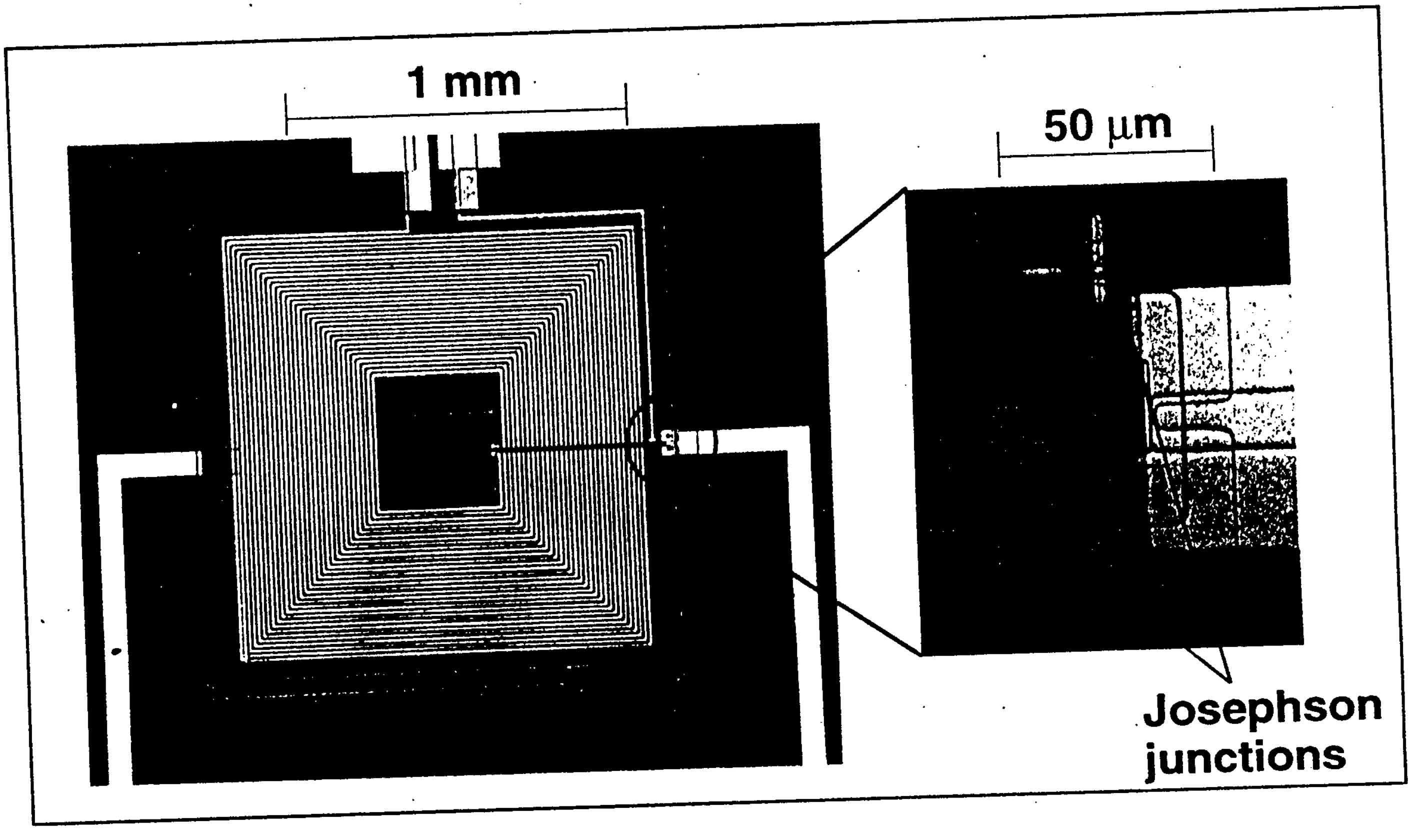
1 mm
50 μm
Josephson
junctions

# Conventional SQUID design

**Top View**

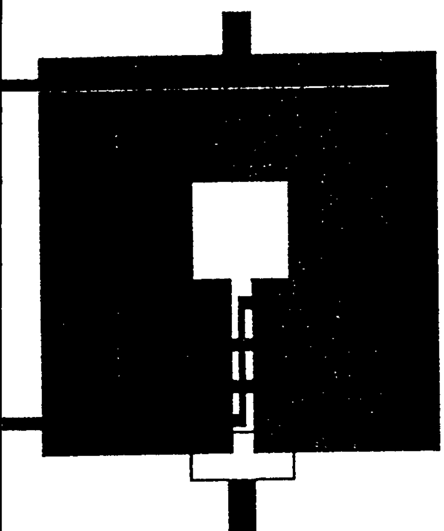

**Side View**

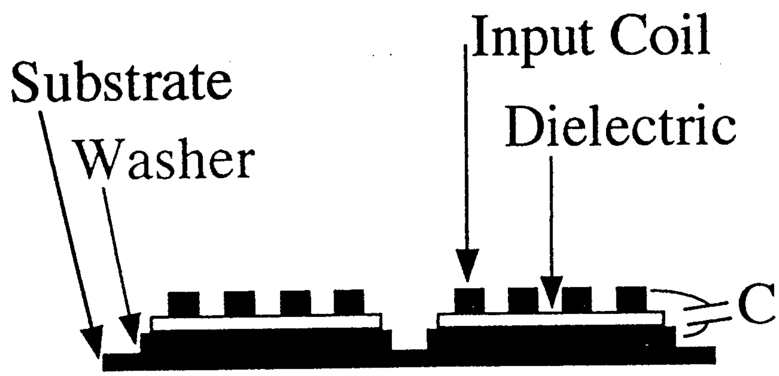


At high frequencies, most of the current flows through the parasitic capacitance rather than the inductance.

This reduces the gain substantially.

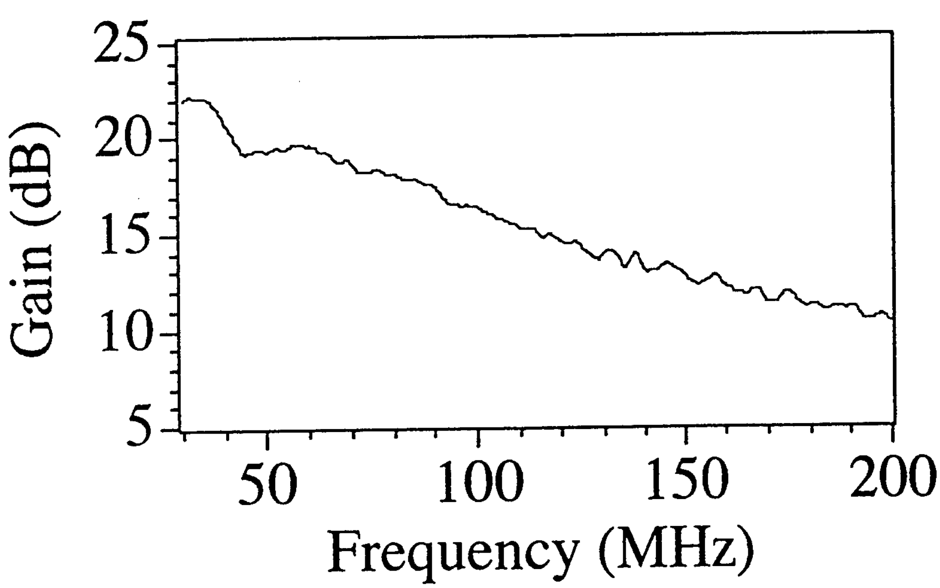

# MICROSTRIPLINE

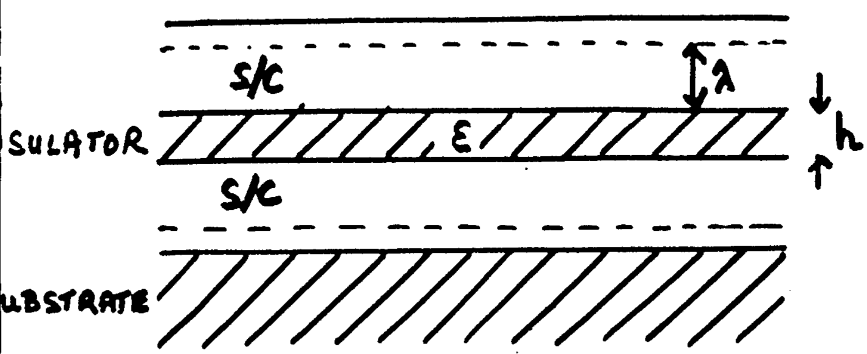


SIDE VIEW

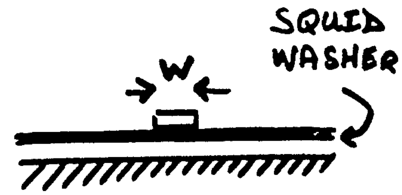


END VIEW

$W \approx 5\mu m$
$h \approx 0.4 \mu m$
$\varepsilon \approx 9$
$\lambda \approx 0.15 \mu m$

NEGLECT FRINGING FIELDS

ASSUME $\lambda$ < FILM THICKNESS

$$C/1m = \frac{\varepsilon \varepsilon_0 W}{h} \approx \underline{1 nF/m}$$

$$L/1m = \frac{\mu_0 h}{W} \underbrace{\left(1 + \frac{2\lambda}{h}\right)}_{\text{INDUCTIVE LOADING}} \approx \underline{175 nH/m}$$

VELOCITY $\bar{c} = \dfrac{c}{\sqrt{\varepsilon}\sqrt{1+2\lambda/h}} \approx \underline{0.25c}$

IMPEDANCE $Z_0 = \sqrt{\dfrac{L}{C}} = \dfrac{h}{W}\sqrt{\dfrac{\mu_0}{\varepsilon\varepsilon_0}\left(1+\dfrac{2\lambda}{h}\right)} \approx \underline{13\Omega}$

# MICROSTRIPLINE RESONANCE

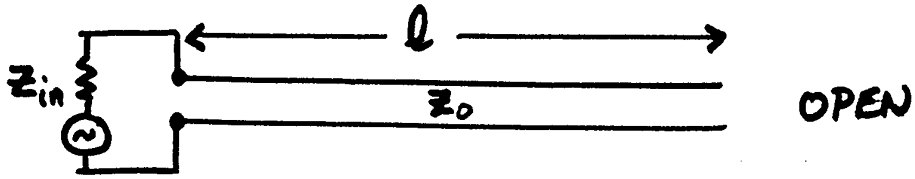


$Z_{in} > Z_0$

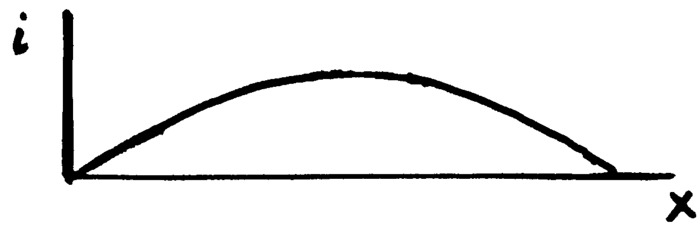


RESONANCE : $$\frac{\lambda}{2} = l = \frac{\bar{c}}{2f}$$

QUALITY FACTOR: $$Q = \frac{\pi Z_{in}}{2 Z_0}$$

# Feedback

Feedback from the output of the SQUID to the input via the capacitance of the microstrip.

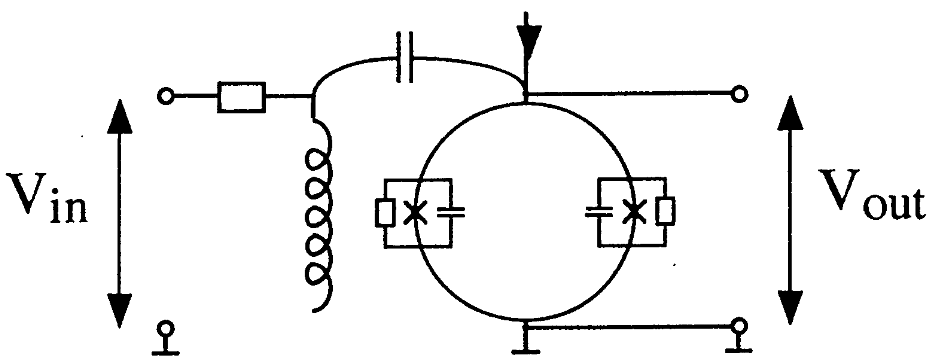


Positive feedback for $V_{\Phi}^{+}$

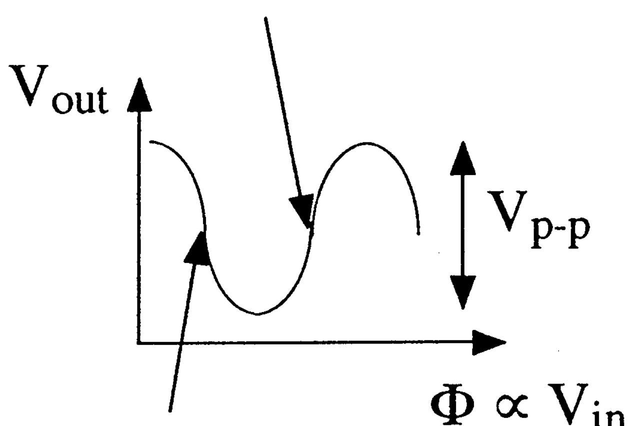


Negative feedback for $V_{\Phi}^{-}$

# Gain Measurements

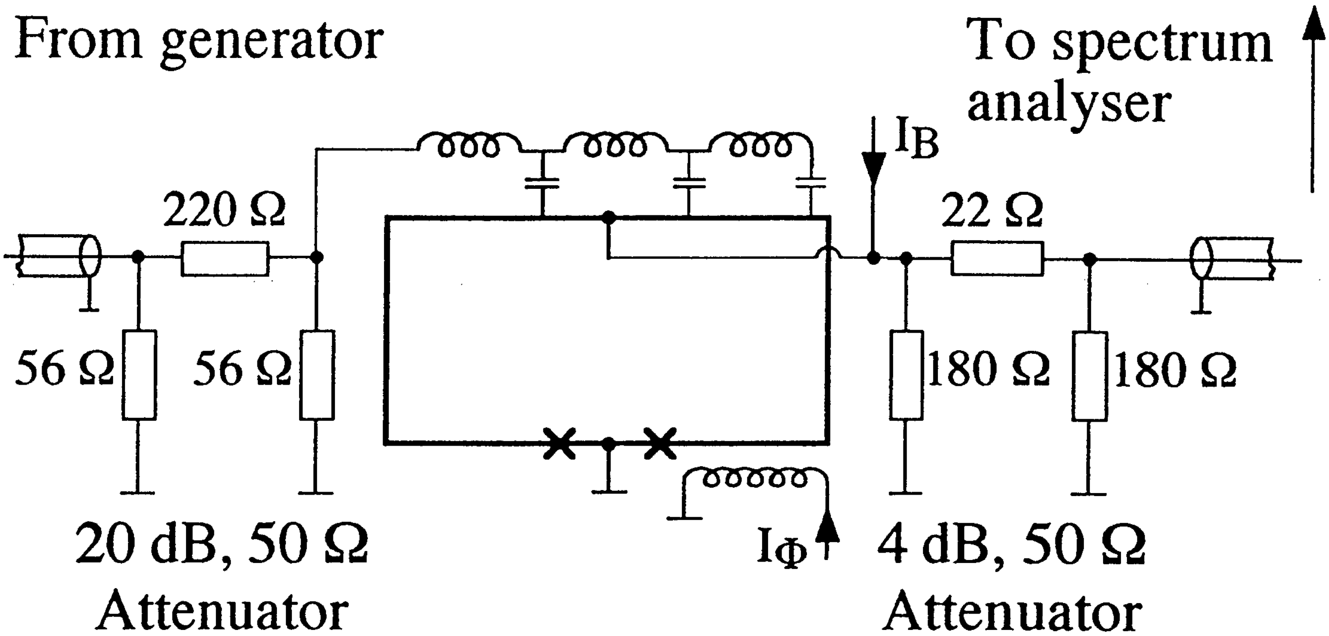


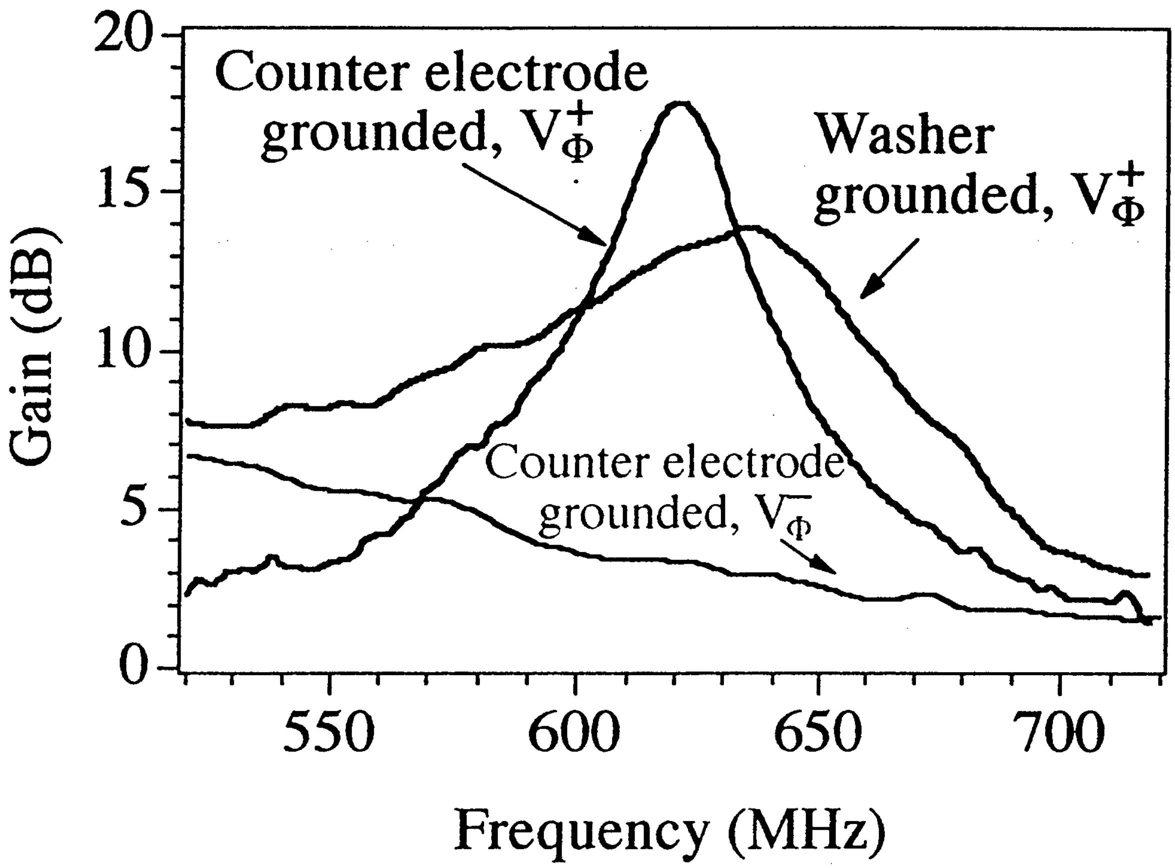

# Gain vs. Coil Length

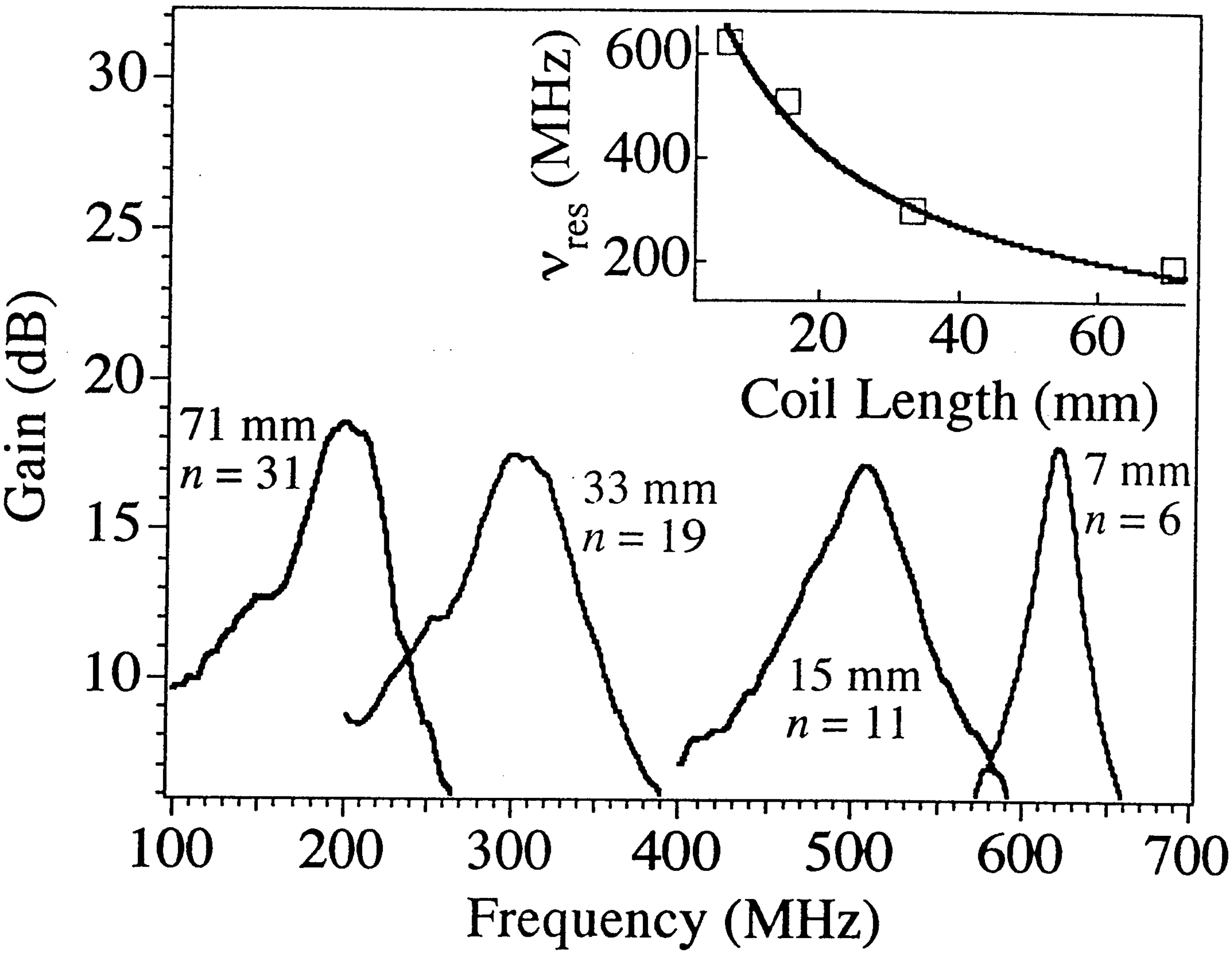


Fitted line in inset: $\nu_{res} = \dfrac{c}{2\sqrt{\varepsilon_r \kappa \chi (l + 16)}}$ ($l$ in mm)

- $c = 3\text{x}10^8$ m/s
- $\varepsilon_r$ (Si) $\approx 9$
- $\kappa \approx 1.75$ arises from inductive loading.
- $\chi \approx 9$ accounts for the SQUID inductance coupled into the microstrip.

# RESONANT FREQUENCY

31-TURN COIL : $\ell = 71\,mm$

FUNDAMENTAL RESONANCE $\underline{\frac{\bar{c}}{2\ell} \approx 530\,MHz}$ FOR $\bar{c} = 0.25c$

MEASURED RESONANT FREQUENCY $\approx$ <u>200MHz</u>

## SCALE MODEL 195:1

31-TURN COPPER COIL ON ONE SIDE OF PC BOARD.

HOLE & SLIT ON THE REVERSE SIDE.

MEASURE RESONANT FREQUENCY OF COIL.

- HOLE & SLIT COVERED WITH Cu SHEET :

  RESONANCE AT EXPECTED FREQUENCY

- HOLE & SLIT UNCOVERED :

  RESONANT FREQUENCY DROPS BY FACTOR ~3

- HENCE IT APPEARS THAT INDUCTANCE COUPLED INTO THE COIL SLOWS THE WAVE VELOCITY.

# Noise Temperature Measurements

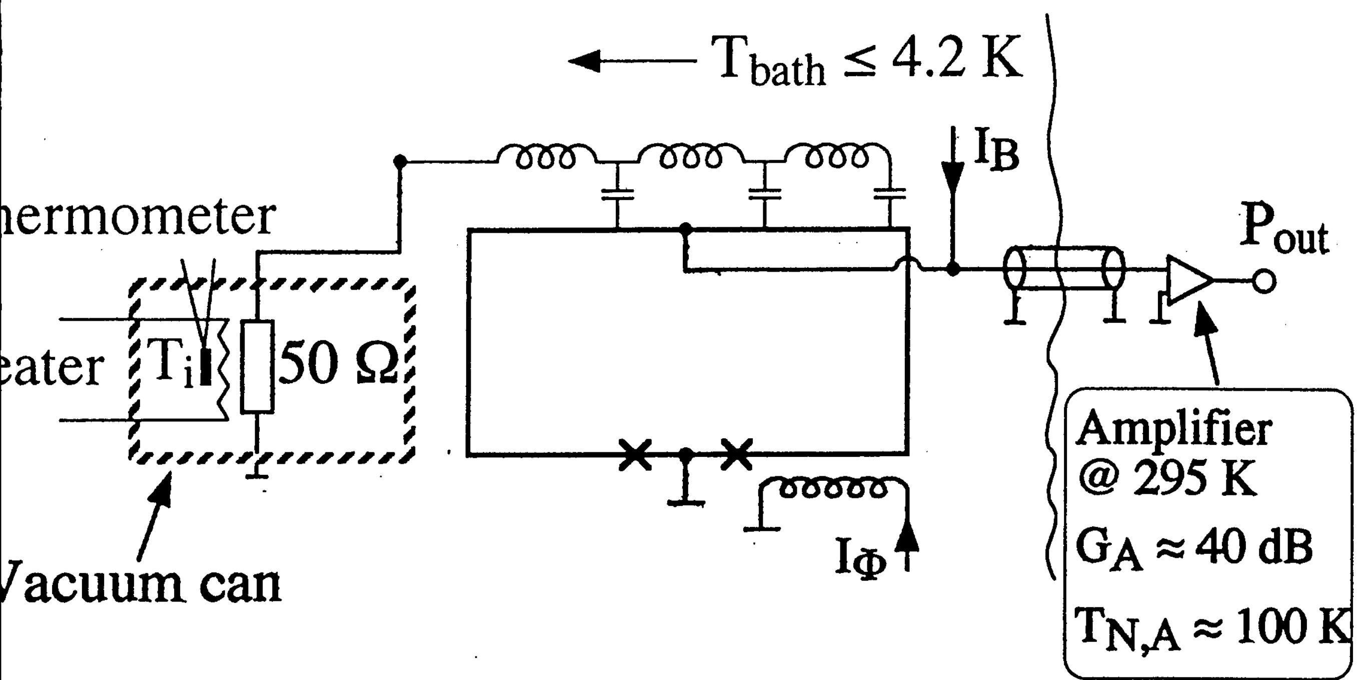


IF WE NEGLECT THE NOISE OF THE POSTAMPLIFIER

$$P_{OUT} = 4k_B(T_i + T_{SQ})G_{SQ}G_A$$

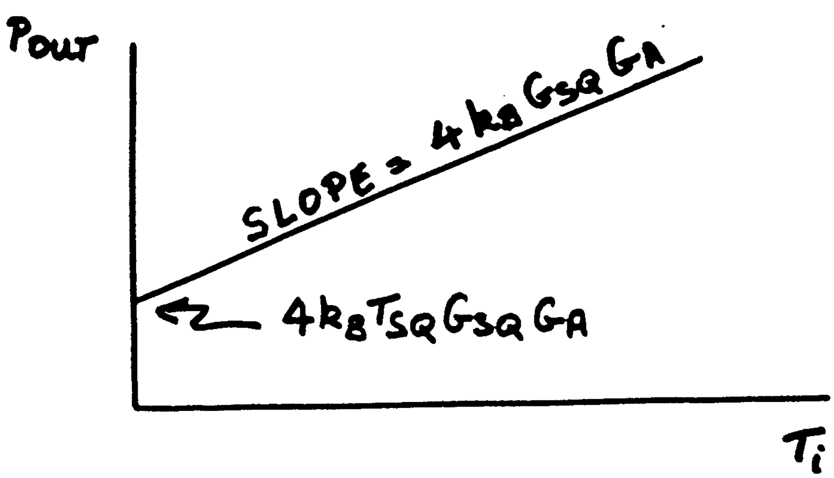

# Results

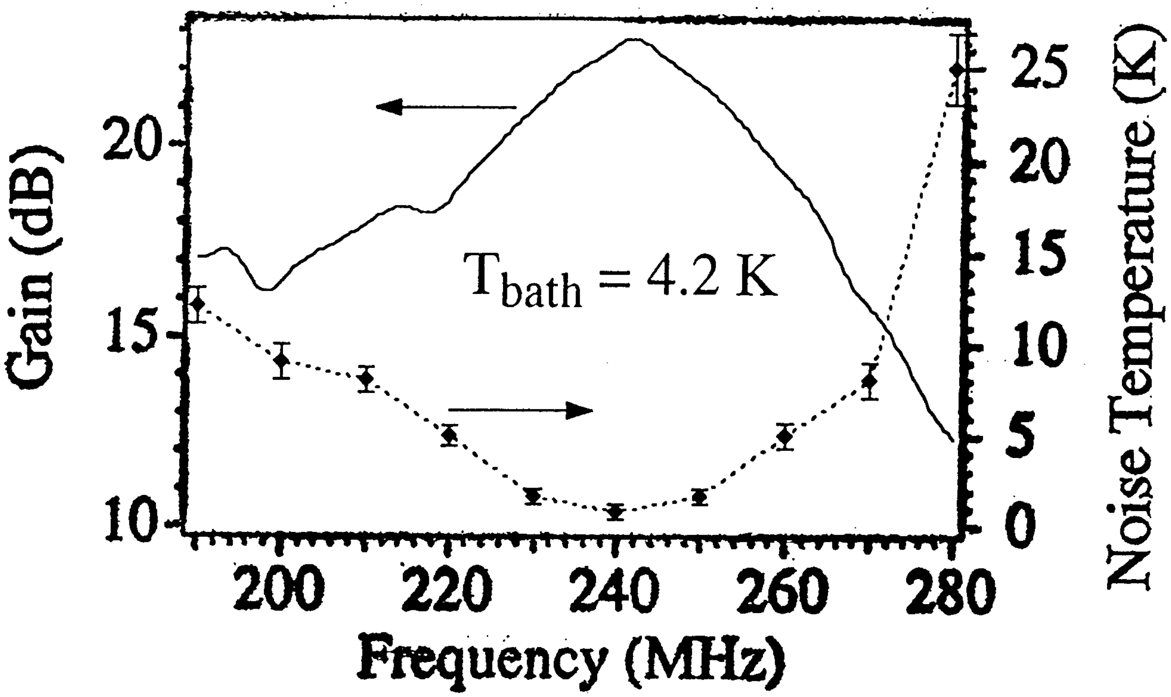


Noise temperature of the 295 K post-amplifier: ~ 100 K.

SQUID Gain ≈ 200 ⟷ 0.5 K at SQUID input.

Using a cold HEMT post-amp ($G_A$ ≈ 17 dB, $T_{N,A}$ ≈ 8 K)

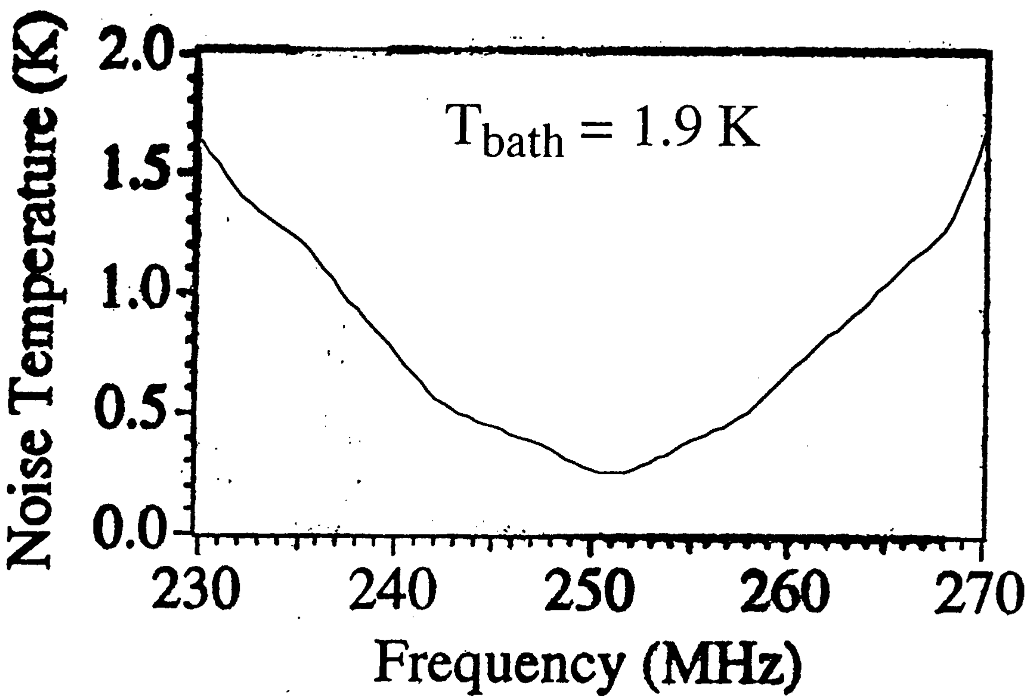

# PERFORMANCE OF MICROSTRIP SQUID AMPLIFIERS WITH COOLED HEMT POSTAMPLIFIER

| FREQUENCY (MHz) | T | GAIN | $T_N^{(SYS)}$ | $T_N^{(SQ)}$ |
|---|---|---|---|---|
| 90 | 4.2 | 24 | $0.90 \pm 0.12$ | $0.86 \pm 0.12$ |
| 90 | 0.4 | 24.5 | $0.10 \pm 0.02$ | $0.06 \pm 0.02$ |
| 438 | 4.2 | 20 | $1.40 \pm 0.18$ | $1.02 \pm 0.19$ |
| 438 | 0.5 | 20 | $0.50 \pm 0.07$ | $0.12 \pm 0.10$ |

NOTE: AT 438 MHz, $T_N^{QL} = hf/k_B \ln 2 \approx \underline{0.03K}$

# RESONANT FREQUENCY

31-TURN COIL : $\ell = 71\text{mm}$

FUNDAMENTAL RESONANCE $\frac{\bar{c}}{2\ell} \approx 530\text{MHz}$ FOR $\bar{c} = 0.25c$

MEASURED RESONANT FREQUENCY $\approx$ 200MHz

## SCALE MODEL 195:1

31-TURN COPPER COIL ON ONE SIDE OF PC BOARD.

HOLE & SLIT ON THE REVERSE SIDE.

MEASURE RESONANT FREQUENCY OF COIL.

- HOLE & SLIT COVERED WITH Cu SHEET :

  RESONANCE AT EXPECTED FREQUENCY

- HOLE & SLIT UNCOVERED :

  RESONANT FREQUENCY DROPS BY FACTOR ~3

- HENCE IT APPEARS THAT INDUCTANCE COUPLED INTO THE COIL SLOWS THE WAVE VELOCITY.

# Noise Temperature Measurements

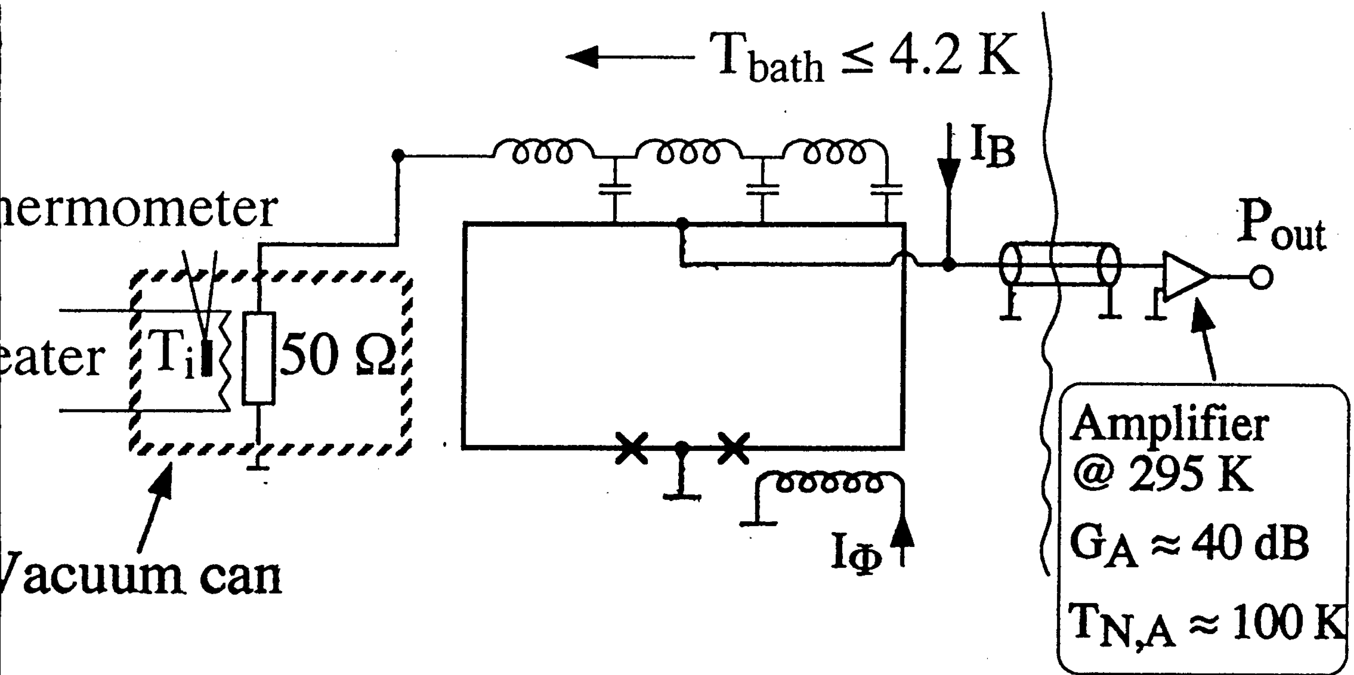


IF WE NEGLECT THE NOISE OF THE POSTAMPLIFIER

$$P_{OUT} = 4k_B (T_i + T_{SQ}) G_{SQ} G_A$$

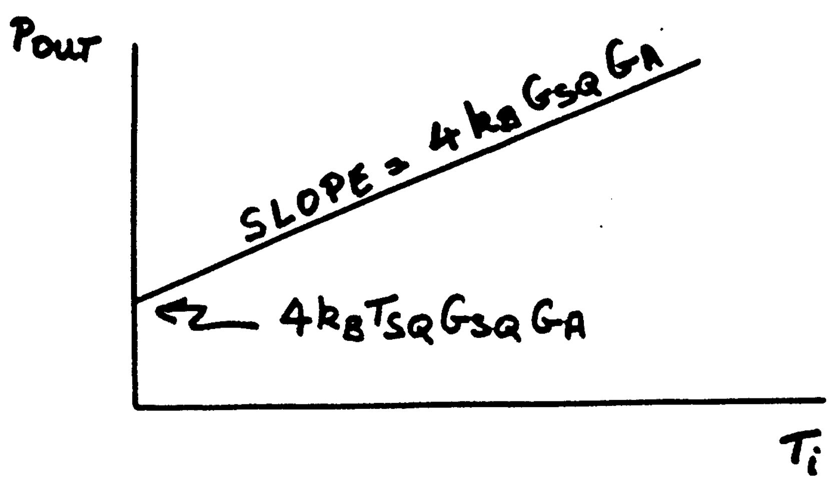

# Results

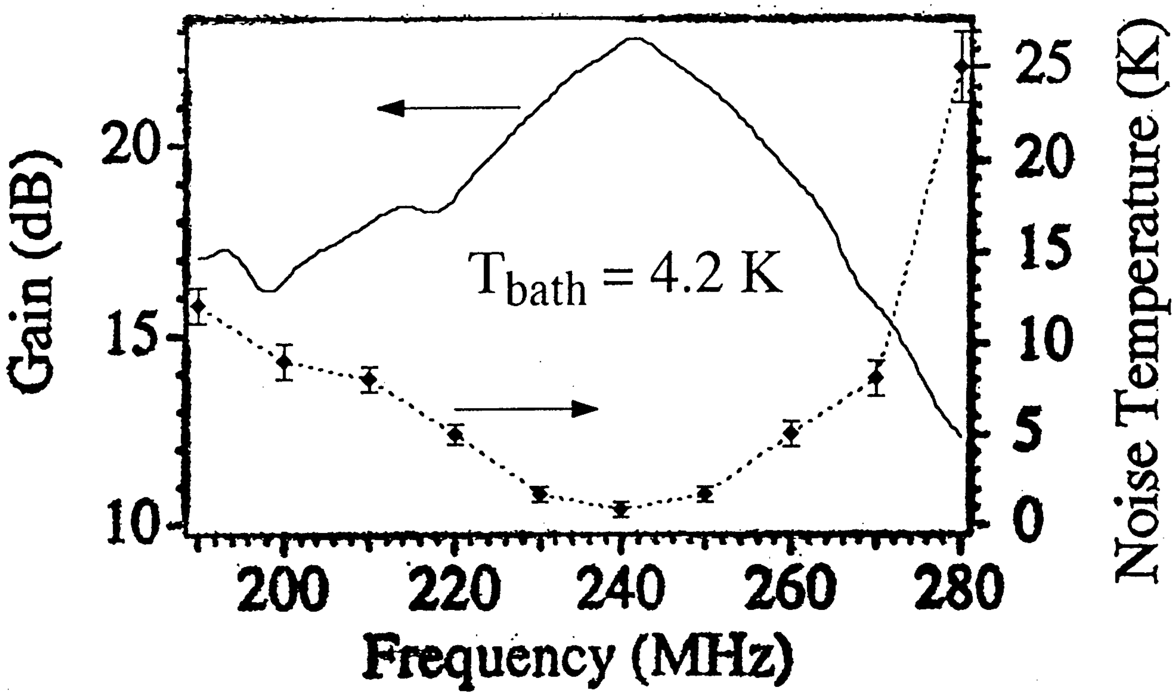


**oise temperature of the 295 K post-amplifier:** ~ 100 K.

**QUID Gain ≈ 200** ⟷ 0.5 K at SQUID input.

**sing a** cold **HEMT post-amp ($G_A$ ≈ 17 dB, $T_{N,A}$** ≈ 8 K)

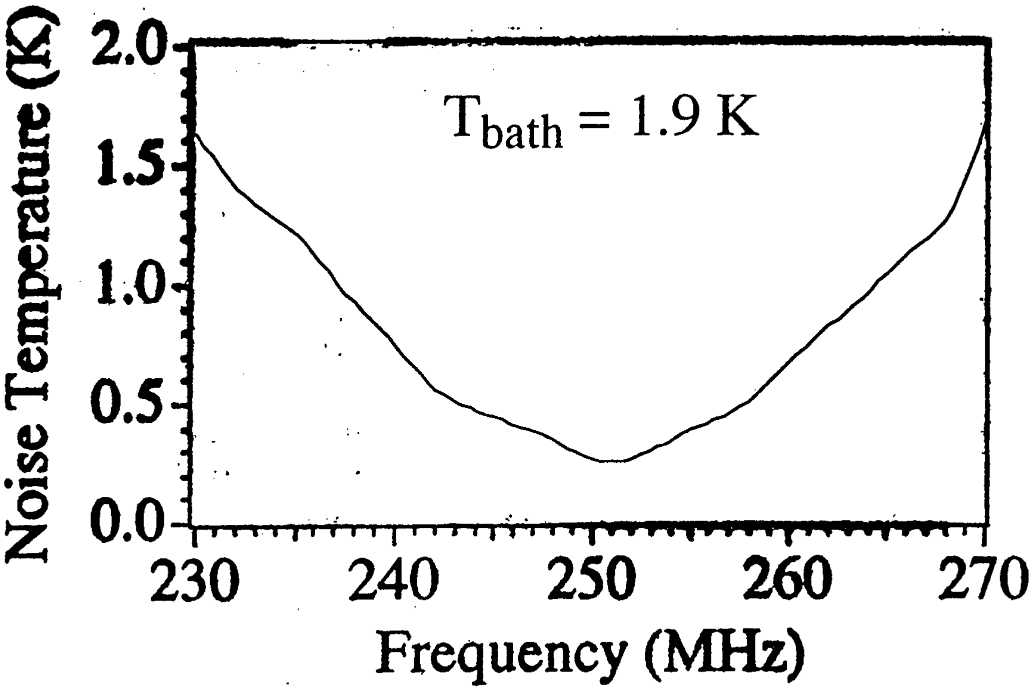

# PERFORMANCE OF MICROSTRIP SQUID AMPLIFIERS WITH COOLED HEMT POSTAMPLIFIER

| FREQUENCY (MHz) | T | GAIN | $T_N^{(SYS)}$ | $T_N^{(SQ)}$ |
|---|---|---|---|---|
| 90 | 4.2 | 24 | $0.90 \pm 0.12$ | $0.86 \pm 0.12$ |
| 90 | 0.4 | 24.5 | $0.10 \pm 0.02$ | $0.06 \pm 0.02$ |
| 438 | 4.2 | 20 | $1.40 \pm 0.18$ | $1.02 \pm 0.19$ |
| 438 | 0.5 | 20 | $0.50 \pm 0.07$ | $0.12 \pm 0.10$ |

NOTE: AT 438 MHz, $T_N^{QL} = hf/k_B \ln 2 \approx \underline{0.03K}$

# LC - Resonator Input

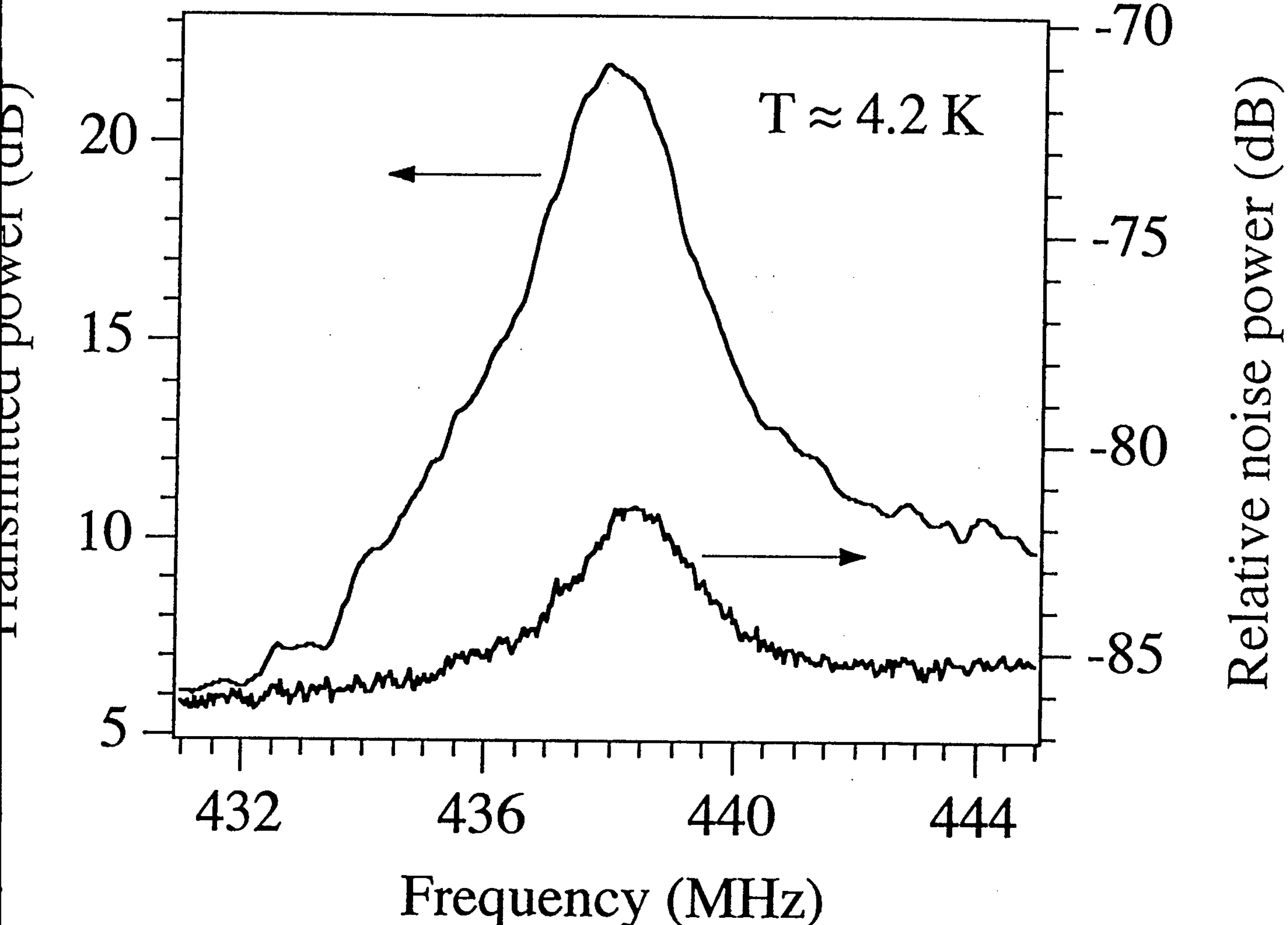

# LC - Resonator Input

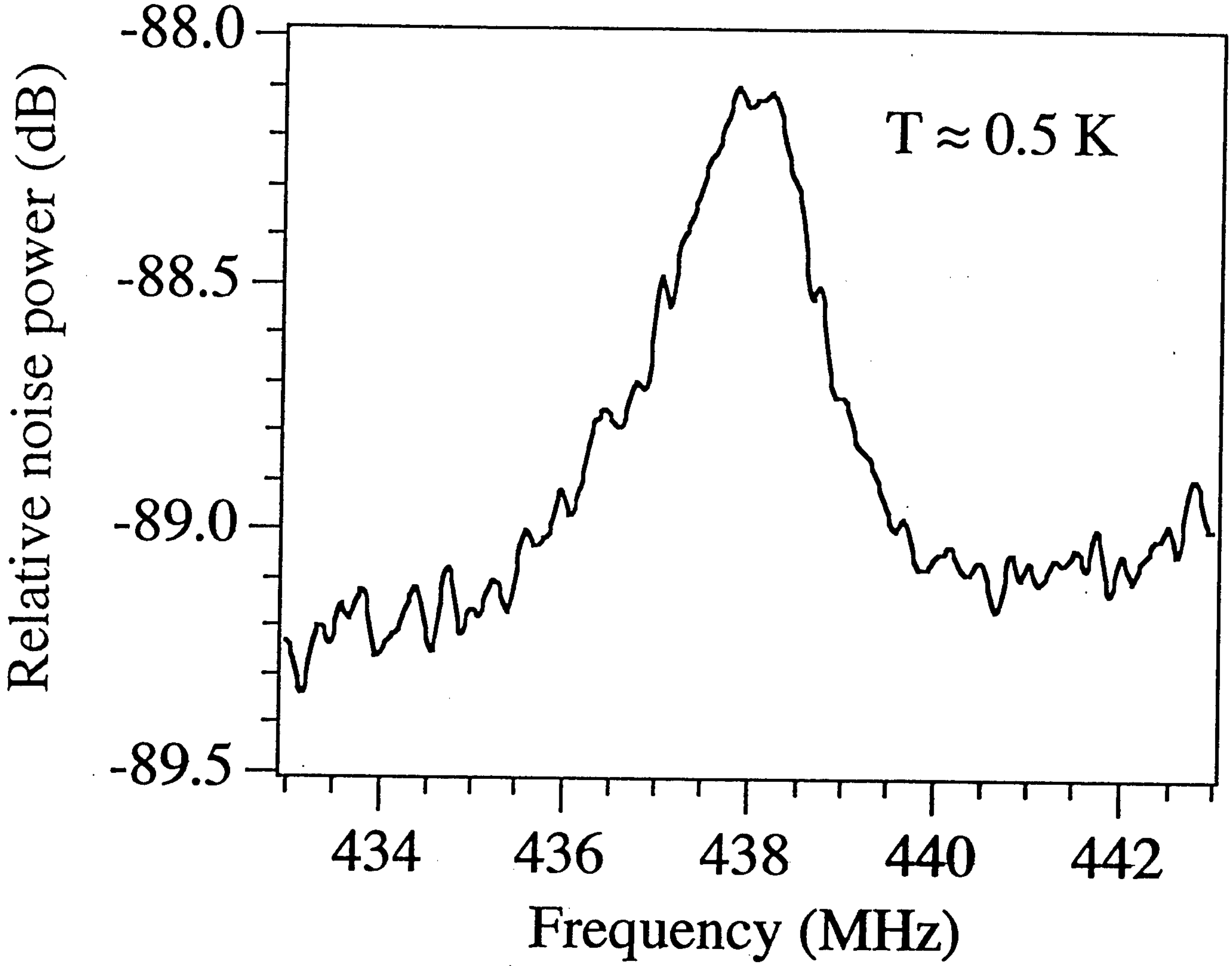


INFER $T_N^{(SYS)} \approx \underline{0.5\ K}$

[MEASURED $T_N^{(SYS)} = 0.50 \pm 0.07 K$]

# TERMINATION OF MICROSTRIP

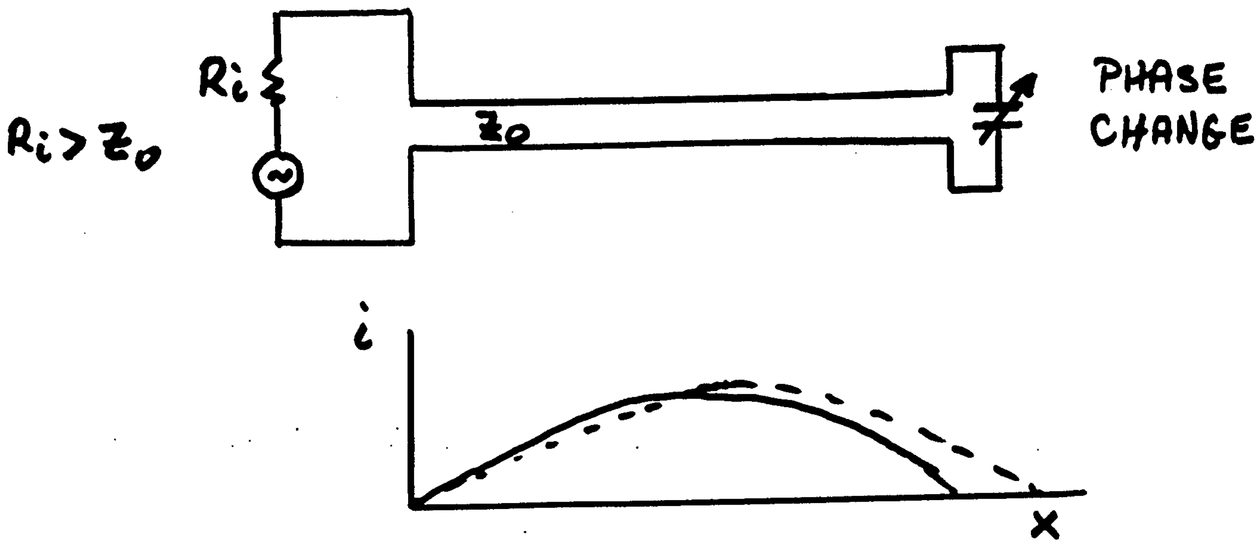

# aractor tuning of microstrip SQUID

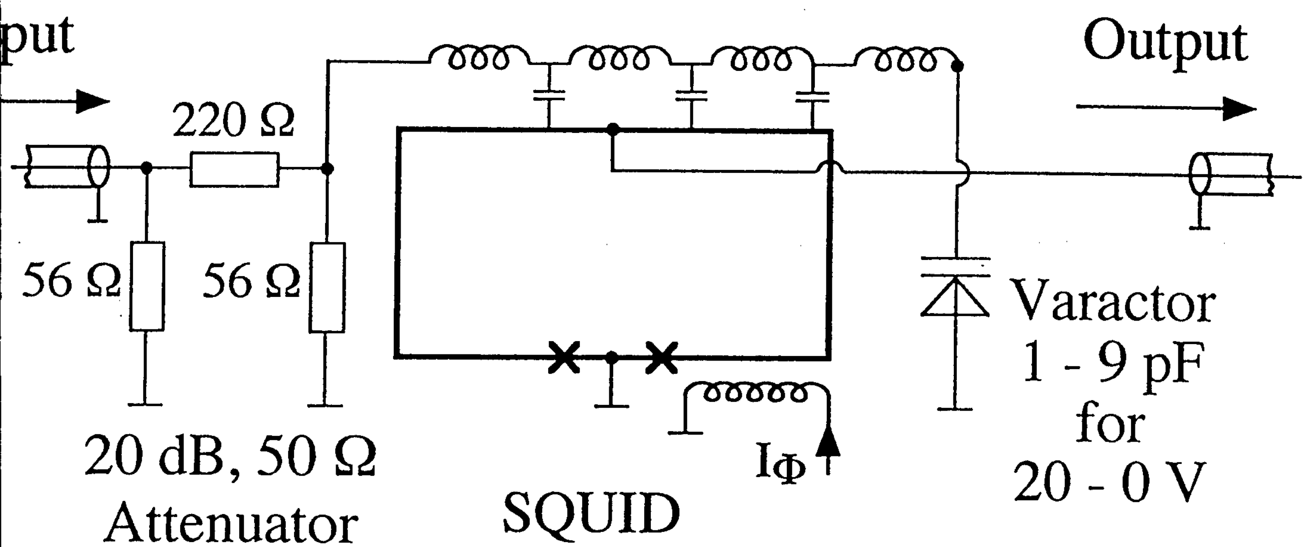


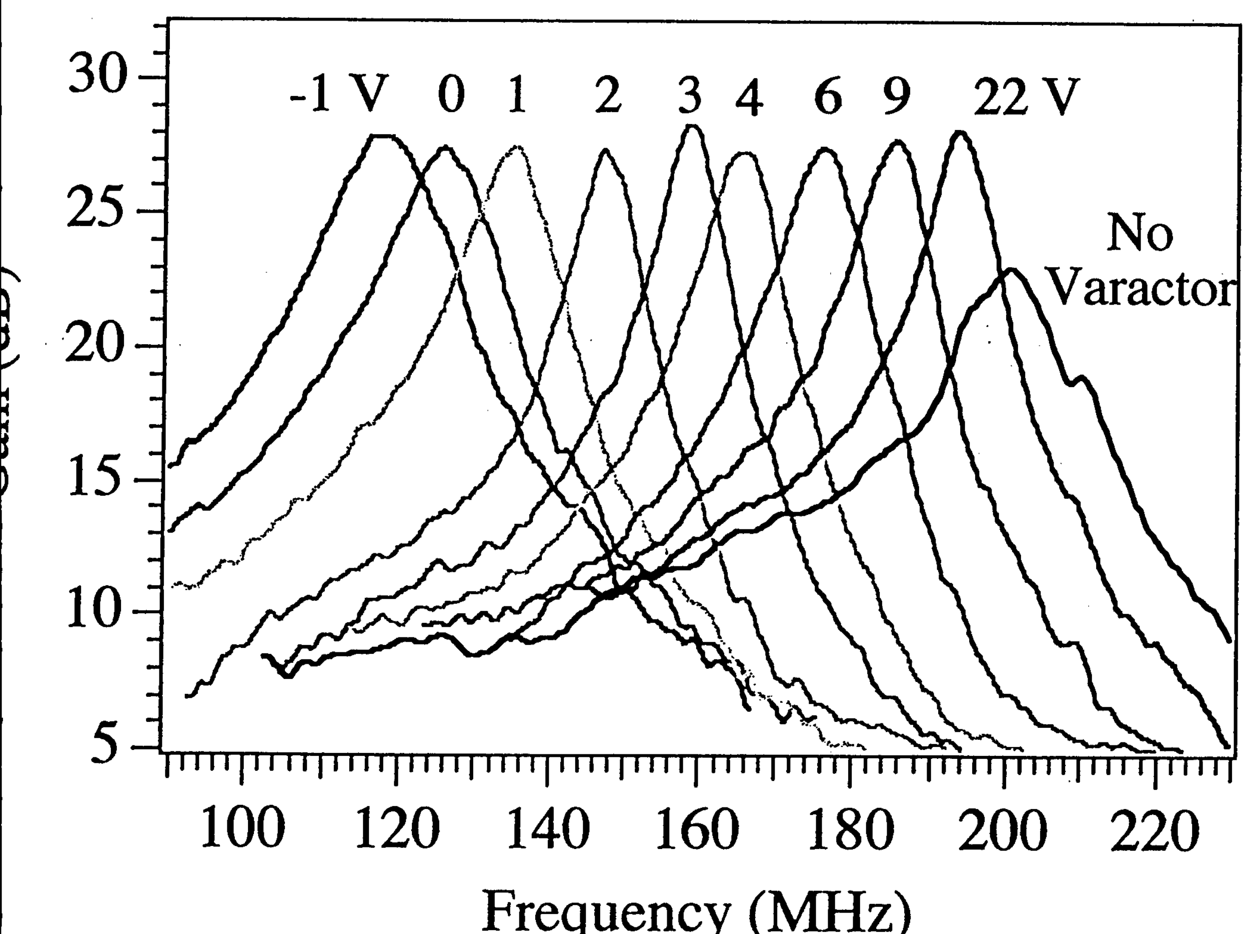

# SQUID Postamplifier

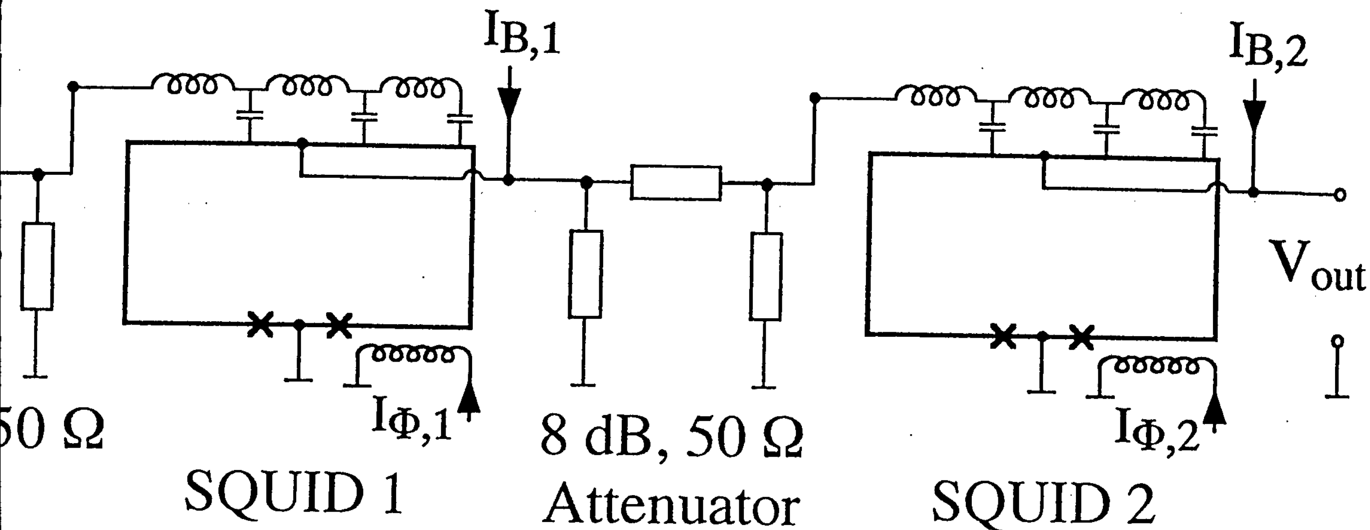


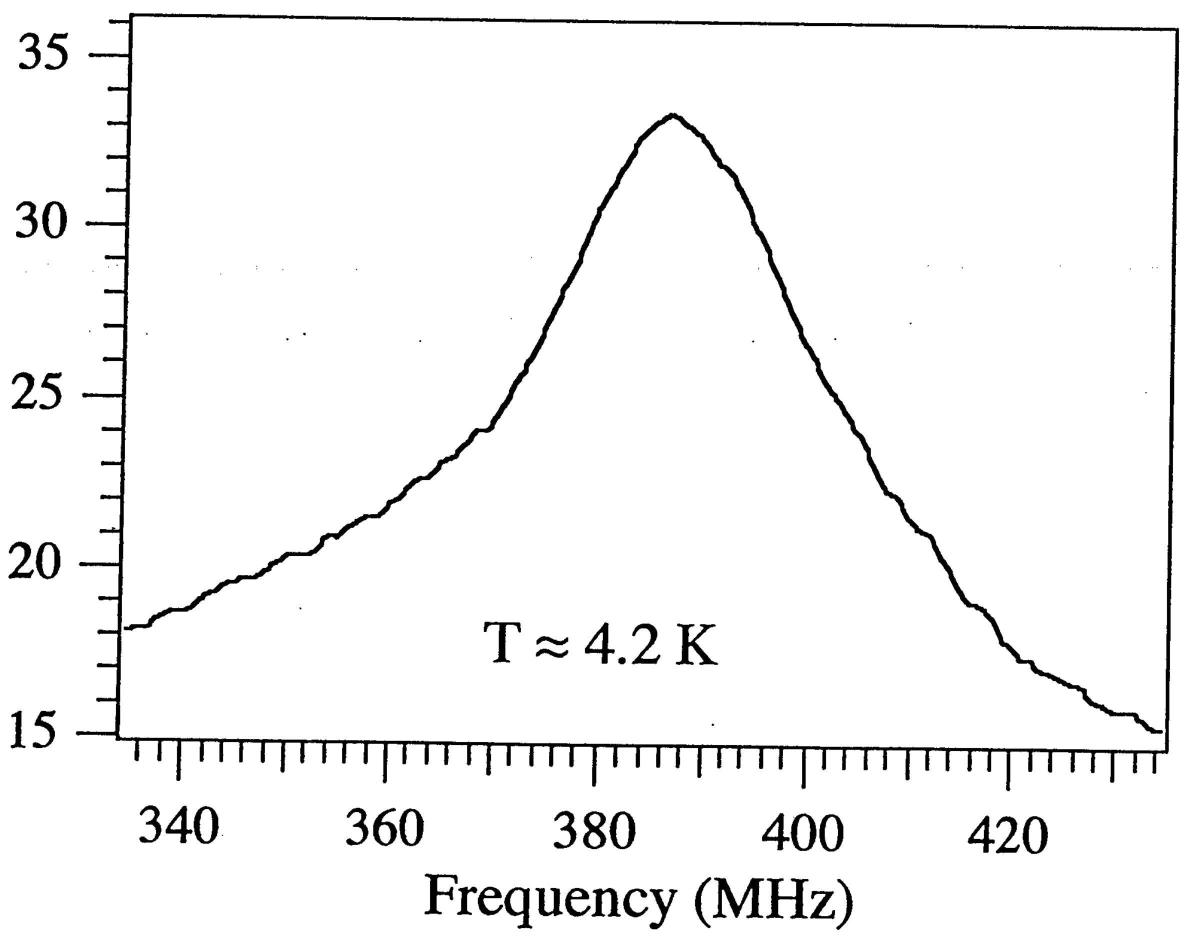

## Microstrip SQUID Amplifier: Summary

- Gain $\gtrsim$ 20 dB for frequencies $\lesssim$ 1 GHz
- With cooled postamplifier and T = 0.4 – 0.5 K:

  $$T_N^{(SQ)} \sim 0.1 \text{ K}$$
- Tunable over factor of 2 with varactor diode
- Second SQUID used as postamplifier
- Cooled to 0.1 K, SQUID should be

  Quantum Limited ($f \gtrsim 1/2$ GHz)

# Magnetotactic Bacteria

- Yann Chemla

  Helene Grossman

  Tom Lee

- Bob Buchanan -- Microbiology

  Mike Adamkiewicz

# MICROSCOPE SCHEMATIC

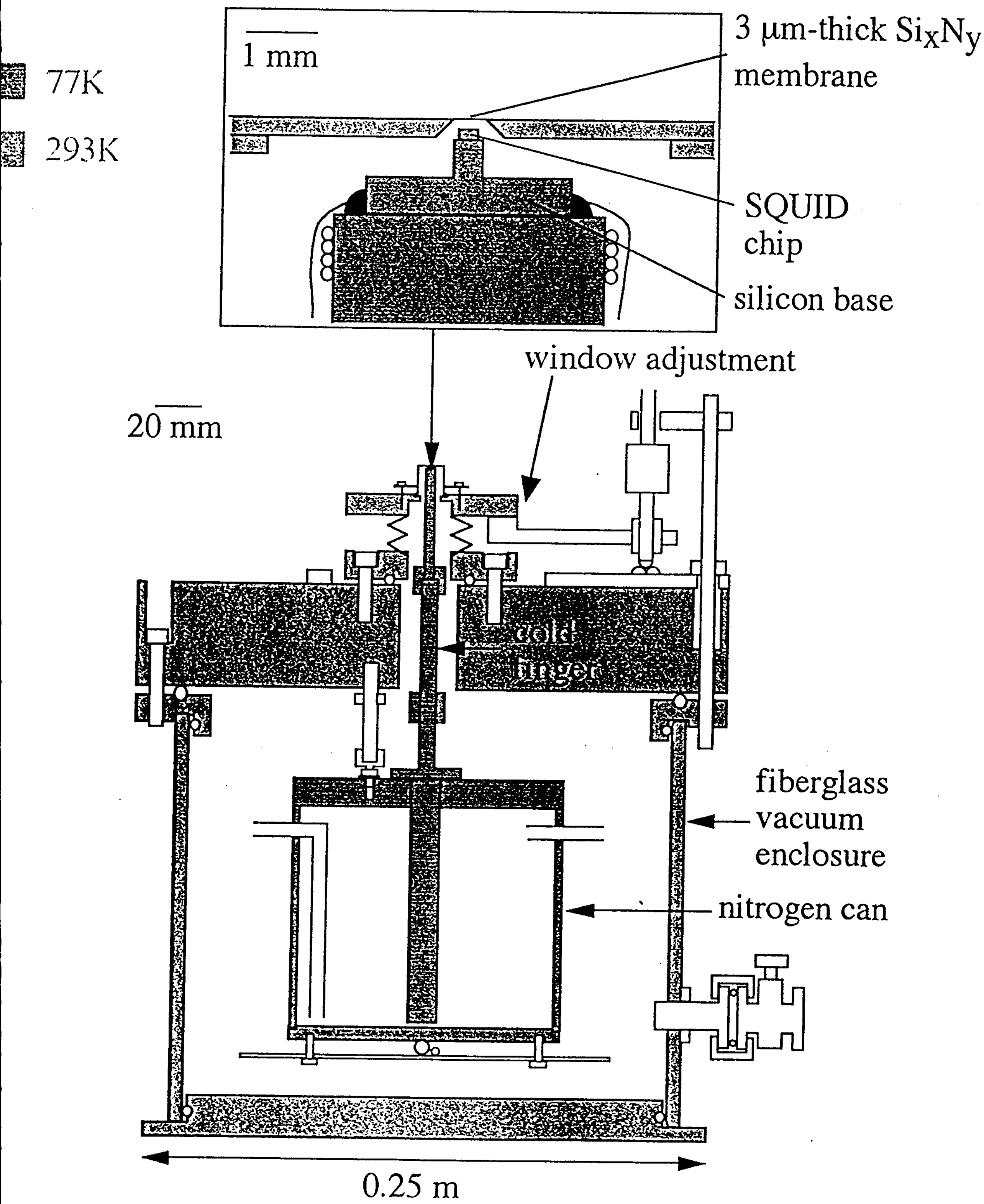

# Magnetotactic Bacteria

Bacteria MS-1 (*Magnetospirillum magnetotacticum*):

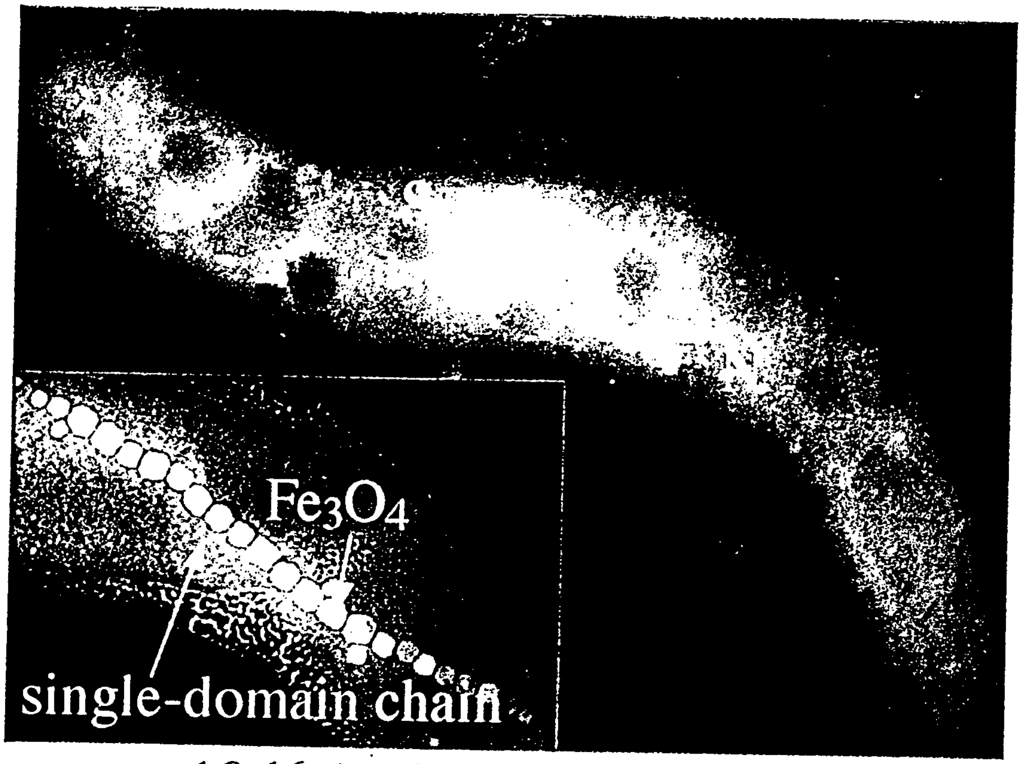


$\mathbf{m} \sim 10^{-16}\ Am^2$

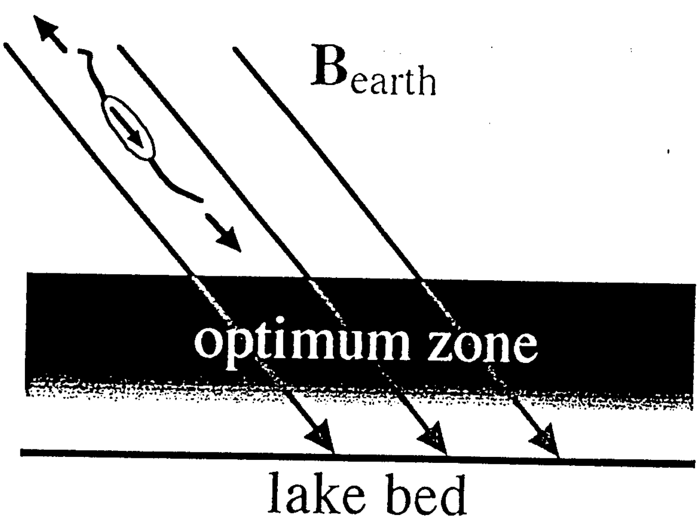


Magnetotaxis:
- $-\mathbf{m} \bullet \mathbf{B} \sim 10\ k_BT$
- 3-D $\Rightarrow$ 1-D

A. S. Bahaj, et. al. http://www.soton.ac.uk)
R. P. Blakemore (1982) *Ann. Rev. Microbiol.* **36**, 217-38)

# Experimental Setup

- Observe bacteria in solution
- Parameters:
  - shielded environment ($B<2x10^{-5}$ $B_e$)
  - cell concentrations: $10^7$-$10^8$ cells/ml
  - SQUID ~30μm away

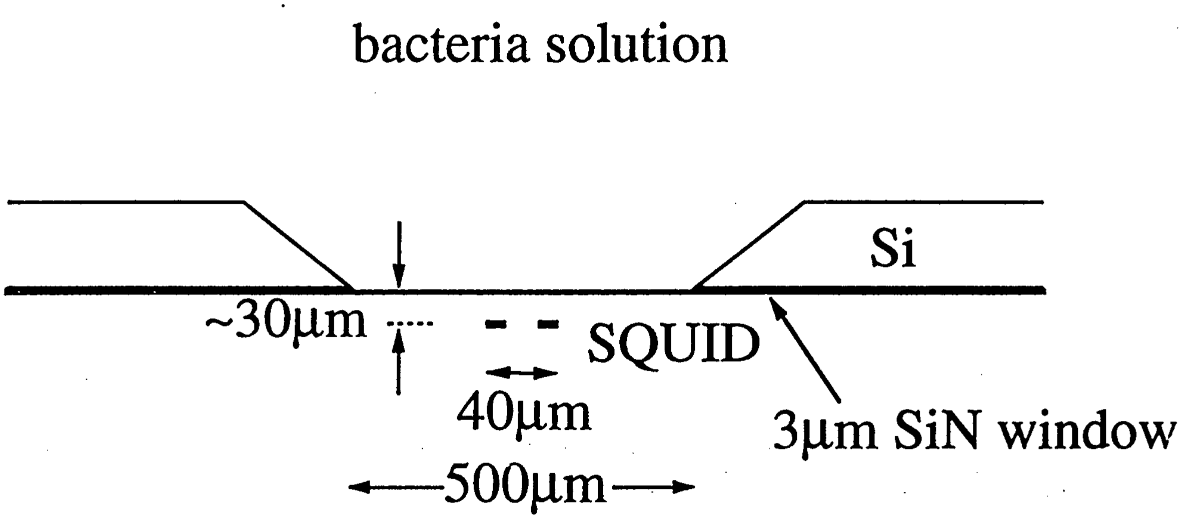


- Measurement:

motion of bacteria in solution

↓

magnetic flux fluctuations

↓

measure flux noise spectral density: $\mathbf{S_\Phi(f)}$

# Dead Bacteria

Rotational Brownian motion of magnetic dipoles:

$$\Rightarrow S_\Phi(f) \sim \frac{2\tau_o}{1+(2\pi\tau_o f)^2} \quad \tau_o = \alpha_r/2k_BT, \quad \alpha_r = \text{rotational drag coeff.}$$

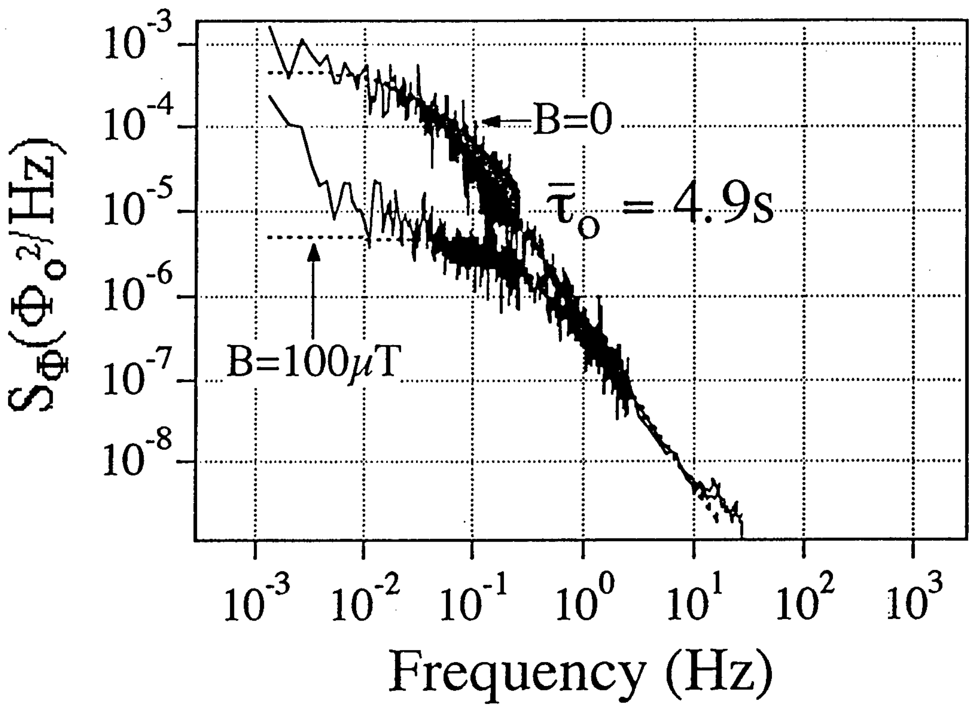


Model bacteria as cylinders:

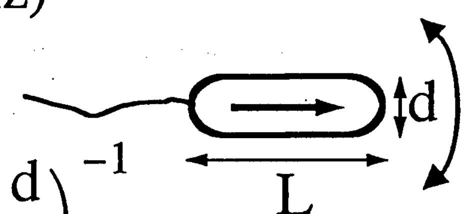


$$\tau_o \approx \frac{\pi\eta L^3}{6k_BT}\left(\ln\frac{L}{d} - 0.662 + 0.92\frac{d}{L}\right)^{-1}$$

For $d \sim 0.7\mu m \Rightarrow L \approx 3.5\mu m, \Delta L \approx 0.7\mu m$

In a field, noise is reduced and $\tau_o \Rightarrow \tau_B = \alpha_r/2mB$

$$\Rightarrow m = 3.0 \times 10^{-16} Am^2$$

(M. M. Tirado, et al (1980) *J. Chem. Phys.* **73**(4), 1986-93)

# Relaxation in a Field

- Turn off a field & measure randomization time:

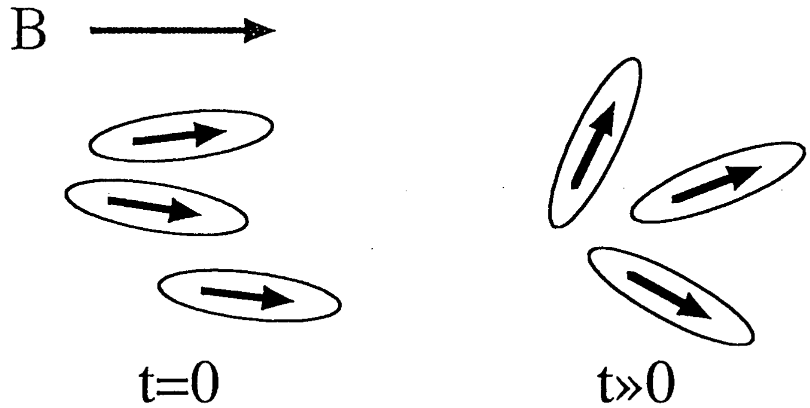


$$\Rightarrow \Phi(t) \sim e^{-t/\tau_o}$$
$$\tau_o = \alpha_r / 2k_B T$$

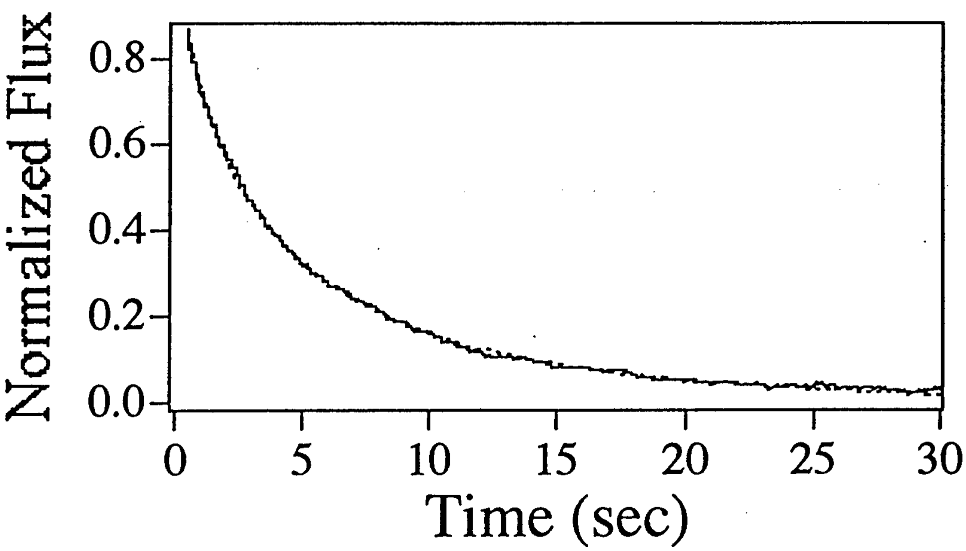


$$\Rightarrow \bar{\tau}_o = 4.8\text{s}$$

# Alignment in a Field

- Turn on a field & measure alignment time:

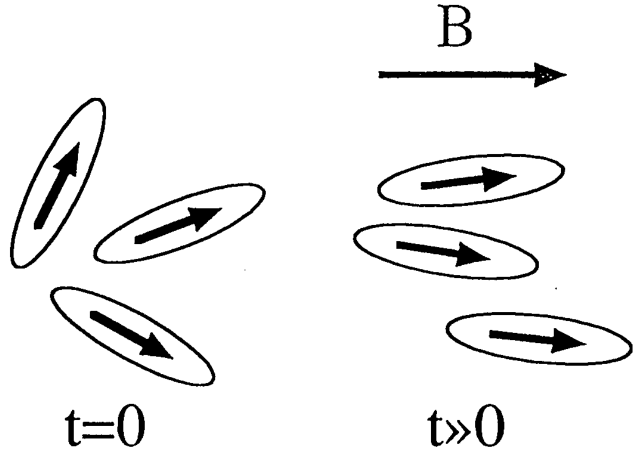


$$\Rightarrow \Phi(t) \sim e^{-t/\tau_B}$$
$$\tau_B = \alpha_r / 2mB$$

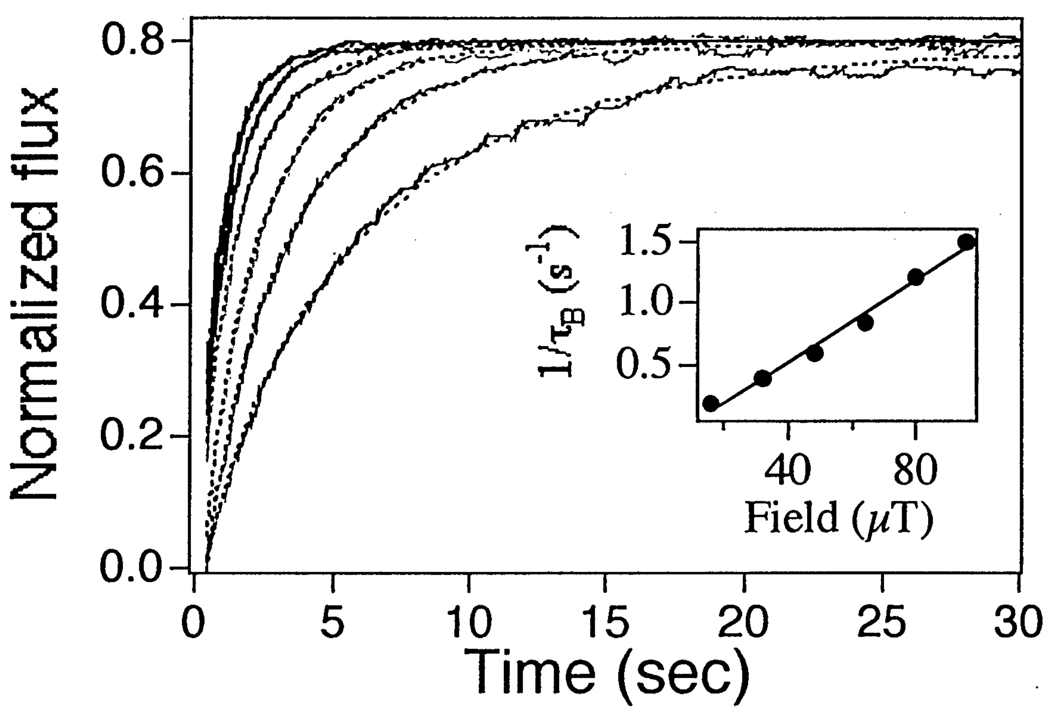


$$\Rightarrow m = 3.2 \times 10^{-16} \mathrm{Am}^2$$

# Live Bacteria

Universal features:
- high frequency peaks: (1) ~65Hz, (2) ~25Hz
- shift in low freq. knee: (3) ~0.1Hz
- deviation from Lorentzian

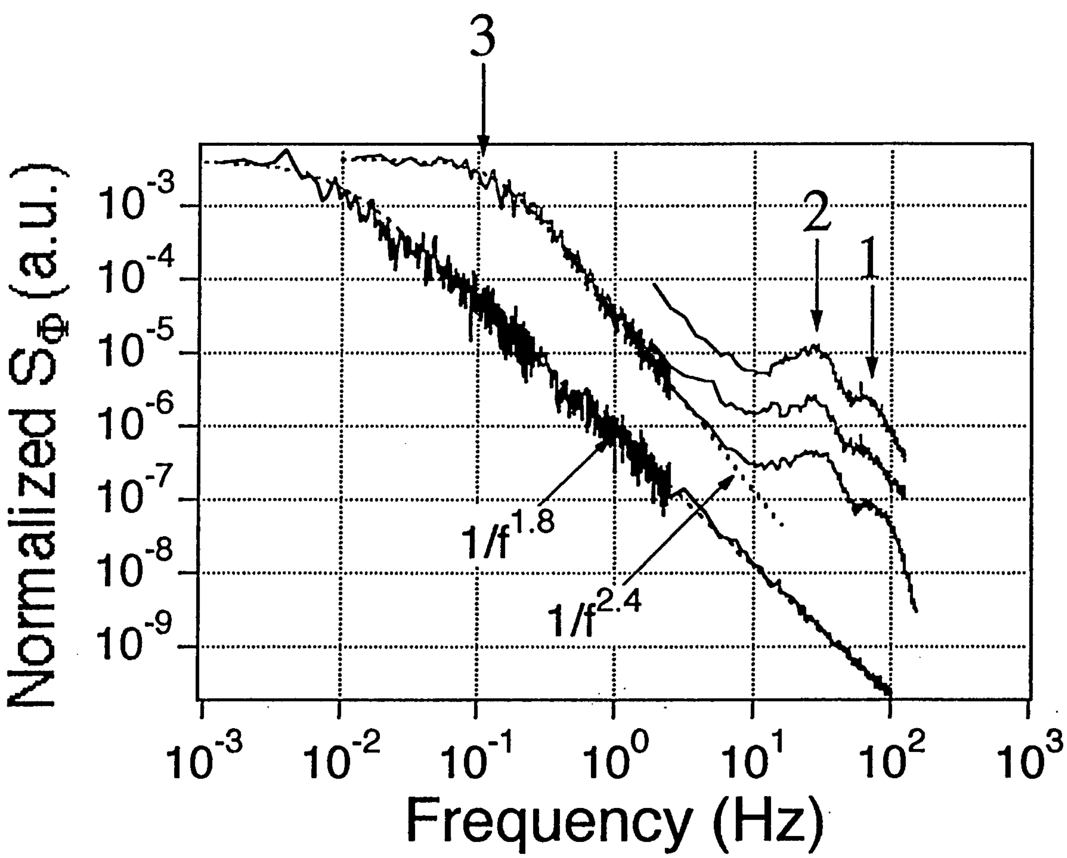

# Modeling

- Vibration or "gyration"
  - imbalance in drag forces
  - vibration at flagellar frequency ~ 100Hz

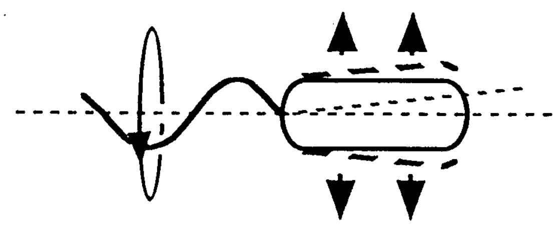

- Precession or "wobble"
  - body rolls counter to flagellum
  - body & flagellar axes not collinear
  - precession at lower frequency

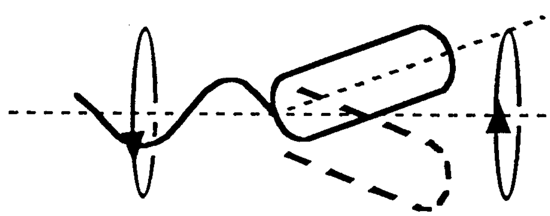

- Model vibration & precession as rotations of dipole about two axes:

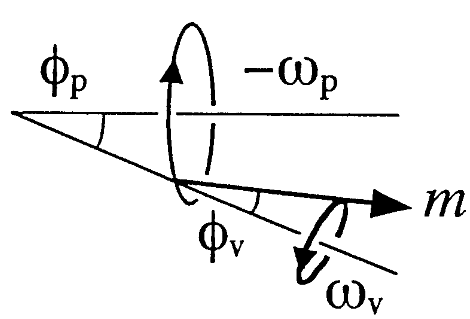


- In lab frame, measure peaks at $f_p$ and $f_v$-$f_p$.

# High Frequency Behavior

Model vibration & precession as rotations of dipole about two axes:

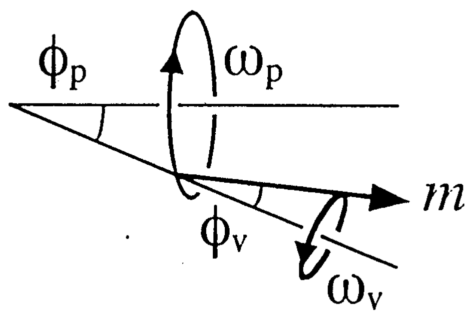


Fit spectrum to Gaussian distribution of frequencies:
- $\phi_v$, $\phi_p$ determined by scaling to $S_\Phi(f=0)$

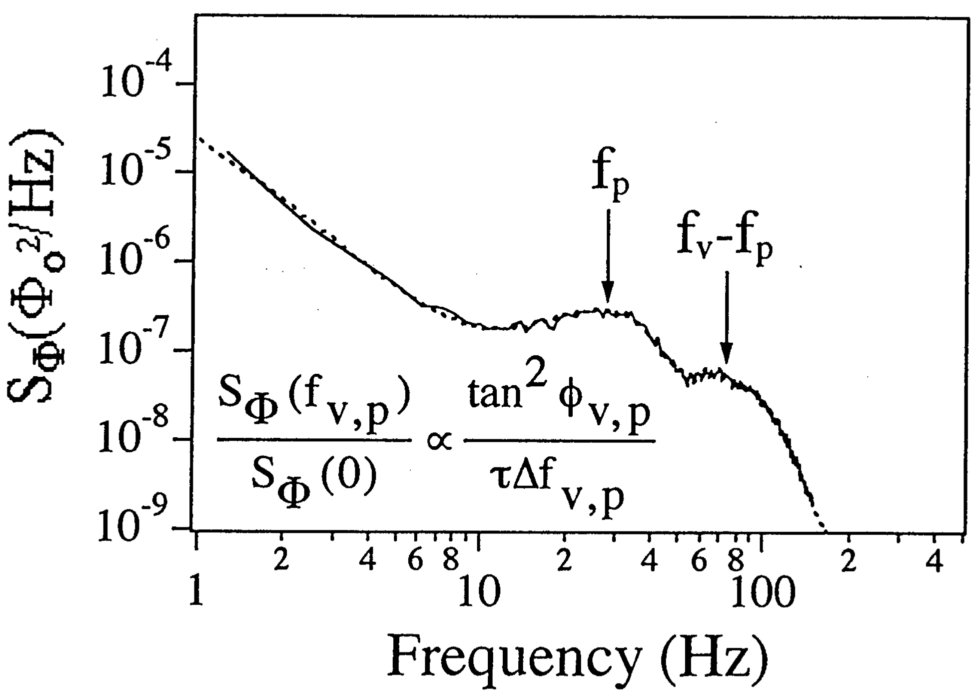


$f_v$=89Hz, $\Delta f_v$=30Hz, $\phi_v$=5.5°

$f_p$=26Hz, $\Delta f_p$=10Hz, $\phi_p$=7.0°

# Time scan of single bacterium

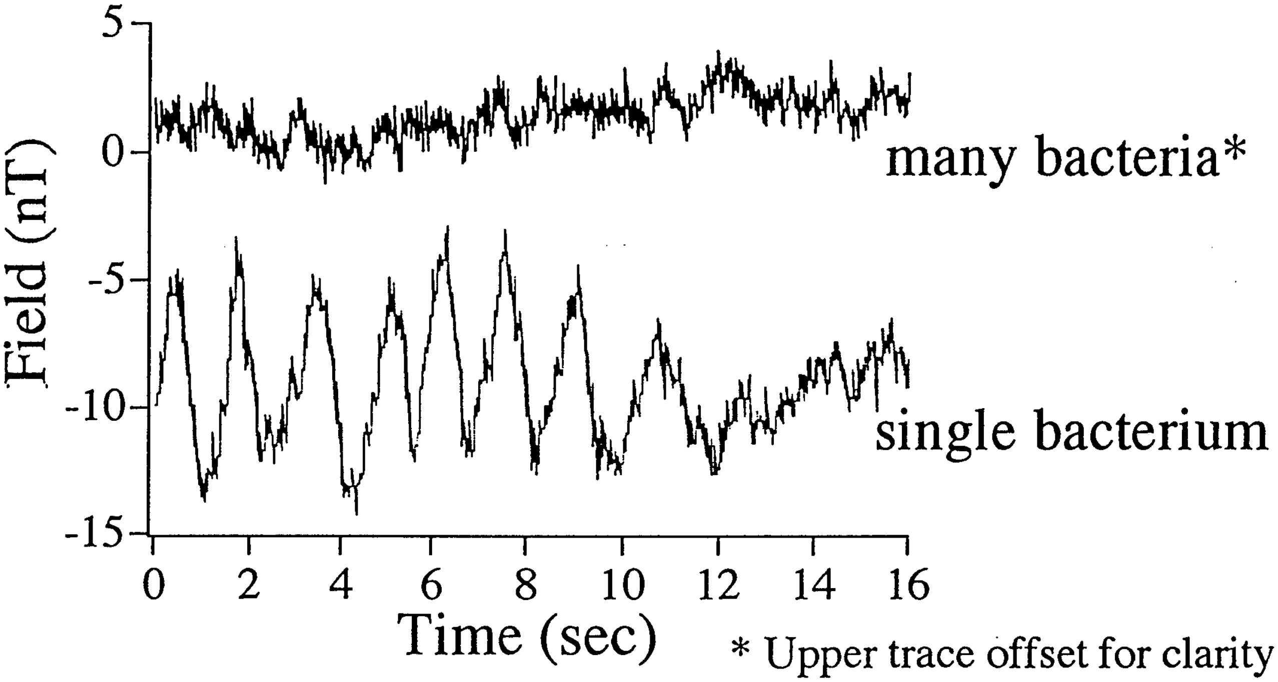


* Upper trace offset for clarity

Interpretation: orbits near surfaces

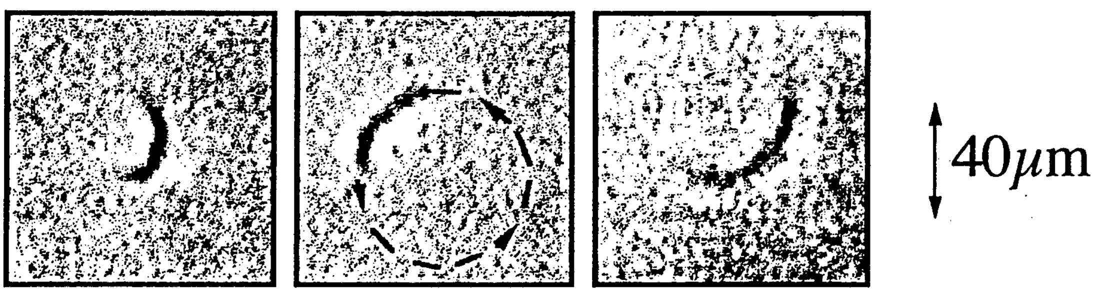


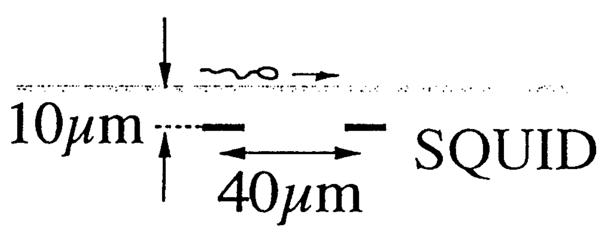


Amplitude and period consistent

Sensitivity: $<10^{-17}$ Am$^2$ in 1Hz ⇔ one 35nm particle ~15-30$\mu$m away

P. D. Frymier, et al (1995) *Proc. Natl. Acad. Sci USA* **92**, 6195-99)

## MAGNETIC MOMENT RESOLUTION

- MAGNETIC MOMENT OF ONE BACTERIUM $\approx 3 \times 10^{-16}\ Am^2$

- S/N RATIO OF SWIMMING BACTERIUM
  $\approx$ 20:1 IN 25 Hz BANDWIDTH

- THUS, MICROSCOPE RESOLUTION $\approx 3 \times 10^{-18}\ Am^2/Hz^{1/2}$
  $\approx 3 \times 10^{5}\ \mu_B/Hz^{1/2}$

- NOTE: EACH BACTERIUM CONTAINS $\sim$ 30 MAGNETOSOMES
  WITH A MAGNETIC MOMENT $\sim 10^{-17}\ Am^2$.
  THUS, ONE COULD DETECT 1 MAGNETOSOME
  WITH A S/N RATIO $\sim 3\ (Hz^{-1/2})$

# Immunoassay

Physikalisch Technische Bundesanstalt, Berlin
Institut für Diagnostikforschung GmbH, Berlin
Schering Ag, Berlin

Magnetically tag antibody

Attach antigen to substrate

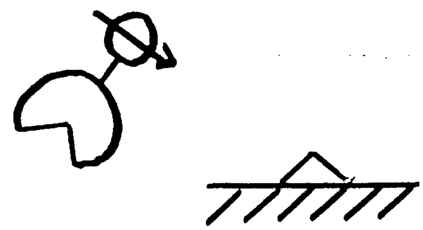

Allow interaction to take place

Apply magnetic field for a few seconds

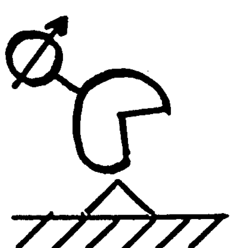

Brownian rotation of antibody yields zero average magnetic field

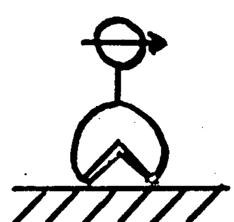

Remanent magnetization of magnetic tag produces nonzero field

# MAGNETIC FIELD GRADIENTS

MAGNETIC DIPOLE MOMENT $m$

$$B \sim \frac{m}{r^3}$$

$$\frac{dB}{dr} \sim \frac{m}{r^4}$$

$$\frac{d^2B}{dr^2} \sim \frac{m}{r^5}$$

# FLUX TRANSFORMERS

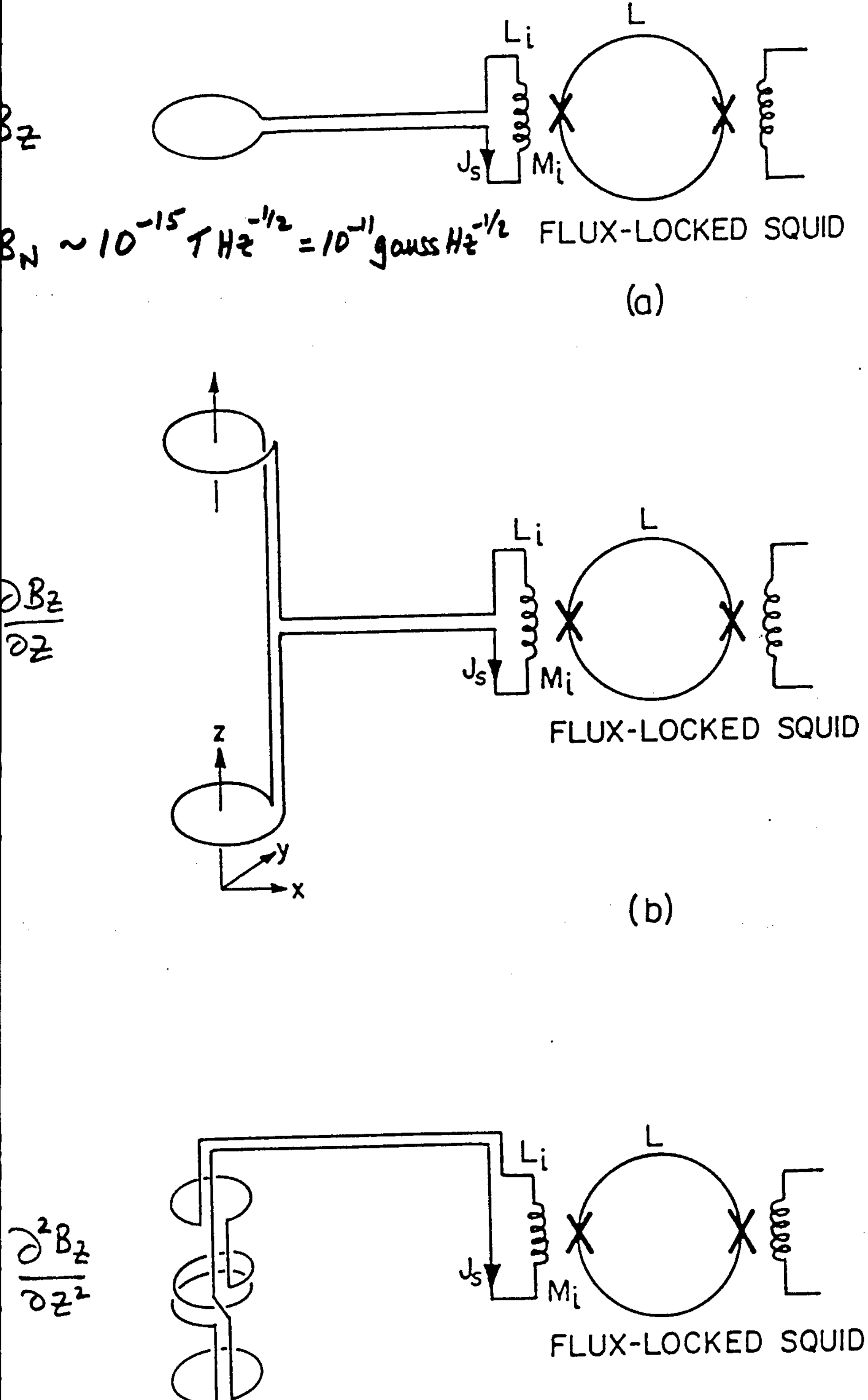


XBL 766-7138A

# JÜLICH GRADIOMETER (TAVRIN ET AL.)

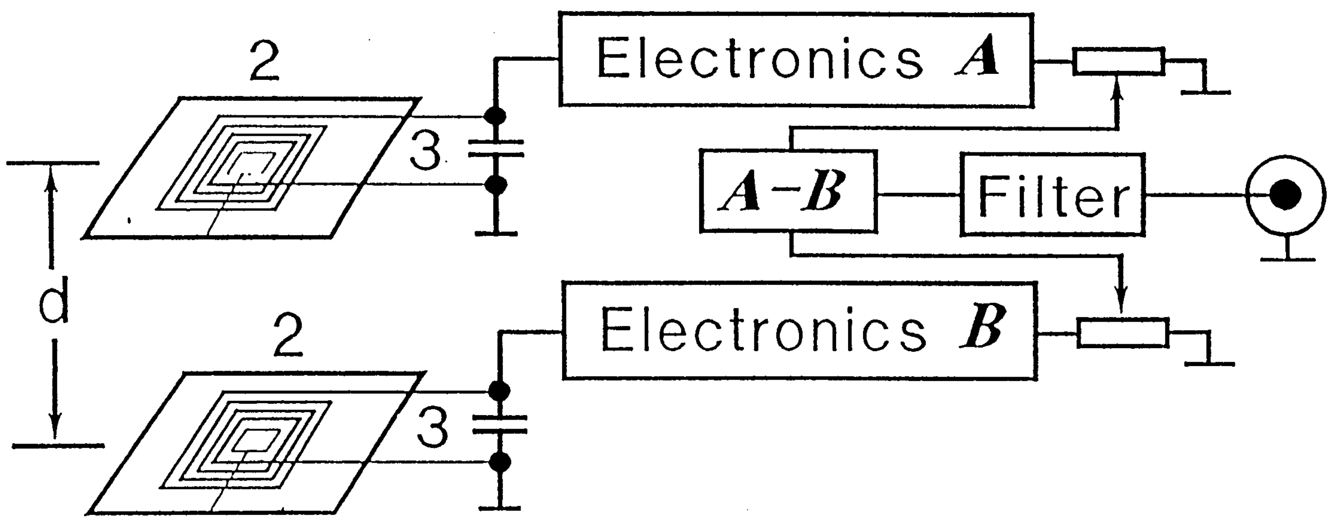


ALSO : 2ND DERIVATIVE

# THREE - SQUID GRADIOMETER (KOCH ET AL.

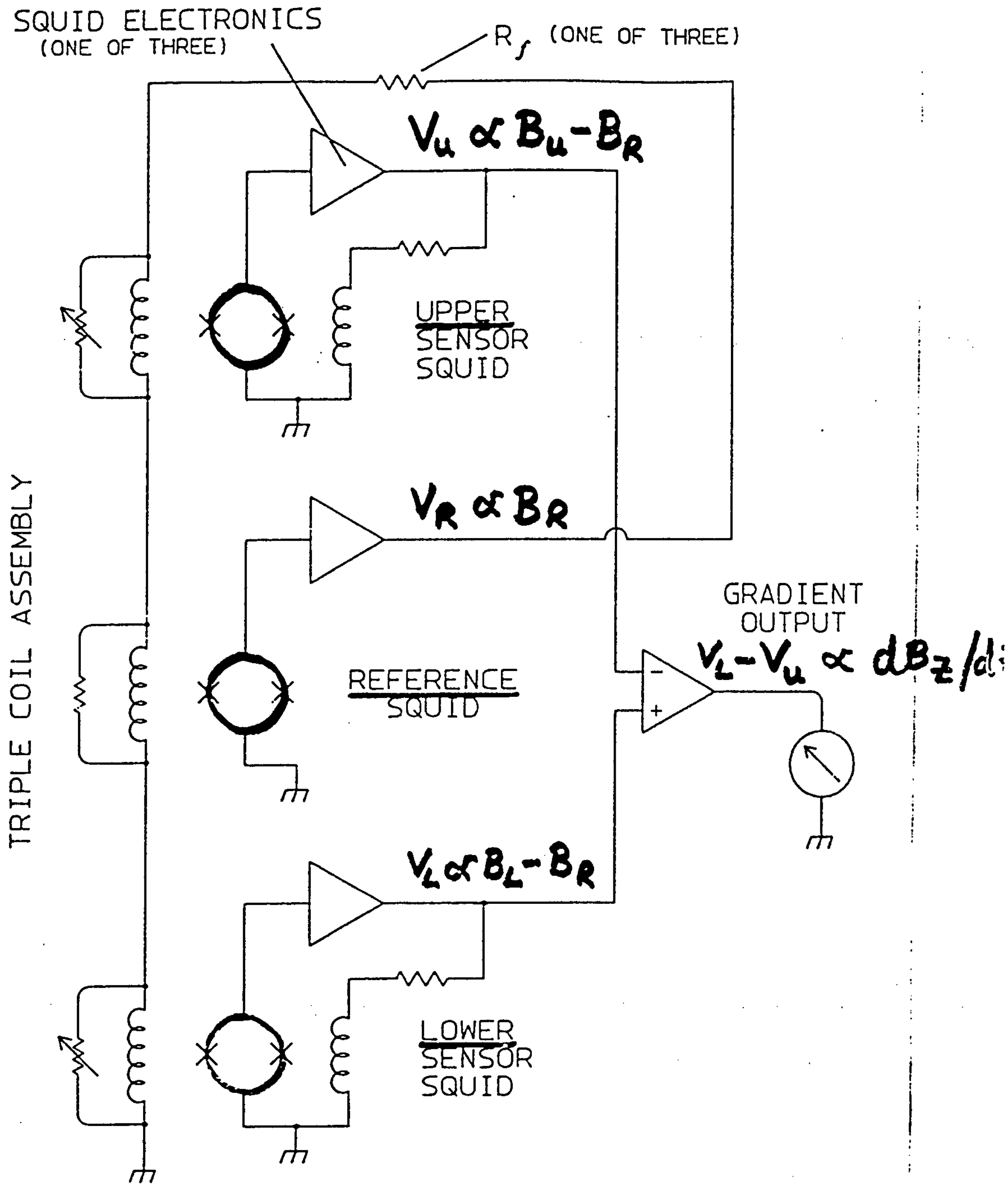


- REFERENCE SQUID PROVIDES QUIET ENVIRONMENT FOR UPPER AND LOWER SQUIDS
- NOISE OF REFERENCE SQUID IS SUBTRACTED OU

# PLANAR GRADIOMETER

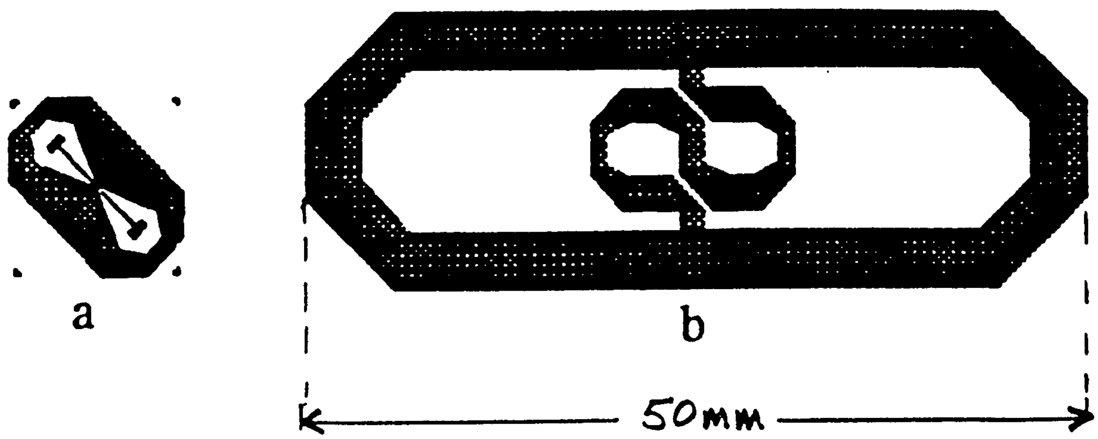


FALEY ET AL. (JÜLICH)

BALANCE: 1 PART IN 1800

$5\,pT\,m^{-1}\,Hz^{-1/2}$ AT 1kHz

# Collaborators

UCB/LBNL

Sherry Cho
Gene Dantsker
Oliver Froelich
Achim Kittel
Konstantin Kouznetsov
Robert McDermott
Byungdu Oh
Saburo Tanaka
JÖRG BORGMANN

Conductus, Inc.

Kookrin Char
Z. Lu
Vlad Matijasevic
C. Soble

IBM

Roger Koch

# FLIP- CHIP GRADIOMETER : PRINCIPLE

ZIMMERMAN 1977

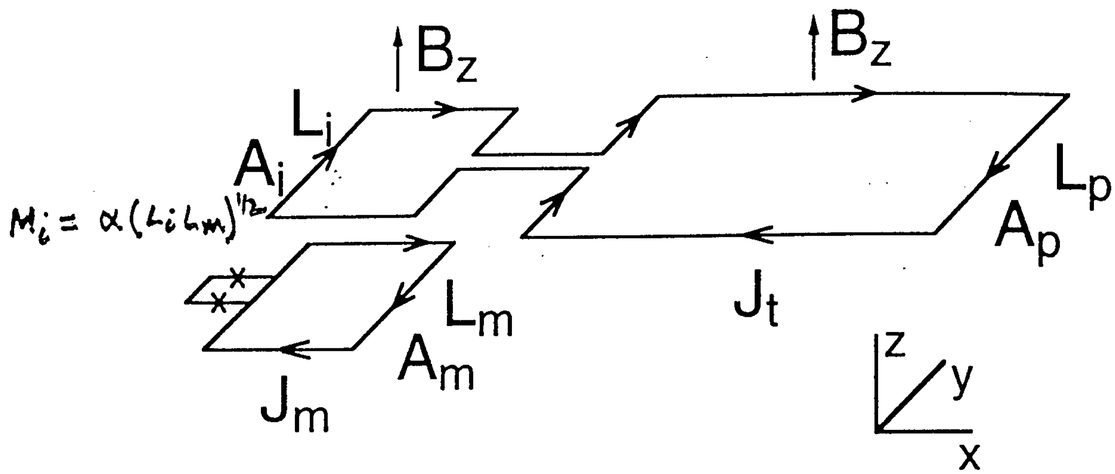


## CONDITION FOR BALANCE : ZERO RESPONSE TO UNIFORM $B_z$

TRANSFORMER: $\quad B_z (A_p + A_i) - (L_p + L_i) J_t - M_i J_m = 0$

MAGNETOMETER: $\quad B_z A_m - L_m J_m - M_i J_t = 0$

REGARD $\alpha$ AS THE VARIABLE PARAMETER, CHOOSING IT SO THAT $J_m = 0$:

$$\alpha = \frac{A_m}{A_p + A_i} \cdot \frac{L_p + L_i}{(L_i L_m)^{1/2}}$$

THIS IS THE CONDITION TO <u>BALANCE</u> THE GRADIOMETER

# FLIP-CHIP GRADIOMETER: PRINCIPLE

ZIMMERMAN 1977

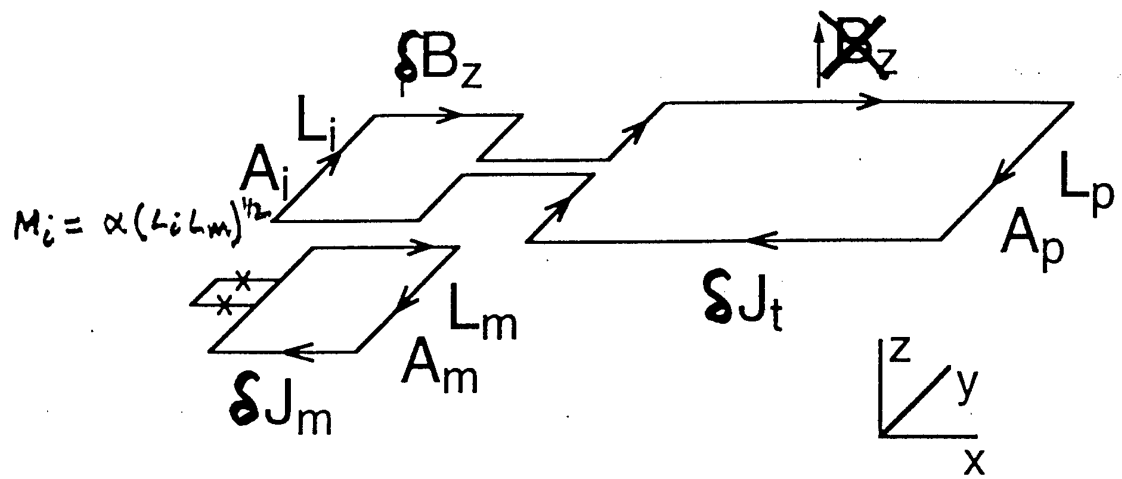


GRADIENT RESPONSE: APPLY $\delta B_z$ TO MAGNETOMETER AND INPUT LOOP ONLY

TRANSFORMER: $\delta B_z A_i - (L_p + L_i)\,\delta J_t - M_i\,\delta J_m = 0$

MAGNETOMETER: $\delta B_z A_m - L_m\,\delta J_m - M_i\,\delta J_t = 0$

SOLVING FOR $\delta J_m$:

CURRENT IN BARE MAGNETOMET

$$\delta J_m = \eta\, \boxed{\delta B_z \frac{A_m}{L_m}}$$

WHERE $$\eta = \frac{L_p/L_i + 1 - \alpha (A_i/A_m)(L_m/L_i)^{1/2}}{L_p/L_i + 1 - \alpha^2}$$

FACTOR $\eta$ REPRESENTS THE REDUCTION IN THE SENSITIVITY OF THE MAGNETOMETER DUE TO THE TRANSFORME

# FABRICATION OF GRADIOMETER

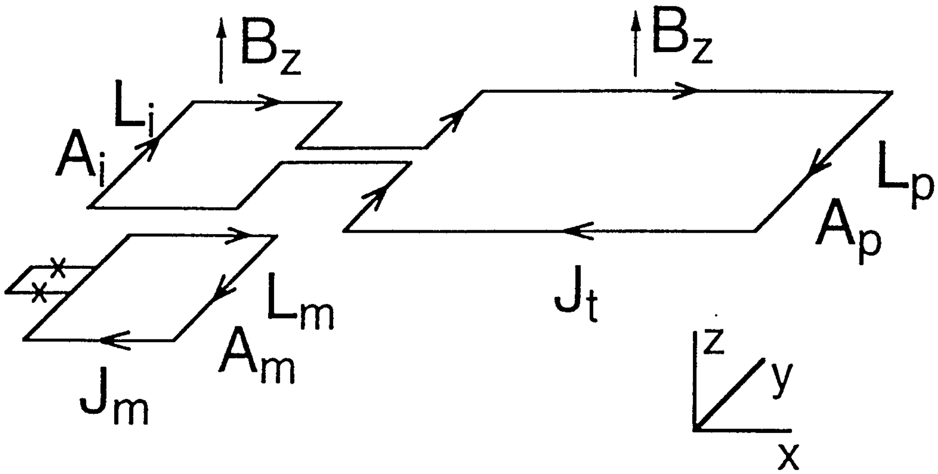


onm YBCO
u
ATITJASENC
HAR
NDUCTUS)

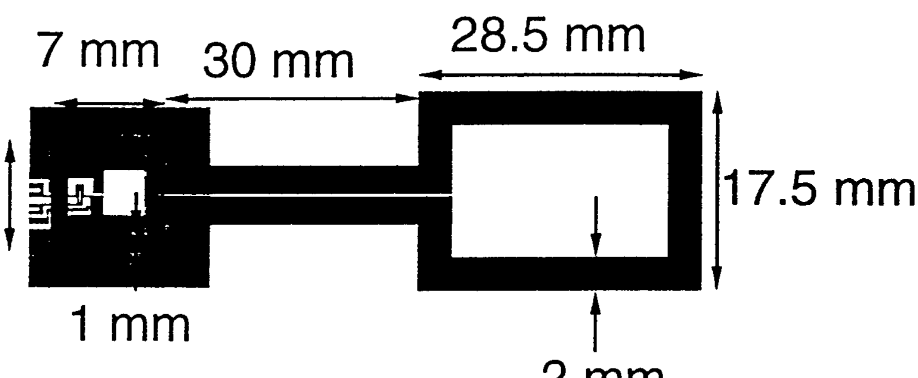


ESTIMATED PARAMETERS:

TRANSFORMER: $L_i \approx 10\,nH$, $A_i \approx 36\,mm^2$, $L_p \approx 50\,nH$, $A_p \approx 411\,mm^2$

SQUID: $L \approx 50\,pH$, $R \approx 1.2\,\Omega$, $I_0 \approx 200\,\mu A$

MAGNETOMETER: $L_m \approx 4\,nH$, $A_m \approx 20\,mm^2$

THUS: $\alpha = 0.43$

$\eta = 0.95$ – ONLY 5% REDUCTION IN SENSITIVITY

BASELINE : 48mm

# First-order asymmetric gradiometer

(a)

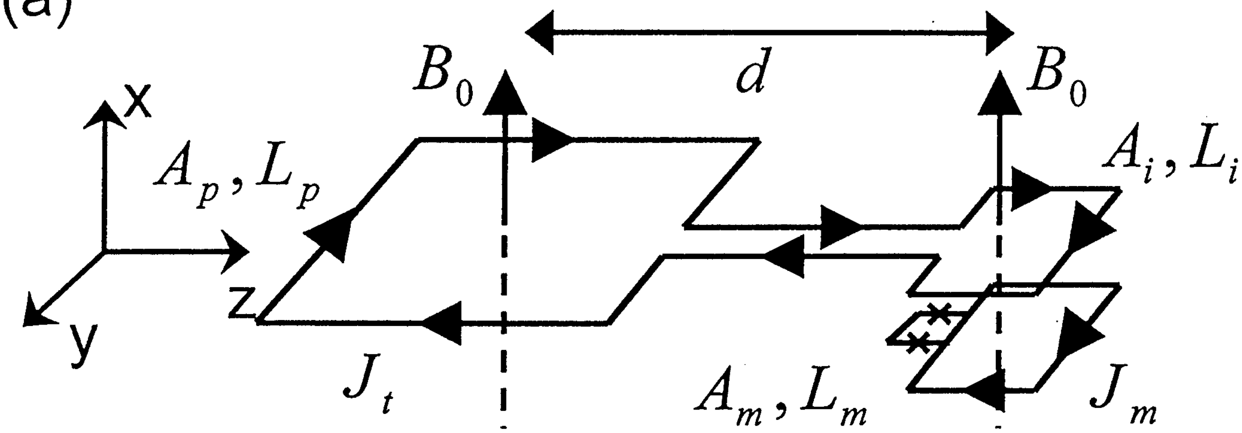


(b)

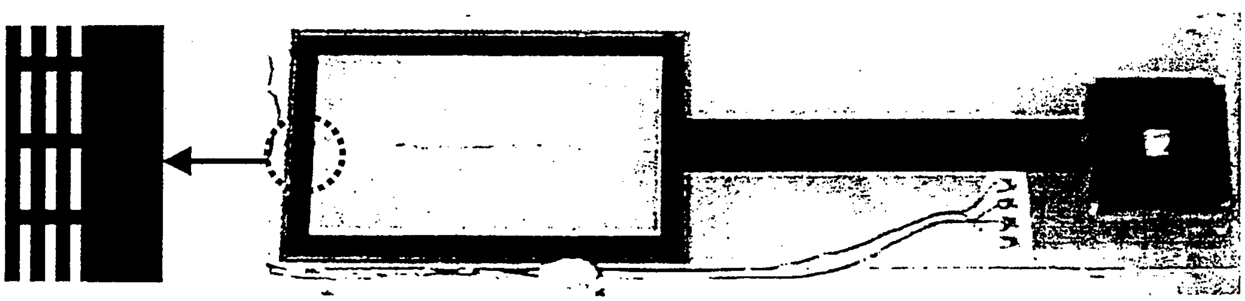

TYPICAL BALANCE 1 : 300

# Probe with two gradiometers and three magnetometers

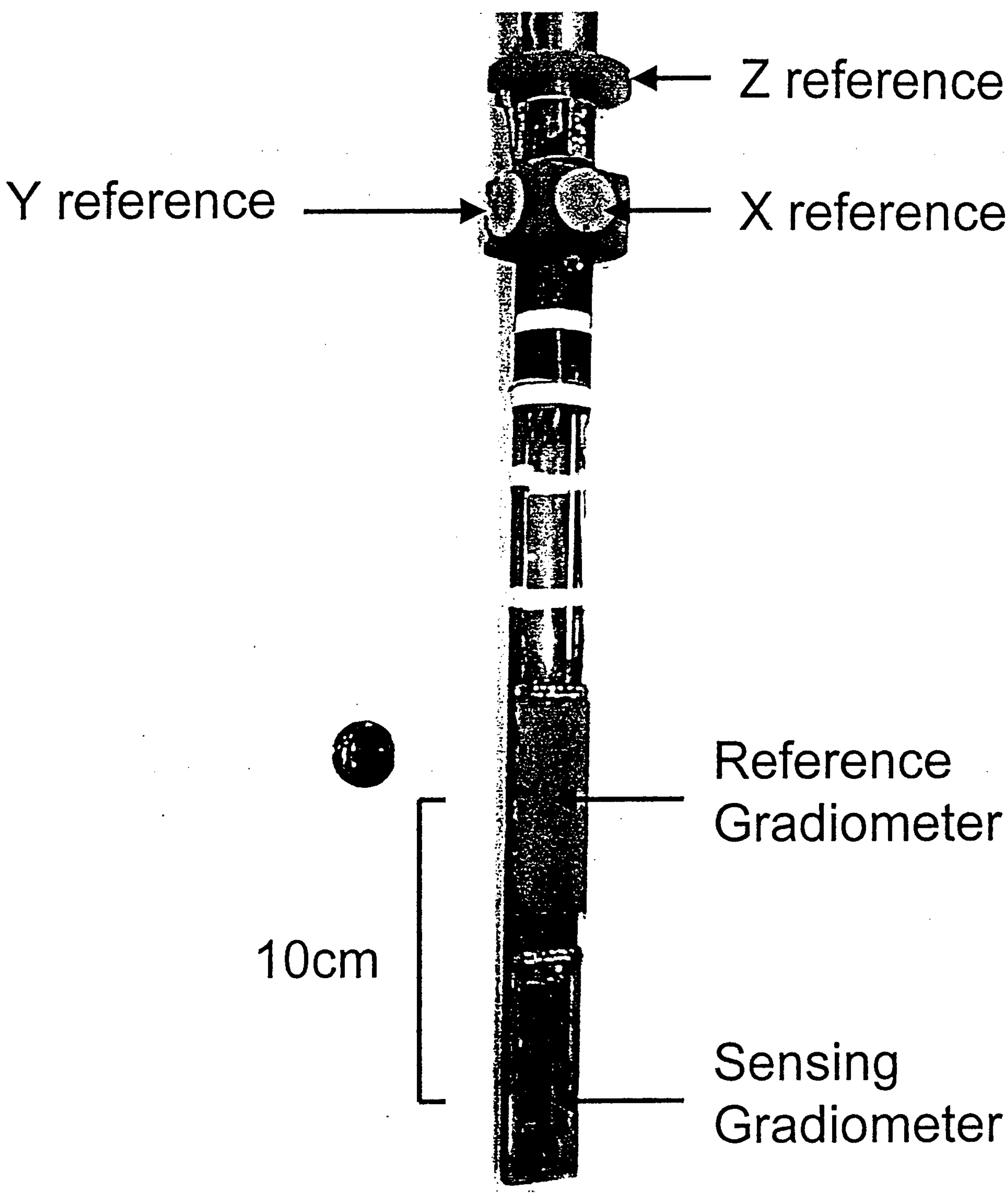

# Balance of First-Order Gradiometer

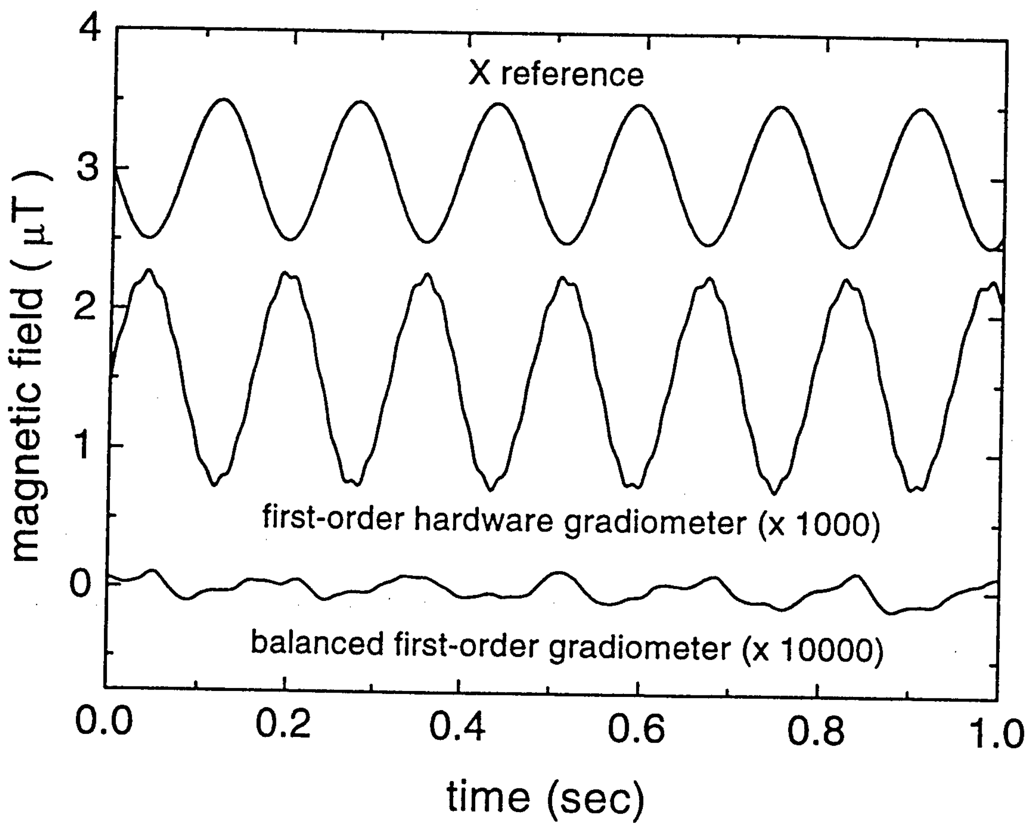


BALANCE : 20 ppm

Noise Spectra of Magnetometer and Gradiometer

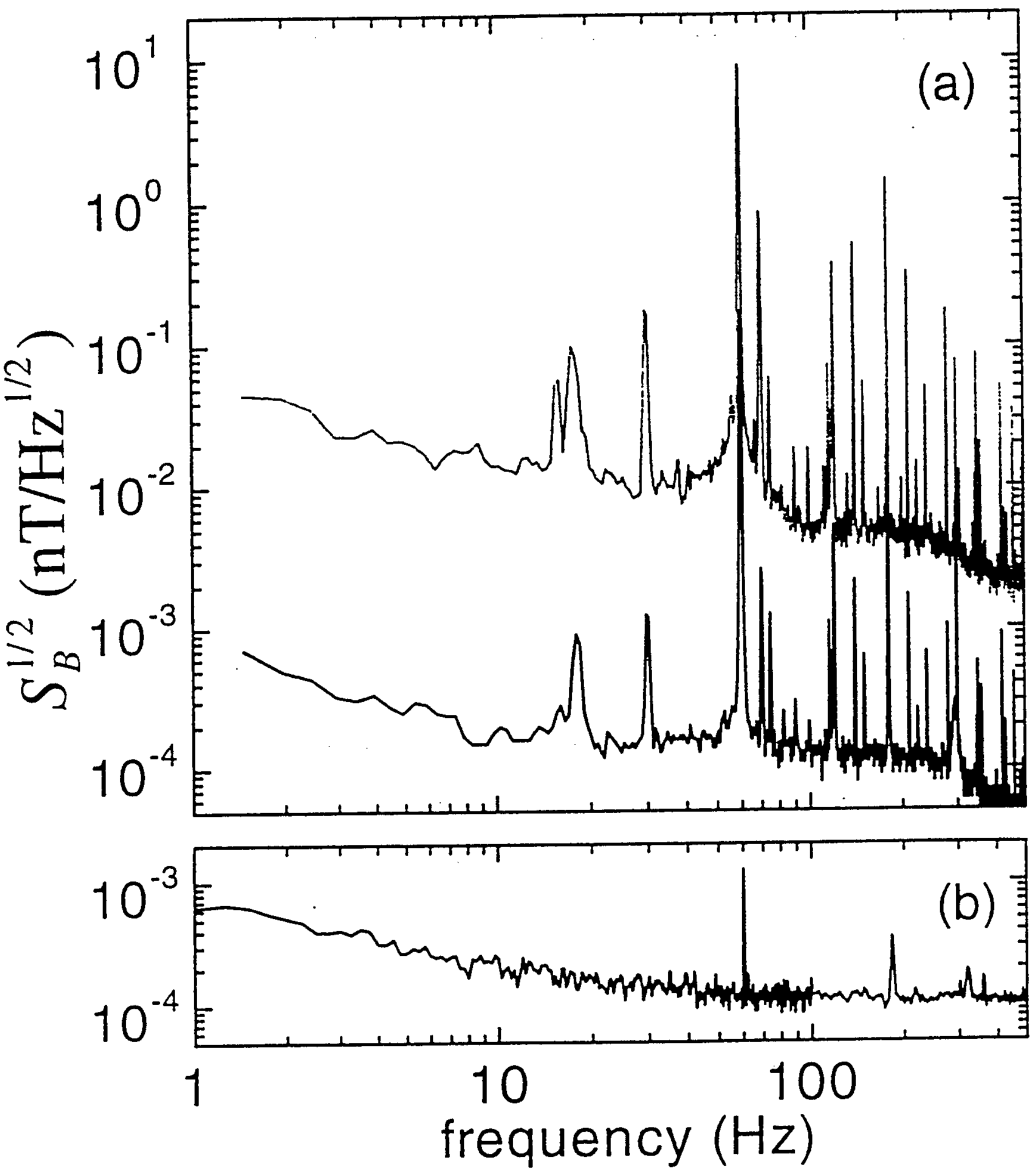

# Magnetocardiogram in an Unshielded Environment

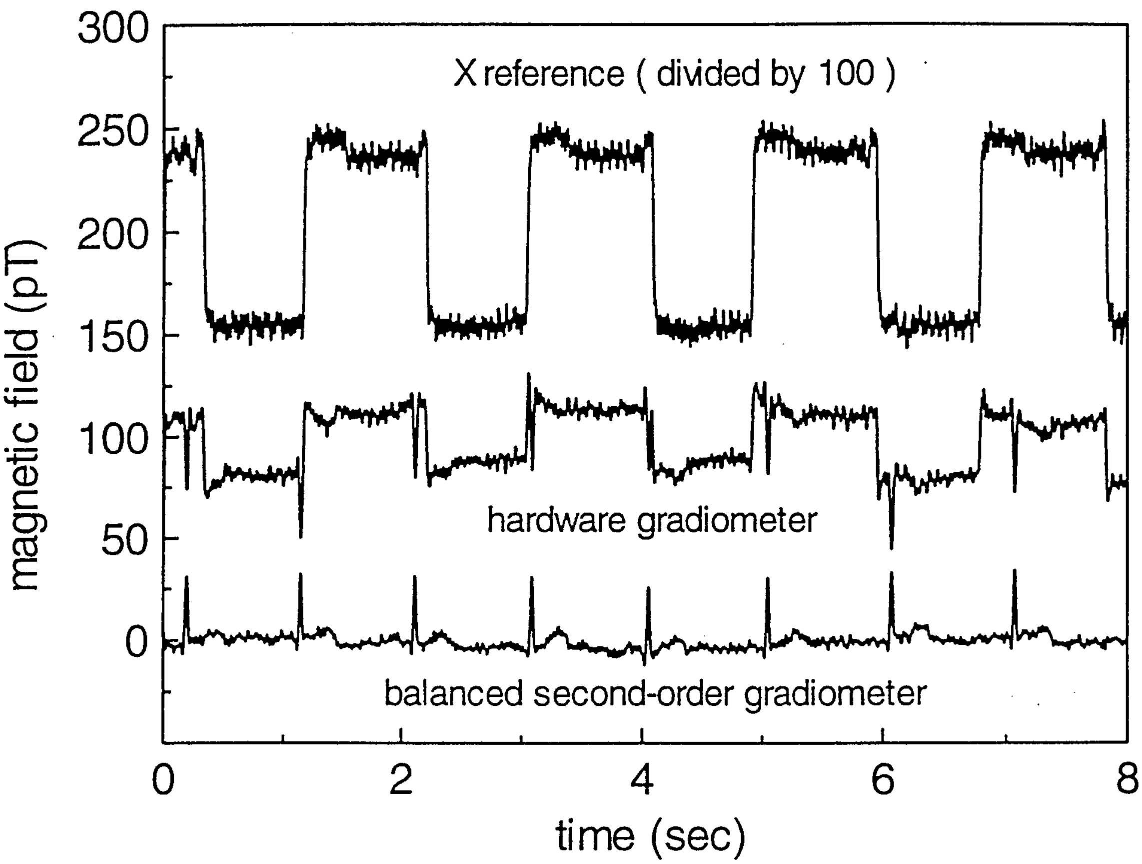

## Magnetocardiogram in an Unshielded Environment
## (averaged 119 times)

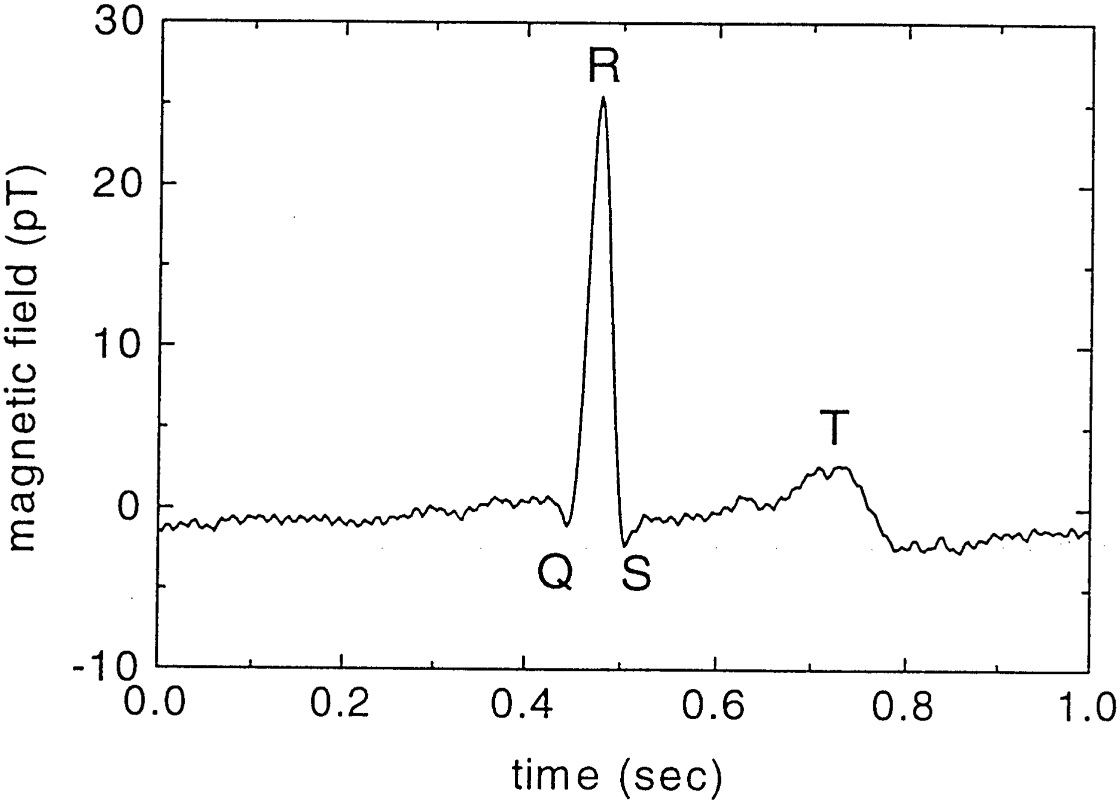

# Frequency range of the dc SQUID

| | |
|---|---|
| Magnetotactic bacteria: | $\sim 10^{-3}$ Hz |
| Axion detector: | $\sim 1$ GHz |

Over 12 decades of frequency, appropriately used the dc SQUID is the most sensitive detector available.

# The Use of SQUIDs in the Non-Destructive Evaluation of Engineering Structures

Gordon B Donaldson
Department of Physics & Applied Physics
University of Strathclyde
Glasgow
Scotland

# North Sea Oil and Gas Pipes- Welds

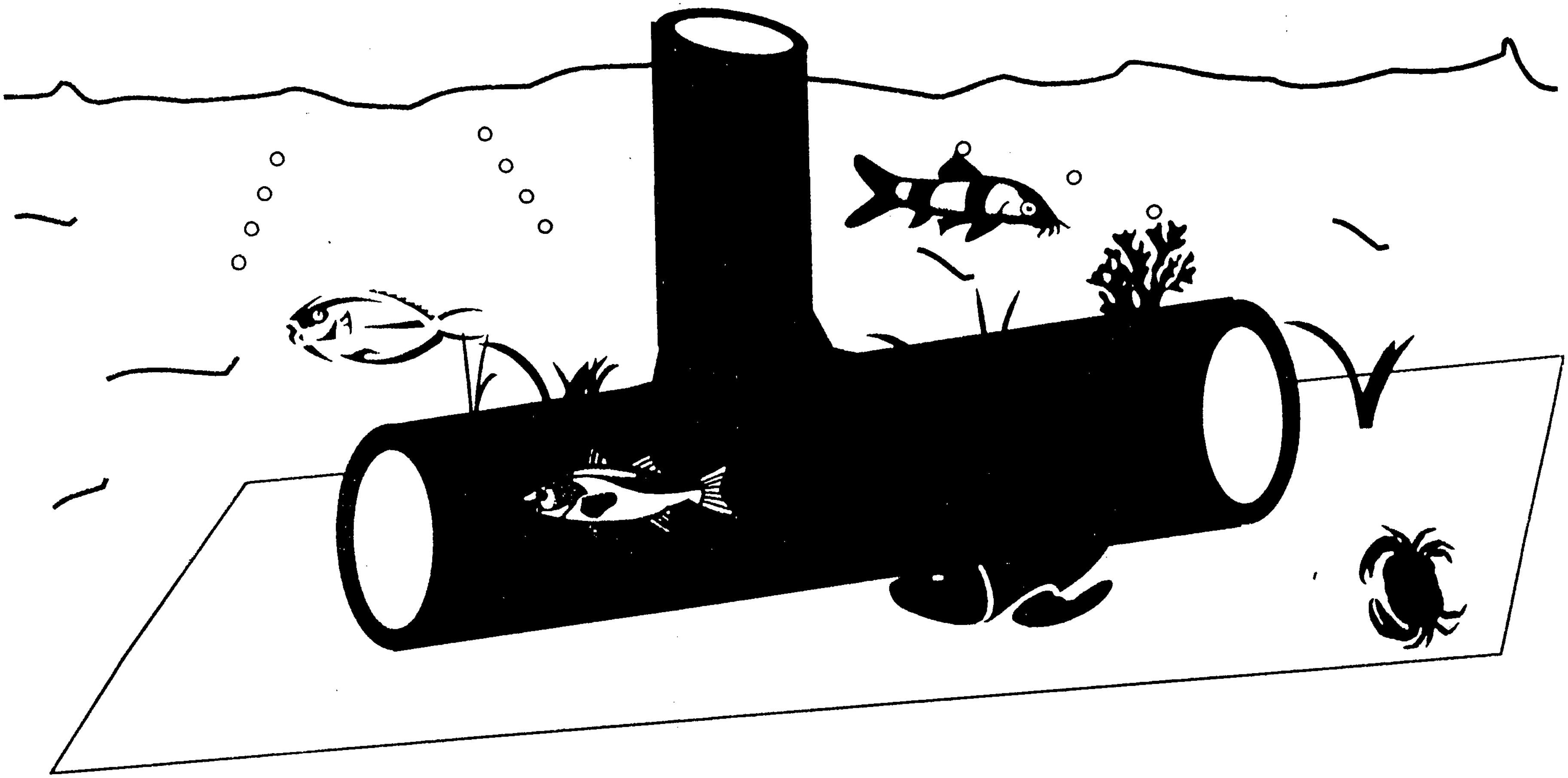

Harold Weinstock DHC, INSA Lyon 1999

# A Brief History of SQUID NDE

| | | |
|---|---|---|
| 1985 | 'Buried' Gas Pipes | NRL/AFOSR |
| | 'North Sea' Oil Pipelines | Strathclyde |
| 1987 | AC injection and eddy current techniques | |
| | | Vanderbilt |
| 1988 | Corrosion currents | MIT |
| 1990 | HTS | |
| 1991.. | Aircraft 'bodies' | SQM |
| | Concrete bridges | |
| | Ageing in reactor steels | Hitachi |
| | Fish | |
| | Inclusions in fine copper wire | Sumitomo |
| | Stressed steels | ETL |
| | Microscope | Maryland |
| | Aircraft wheels | Julich |
| ..1998 | Turbine blades | FIT |

# Magnetic Detection

## Advantages

Non-contacting- significant lift off possible
Skin depth dependence allows probing

## Disadvantages

Can need large excitations
No Time-of-flight or Phased array methods possible-
spatial location comparable only to stand-off

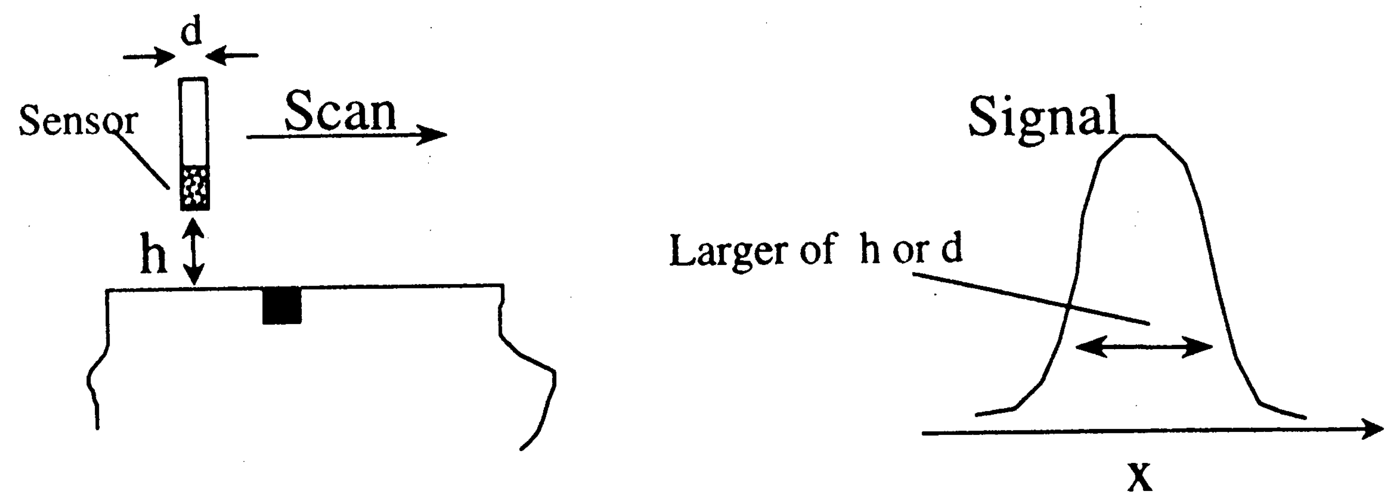

# SQUIDs

Vector device

Gradiometer

Measures $\Phi$, not $d\Phi/dt$ so useable to DC

In fact, measures $\Delta\Phi$ in large $\Phi_{background}$, equivalent to $10^{-7}$T in 4 x $10^{-2}$T

Can use tiny pick-up coils to improve spatial resolution (SQUID microscope)

# MAGNETIC SENSORS FOR NDE

**Table 2: Magnetic sensors for eddy current NDE**

| Sensor | Sensor Package Size (Sensing Volume) | Spatial Resolution | Frequency Dependence | Signal Sensitivity | Cost |
|---|---|---|---|---|---|
| Induction coils | Small (1.5mmϕ x 4mm) | Good | Signal ∝ 1/f | | Low (£'s) |
| Hall Sensors | Small ($1mm^3$) | Good | Good | Poor | Low (£'s) |
| Magnetoresistors | Medium ($10mm^3$) | Good | Good | Medium | High (£1k)[1] |
| Fluxgates | Medium (1mmϕ x 15mm) | Medium | Good | Medium | High (£1k) |
| SQUIDs | High[2] ($1mm^2$ thin film) | Good | Good | Good | High (£1k)[3] |

[1]Magnetoresistors are not widely available commercially. [2]While the sensing area of a HTS SQUID is small, the size of the cryostat has to be taken into account. [3]The initial outlay for a HTS SQUID is comparable to that of a fluxgate. Liquid nitrogen cryogen is inexpensive.

Why use SQUIDs?

- flaws in airframes at depths ~10-20mm require low noise at f<200Hz which only SQUIDs posses.
- low noise can also mean a much larger standoff compared to other sensors.
- often the cost of operating the SQUID is buried.

But

A £40K SQUID system is not state of the art technology. A fluxgate magnetometer detection system costing £40K is.

[General Reference — Jenks et al, "SQUIDs for Nondestructive Evaluation", Journal of Physics D: Applied Physics, vol. 30, pp. 293-323, 1997].

# NDE Techniques

- Static field mapping

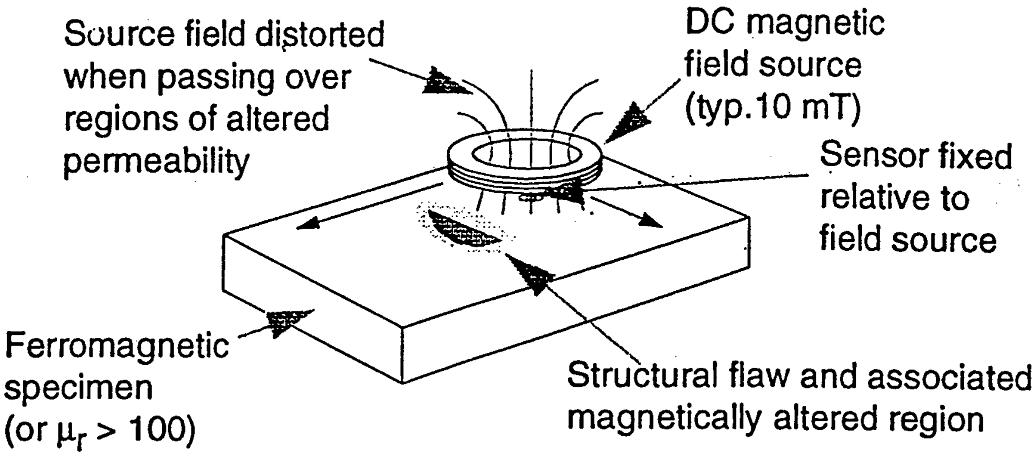


- Directly injected current mapping

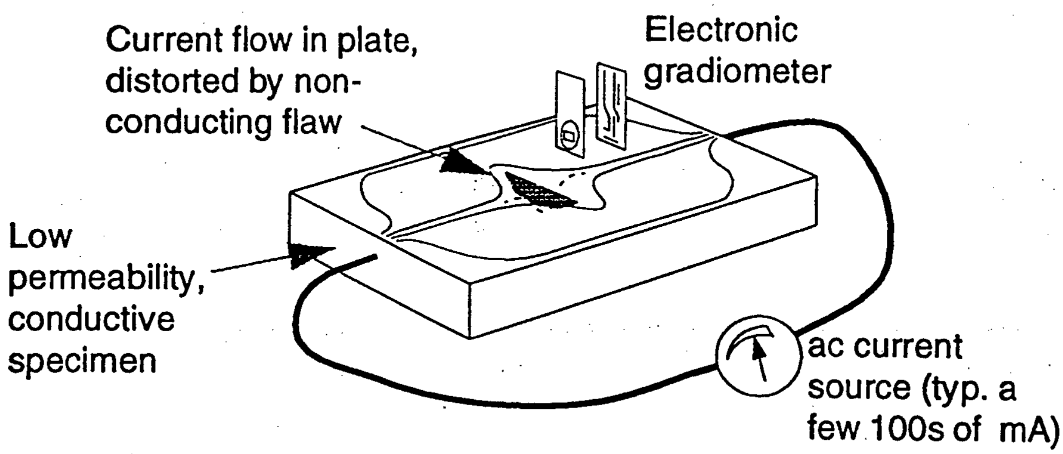


- **Eddy current measurement**

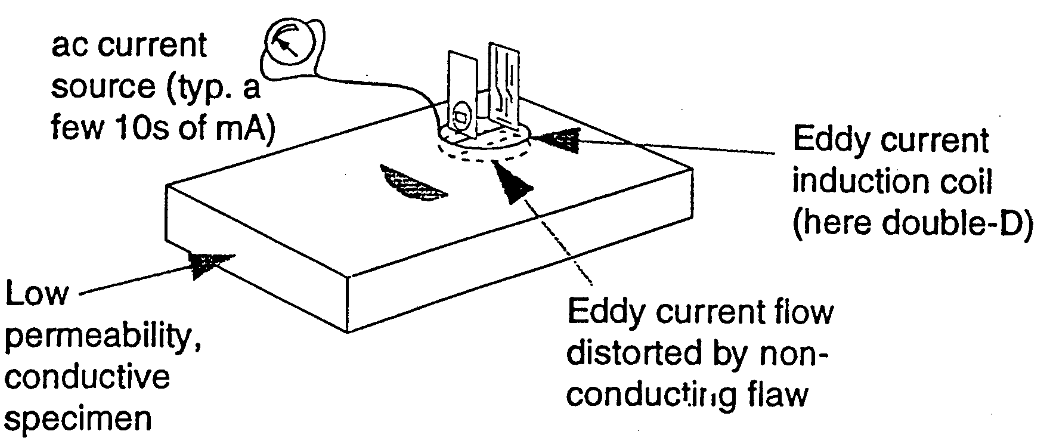

*5.2.1. Pipelines.* In early work, Weinstock and Nisenoff [43] showed that when a 1 A, 4.6 Hz, current was passed along a metal pipe, the pipe could be accurately located using an axial SQUID gradiometer. A scan across the line of the pipe, given in Fig. 12, shows that when the pipe lies directly along the gradiometer axis there is a sharp zero in the detected signal, which is then purely transverse. The horizontal resolution here is rather better than the stand-off limit discussed earlier. Triangulation to determine the pipe position depends on a second scan with the gradiometer axis at about 30° to the vertical.

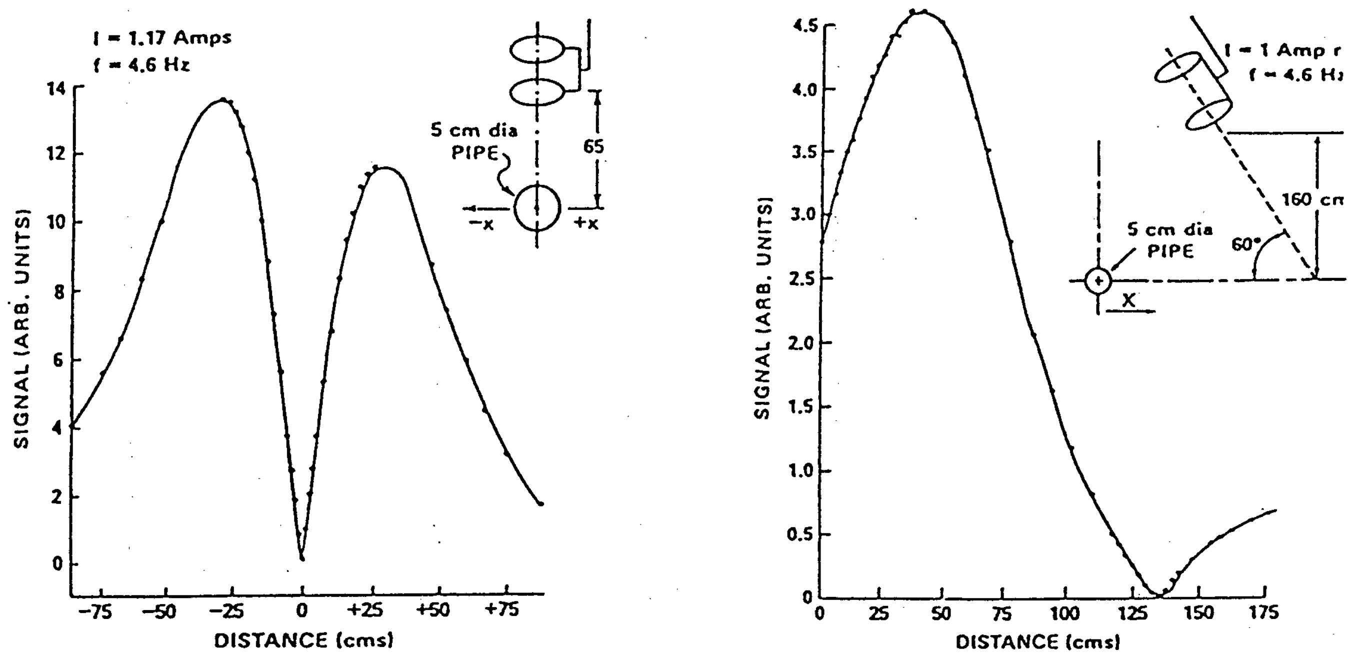


Figure 12. SQUID pipeline detection results [43].

Distances up to 1.6 m were studied, but much greater values should be possible and the method should be applicable to buried pipelines.

Holes and welds in the pipe could also be seen. They divert the flow of current, producing anomalies in the field measured by the SQUID as it is tracked along the line of the pipe.

# SQUID Gradiometer

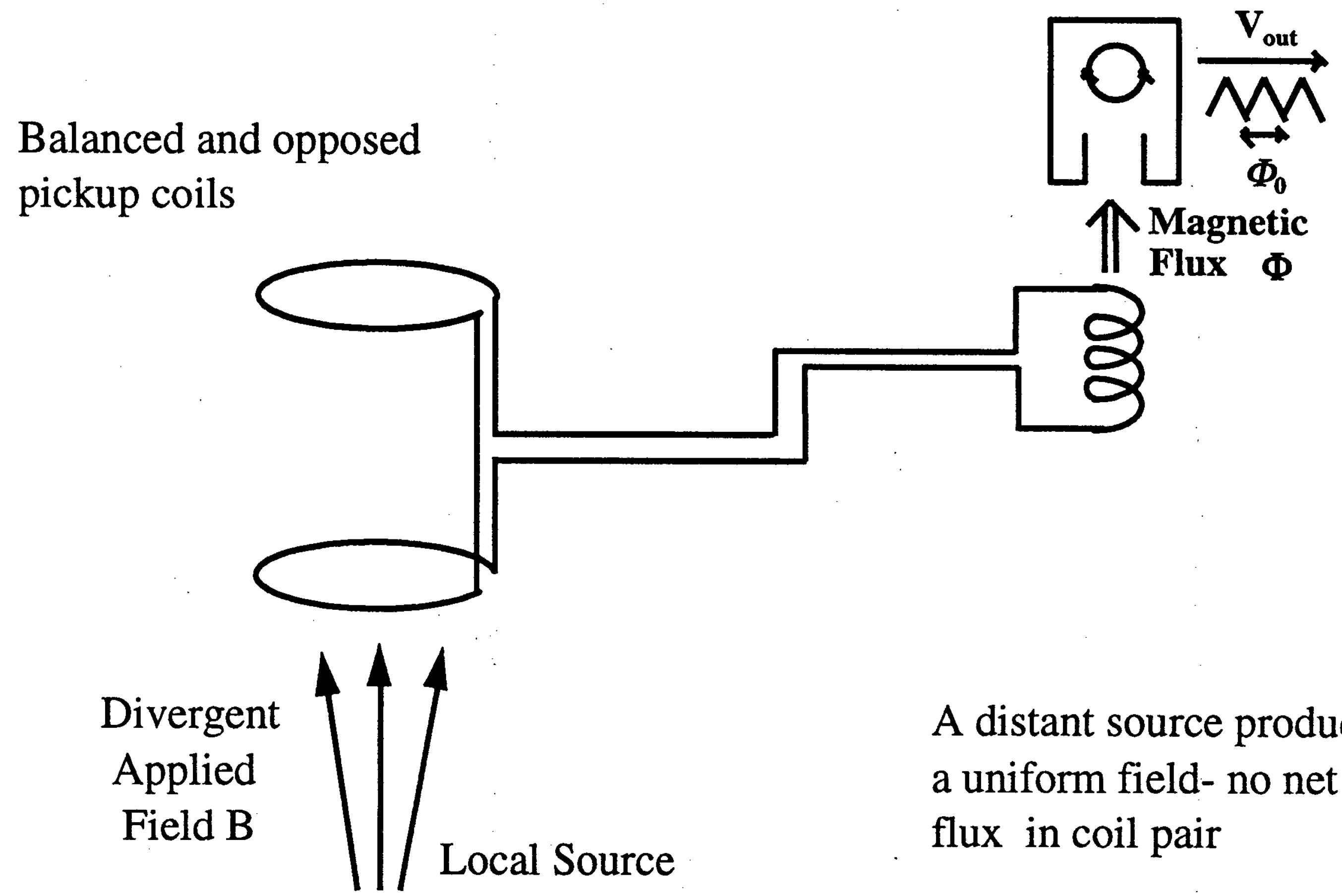


A distant source produces a uniform field- no net flux in coil pair

Harold Weinstock DHC, INSA Lyon 1999

# 110 SQUID(超電導量子干渉素子)センサによる2相ステンレス鋼の時効変化の検出 要旨


正 ※大高 正廣 (日立機械研)　正 長谷川 邦夫 (日立機械研)
正 清水 翼 (日立機械研)　正 高久 和夫 (日立日立)
S.Evanson (Univ. of Strathclyde)　G.B.Donaldson (Univ. of Strathclyde)


ルに置き、試験片がSQUIDセンサの下部を通

Table 1. Chamical composition and ferrite content of cast stainless steels

| Material | C | Si | Mn | P | S | Cr | Ni | Mo | Co | N | Ferrite content (%) |
|---|---|---|---|---|---|---|---|---|---|---|---|
| A | 0.016 | 1.36 | 0.16 | 0.014 | 0.005 | 19.4 | 10.05 | 2.21 | 0.03 | — | 12.5 |
| B | 0.01 | 1.25 | 0.63 | 0.010 | 0.006 | 20.30 | 9.54 | 2.14 | 0.03 | 0.04 | 21.3 |
| C | 0.02 | 1.39 | 0.59 | 0.018 | 0.006 | 20.74 | 9.67 | 2.30 | 0.04 | 0.03 | 26.1 |

ル方向が反転するためである。また、SQUIDセ

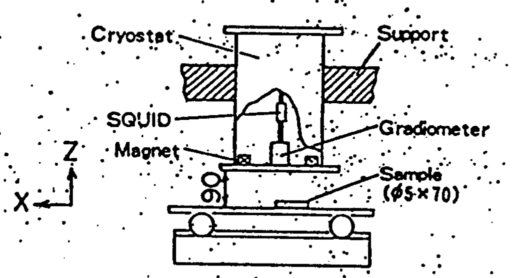


Fig. 1 Schematic of experimental apparatus

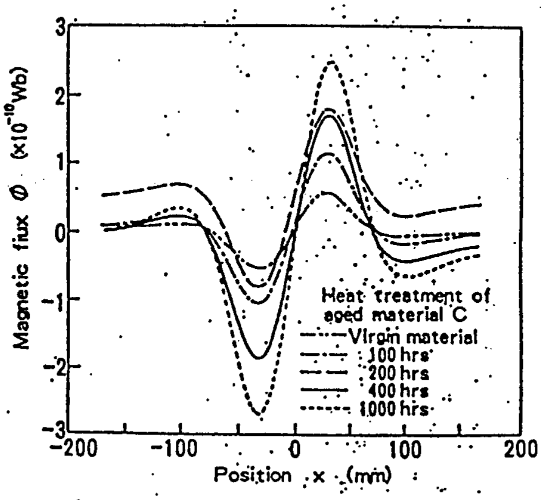


Fig.2 Intensity of SQUID sensor

Remanence

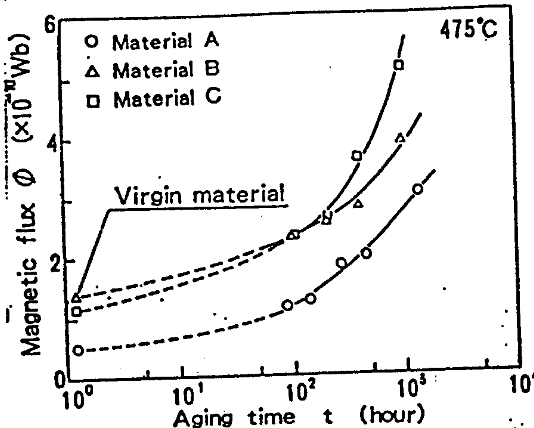


Fig.3 Intensity of SQUID sensor as a function of aging time

Saturation

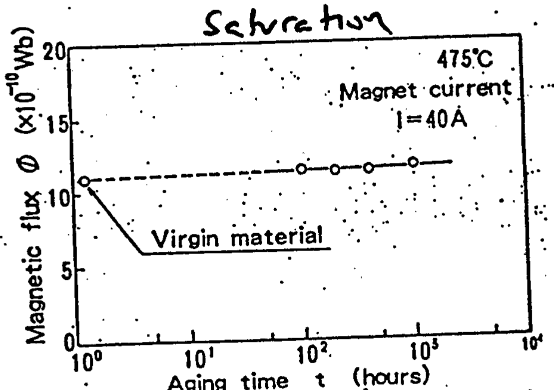


Fig. 4 Intensity of SQUID sensor as a function of aging time (Material C)

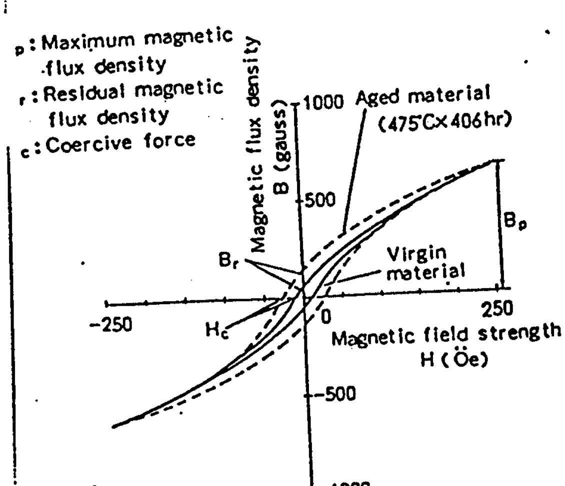


ig.5 Magnetization characteristics of virgin and aged cast stainless steel (Material C)

# Magnetic

*Remote Magnetometry*

Measure spontaneous fields of magnetised inclusions
Measure induced fields of magnetisable inclusions
Measure effective difference dipoles of inclusions of permeability different ($\Delta\mu$) from host (including void $\mu$=0)
Measure diverted fields
Measure flux leakage

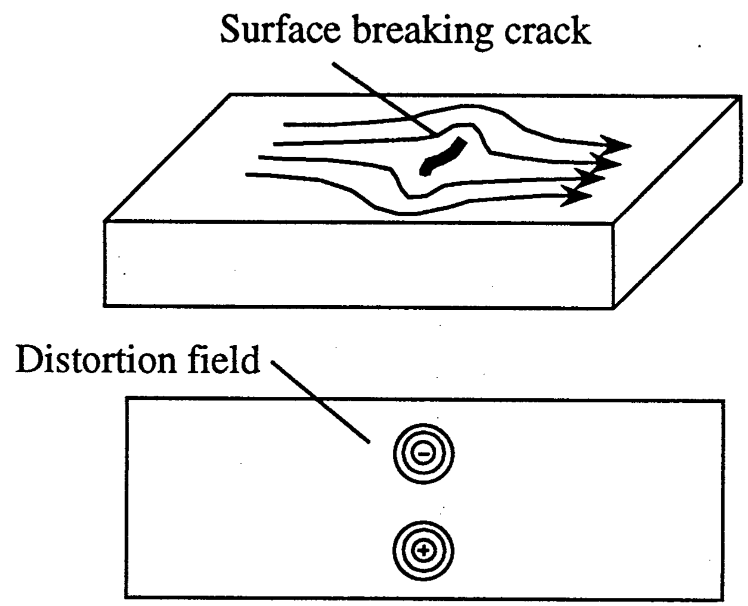


*Remote Galvanometry*

Measure difference fields caused by distorted flow of injected or induced (eddy) currents, close to flaw
Measure fields due to noise currents

# Non-Destructive Evaluation (NDE)

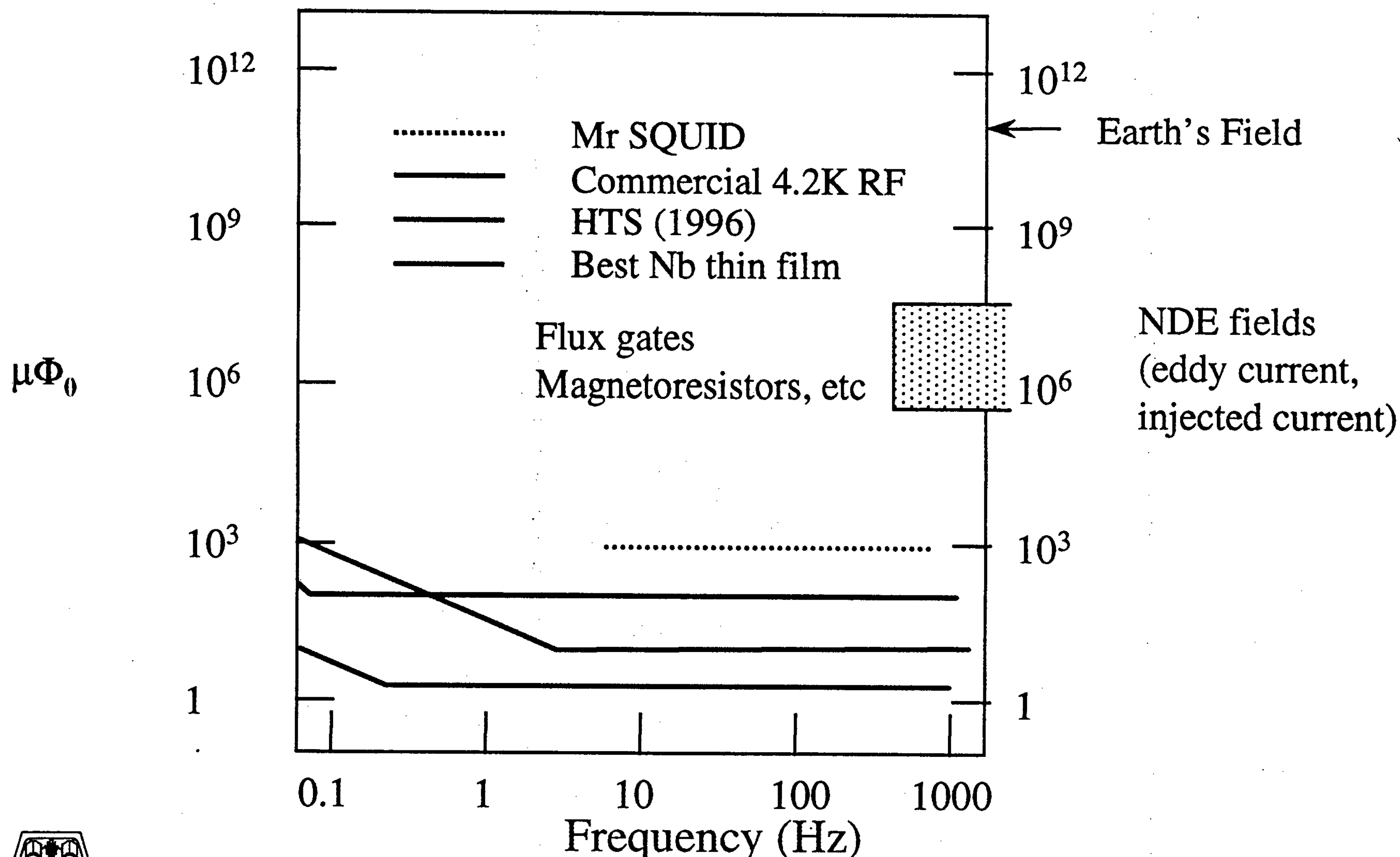


Harold Weinstock DHC, INSA Lyon 1999

STR LTS

# STATIC FIELD MAPPING AND MATERIAL CHARACTERISATION

A MILD STEEL PLATE WAS ARTIFICIALLY CRACKED BY CYCLIC THREE-POINT LOADING AND WAS SCANNED BENEATH A LOW TEMPERATURE SQUID SENSOR. NO CONTACT WITH THE STEEL PLATE WAS MADE. THE CRACK WAS DETECTED BY MEASURING APPLIED FIELD DISTORTIONS CAUSED BY ASSOCIATED MAGNETIC PERMEABILITY VARIATIONS.

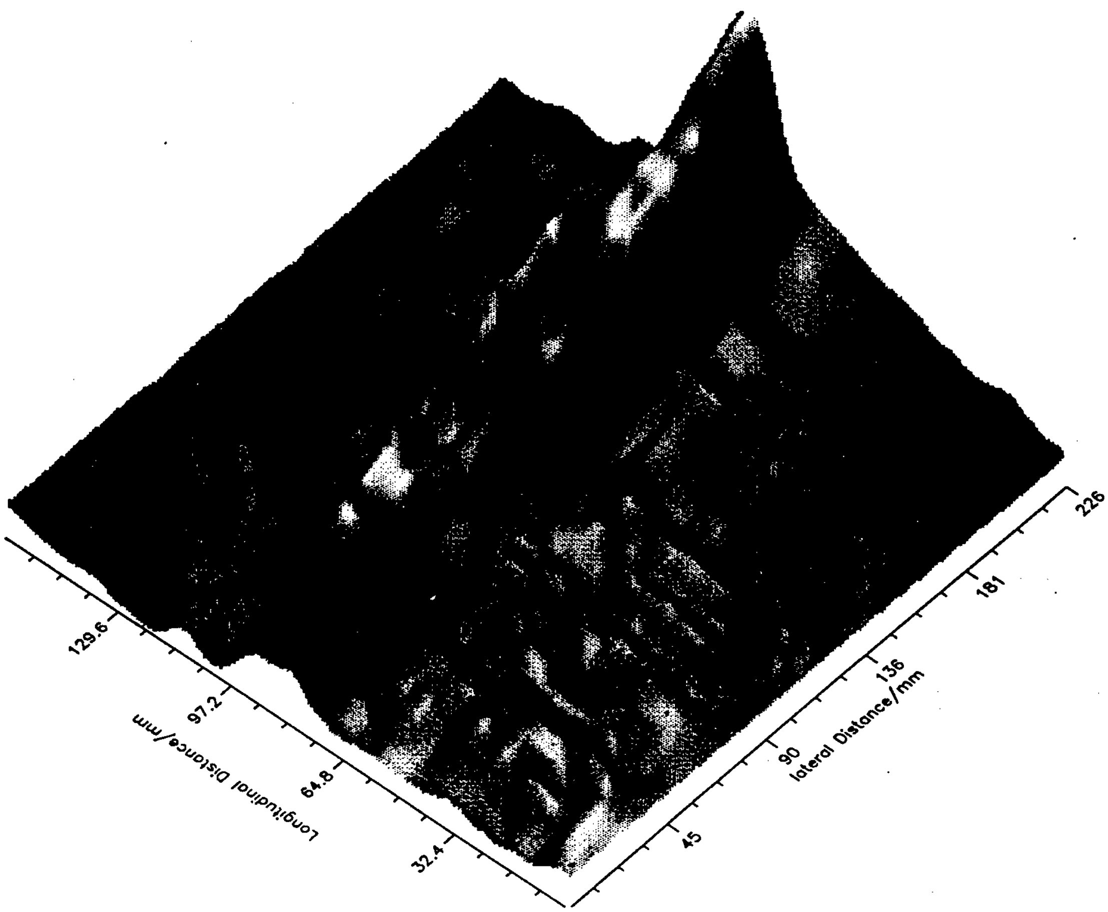


THIS TECHNIQUE HAS BEEN HIGHLY SUCCESSFUL FOR PREDICTING POSSIBLE CRACK SITES, EVEN THROUGH A THICK LAYER OF NON-MAGNETIC MATERIAL.

# Experimental Apparatus

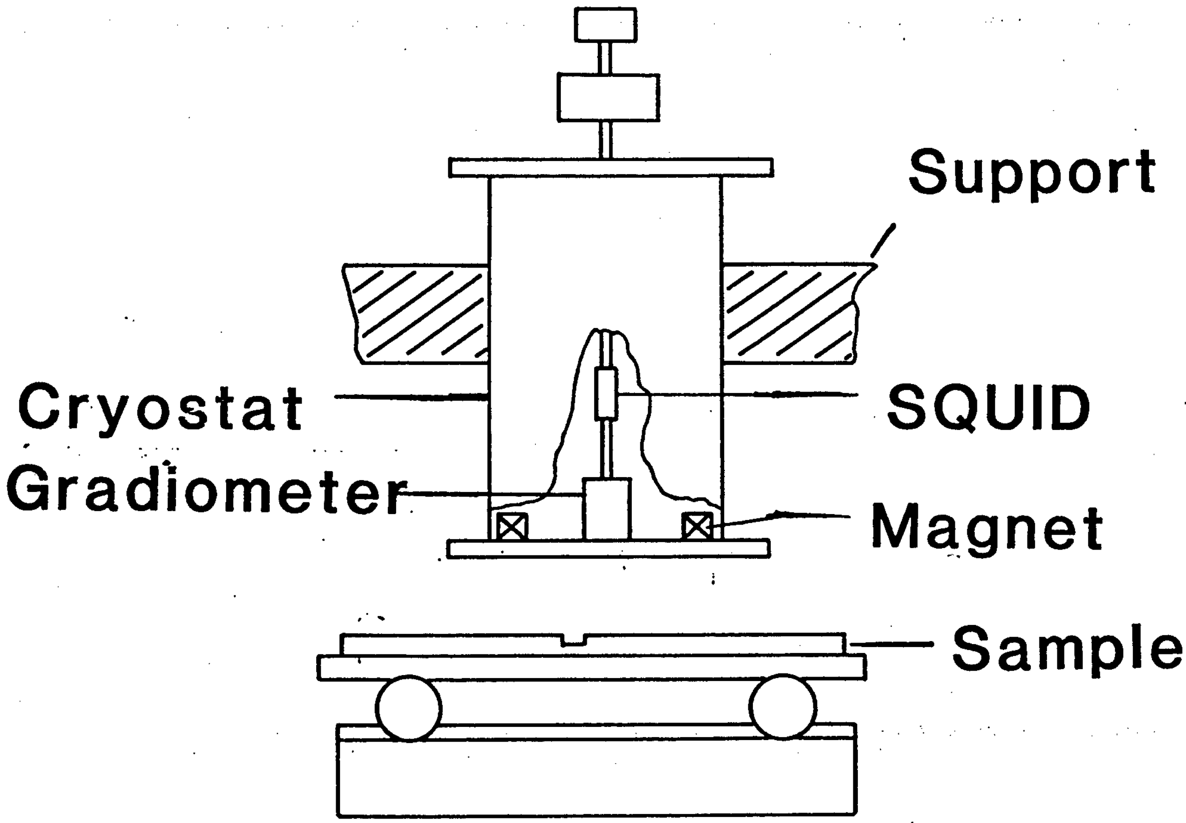


'Room temperature' application

Planar gradiometers

Heavy ~~dep~~ use of computer data acquisition and processing

# Non-Destructive Evaluation (NDE)

Corrosion and embrittlement in

- Chemical and nuclear reactors
- Pipelines (especially coated, sub-sea, etc.)
- Ageing aircraft

are major, and expensive problems.

E.g.

- Extension of KC135 (Boeing 707), now 35 years old to 70 year life
- Japanese reactor accident

STR. INV.

# CURRENT FLOW <-> MAGNETIC FIELD TRANSFORMATIONS

STARTING WITH THE BIOT-SAVART LAW:

$$\underline{B}(\underline{r}) = \frac{\mu_0}{4\pi}\int \frac{\underline{J}(\underline{r}') \times (\underline{r}-\underline{r}')}{|\underline{r}-\underline{r}'|^3} d^3\underline{r}'$$

EXTRACTING THE VERTICAL COMPONENT AND EXPRESSING IN TERMS OF GREEN'S FUNCTIONS GIVES:

$$B_z(\underline{r}) = J_x(x, y) \otimes G_y(x, y, z) + J_y(x, y) \otimes G_x(x, y, z)$$

THE TWO GREEN'S FUNCTIONS ARE:

$$G_x(x, y, z) = \frac{\mu_0 dz}{4\pi}\left[\frac{x}{(x^2+y^2+z^2)^{3/2}}\right]$$

AND

$$G_y(x, y, z) = \frac{\mu_0 dz}{4\pi}\left[\frac{y}{(x^2+y^2+z^2)^{3/2}}\right]$$

TRANSFORMING INTO FREQUENCY SPACE AND APPLYING THE LAW OF CONTINUITY, GIVES A SIMPLE TRANSFORM BETWEEN CURRENT DENSITY AND MAGNETIC FIELD:

$$b_z(k_x,k_y,z) = i\frac{\mu_0 d}{2}\frac{k}{k_y}e^{-kz}j_x(k_x,k_y)$$

BY REARRANGEMENT THE INVERSE IS GIVEN BY:

$$j_x(k_x,k_y) = -i\frac{2}{\mu_0 d}\frac{k_y}{k}e^{kz}b_z(k_x,k_y,z)$$

# AN EXAMPLE OF MAGNETIC FIELD TO CURRENT FLOW TRANSFORMATIONS

A PRINTED CIRCUIT BOARD IN THE SHAPE OF AN SU WITH A SMALL CURRENT FLOWING IN IT. WAS SCANNED BENEATH A LOW TEMPERATURE SQUID SENSOR, PRODUCING A MAGNETIC FIELD MAP AS SHOWN BELOW:

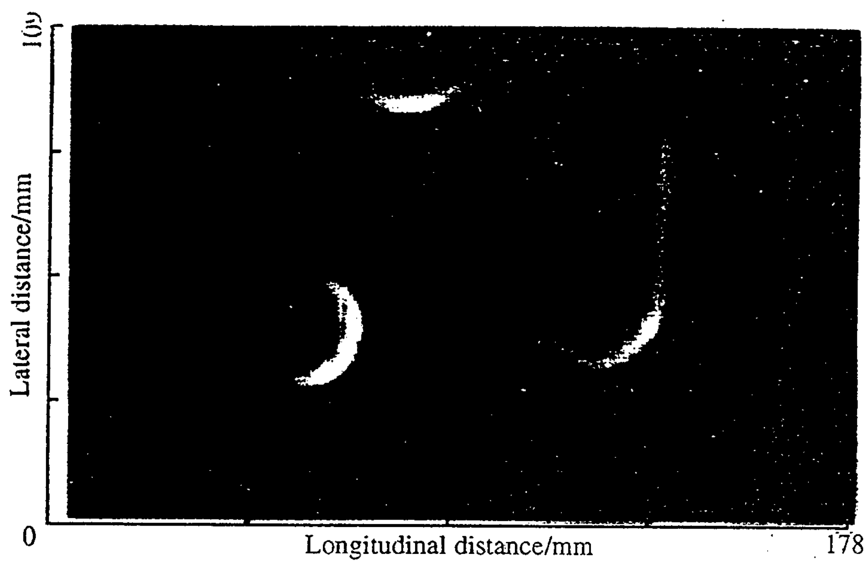


BY USING THE ALGORITHM DESCRIBED ABOVE THE CURRENT DENSITY WAS CALCULATED FROM THE Z COMPONENT OF THE MAGNETIC FIELD:

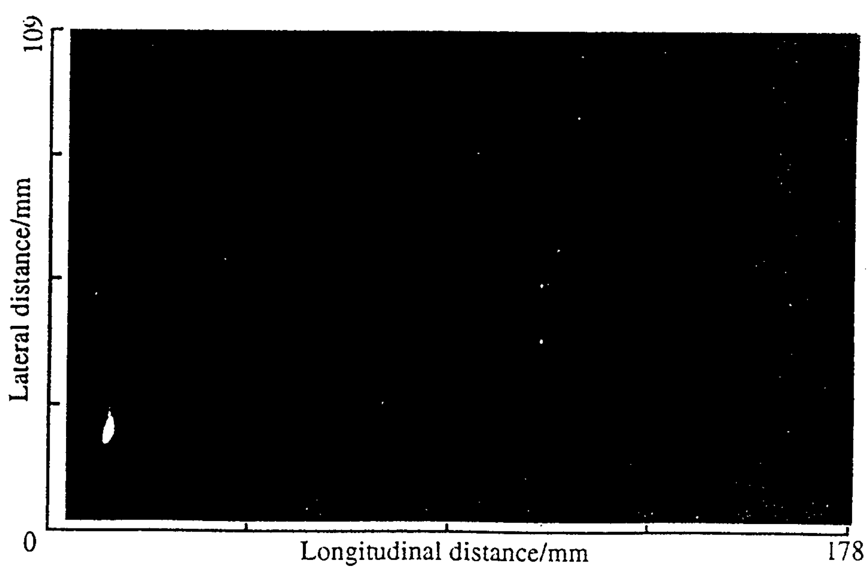


VARIATIONS IN PCB TRACK WIDTH AND THE SOLDER TAGS CAN EASILY BE RESOLVED.

# Depth profiling by frequency scanning

$$\delta = \sqrt{\frac{\rho}{\mu\mu_0\pi f}} = \sqrt{\frac{1}{\mu\mu_0\sigma\pi f}} = \frac{10^6}{2\pi}\sqrt{\frac{10}{\mu\sigma f}}\ mm$$

| Material parameter | Cu | Al | NiCr | Stainless steel | Mild steel | Si steel | Graphite |
|---|---|---|---|---|---|---|---|
| $\rho$ (x $10^{-8}$) Ωm | 1.8 | 2.7 | 103 | 43 | 10 | 43 | 1000 |
| $\mu$ | 1 | 1 | 1 | 1 | 800 | 50,000 | 1 |
| Frequency | Skin depth (mm) | | | | | | |
| 1 Hz | 67 | 83 | 510 | 330 | 5.6 | 1.4 | 1591 |
| 100 Hz | 6.7 | 8.3 | 51 | 33 | 0.56 | 0.14 | 159 |
| 10 kHz | 0.67 | 0.83 | 5.1 | 3.3 | 0.056 | 0.014 | 15.9 |
| 1 MHz | 0.067 | 0.083 | 0.51 | 0.33 | 0.0056 | | 1.59 |

For crack depth $t$

$\delta << t$

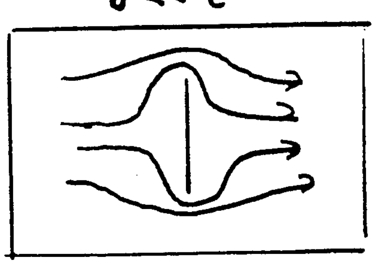

$\delta >> t$

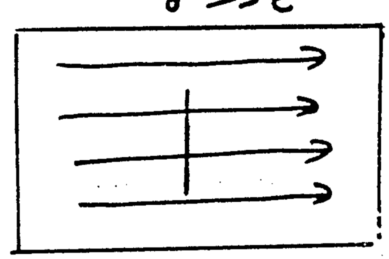

$\delta$

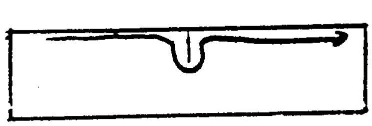

$\delta$

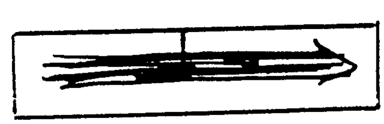

$t$

Depth averaged current

## Experimental procedure

Many AC techniques generate single frequency 1D or 2D scans of a specimen. In contrast, we make measurements over a range of frequencies:

- s(f) at a signal position, near the slot.
- r(f) at a reference position, above a plain piece of plate, far from the slot.

Then we normalise, calculating s(f)/r(f), which contains depth information via the skin effect.

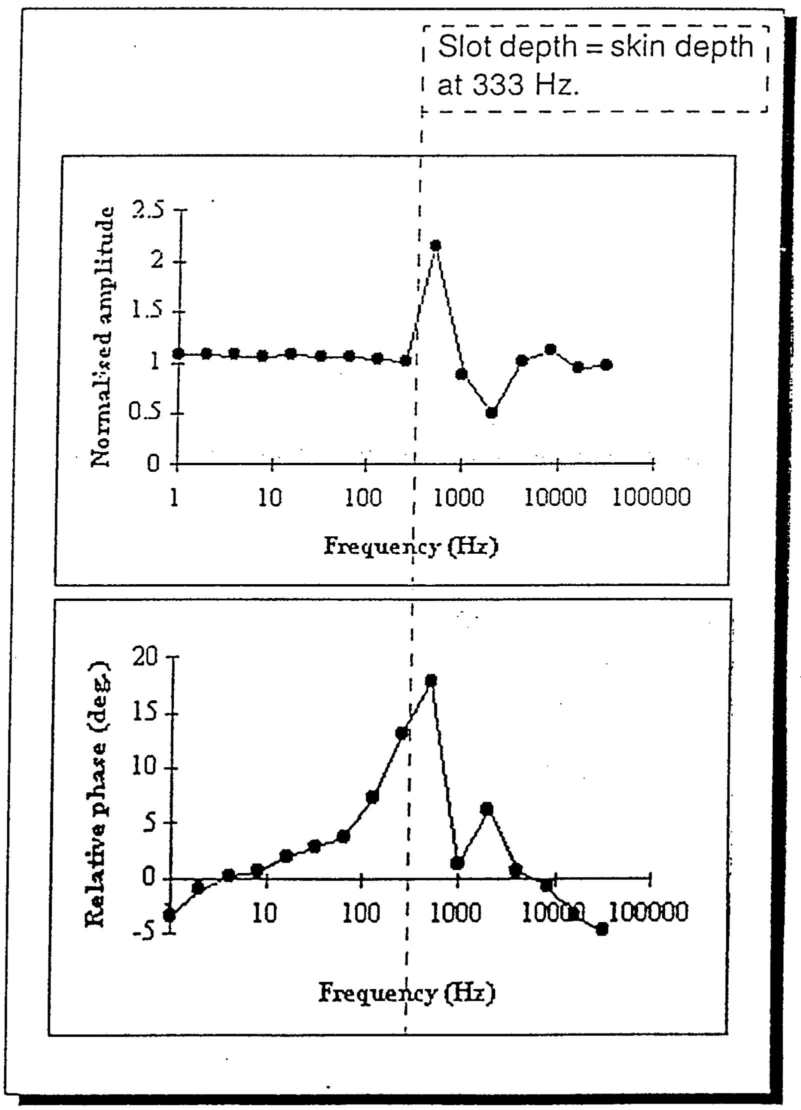


**Figure 3:** a typical experimental result, for a **subsurface** slot 6.5 mm deep.

# NDE WITH LTS SQUID GRADIOMETERS

Uses same scanning system and electronics, but the requirement of a LHe cryostat imposes an additional standoff between the sensor and the sample. (Varying the coil to sample liftoff is much more critical).

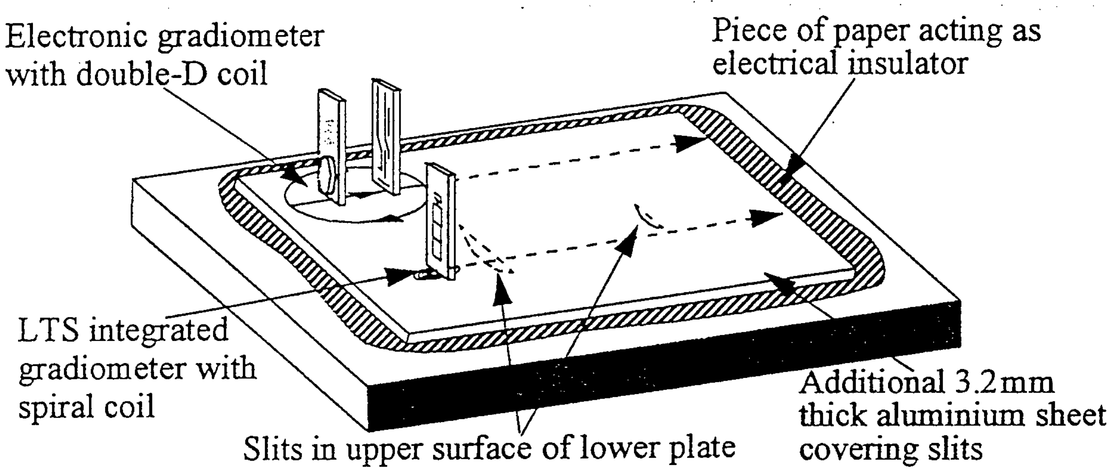


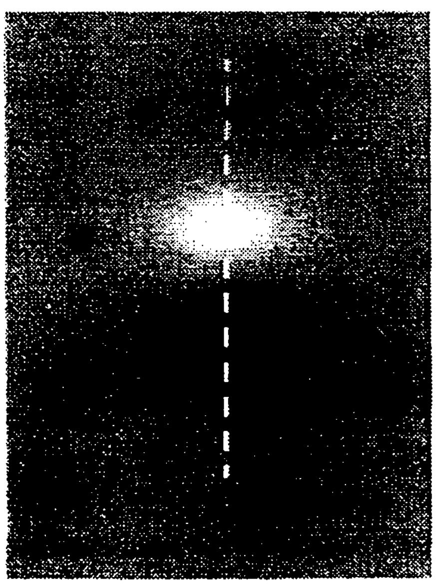

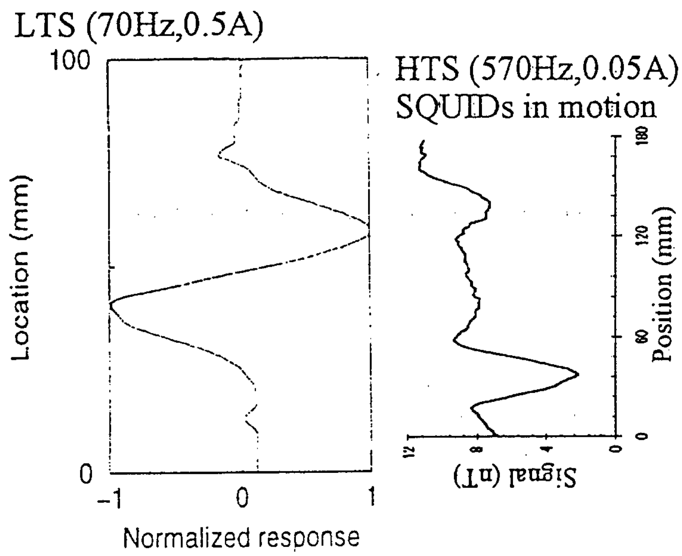


- LTS Gradiometers are overly sensitive for NDE purposes.
- rf or magnetic shielding is often required for operation in a magnetically hostile environment.
- The design and application of higher order asymmetric gradiometers *may* have some future in very specialised areas.

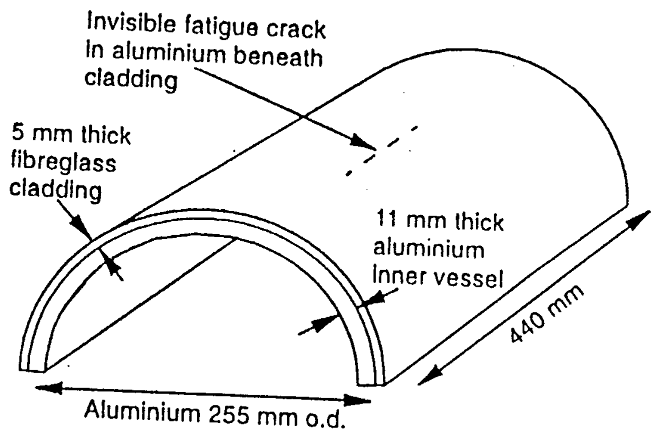


Figure 22. Section of fibreglass-clad aluminium pressure vessel with a fatigue through crack in its metal wall (supplied by British Gas).

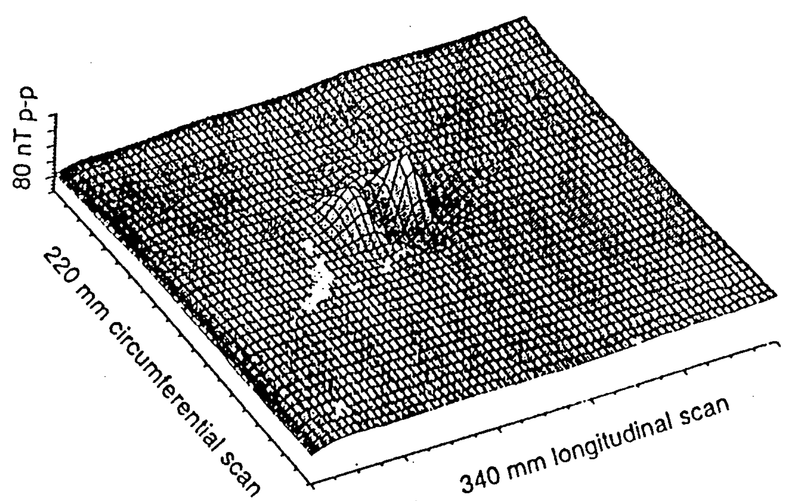

Section 2.1.1.B). The concentration and charge gradients force $Na^+$ into the cell and if the

Figure 2.7 Post-synaptic synapse. Neurotransmitters are released into the synaptic cleft and recombine with the post-synaptic membrane. The recombination of excitatory neurotransmitters, force a change in the permeability of the membrane to $Na^+$ ions which initiates depolarisation. (Gaudin and Jones, 1989).

threshold potential is reached an action potential is initiated in the post-synaptic neurone. The action potential can now propagate along this new neurone. The current distribution of a post-synaptic potential is like that of a single current dipole. The measured biomagnetic signal is not of one axon synapsing with another but is the sum of the magnetic field from many synapses in the nerve bundle.

The post-synaptic potential always occurs at the synapse at the same time for a given nerve and stimulus site. The recordings taken from the spinal cord and cortex in Chapter 6 and 7 are of the magnetic fields induced by post-synaptic potential currents of several hundred neurones. Stimulation of the median nerve at the wrist, causes propagation of an action potential along the nerve bundle to the post-synaptic neurones in the dorsal horn in the spinal cord, 14ms after the stimulation. The signal

# MULTILAYER SPECIMENS

Realistic aircraft lap-joint structures may have flaws beside fasteners in the first, second or even third layers, ie flaws hidden below 6mm of aluminium. The lack of any sealant between the layers makes ultrasonic testing unsuitable.

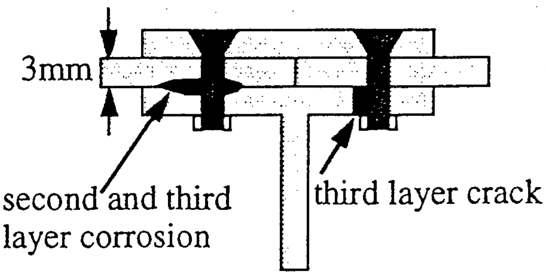


←Cross section of airframe

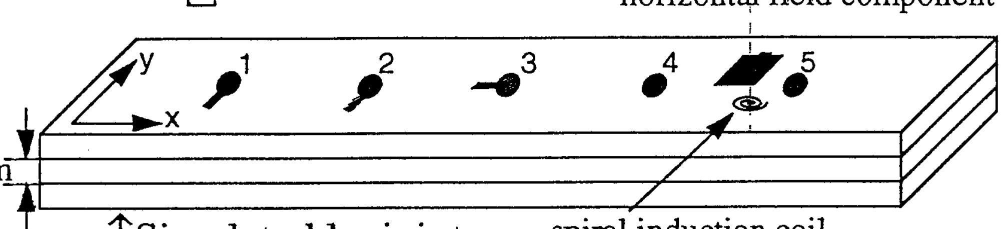


↑Simulated lapjoint

Eddy currents induced in the sample using a spiral coil located on the cryostat tail. $I_{coil}$~0.5A, $f_{coil}$=620Hz. The HTS SQUID magnetometer is scanned across the sample at v~3mms$^{-1}$ and takes 60mins to collect the data.

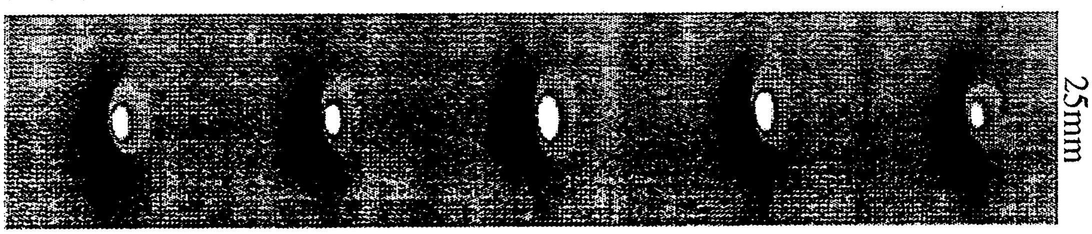


The flaw signal is superimposed onto the rivet signal and identical unflawed rivets do not have identical signatures due to the nature of the contact between the rivet and the plate.

620Hz

Deeper flaws → lower excitation frequency
Reducing the frequency to 170Hz increases the flaw signal at rivet 2. Use digital signal subtraction to remove the rivet signal from the image.

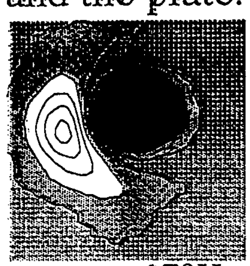

170Hz

# FLUXGATES vs SQUIDS

Both sensors were used to map the features of the lap-joint sample, starting with the top layer.

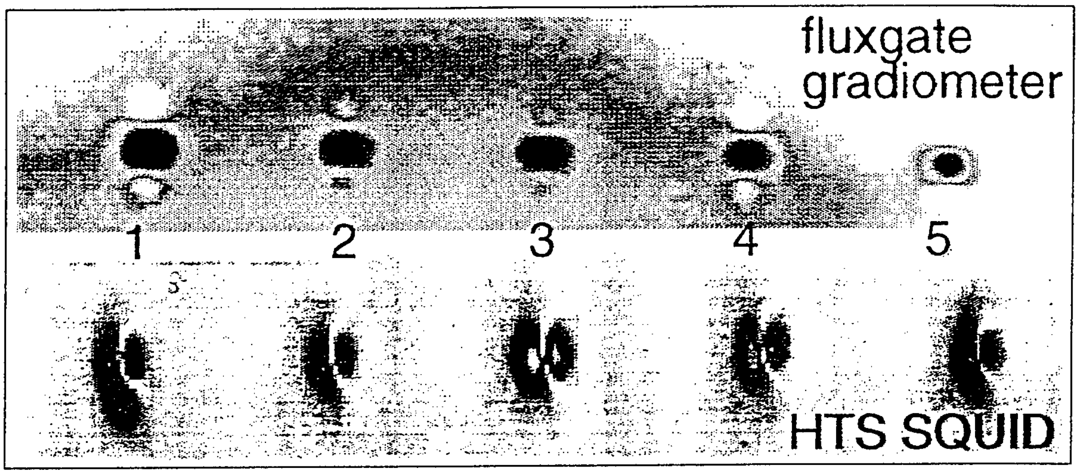


Two-dimensional cross-correlation of the final image with an “ideal, unflawed fastener” can be used to isolate the flaw signal. For the SQUID image:

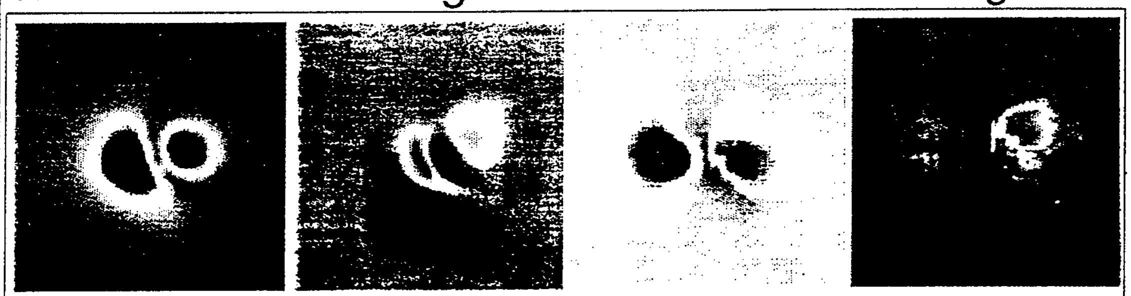

| | | | |
|---|---|---|---|
| Average of 2&4 (both unflawed) | Rivet 1 -Average pk-pk 90 | Rivet 3 - Average pk-pk 67 | Rivet 5 - Average pk-pk 25 |

In the above example, a moderately low noise HTS SQUID performs better than a fluxgate in terms of spatial and signal resolution.

Removal of the rivet signal can also be performed using orthogonal induction of the eddy currents.

## Second generation gradiometers

Aimed at ultra low-noise applications:

- ➔ Fabricate gradiometer on large substrate 30 x 10mm$^2$ --> baseline is 14mm.
- ➔ Improve inductance matching between gradiometer loop and SQUID
- ➔ Use novel coupling scheme where two SQUIDs are connected to gradiometer loops to compensate for parasitic effective area.

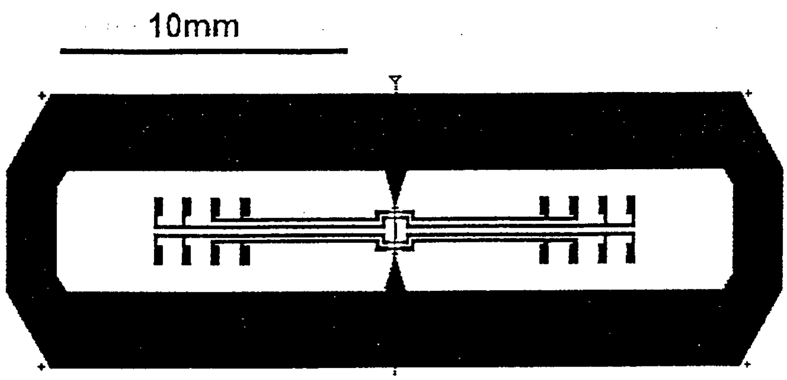


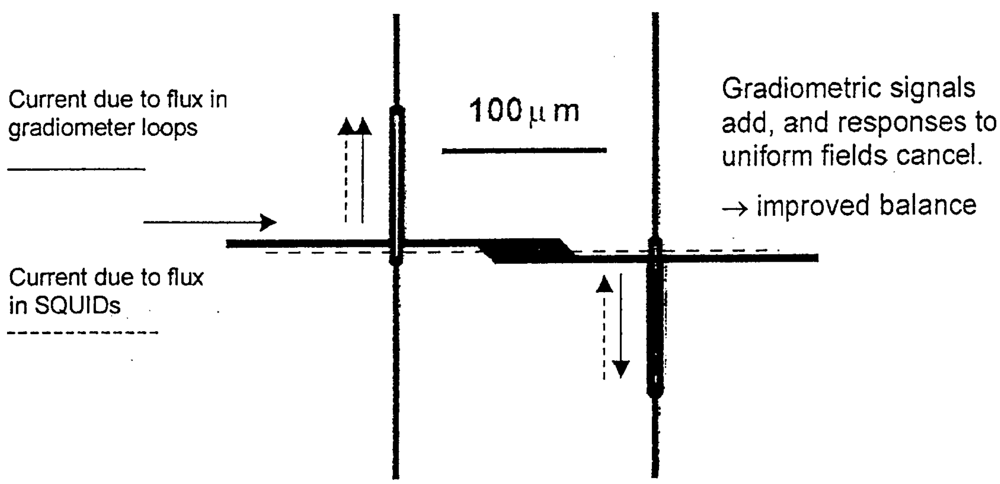


First Tests: Gradient resolution is ~~222~~ 70fT/cm$\sqrt{\text{Hz}}$ --> suitable for biomagnetism
Gradiometer operates well unshielded

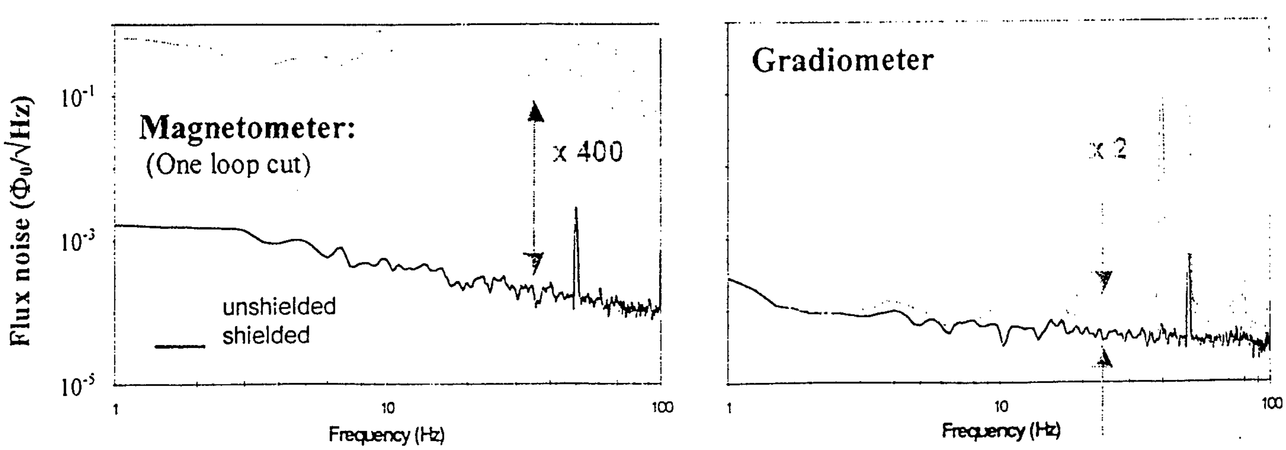

# 4) Mobile Cryostat with SQUID and Scanmaster moving unit

# Mobile Cryostat for SQUID cooling (ILK Dresden)

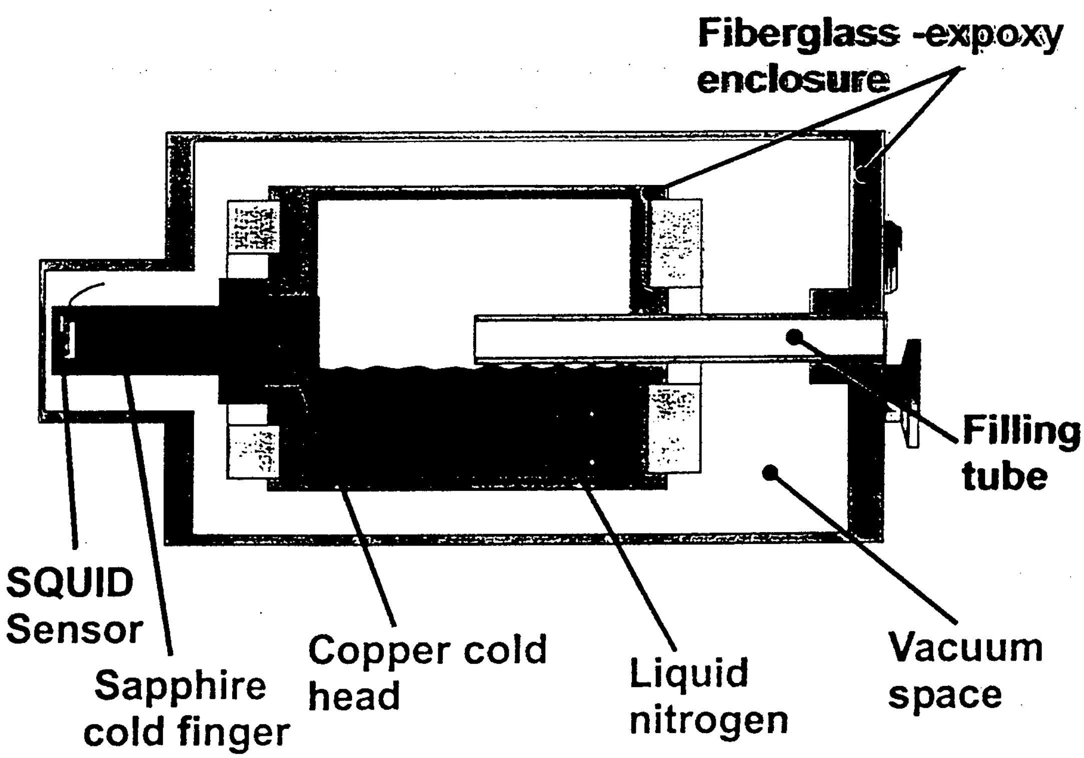

# Flawless Airbus wheel

## Lock-in signal of SQUID (one trace)

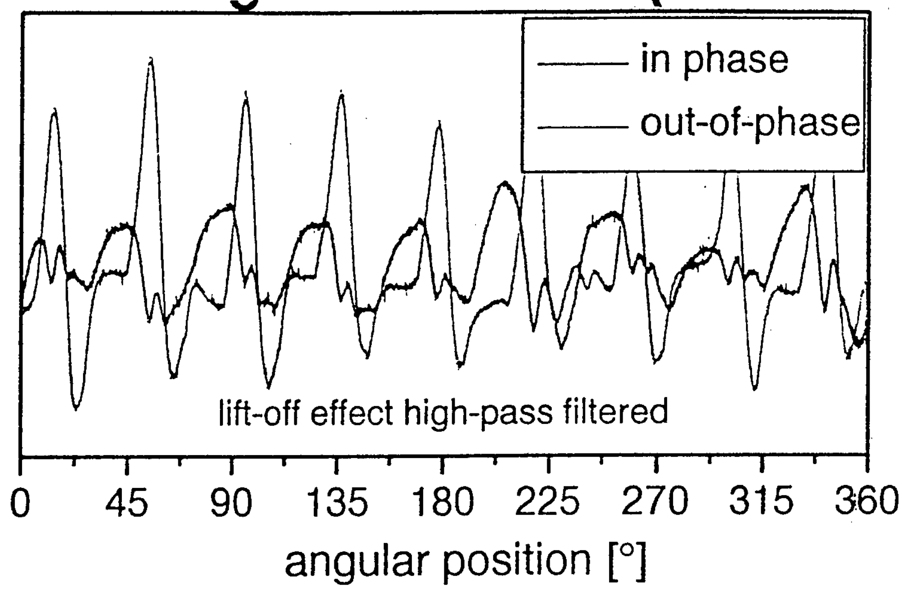


## Signature from ferromagnetic keys

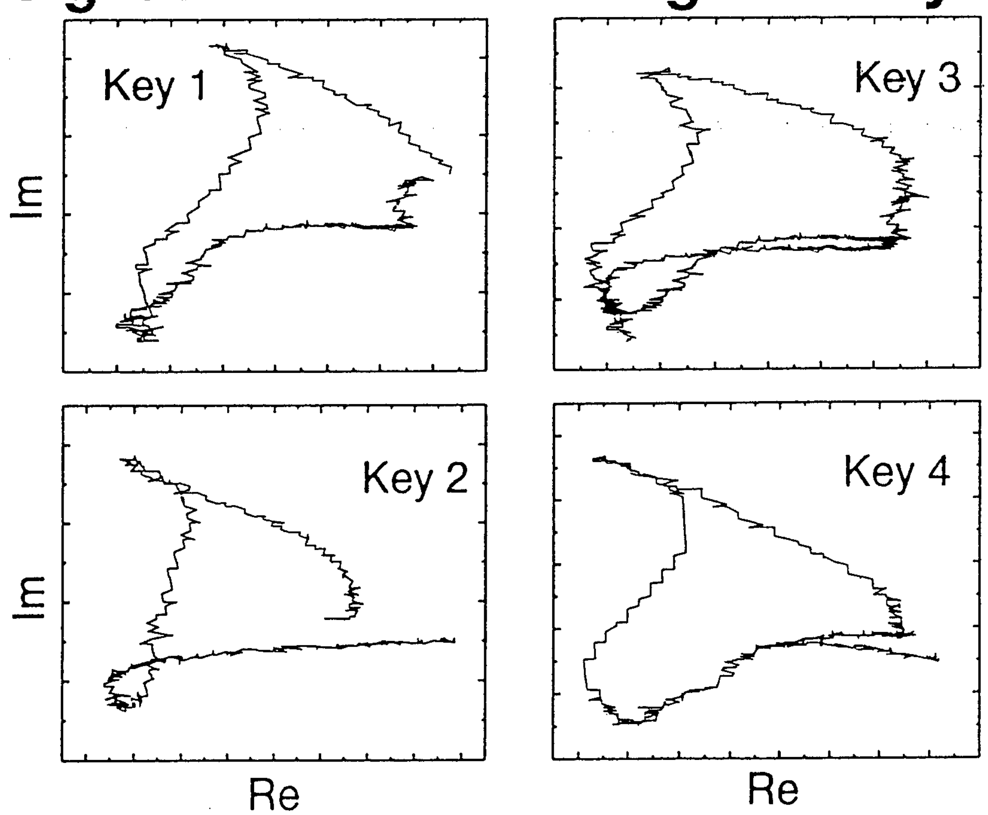

# Aircraft Wheel Testing

rf-Gradiometer, f = 215 Hz, I = 200 mA
trace with 65 % crack and 25 % crack

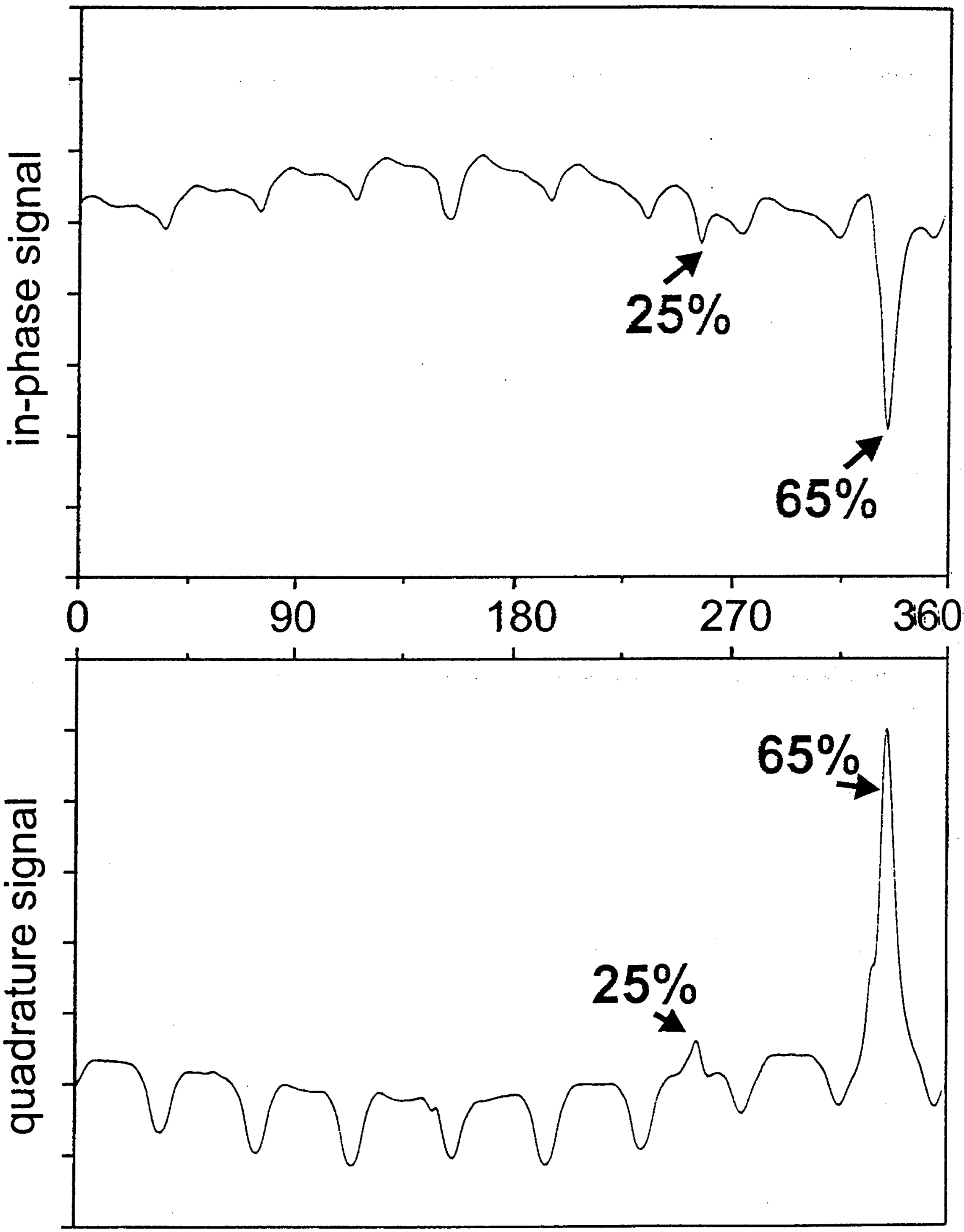

# Orthogonal Excitation with Planar Gradiometer and Sheet Inducer

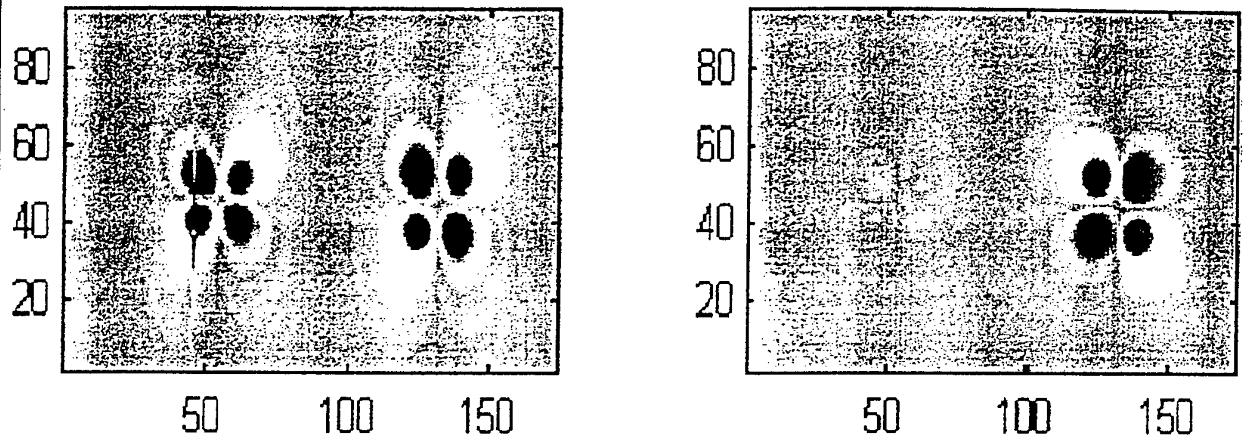


↑ Signal ↓ integrated along gradiometer baseline

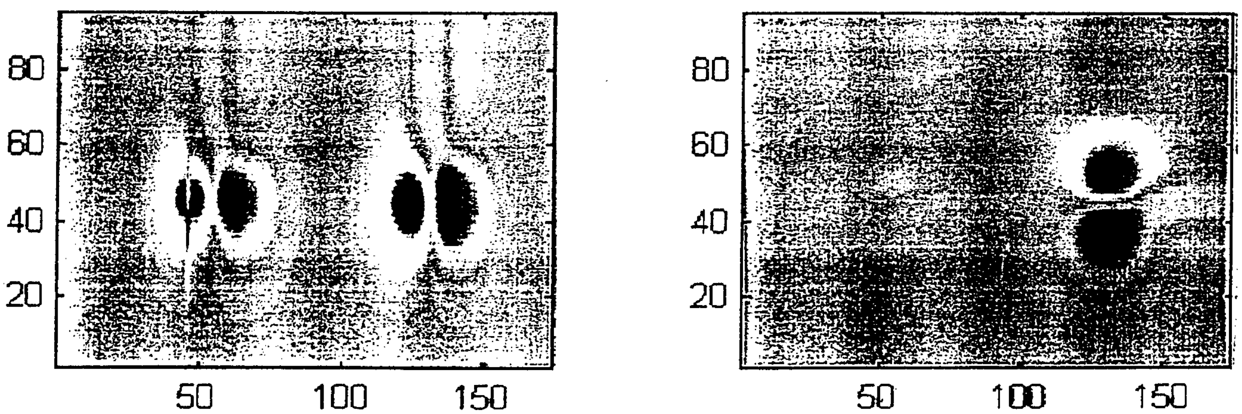


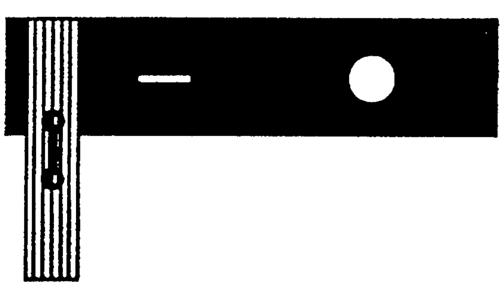

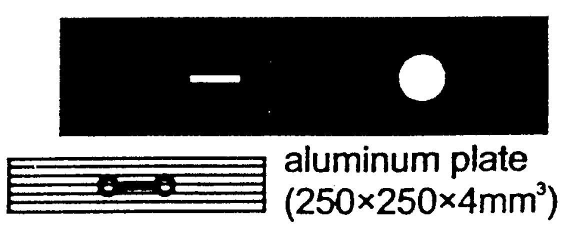

aluminum plate ($250 \times 250 \times 4 mm^3$) with 12.5mm slot and 12.5 mm hole

Sheet inducer.with planar rf gradiometer

Excitation current: 5 mA @ 500 Hz

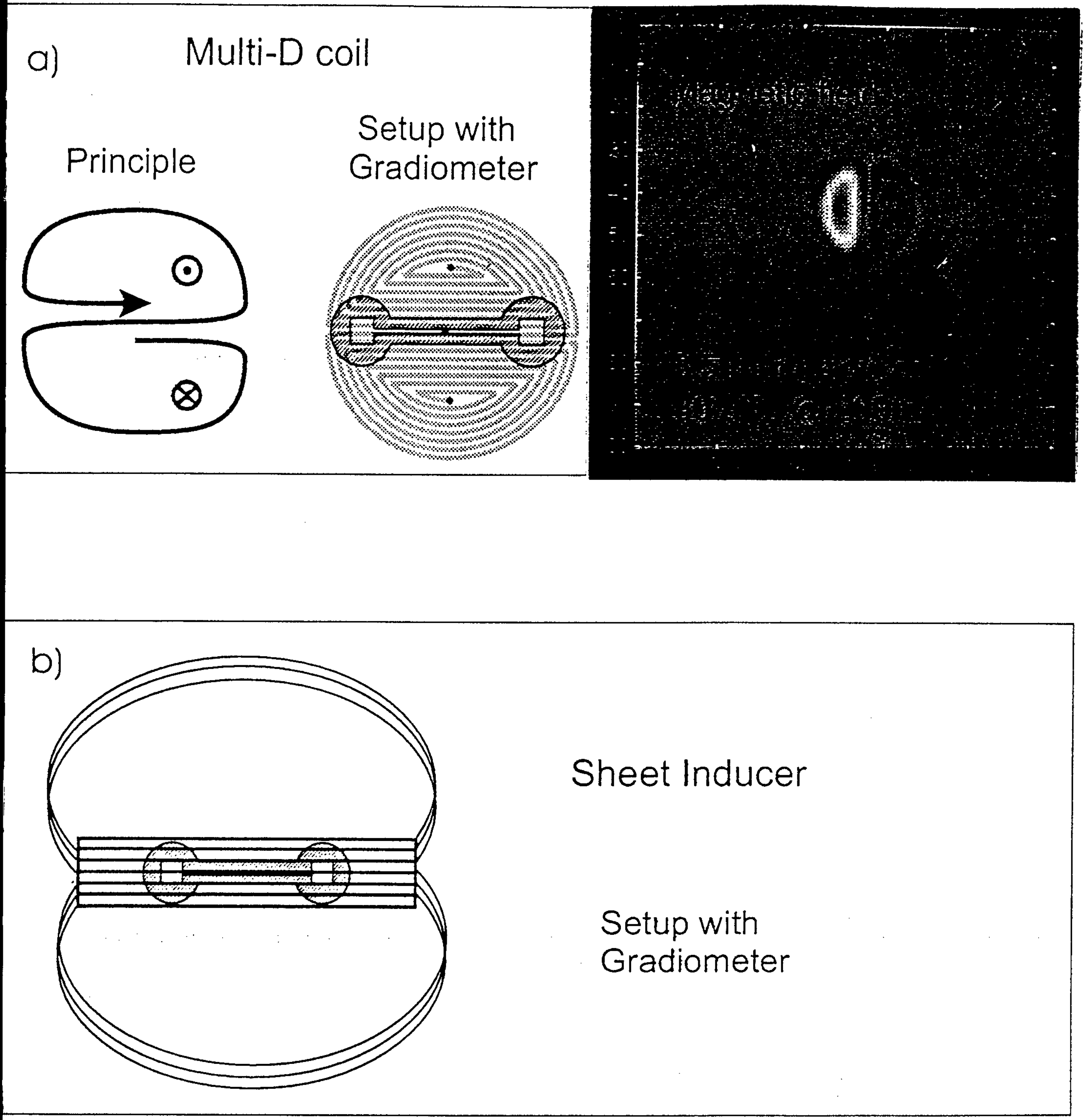


Fig. 6: MULTI-D COIL AND SHEET INDUCER
WITH SQUID SETUP

Forschungszentrum Jülich

# Rotation of excitation current

## Software Evaluation of Orthogonal Measurements with Planar Gradiometer and Sheet Inducer

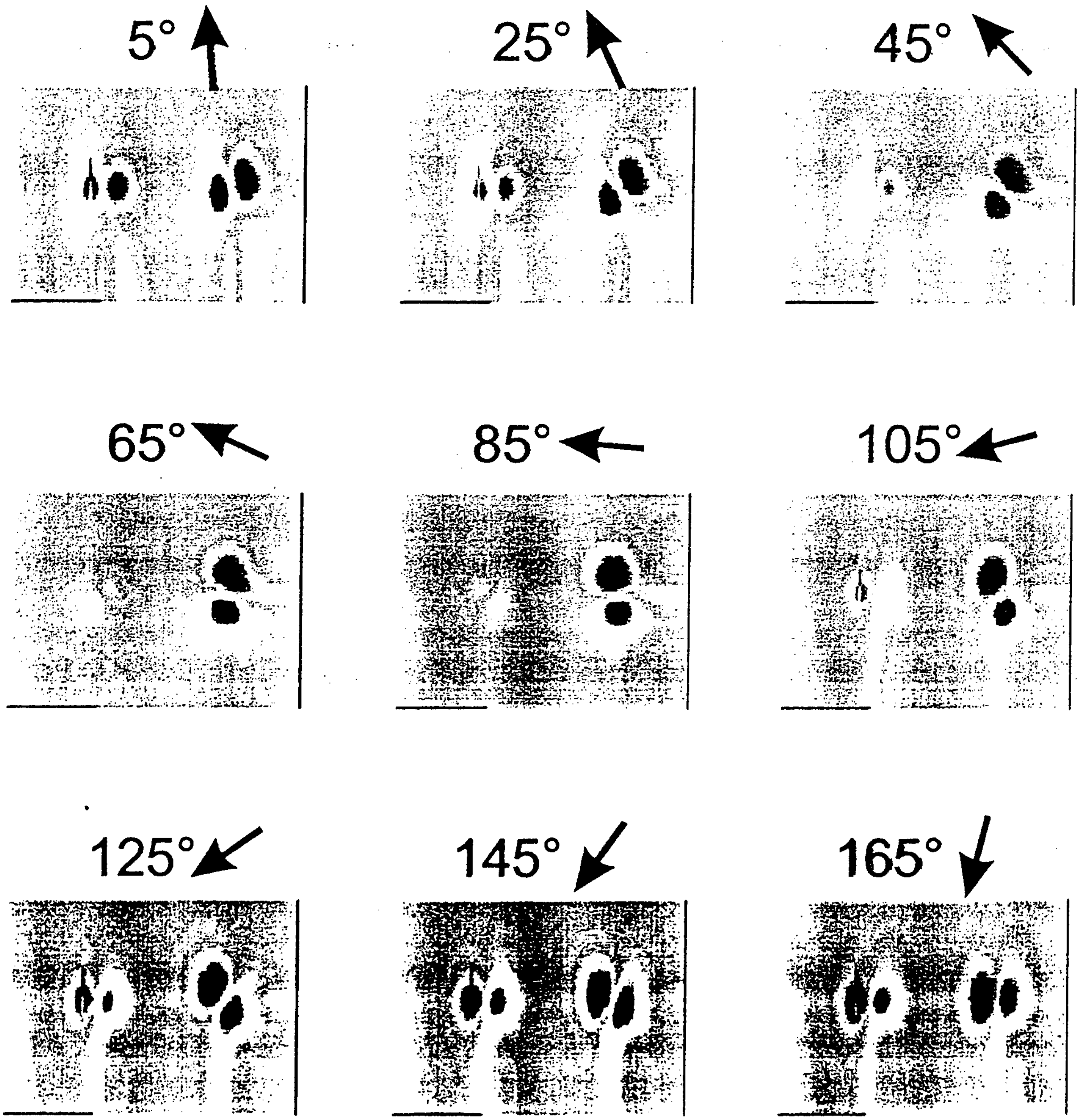


Excitation: 5 mA @ 500 Hz

aluminum plate ($250\times250\times4 mm^3$)
with 12.5mm slot and 12.5 mm hole

# Orthogonal Excitation with Planar Gradiometer and Multi-D Coil

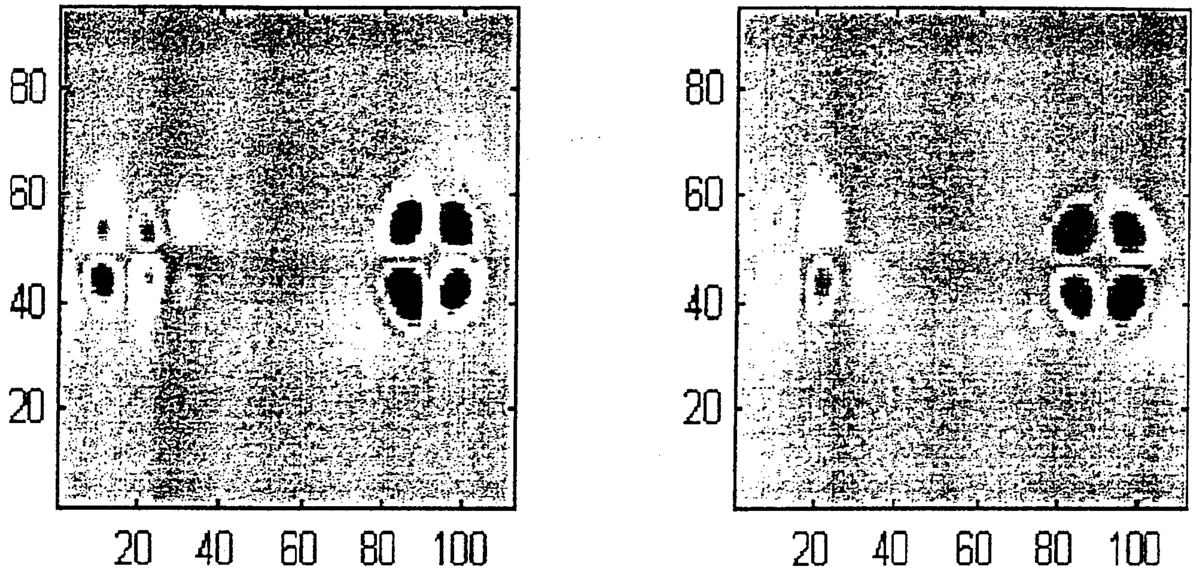


↑ Signal ↓ integrated along gradiometer baseline

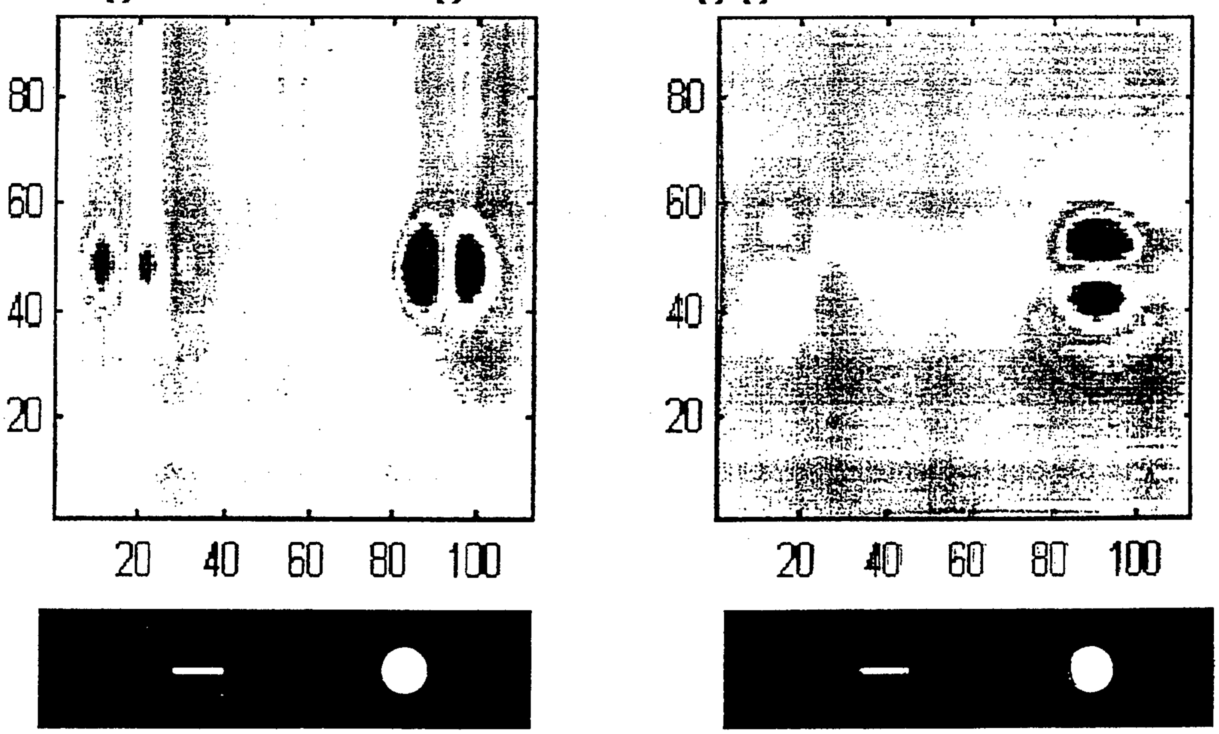


aluminum plate (250×250×4mm³) with 12.5mm slot and 12.5 mm hole

Multi-D coil with planar gradiometer

Excitation current: 1 mA @ 500 Hz

# SQUID measurement of DASA Calibration Sample

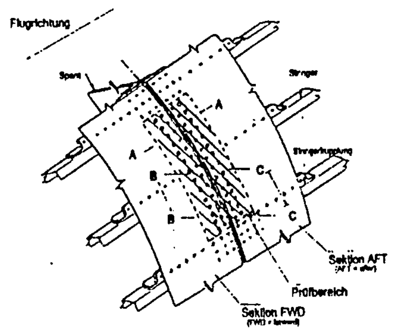


15 190 (k 4)..190 (k 5) 1

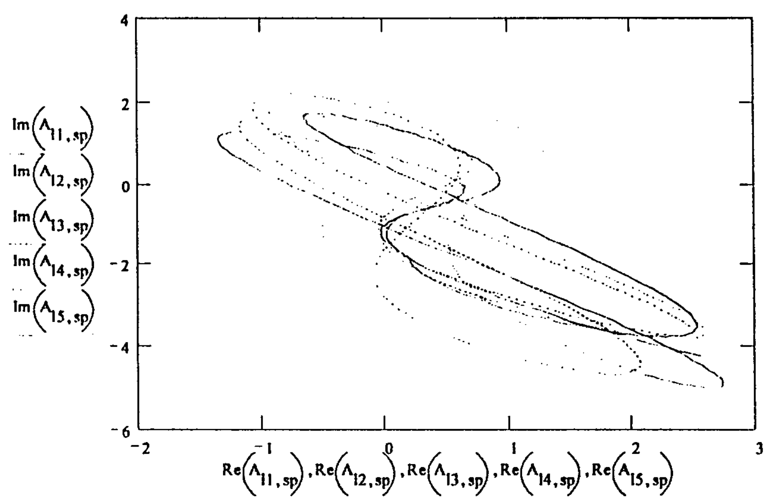


Conventional measurement:
(Eddyscan)

Rivet distance: 25 mm
Rivet diameter: 4.8 mm

Section FWD

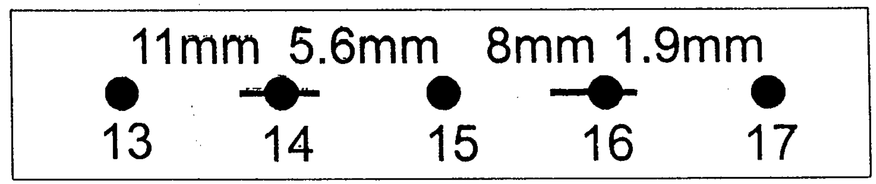



Quadrature Signal

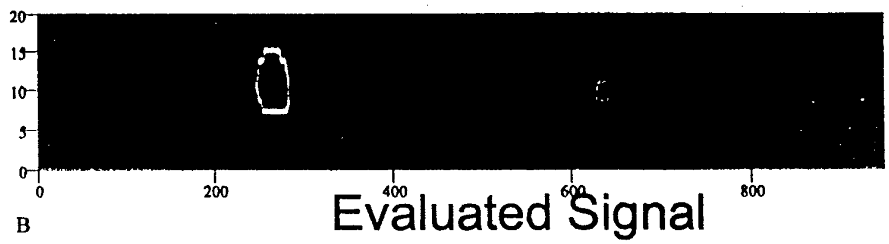


Evaluated Signal

# Harold Weinstock (AFOSR) -1997

"Those of us who are seeking potential SQUID NDE applications would do well to spend more time at NDE meetings. At these meetings we will learn what the real problems are, and how far we must go to outperform the existing and emerging competition. Furthermore, we must visit manufacturing and processing plants to learn how a SQUID might be used to speed production and improve quality control. The results of such forays into the world of NDE will have a major impact on the future of SQUID technology."